SOFIA ISABEL FRANCO CAVACO

STUDIES TOWARDS UNVEILING THE ASSOCIATION OF GLA-RICH PROTEIN WITH OSTEOARTHRITIS

UNIVERSIDADE DO ALGARVE

Faculdade de Ciências e Tecnologia

2016

SOFIA ISABEL FRANCO CAVACO

STUDIES TOWARDS UNVEILING THE ASSOCIATION OF GLA-RICH PROTEIN WITH OSTEOARTHRITIS

Doutoramento em Ciências Biológicas

Trabalho efetuado sob a orientação de:

Professora Doutora Dina Simes

Doutora Carla Viegas

UNIVERSIDADE DO ALGARVE

Faculdade de Ciências e Tecnologia

2016

Studies towards unveiling the association of Gla-rich protein with osteoarthritis

Declaração de autoria de trabalho

Declaro ser a autora deste trabalho, que é original e inédito. Autores e trabalhos consultados estão devidamente citados no texto e constam da listagem de referências incluída.

Aos meus pais, Ana Maria e José Manuel

If we stop learning we stop living

Mary-Frances Winter

Agradecimentos

Durante o decorrer deste projeto contei com o apoio de diversas pessoas, às quais gostaria de agradecer.

Em primeiro lugar gostaria de agradecer à Professora Doutora Dina Simes, que tem acompanhado todo o meu percurso pela ciência, desde o meu estágio de Licenciatura em Bioquímica, do qual foi co-orientadora, até ao momento. O tempo voa e parecendo que não já se passaram mais de 13 anos, dentro dos quais concluí a minha Licenciatura, trabalhei como bolseira de investigação, realizei o meu Mestrado em Biologia Molecular e Microbiana e me encontro agora a concluir o Doutoramento em Ciências Biológicas, sempre sob a sua orientação. Também durante este período vivi a formação do atual grupo de investigação FBP (Functional Biochemistry and Proteomics), ajudei aestabelecer um laboratório provisório para o grupo e o actual laboratório de investigação. Agradeço à Professora Dina o constante empenho, preocupação e a oportunidade por realizar este projeto no seu laboratório.

À Doutora Carla Viegas, minha co-orientadora, agradeço pelos conhecimentos transmitidos, não só durante o meu projeto de Doutoramento mas desde o início do meu percurso pela ciência, uma vez que por diversas vezes contei com a sua ajuda para desenvolver as minha atividades laboratoriais. Agradeço também o entusiamo e empenho demonstrados em relação à ciência, e em especial no que remete às linhas de investigação do grupo FBP, que fazem com que seja impossível não suscitar interesse pela temática.

Um especial agradecimento ao Doutor Acácio Ramos, o principal responsável pela colheita de material biológico do projeto e pela familiarização do grupo com a parte clínica da osteoartrite. Apesar da sua agenda preenchida, o Doutor Acácio mostrou-se sempre muito interessado pelo projeto e esteve sempre disponível para responder a quaisquer questões que eventualmente íam surgindo.

Agradeço também à Doutora Joana Luz, responsável pela colheita de material biológico controlo do projecto, na Delegação do Sul do Instituto Nacional de Medicina Legal e Ciências Forenses.

I would like to thank Doctor Cees Vermeer for granting me the opportunity to work at his laboratory (VitaK BV) for a period of time and perform experimental procedures that I would not have been able to do in the FBP laboratory. At Vitak BV, I greatly thank Marjolein Herfs and Cynthia van't Hoofd for their help and guidance.

Muito obrigado ao Doutor Francisco Blanco por permitir a colaboração entre o seu grupo de investigação (Grupo de Bioingeniería Tisular y Terapia Celular) e o nosso, que possibilitou a aquisição de culturas primárias de células essenciais ao decorrer do projeto. Dentro deste grupo quero agradecer particularmente à Doutora Joana Magalhães, a responsável pelo desenvolvimento das culturas de células fornecidas, e que para além disso foi sempre super prestável e eficaz.

Também gostaria de agradecer ao Doutor José Enriquez, em primeiro lugar por permitir a colaboração entre o Departamento de Anatomia Patológica do Centro Hospitalar do Algarve e o nosso laboratório, mas também por se disponibilizar a analisar algumas das *minhas* amostras patológicas. Neste departamento, agradeço também em particular à Técnica Alexandra Teixeira, que realizou todas as inclusões de tecidos em parafina do projeto e alguns dos cortes histológicos.

Quero agradecer à Denise e Marta Valente, que trabalhando noutros laboratórios de investigação, tantas vezes me auxiliaram e disponibilizaram para ajudar.

Agradeço aos meus colegas de laboratório, que no geral se tornaram grandes amigos. Começando pela malta do "Gang do E4", com quem já trabalhava antes de iniciar o Doutoramento, nomeadamente a Odete, Palma, Ricardo, Tomé, Daniel, Mahaut e Nadège. Com eles partilhei e continuo a partilhar bons momentos, muitos deles ao som do José Cid. Já

durante o projeto de Doutoramento, chegam ao laboratório o Miguel e o Tiago, depois a Vera e a Marta. Mais tarde o Brecht, embora que não por muito tempo, mas que tão bem me acolheu quando foi a minha vez de visitar o "seu" laboratório na Holanda. Depois chegaram o Rúben, a Andreia, a Inês e a Sofia! E por fim a Lúcia e a Nuna! Obrigado pela ajuda sempre que necessária, pelos bons momentos e também por estarem lá nos momentos menos bons! Agradeço especialmente à Marta, Odete e Palma, que se tornaram parte do meu grupo de amigos mais próximos e sempre puxaram e continuam a puxar por mim!

Agradeço ainda àqueles que mesmo não directamente relacionados com o projeto, me incentivaram durante estes anos. Acho que sou uma pessoa bastante afortunada com as minhas amizades. Sem nenhuma ordem em particular agradeço ao Eduardo, Liliane, Márcio, Cátia, Mónia, Rita, Zé António, António, Santana, Rutezinha, Joana Rosa, Betinha, Sr. Humberto, Jorge Graça, Sara Brás, à minha maninha Tânia, às Catarinas, à minha loura Inês e às internacionais Susana, Brigite e Joana. Agradeço ainda ao grupo Marafados do Ludo, com quem partilhei e partilho momentos espectaculares, desportivos e de convívio, que foram e são fundamentais para a mantutenção do meu bem-estar físico e psicológico.

Aos meus pais, agradeço todos valores transmitidos e agradeço pelas pessoas fora de série que são, tanto um como o outro, cada um à sua maneira!

Finalmente agradeço ao Henrique, pelo amor, amizade, disponibilidade e compreensão. Obrigado pela paciência e ajuda, em special nos últimos momentos. Obrigado pelo optiminsmo e capacidade de ultrapassar cada obstáculo. Sem ti tudo teria sido muito mais difícil.

A produção deste trabalho teve o financiamento da Fundação para a Ciência e Tecnologia (SFRH/BD/60867/2009), à qual expresso os meus agradecimentos.

Abstract

Osteoarthritis (OA) is a whole-joint disease believed to onset after articular cartilage damage and accompanied by tissue inflammation, abnormal bone formation and extracellular matrix (ECM) mineralization. Gla-rich protein (GRP), the latest discovered vitamin K-dependent protein (VKDP), was shown to accumulate in mouse and sturgeon cartilage, and sites of skin and vascular calcification in human. Therefore, we investigated the possible involvement of GRP with OA development. An osteoarthritic and control samples human biobank was collected and used for the comparative analysis of GRP patterning at transcriptional and translational levels. Two novel GRP alternative spliced transcripts were unveiled in human (GRP-F5 and F6), yet GRP-F1, corresponding to the full-length protein, was shown to be the predominant variant in articular tissues and upregulated in osteoarthritic cartilage. Undercarboxylated GRP was the prevalent protein form found associated with osteoarthritic cartilage and synovial membrane tissues, highly accumulated at sites of calcification, indicating that the impairment of VKDPs γ-carboxylation may be related with OA. Using a chondrocyte and synoviocyte cell system developed within this project, we further investigated the association of GRP with OA mineralization and inflammatory processes. Upregulation of GRP was found during induced mineralization and inflammation, and associated to cell differentiation towards ECM mineralization and inflammatory responses, in both cellular types. Moreover, the role of GRP was highlighted through functional assays, showing the inhibition of ECM mineralization and decreased inflammatory response following GRP supplementation. While γ-carboxylation was required for GRP anti-mineralization function, its anti-inflammatory effect was independent of protein γ-carboxylation status. Ultimately, using serum samples from our biobank and a comparative proteomic approach, candidate OA biomarkers were identified. Overall, our results demonstrated, for the first time, the involvement of GRP in two of the main pathological processes occurring in OA, contributing for new knowledge regarding disease progression.

Keywords: Gla-rich protein (GRP), osteoarthritis (OA), ectopic calcification inhibitor, anti-inflammatory effect, γ-carboxylation status, biomarkers

Resumo

A osteoartrite (OA) representa a forma mais comum de doenças degenerativas das articulações, sendo a principal causa de incapacidade física crónica na população acima dos 50 anos de idade. A origem da OA está geralmente associada a danos na cartilagem articular, acompanhados por uma remodelação da matriz extracelular (ECM), que numa sucessão de eventos acabam por comprometer toda a articulação. A perda de cartilagem articular, inflamação tecidular, formação óssea anormal e a mineralização da ECM, são características comuns desta patologia. No entanto, o conhecimento sobre mecanismos moleculares da OA ainda é limitado, o seu diagnóstico é tardio e não existem atualmente medicamentos eficazes para o tratamento da doença. É portanto essencial a descoberta de novos alvos moleculares e biomarcadores que beneficiem a patologia. A proteína rica em Glas (GRP), último membro descoberto pertencente à família de proteínas dependentes da vitamina K (VKDPs), representa um potencial alvo para o estudo de mecanismos da OA. Esta proteína é bastante acumulada na cartilagem de ratinho e esturjão, e em zonas calcificadas na pele e sistema cardiovascular em humano. Além disso, a GRP é considerada um regulador negativo da osteogénse. Partículas de calciproteínas (CPP) presentes em circulação em fluidos biológicos, representam igualmente um alvo para o estudo de processos moleculares da OA uma vez que estas também são associadas a situações de calcificação patológica e mesmo a processos inflamatórios. Neste âmbito, o principal objetivo do presente estudo foi a análise da possível associação entre a GRP e o desenvolvimento da osteoartrite. Um objetivo adicional foi a procura de biomarcadores para a patologia, com especial interesse na GRP.

Durante o decorrer deste projeto, foi coletado um biobanco bem caracterizado contendo tecidos e fluidos biológicos de pacientes com osteoartrite do joelho e indivíduos sem histórico de patologias nas articulações. As amostras deste banco biológico foram utilizadas para a realização de análises comparativas de padrões de expressão e acumulação da GRP. Haviam sido anteriormente identificadas em ratinho e esturjão quatro variantes por splicing alternativo do gene da GRP, nomeadamente a GRP-F1, F2, F3, e F4. Aqui, utilizando uma estratégia de RT-PCR, foram identificados em humano dois novos transcritos da GRP, denominadas GRP-F5 e F6 e caracterizados pela perda de domínios de γ-carboxilação e secreção. No entanto, os nossos resultados evidenciaram a variante GRP-F1, correspondente à proteína total, como a maioritariamente expressa em cartilagem e membrana sinovial, sugerindo que associações existentes entre a GRP e a OA reflitam sobretudo a contribuição

deste transcrito. Além disso, também se verificou que a GRP-F1 era sobrexpressa em cartilagem osteoartrítica em comparação com tecidos controlo. O estudo entre a possível associação da GRP com a OA prosseguiu utilizando técnicas imunológicas e anticorpos conformacionais específicos contra as formas carboxilada (cGRP) e subcarboxilada (ucGRP) da GRP. Esta abordagem revelou que embora ambas as entidades sejam acumuladas em tecidos articulares e fluidos osteoartríticos, bem como zonas de calcificação ectópica, a ucGRP é a forma predominante associada à cartilagem e membrana sinovial osteoartríticas, enquanto que a cGRP é preferencialmente acumulada nos mesmos tecidos em condições controlo. A forma subcarboxilada da proteína Gla da matriz (ucMGP) foi também a predominantemente associada à cartilagem osteoartrítica. A combinação destes resultados sugere que deficiências na γ-carboxilação de VKDPs estejam possivelmente relacionadas com mecanismos moleculares da OA. Os nossos resultados imunohistológicos também revelaram que a acumulação de GRP em membranas sinoviais osteoartríticas não era restrita a zonas de calcificação, ocorrendo também nas camadas que revestem estes tecidos e sugerindo associações a outros processos. Utilizando um sistema celular de linhas primárias de condrócitos e sinoviócitos desenvolvido no âmbito deste projeto, o estudo da associação entre a GRP e a mineralização associada à OA foi aprofundado, bem como o seu possível envolvimento com processos inflamatórios. A análise comparativas do padrão de expressão de GRP entre células osteoartríticas e controlo, revelou que esta era sobrexpressa em células osteoartríticas, em concordância com os resultados obtidos *in vivo* com amostras de cartilagem. Também se verificou que a GRP era sobrexpressa mediante a indução de mineralização e inflamação do sistema, e associada a processos de diferenciação celular inerentes à mineralização da ECM e respostas inflamatórias, em ambos os tipos celulares. Notavelmente, foram evidenciadas funções biológicas da GRP na OA através de estudos funcionais: a sua capacidade de inibição da mineralização da ECM e a diminuição de respostas inflamatórias após suplementação da proteína. Curiosamente, a γ-carboxilação da GRP revelou ser essencial para a sua função anti-calcificante enquanto que o efeito anti-inflamatório observado mediado pela GRP ou GRP-acoplada a cristais de fosfato de cálcio básico foi independente do seu estado de γ-carboxilação, evidenciando funções alternativas para a ucGRP em particular. Os nossos novos resultados sugerem que na OA ocorra um aumento da expressão de VKDPs, como a GRP e MGP, possivelmente associado ao combate de processos de calcificação ectópica. No entanto, a sobrecarga do sistema pode resultar numa capacidade de γ-carboxilação deficiente, culminando na prevalência de ucGRP e ucMGP. Por sua vez, a ucGRP pode estar associada ao controlo de níveis de mediadores de inflamação

através de mecanismos ainda desconhecidos. A última parte deste trabalho pretendia identificar candidatos a biomarcadores da OA, para fins de diagnóstico da patologia ou de monitorização de tratamentos, sendo de particular interesse a análise do potencial da GRP como um destes biomarcadores. Contudo, o uso da técnica clássica de electroforese bidimensional revelou ser inadequado para o estudo desta proteína. Em alternativa, utilizando a mesma abordagem proteómica e amostras de soro do biobanco colecatdo, foi realizada a procura de potenciais biomarcadores para a patologia associados a CPP. Esta análise permitiu a identificação de 19 proteínas diferencialmente expressas entre condições controlo e osteoartríticas, que podem ser consideradas potenciais biomarcadores para a OA. Além disso, algumas das proteínas identificadas associadas a estes complexos estão relacionadas com processos de calcificação patológica e inflamatórios, o que sugere um possível envolvimento entre CPP e osteoartrite.

Os nossos resultados abrem novas portas no domínio de investigação científica da osteoartrite, sobretudo através da associação nunca antes descrita entre a GRP e a patologia. Os dados coletados durante o projeto revelaram o envolvimento da GRP, aparentemente com efeitos benéficos, em dois dos principais processos patológicos que ocorrem na OA, nomeadamente a calcificação patológica e inflamação, o que contribuiu para um melhor conhecimento relativo à progressão da patologia.

Palavras-chave: Proteína rica em Glas (GRP), osteoartrite (OA), inibidor de calcificação ectópica, efeito anti-inflamatório, estado de γ-carboxilação, biomarcadores

Table of contents

Abbreviation list

2-DE	Two-dimensional gel electrophoresis
3D	Three-dimensional
aa	Amino acid
ADAMTS	A disintegrins and metalloproteinases with thrombospondin motifs
ACTB	Actin cytoplasmic 1
AGAL	α-galactosidase A
ALP	Alkaline phosphatase
AMPL	Cytosol aminopeptidase
ANOVA	Analysis of variance
APOA4	Apolipoprotein A-IV
ATP	Adenosine triphosphate
BCP	Basic calcium phosphate
BMI	Body mass index
BMP	Bone morphogenetic protein
bp	Base pairs
BPG	β-glycerophosphate
BRC	Bone-remodelling compartment
BSA	Bovine serum albumin
CAVD	Calcified aortic valve disease
CATD	Cathepsin D
CBS	Centre for Biological Sequence analysis
CBB	Coomassie brilliant blue
CCMar	Centro de Ciências do Mar
CD	Cluster of differentiation
cDNA	Complementary DNA
CDS	Coding DNA sequence
cGRP	γ-carboxylated GRP
CKD	Chronic kidney disease
cMGP	γ-carboxylated MGP
COF1	Cofilin 1
Col1a1	Type I collagen
Col2a1	Type II collagen
Col10a1	Type X collagen
COX2	Cyclooxygenase 2
CPC	Cetylpyridinium chloride
CPP	Calciprotein particles
CPPD	Calcium pyrophosphate dihydrate
CTX-II	C-terminal telopeptides of type II collagen
DAMPs	Damage-associated molecular patterns
DAPI	4,6-diamidino-2-phenylindole
DBS	4-diazobenzene sulfonic acid
DM	Type II diabetes mellitus
DMEM	Dulbecco's modified Eagle's medium
DMM	Destabilization of the medial meniscus
DMOADs	Disease-modifying osteoarthritis drugs
DNA	Deoxyribonucleic acid
DTT	Dithiothreitol

DXM	Dexamethasone
E	Extinction coefficient
ECM	Extracellular matrix
EDTA	Ethylenediamine tetraacetic acid
ELISA	Enzyme-linked immunosorbent assay
EVs	Extracellular vesicles
FBS	Fetal bovine serum
FBP	Functional Biochemistry and Proteomics
FCT	Fundação para a Ciência e Tecnologia
HA	Hydroxyapatite
HFLS	Human fibroblast-like synoviocytes
HT	Hypertension
GGCX	γ-glutamyl carboxylase
Gla	γ-carboxyglutamic acid
Glc-Gal-Pyd	Glucosyl-galactosyl-pyridinoline
Glu	Glutamate
GRP	Gla-rich protein
GRP2	Gla-rich protein paralog
IBET	Instituto de Biologia Experimental e Tecnológica
IEF	Isoelectric focusing
IF	Immunofluorescence
IGHG1	Immunoglobulin γ 1 chain C region
IGHM	Immunoglobulin mu chain C region
IHH	Indian hedgehog
IHC	Immunohistochemistry
IL	Interleukin
ILEU	Leukocyte elastase inhibitor
IPG	Immobilized pH gradient
IR	Infrared
ITA2B	Integrin α-IIb
ITIH4	Inter-α-trypsin inhibitor heavy chain H4
ITQB	Instituto de Tecnologia Química e Biológica
K	Quinone form of vitamin K
K1	Phylloquinone
K2	Menaquinones
KH_2	Vitamin K hydroquinone
KL	Kellgren-Lawrence
KO	Vitamin K 2,3-epoxide
LC-MS/MS	Liquid chromatography-MS/MS
LDS	Lithium dodecyl sulphate
MALDI	Matrix-assisted laser desorption/ionization
MAPK	Mitogen-activated protein kinases
MetS	Metabolic syndrome
MVs	Matrix vesicles
MS	Mass spectrometry
MS/MS	Tandem mass spectrometry
MGP	Matrix Gla protein
MK	Menaquinone
MK-n	Menaquinone with a n number of prenyl repeats
MMLV-RT	Moloney-murine leukemia virus-reverse transcriptase

MMP	Matrix metalloproteinase
MW	Molecular weight
NC	Normal chondrocytes
NCBI	National Centre for Biotechnology Information
NHAC	Normal human articular chondrocytes
NF-κB	Nuclear factor κB
NO	Nitric oxide
NOS	Nitric oxide synthase
NSAIDs	Nonsteroidal anti-inflammatory drugs
OA	Osteoarthritis
OA-HAC	Osteoarthritic human articular chondrocytes
OA-HFLS	Osteoarthritic human fibroblast-like synoviocytes
OAC	Osteoarthritic articular chondrocytes
OC	Osteocalcin
OPN	Osteopontin
Osx	Osterix
PBS	Phosphate buffered saline
PCR	Polimerase chain reaction
PGE	Prostaglandin E
pI	Isoelectric point
Pi	Inorganic phosphate
PKP1	Plakophilin 1
PLAK	Junction plakoglobin
PPi	Inorganic pyrophosphate
PRP	Platelet-rich plasma
PTH	Phenylthiohydantoin
PRS	Pararosaniline
PTHr	Parathyroid hormone-related
PVDF	Polyvinylidene fluoride
PXE	Pseudoxanthoma elasticum
RA	Rheumatoid arthritis
RNA	Ribonucleic acid
ROS	Reactive oxygen species
RP-HPLC	Reverse phase-high performance liquid chromatography
RT	Room temperature
RT-PCR	Reverse transcription-polymerase chain reaction
Runx2	Runt-related transcription factor 2
SDS-PAGE	Sodium dodecyl sulphate-polyacrylamide gel electrophoresis
SNR	Normal fibroblast-like synoviocytes
SOAR	Osteoarthritic fibroblast-like synoviocytes
Sox9	SRY-box 9
TBST	Tris buffered saline
TGF-β	Transforming growth factor β
TLR	Toll-like receptors
TLN1	Talin 1
TNF-α	Tumour necrosis factor α
TPM4	Tropomyosin α 4 chain
TRAP	Tartrate-resistant acid phosphatase
TRFE	Serotransferrin
ucGRP	Undercarboxylated GRP

UCMA	Upper zone of growth plate and cartilage matrix associated protein, former unique cartilage matrix associated protein
ucMGP	Undercarboxylated MGP
ucOC	Undercarboxylated OC
VEGF	Vascular endothelial growth factor
VINC	Vinculin
VKDP	Vitamin K-dependent protein
VKOR	Vitamin K epoxide reductase
VSMCs	Vascular smooth muscle cells
VWDE	Von Willebrand factor D and EGF domain-containing protein
WB	Western blot
WDR1	WD repeat-containing protein 1
Wnt	Wingless/Int

Chapter 1

General introduction

© Centro Hospitalar do Algarve

1.1 Vitamin K-dependent proteins associated with calcification

Vitamin K-dependent proteins (VKDPs) comprise a family characterized by the presence of γ-carboxyglutamic acid (Gla) residues, which result from the post-translational modification of glutamate (Glu) residues [1]. The conversion of Glu to Gla residues is termed γ-glutamyl carboxylation and vitamin K is an essential cofactor of this process [1]. Vitamin K metabolism was initially considered in the context of haemostasis [2], yet with the discovery of VKDPs this vitamin has been associated to multiple biological processes [1]. Vitamin K-dependent proteins may be categorized into two main groups: hepatic and extrahepatic VKDPs [3]. Hepatic VKDPs are mainly involved in balancing blood coagulation, by bridging their Gla residues through calcium with negatively charged phospholipids [4,5], whereas extrahepatic VKDPs are described to have distinct functions, ranging from roles in bone and cardiovascular health [6,7] to the regulation of energy metabolism [8]. Three extrahepatic VKDPs have been associated with calcification processes: osteocalcin (OC), matrix Gla protein (MGP) and Gla-rich protein (GRP). Osteocalcin was the first identified extrahepatic VKDP [9] and has two proposed roles in calcification, the regulation of bone mineralization, and osteoblast and osteoclast activity [6,10]. Some years later MGP was discovered [11], subsequently related with the inhibition of ectopic calcification [12], and the regulation of osteogenesis and chondrocyte maturation [13]. More recently, GRP was identified and proposed as a modulator of calcium availability [14,15] and an inhibitor of calcification in the cardiovascular system, although its mechanism of action requires further investigation [16].

1.1.1 Vitamin K

Vitamin K is a lipid-soluble vitamin, that in nature may occur in form of phylloquinone (K1) or menaquinones (K2) (**Fig. 1.1**), yet both forms present the cofactor activity required for the γ-carboxylation reaction [17]. These vitamin K compounds share a common 2-methyl-1,4-naphthoquinone ring structure and an isoprenoid side chain, that differs in length and degree of saturation (**Fig. 1.1**), depending on the organism by which they are synthesised [17]. Phylloquinone contains a phytyl side chain, which has only one unsaturated bond (**Fig. 1.1**), and is found in plants and cyanobacteria [18]. Menaquinones are composed by a side chain with repeating isoprene residues, each containing an unsaturated bond (**Fig. 1.1**) [17]. Depending on the number of prenyl repeats, menaquinones are

subcategorized as MK-n, with n corresponding to the number of isoprenoid units, generally ranging from 5 to 13 (**Fig. 1.1**) [18]. Menaquinones are majorly obtained nutritionally from bacterially fermented food and liver, but intestinal bacteria also synthesize these vitamin K forms [17]. Although K1 is the major type of vitamin K present on a typical western diet, its concentrations in animal tissues are remarkably low compared with those of menaquinones, especially MK-4, the major form of vitamin K present in tissues [19]. The origin of tissue MK-4 is postulated to be resultant from K1 conversion via integral side-chain removal, with subsequent MK-4 accumulation in extrahepatic tissues [19].

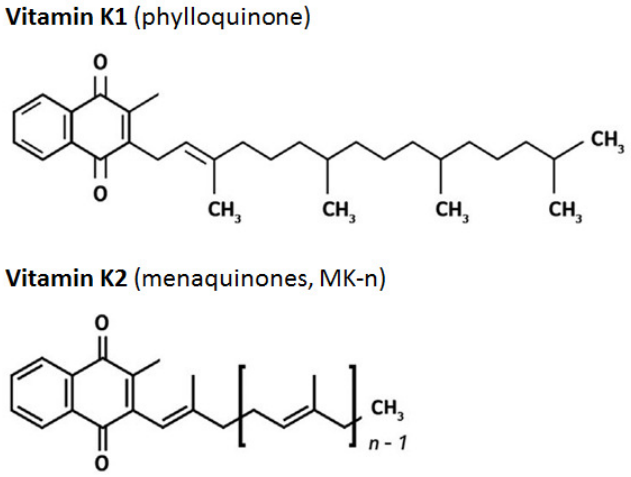

Fig. 1.1 – Chemical structures of naturally occurring vitamin K forms. Vitamin K1, also termed phylloquinone, contains a phytyl side chain with only one unsaturated bond and vitamin K2, known as menaquinones (MK-n), contain a side chain with repeating isoprene residues, each containing an unsaturated bond. The respective menaquinone is indicated by the number of prenyl units (n) (Adapted from Willems et al., 2014 [3]).

The γ-carboxylation reaction of VKDPs requires the presence of three cofactors: a reduced form of vitamin K (vitamin K hydroquinone, KH_2), carbon dioxide and oxygen (**Fig. 1.2**) [1]. Therefore, the continuous recycling of vitamin K 2,3-epoxide (KO) to its quinone (K) and KH_2 forms, in successive reactions catalysed by vitamin K reductases, is essential for the γ-carboxylation process (**Fig. 1.2**) [20]. Gamma-glutamyl carboxylase (GGCX) is the enzyme responsible for the conversion of Gla to Glu residues, a process concomitant with KH_2 oxidation to KO (**Fig. 1.2**) [1]. Subsequently, KO is converted back to KH_2, through a two-step reduction, using the enzymes vitamin K epoxide reductase (VKOR) and vitamin K reductase (VKR) (**Fig. 1.2**), in order that each KO molecule may be reused several times [1].

This pathway is known as the vitamin K cycle (**Fig. 1.2**) [1]. Gamma-glutamyl carboxylase is an integral membrane protein localized at the endoplasmic reticulum membrane, where luminal VKDPs carboxylation takes place as part of proteins secretion pathway [20]. Specific protein binding is accomplished by GGCX interaction with the propeptide region (with the exceptions of MGP and periostin [21]), located at the N-terminal part of the VKDPs [1]. The carboxylated VKDPs then transit from the endoplasmic reticulum, their propeptide is removed in the Golgi apparatus and proteins are secreted [20]. The γ-carboxylation of multiple Glu residues is believed to occur through a GGCX processive mechanism, in which all Glu residues are carboxylated as a result of one single binding event [20]. The γ-carboxylation of specific Glu residues within most VKDPs, induces a calcium-dependent conformational change in the Gla domain, associated with the binding of calcium ions or calcium crystals [20].

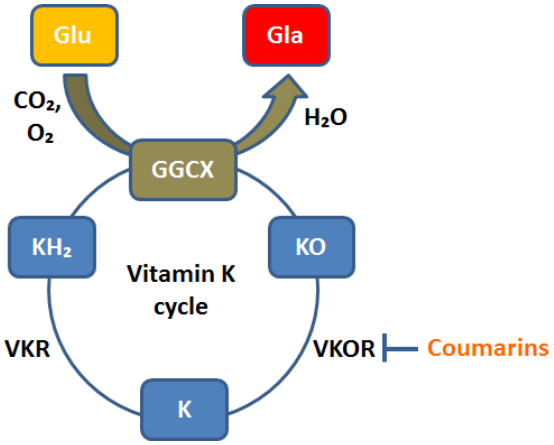

Fig. 1.2 – Vitamin K cycle. Representation of the enzymes and cofactors required for the continuous recycling of vitamin K to its hydroquinone active form (KH_2), used as cofactor by γ-carboxylase (GGCX), for the conversion of glutamate (Glu) residues into γ-carboxyglutamic acid (Gla) residues. Coumarins inhibit vitamin K epoxide reductase (VKOR). KO, vitamin K 2,3-epoxide; K, quinone form; VKR, vitamin K reductase (Adapted from Tie et al., 2015 [1]).

Vitamin K recycling may be inhibited by coumarins, such as warfarin, a drug used to treat coagulation-related problems which blocks VKOR activity (**Fig. 1.2**) [22]. As a consequence, depletion of tissue vitamin K reserves occurs, resulting in the undercarboxylation of VKDPs [3]. One result of vitamin K antagonists treatment is the increased calcification of the vasculature, which was first observed in rats injected with daily

doses of warfarin combined with vitamin K1, to prevent lethal haemorrhages [23]. The treatment resulted in vitamin K depletion in extrahepatic tissues and consequent aortic calcifications, ascribed to the inhibition of MGP γ-carboxylation [23].

In the past decade, biological functions of vitamin K other than as a cofactor of GGCX have been extensively studied [24]. In concordance, vitamin K has been described to possess significant anti-inflammatory and antioxidant actions, among other biological roles [24,25]. Vitamin K was shown to be inversely correlated with circulating markers of inflammation and suggested to suppress inflammation by decreasing the expression of genes for individual cytokines [26,27]. Vitamin K was also described to exert an anti-inflammatory effect by suppressing nuclear factor κB (NF-κB) signal transduction [28,29], a proinflammatory signalling pathway activated by proinflammatory cytokines [30]. Moreover, vitamin K has been shown to have a protective effect against oxidative stress that is independent of carboxylation and may be an alternative anti-inflammatory mechanism associated with this vitamin [31]. Oxidative stress protection by vitamin K was suggested to function through the blocking of reactive oxygen species (ROS) generation [25].

1.1.2 Physiological cartilage calcification

Calcification is a physiological process required to create mineralized tissue such as teeth and bones [3]. The majority of the mammalian skeleton bones originates from cartilage templates through a process known as endochondral ossification [32]. The transition from cartilage to bone is a multifactorial and complex process tightly coupled with chondrocyte and osteoblast differentiation, and vascularization [32].

Endochondral bone development begins with mesenchymal cells condensation from the mesoderm [32]. Bone morphogenetic proteins (BMPs), members of transforming growth factor β (TGF-β) superfamily, are essential for chondrogenic mesenchymal condensation signalling, and the transcription factor SRY-box 9 (Sox9) plays a fundamental role maintaining such condensation [32,33]. Chondrogenic differentiation proceeds stimulated by BMPs and Sox9 originating chondrocytes, the exclusive cartilage cell type, which secrete an enriched extracellular matrix (ECM) in type II collagen (Col2a1) and proteoglycans such as aggrecan [32-34]. After the formation of cartilage primordia chondrocytes undergo a rapid proliferation that drives the linear growth of bones and at a certain stage central chondrocytes follow progressive maturation [32]. Chondrocytes proliferation and maturation is regulated by

extracellular signals such as the Indian Hedgehog (IHH) and parathyroid hormone-related (PTHr) proteins, which manage the processes through negative-feedback mechanisms, and BMPs [32,35]. Chondrocytes eventually exit the cell cycle and undergo hypertrophy marked by a 10-fold increase in cell volume, ECM remodelling and terminal differentiation markers expression, including matrix metalloproteínase 13 (MMP13), type X collagen (Col10a1) and alkaline phosphatase (ALP) (**Fig. 1.3**) [36,37]. Hypertrophy is regulated by nuclear factors such as runt-related transcription factor 2 (Runx2) and pathways including β-catenin activation by canonical Wingless/Int (Wnt) signalling [32,38]. Runx2 drives the expression of MMP13 and Col10a1, and secreted MMP13 degrades Col2a1 and aggrecan (**Fig. 1.3**) [38,39]. Col10a1 deposition within the hypertrophic cartilage ECM serves as framework for subsequent calcification, which originates from matrix vesicles (MVs) secreted from chondrocytes outer plasma membranes (**Fig. 1.3**) [38,40]. These vesicles contain ALP, subsequently anchored to the Col10a1 matrix, and are secreted in response to increased calcium levels (**Fig. 1.3**) [38,40]. In the first step of mineralisation, ALP hydrolyses pyrophosphate (PPi) to inorganic phosphate (Pi) inside the MVs forming hydroxyapatite (HA) crystals ($Ca_{10}(PO_4)_6(OH)_2$) in the presence of calcium (**Fig. 1.3**) [41]. Phospholipids hydrolysis and the influx through type-III Na/Pi co-transporter may represent other sources of phosphate in the MVs, while calcium influx is believed to be regulated by annexins II, V and VI, with annexin V activity directly stimulated by the binding to Col2a1 and Col10a1 fibrils [38,42]. The second step of mineralisation is initiated by the infiltration of HA crystals into the ECM (**Fig. 1.3**) [38], a process considered to be regulated by proteins such as OC [43] secreted by hypertrophic chondrocytes and osteoblasts [44]. Chondrocyte hypertrophy is accompanied by vascular endothelial growth factor (VEGF)-mediated vascular invasion of cartilage and differentiation of the inner perichondrium (connective tissue layer that surrounds cartilage during bone formation) cells into osteoblasts [32,38]. MMP13 plays a crucial role cleaving ECM proteins within hypertrophic cartilage, facilitating vascular invasion [39]. Cartilage vascular invasion leads to further degradation of the mineralized matrix by MMP9 produced by chondroclasts, a resorptive cell type associated with capillary walls [32]. Osteoblast differentiation is regulated by extracellular signals and transcription factors such as IHH, Runx2, osterix (Osx), Wnt proteins and BMPs [32,38]. Osteoblasts secrete a type I collagen (Col1a1)-enriched ECM, in which HA fills the space between Col1a1 fibrils in the skeletal matrices, establishing the primary ossification centre to form trabecular bone [32,45]. Final stages of endochondral ossification may include chondrocyte apoptosis and generate

apoptotic bodies, which exteriorize phosphatidyl serine contributing for calcium binding, that in turn may promote more ECM mineralization in the presence of phosphate [46].

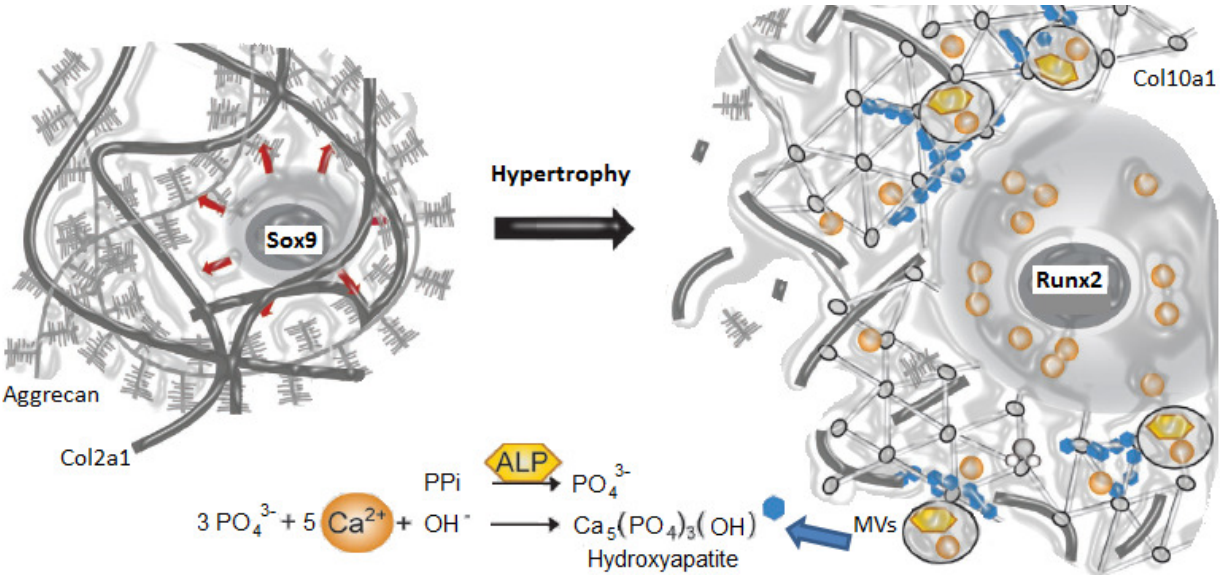

Fig. 1.3 – Chondrocytes hypertrophic differentiation and mineralization. After chondrocyte formation, regulated by Sox9, upon endochondral bone formation, cells proliferate, maturate and reach hypertrophy, marked by cell increased volume (red arrows) and extracellular matrix (ECM) remodelling. These changes are regulated by transcription factors such as runt-related transcription factor 2 (Runx2), which induces the expression of type X collagen (Col10a1) and matrix metalloproteínase 13 (MMP13). MMP13 degrades aggrecan and type II collagen (Col2a1). Col10a1 facilitates mineralization in association with matrix vesicles (MVs), that transport alkaline phosphatase (ALP). ALP dephosphorylates pyrophosphate (PPi) to phosphate (PO_4^{3-}, Pi), leading to hydroxyapatite (HA) formation (Adapted from Studer et al. 2012 [38]).

1.1.3 Pathological cartilage calcification

Calcification can also be detrimental and tissue ectopic calcification is considered pathological [3]. Uncontrolled mineralization, first considered to be a passive process occurring as a nonspecific response to tissue injury or necrosis, is now believed to naturally occur, thus it must be actively inhibited [47]. Pathological calcification can occur throughout the body, yet articular cartilage, the cardiovascular system and kidneys seem to be particularly prone to calcify [46]. Unlike physiological mineralization deposits, which only contain HA crystals, ectopic mineralization depositions may also include other basic calcium phosphate (BCP) crystals, such as octacalcium phosphate ($Ca_8(HPO_4)_2(PO_4)_4.5H_2O$) and apatite-

containing magnesium ($Ca_9Mg(PO_4)_6(OH)_2$), calcium pyrophosphate dihydrate ($Ca_2P_2O_7.2H_2O$, CPPD) or calcium oxalate (CaC_2O_4) [46,48,49], the latter more rare [48]. Cartilage deposition of BCP and CPPD crystals, is associated with acute pain and decreased mobility in destructive arthropathies involving abnormal cartilage homeostasis, such as osteoarthritis (OA) [48]. These calcifications modify the biomechanical properties of cartilage and ultimately trigger crystal-induced stress, leading to proinflammatory cytokine and MMPs production, and eventually chondrocyte apoptosis (**Fig. 1.4**) [48].

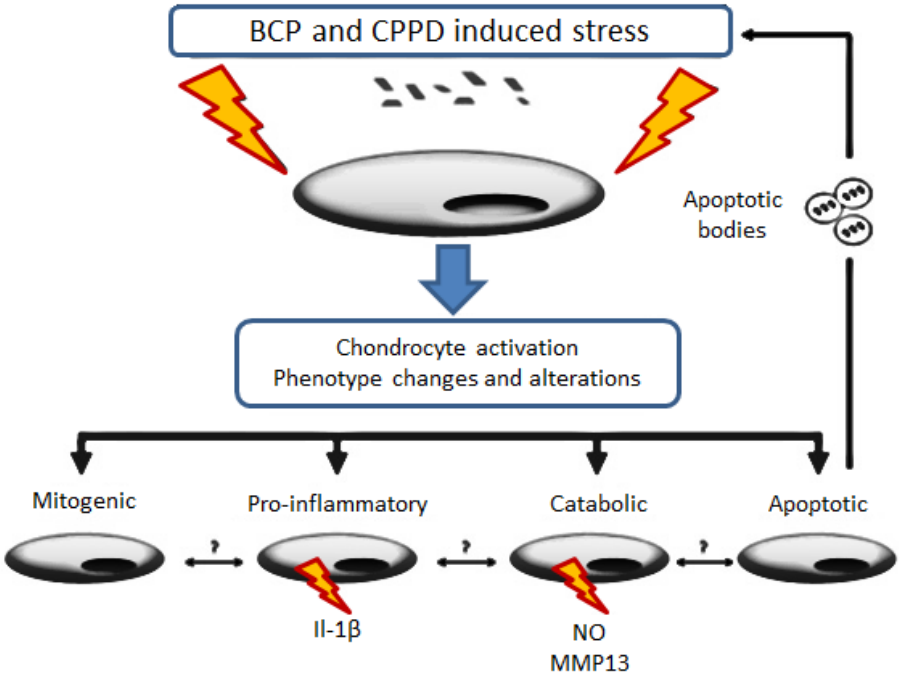

Fig. 1.4 – Effects of BCP and CPPD crystals on articular chondrocytes. Basic calcium phosphate (BCP) and calcium pyrophosphate dihydrate (CPPD) crystals activate articular chondrocytes through crystal-induced stress. Cell activation may lead to significant articular chondrocyte phenotype changes including mitogenic, proinflammatory, catabolic and apoptotic chondrocytes. Proinflammatory cells may produce cytokines, such as interleukin-1β (IL-1β). Catabolic chondrocytes can secrete prodegradative soluble factors, such as nitric oxide (NO) and proteases like matrix metalloproteínase 13 (MMP13). Apoptotic cells are able to release promineralizing apoptotic bodies prone to enhance crystal-induced stress in the vicinity of articular cartilage (Adapted from Ea et al., 2011 [50]).

The triggers for pathological calcification are still not completely understood, however, like in physiological calcification, ectopic mineralization is believed to be initiated in MVs, where calcium crystals are formed and then propagated into the ECM, inducing their further expansion [46]. Chondrocyte apoptosis and their apoptotic bodies are also believed to

contribute for cartilage ectopic mineralization (**Fig. 1.4**) [46]. Articular cartilage is supposed to be resistant to ECM mineralization due to the synthesis of calcification inhibitors and the maintenance of articular chondrocytes in a mature state, without undergoing hypertrophic differentiation [50]. Calcification can proceed when this equilibrium is disrupted by factors of multiple origins: genetics, aging, ECM modifications, imbalance between inhibitors and promineralizing factors, dysregulation of PPi and Pi metabolism, changes in extracellular calcium levels, and chondrocyte phenotype alterations including articular chondrocyte hypertrophic differentiation, apoptosis, and altered responses to growth factors, inflammatory cytokines, and mediators of inflammation [49,50].

Among ECM components, extracellular Pi and PPi concentrations are critical determinants of mineralization and the type of calcium-containing crystal accumulating in cartilage depends on their levels [49]. High PPi levels promote CPPD crystal formation and inhibit BCP crystal nucleation, whereas high Pi concentration and low PPi favour BCP crystal formation [49].

1.1.4 Vitamin K-dependent proteins associated with pathological calcification

Several gene and protein alterations have been associated with ectopic calcification [51], including impairments in the extrahepatic VKDPs OC, MGP and GRP [12,16,52]. In fact, OC and MGP are implicated in the regulation of endochondral calcification, controlling HA deposition [43,53], and deficiencies in these VKDPs interfere with endochondral bone formation, generating pathological calcification [12,52]. With the discovery of GRP, initially identified in cartilaginous tissues and containing an unprecedented high number of Gla residues [54], its potential involvement with physiological and pathological calcification was hypothesized, and studies have been conducted in the past years to further elucidate this question.

In vertebrates, all extracellular body fluids are supersaturated with calcium and phosphate, resulting in a tendency for spontaneous calcium phosphate precipitation [55]. Potent inhibitors of calcium salt precipitation and crystallization are therefore essential for survival, and indeed, a broad range of inhibitors are found in circulation [56]. Fetuin-A, a glycoprotein synthesized in the liver and secreted into circulation, is considered the most important systemic inhibitor of soft-tissue calcification [57]. Fetuin-A binds and sequesters

mineral nuclei, forming soluble colloidal high molecular weight calciprotein particles (CPP), inhibiting crystal growth and aggregation [57,58]. This mechanism is believed to facilitate the clearance of calcium crystals from extracellular fluids, that otherwise could seed and possibly promote ectopic calcification [58]. Enhanced CPP levels are encountered upon increased bone resorption events, where calcium phosphate crystal nuclei are believed to be formed in a bone-remodelling compartment (BRC) and released into the circulation, accompanied by the complex formation in the BRC [59]. Notably, BRC structures were also identified in the vasculature [60], suggesting that calcium crystals and CPP may be formed in other locations, such as sites of pathological calcification. Besides fetuin-A, small extrahepatic VKDPs have been discovered acting as potent calcification inhibitors, namely OC and MGP [56]. Interestingly, a circulating MGP-containing CPP was described and suggested to inhibit calcium phosphate crystal precipitation [61], indicating that both fetuin-A and MGP may function in association. In contrast to fetuin-A, OC and MGP are local inhibitors of calcification, being synthetized in the tissues in which they exert their function [56]. Osteocalcin is primarily synthesized by osteoblasts, and OC-deficient mice show increased bone mineral content [62]. Matrix Gla protein is majorly synthesized by chondrocytes and vascular smooth muscle cells (VSMCs), and MGP-deficient mice show impaired growth, resulting from excessive growth plate calcification, and massive calcification of the arterial tunica media [12]. In agreement with its local inhibitory activity, and in contrast to MGP, OC is not able to inhibit ECM calcification in arteries [63]. An interesting question is why fetuin-A alone is unable to stop calcification of the former mentioned tissues. A possible answer to this issue was provided by studies which demonstrated that fetuin-A is too large to penetrate the luminal space within collagen and elastin fibrils while small calcification inhibitors, such as OC and MGP, may penetrate the fibrils and prevent mineral growth [43]. This finding could explain why elastin fibrils are prone to calcify, especially during vitamin K insufficiency, and evidenced the vital importance of vitamin K in the prevention of soft-tissue calcification [43].

The calcification inhibitory effect of MGP is partly based on its direct calcium crystals binding ability through the Gla residues [64]. Accordingly, Keutel disease, caused by mutations in the human MGP gene resulting in non-functional protein, originates, among other features, cartilage calcification similar to that of MGP-deficient mice [65]. Transgenic mice with a MGP mutant that could not be carboxylated, also acquired a similar phenotype [63]. Moreover, MGP is described to affect osteogenesis, chondrocyte maturation and ECM calcification inhibition, by interacting with BMP2, a potent inducer of bone formation in both

skeletal and soft tissues [13]. Matrix Gla protein regulates BMP2 activity via binding through its Gla residues, emphasizing the need of MGP γ-carboxylation in bone and cartilage formation [66]. In concordance, the ectopic calcification of connective tissues observed in pseudoxanthoma elasticum (PXE), an autosomal recessive disease [67], is believed to be originated, in part, from local tissue deficiency in MGP γ-carboxylation [68]. Also, increased circulating levels of undercarboxylated MGP (ucMGP), possibly reflecting local synthesis, have been proposed to serve as a predictor for vascular calcifications [69]. A striking difference between Keutel syndrome and MGP-deficient animals is that the effects on the vasculature are less prominent in human, suggesting that other calcification inhibitors could form a backup system for MGP deficiency in humans [56]. Gla-rich protein, the most recently discovered VKDP [54], may represent such a calcification inhibitor. Although the function of GRP in humans has not yet been completely established, GRP has been associated to sites of pathological calcification in human [14-16] and proposed as a modulator of calcium availability [14,15] and a calcification inhibitor in the cardiovascular system, depending on its γ-carboxylation status [16]. These findings highlight the possibility of GRP association to other ectopic calcification-related pathologies, such as OA.

1.1.4.1 Gla-rich protein

Gla-rich protein was originally identified in Adriatic sturgeon calcified cartilage extracts, when analysing OC and MGP protein content [54]. Gla-rich protein revealed to be a small secreted protein containing 16 Gla residues in sturgeon (**Fig. 1.5**), the highest Gla percent of any known protein, and it was therefore named Gla-rich protein [54]. This high content of Gla residues present in GRP is in clear contrast with the 3 to 5 Gla residues present in OC and MGP [70,71]. GRP primary sequence analyses revealed a high content of charge density (36 negative and 16 positive with a total of 20 net negative), yet it is insoluble at neutral pH [54].

Gla-rich protein orthologs were identified in all taxonomic groups of vertebrates, and a paralog (GRP2) in bony fish [54,72,73]. The protein sequence of this VKDP was shown to be highly conserved, with 78% identity between sturgeon and human GRP (**Fig. 1.5**) and no significant sequence homology was identified between GRP and the Gla-containing region of any presently known VKDP [54]. Gla-rich protein was verified to contain a transmembrane signal peptide of 26-27 amino acids, a propeptide with 38-39 amino acids containing GGCX

recognition site, an AXXF motif (first observed in MGP, serving as a proteolytic cleavage site), a furin-like cleavage site (for propeptide cleavage at the RXXR polybasic site), and a mature protein with dimensions between 67 and 75 amino acids, depending on the species, containing 14 highly conserved Glu residues, each of them γ-carboxylated in sturgeon [54] (**Fig. 1.5**). The high level of evolutionary conservation and unprecedented number of Gla residues verified for GRP, pointed for a fundamental role of this protein, most likely related with the regulation of calcium in the extracellular environment [54].

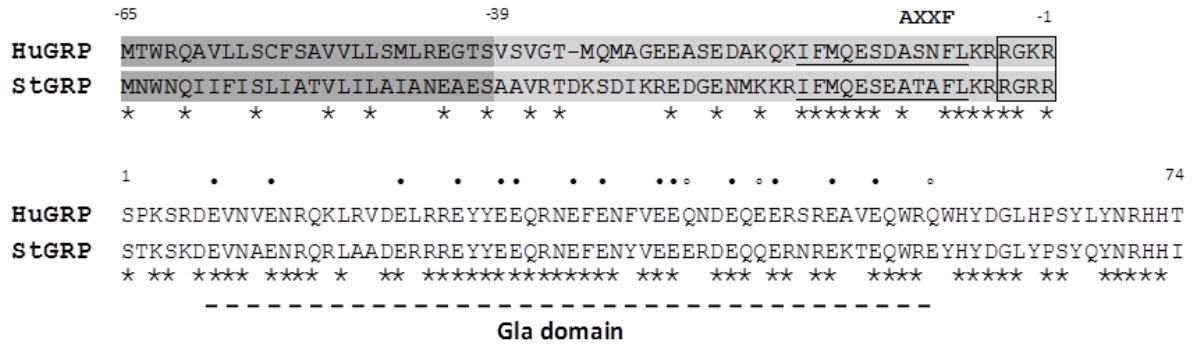

Fig. 1.5 – Alignment of complete human (HuGRP) and sturgeon (StGRP) GRP deduced proteins showing conserved residues in particular positions and highlighting important functional domains and motifs. Stars indicate identical residues; the underlined sequences, γ-glutamyl carboxylase (GGCX) putative recognition site; AXXF motif is evidenced; rectangle, furin-like proteolytic site (RXXR); black dots, conserved putative γ-carboxylated Glu residues; white dots, non-conserved putative γ-carboxylated Glu residues; Gla domain is highlighted with a dashed line; signal peptide is shown in dark grey while propeptide in light grey. First residue of mature protein is assigned as number 1 and signal peptide, propeptide and mature protein are indicated accordingly (Adapted from Viegas et al., 2008 [54]).

Gla-rich protein mRNA was found in several skeleton-associated tissues and soft tissues in sturgeon, although its highest expression was seen in cartilage, with GRP expressing cells including chondrocytes, chondroblasts, osteoblasts and osteocytes [54]. In rat, GRP was expressed in chondrocytes and bone cells suggesting a widespread role throughout skeletal formation [54].

In the same year that GRP was identified in sturgeon cartilage extracts, it was also described by other group as a novel transcript in human fetal growth plate cartilage, which was termed unique cartilage matrix associated protein (UCMA) [74]. Using RNA *in situ* hybridization, immunohistochemistry analysis and a mouse model, the same group hypothesized that GRP could be a secretory marker for resting chondrocytes and suggested an

important function in the early phase of chondrocyte differentiation [74]. Further, GRP was suggested as cartilage specific and to be involved in the negative control of osteogenic differentiation of osteochondrogenic precursor cells in the peripheral zones of fetal cartilage and at the cartilage-bone interface [75]. Accordingly, GRP was shown to be downregulated in mice chondrogenic cells by BMP2, associated to chondrocyte maturation towards a hypertrophic phenotype, and to downregulate ALP activity and OC expression in mice pre-osteoblastic cells [75]. Unique cartilage matrix associated protein nomenclature was later altered to upper zone of growth plate and cartilage matrix associated protein (National centre for biotechnology information, NCBI, database). Gla-rich protein downregulation by BMP2 was also verified in mice chondrocytes in other study [76], supporting the previous results. Yet, recent data showed GRP upregulation in response to Runx2 and Osx, promoting osteoblast differentiation and nodule formation in mice pre-osteoblastic cell cultures [77]. Gla-rich protein knocked-down studies in zebrafish also supported a role for GRP in cartilage development and initial skeletal formation, with reduction of Col2a1 and aggrecan content in cartilage, and severe growth retardation and skeletal defects [72]. Interestingly, this phenotype could be reproduced by treating zebrafish with warfarin, suggesting that the observed effect was ascribed to the inhibition of GRP γ-carboxylation, since VKDPs like MGP and OC are only expressed at later time points of zebrafish skeletal development [72]. Surprisingly, GRP-deficient mice did not display a clear phenotype during normal development, although GRP involvement in skeletal homeostasis and association with challenging conditions, such as ageing or disease, were not addressed [78]. In human, GRP has been associated to pathological situations involving ectopic calcification. The protein was found co-localized with mineral deposits in skin of diagnosed patients with dermatomyositis and PXE [14], in the vascular system of patients with chronic kidney disease (CKD) [14], in breast carcinomas [15], and in aortic valves in patients with calcified aortic valve disease (CAVD) [16]. These associations supported GRP role as modulator of calcium availability in the ECM [14,15]. Moreover, although both carboxylated (cGRP) and non-carboxylated GRP forms were shown to have *in vitro* BCP crystals binding capacity [15] and both cGRP and undercarboxylated GRP (ucGRP) accumulate at sites of pathological calcification in human carcinomas and calcified aortic valves [15,16], ucGRP was the prevalent form associated to pathological tissues suggesting a role dependent of its γ-carboxylation status. In concordance, cGRP, and not ucGRP, was proposed as an inhibitor of calcification in the cardiovascular system, a function that might be associated with the prevention of calcium-induced signalling pathways and direct mineral binding [16]. This study also shown the presence of GRP in extracellular

vesicles (EVs) isolated from cultured aortic segments media, entities whose mineralization capacity is highly related with vascular calcification [79], and it was hypothesized that GRP could be associated with a fetuin-A-MGP calcification inhibitory system detected in the calcified areas [16]. Altogether, the existing data regarding GRP biological roles and molecular mechanisms of action reinforce the need for additional characterization of GRP regarding human pathological conditions related to ectopic calcification, such as OA.

The entire GRP protein sequence is originated from an RNA sequence that contains 5 exons, and four alternatively spliced transcripts of GRP gene were identified in mice - GRP-F1, F2, F3, and F4 - differing by exon 2, exon 4, or both (**Fig. 1.6**) [76]. The same variants were also detected in zebrafish [72,73], however, no splice variants were yet reported in human. In mice, these variants were associated to early stages of chondrogenesis and suggested to be possibly implicated in skeletal pathologies in case of an imbalanced expression [76]. GRP-F1 and -F3, the first corresponding to the full length protein and the second lacking exon 4 (**Fig. 1.6**), were shown to be secreted, whereas GRP-F2 and -F4, both lacking exon 2 and therefore a portion of the signal peptide sequence (**Fig. 1.6**), were shown to accumulate in the cells [76]. In addition, GRP-F4 also lacks exon 4 (**Fig. 1.6**) [76].

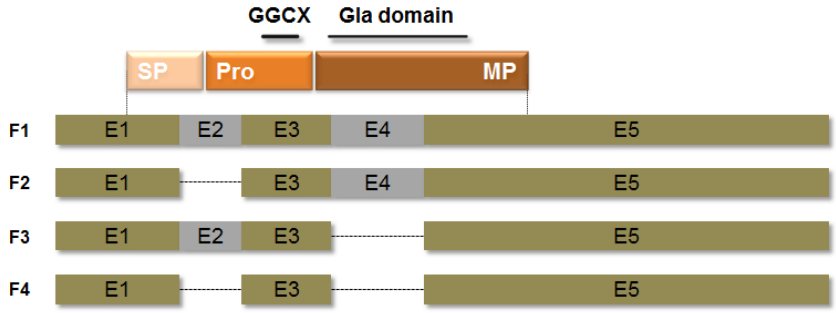

Fig. 1.6 – Four alternatively spliced variants of GRP described to exist in mouse and zebrafish. The RNA structure of the four variants is represented (F1-F4). Exons (E) 2 and 4 are deleted in GRP-F2 and GRP-F3, respectively, and both in GRP-F4. SP, signal peptide; PP, propeptide; MP, mature peptide; GGCX, γ-carboxylase recognition site (Adapted from Le Jeune et al., 2009 [76] by Dr. Marta Rafael).

1.1.5. Vitamin K and calcification-related VKDPs involvement with osteoarthritis

Osteoarthritis is a whole-joint disease characterized by cartilage destruction with cartilage mineralization, subchondral bone modifications and mild synovial inflammation [80], which will be further addressed in the following section. Currently, there is an urgent need for reliable, quantitative and dynamic tests to detect early damage in OA and measure the progress of treatments targeted against joint destruction [81]. Vitamin K and the extra-hepatic VKDPs OC, MGP and GRP represent interesting candidate biomarkers for OA, due to their determinant role in skeletal metabolism and associations with ectopic calcification [3,56].

Several studies have in fact evidenced that subclinical vitamin K levels are associated with increased risk of knee OA development [82-84]. Also, vitamin K2 was suggested to possibly affect bone turnover when medial condyles, showing advanced knee OA, were shown to possess lower menaquinone levels comparing to lateral condyles, showing less advanced OA [85]. Interestingly, vitamin K association with OA may not be restricted to calcification events since this vitamin has been proposed to exert a protective effect against inflammatory events and oxidative stress [24-26,28,29], two features associated with OA progression [86-88].

The absence of functional MGP in animal models has been shown to originate similar processes as those occurring in OA. A study attributed the abnormal growth plate mineralization observed in chicken hypertrophic chondrocyte cultures to impaired MGP synthesis caused by warfarin treatment [89]. The last process can lead to endochondral ossification in a similar way as osteophytes are formed (bony outgrowths occurring at the joint margins in advanced stages of OA) [89]. Also, chondrocytic abnormalities including aberrant chondrocyte proliferation, apoptosis, and defective chondrocyte maturation were observed in mice cell cultures underexpressing MGP [90] and in the MGP-deficient mice [12]. In addition, the lack of organized chondrocyte columns present in the last model [12] are similar to chondrocyte abnormalities occurring in OA [91]. Moreover, osteoarthritic chondrocytes have been demonstrated to produce primarily ucMGP while normal chondrocytes produce functional γ-carboxylated MGP (cMGP) [92]. Interestingly, the last study suggested that MGP lack of function could be associated with pathological cartilage mineralization, and MGP calcification inhibition was proposed to occur via a fetuin-A-MGP complex present in chondrocyte-released MVs in control conditions [92]. Thus, it is most likely that insufficient functional MGP, associated with inadequate concentrations of vitamin K, potentially play a role in OA [92,93]. Vitamin K metabolism deficiency may also affect OC, and in fact, serum undercarboxylated OC (ucOC) is associated with OA and considered a

biomarker for this degenerative disease [94]. Notably, the former association was related with inflammatory processes. A significant correlation was observed between serum ucOC and serum hyaluronic acid, a marker for synovitis, the clinical term for the synovial membrane inflammation occurring in OA [88], suggesting that vitamin K metabolism may be associated with synovitis in patients with knee OA [94]. Moreover, the combined assessment of ucMGP in serum and synovial fluid was suggested as a potential joint inflammatory marker in arthritis patients [95]. Although a precise mechanism of action was not proposed in the last study, it was hypothesized that the synovial inflammation might impair the passage of ucMGP produced by local chondrocytes into circulation, resulting in higher synovial and lower serum ucMGP levels found in inflammatory arthritis [95].

Altogether, the existing associations between vitamin K and the extra-hepatic VKDPs OC and MGP, not only regarding OA pathological calcification but also inflammatory processes, in addition with the notion that other calcification inhibitors may be required to backup MGP functions in human [56], highlighted a possible association of GRP with OA.

1.2 Osteoarthritis

Osteoarthritis is the prevalent form of arthritis, the general term applied to degenerative joint disorders [96]. OA is a chronic health condition and a leading cause of pain and disability among adults, with a high impact worldwide [97]. As the population ages, along with the increasing prevalence of obesity, it is expected that the burden of OA on the population, healthcare system and economy will continue to increase, especially if no major improvements in managing the disease are achieved [96]. Osteoarthritis predominantly affects weight bearing joints like the knee, hip or ankle [98]. Common OA features are articular cartilage degradation and loss, joint space narrowing, subchondral bone changes, osteophytes formation, thickening of the joints, synovial membrane inflammation and pathological calcification [99,100]. Current diagnosis of OA still relays on routine radiography and clinical manifestations, which are unable to evaluate the molecular changes occurring in early stages of OA [81]. Therefore, predicting the disease progression is a very challenging task [81]. Moreover, there are currently no disease modifying OA drugs (DMOADs) [81] and traditional treatments are based on symptom control, trying to post-pone chirurgical interventions [96]. In order to improve the management of OA, it is crucial to enrich the

knowledge on the pathogenesis of the disease, and the wealth of information relating new OA biomarkers with clinical outcomes may permit an earlier diagnosis and better means for accessing the effects of new therapeutic interventions [96,101].

1.2.1 Osteoarthritis epidemiology and burden

Osteoarthritis is a heterogeneous disease characterized by the failure of a synovial joint [101]. Multiple risk factors can affect the development and progression of OA including age, sex, obesity, family history or trauma [97]. When the origin of OA is idiopathic, occurring in the absence of an obvious abnormality, it is termed primary OA, whereas if resulting from trauma or diseases OA is considered secondary [102].

Before the age of 40 the incidence of OA is low and frequently secondary, associated with trauma [103]. The prevalence of OA increases between 40 and 60 years old, with a linear increase in its incidence in later ages [103]. Global estimates indicate that 9.6% of men and 18% of women over 60 years old have symptomatic OA [103]. Osteoarthritis is the first cause of permanent job incapacity, one of the most frequent motifs of inability in the elderly, and one of the most common reasons for primary care visits [104]. USA studies state that OA is responsible for 4 million hospitalizations and the loss of 68 million labour days per year [105]. Also, a survey performed in England based on a 72% response rate from over 26.000 adults with more than 50 years old, showed that half of the sample presented OA [106]. In Portugal, it is estimated that 6% of the population is affected by this joint disorder [103]. Estimates of OA burden need to take into consideration economic, social and/or psychological costs or losses to the patient, family and/or society [103]. In USA alone, the financial burden of OA has been estimated to be $81 billion in medical costs and $128 billion in total cost per year [101]. In Portugal, no published data on specific direct and indirect costs was identified to allow any comparisons, however rheumatic diseases are pointed as the first cause for early retirement [103].

Knee OA is the prevalent form of the disease [97] and the risk of mobility disability attributable to it is greater than due to any other medical condition in people aged over 65 [101]. Recent estimates suggest that the global burden of knee OA affects approximately 250 million people [101]. In Portugal, studies estimate that the incidence of knee OA corresponds to 3.8% of the population and in adults over 40 years old, the prevalence raises to 56.9% in men and 57.7% in women [103].

Age is the strongest predictor of OA development with 64% of the affected population having more than 60 years old [101]. This outcome is mainly consequence of a degenerative process occurring in stable articular cartilage phenotype around the age of 40 in humans, where chondrocytes reach terminal differentiation [107]. Females also present higher risk of developing the disease, and although the reason for these differences is unclear it is suggested to be related with high estrogen levels [99]. In concordance, articular chondrocytes possess functional estrogen receptors and there is evidence that estrogen can upregulate proteoglycan synthesis [99]. Obesity is a key risk factor for knee OA, increasing its incidence three-fold and suggested to accelerate the progression of the disease [97]. Interestingly, obesity appears to affect OA not only because of biomechanical overloading that favours subsequent cartilage degeneration, but also due to a metabolic/inflammatory pathway known as the metabolic syndrome (MetS) [97]. Metabolic syndrome is a cluster of cardiometabolic disorders that result from the increasing prevalence of obesity, having as major components insulin resistance, central obesity, dyslipidaemia (abnormal amounts of lipids in circulation) and hypertension [108]. Although there is still much to clarify regarding the association between MetS and OA, abnormal loading is associated with inflammatory and metabolic imbalances in OA in part because it triggers the same signalling pathways as those induced by inflammatory cytokines [91]. In fact, a clinical study involving 653 participants revealed that in such group almost half of the association between body mass index (BMI) and knee OA was accompanied by high serum leptin levels [109]. The authors suggested that the adipokine leptin may play an important role in the development of knee OA, possibly through an immune-mediated or inflammatory process [109]. In agreement with the existence of associations between OA and MetS, risk factors that contribute to this syndrome are generally considered risk factors for rheumatic diseases, in particular OA [110]. A common feature among OA patients is the existence of comorbidities (presence of one or more additional disorders), which generally increase the impact of OA [103]. Genetic predisposition is also a risk factor for OA and the influence of genetic factors for disease heritability is comprehended between 39 to 65% [111]. Among secondary OA, traumatic joint injury is the major risk factor for OA, particularly at the knee [97]. Diseases that cause inflammation of the joint, such as rheumatoid arthritis (RA), can also increase the risk of developing OA later in life [102].

1.2.2 Pathophysiology of osteoarthritis

Synovial joints are responsible for the movement of articulating bones [111]. They contain articular cartilage, subchondral bone, ligaments, a synovial cavity between bones filled with synovial fluid, a capsule of dense fibrous connective tissue attached to the articulating bones and composed by an outer fibrous membrane and an inner synovial membrane, and periarticular muscles (**Fig. 1.7**) [111].

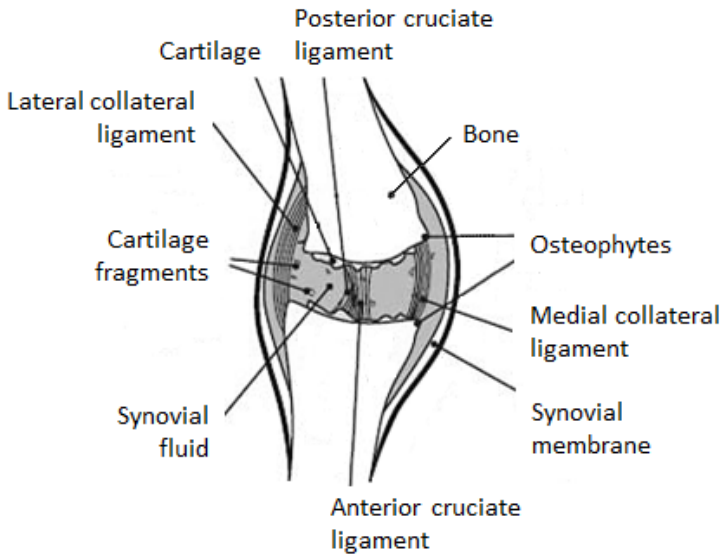

Fig. 1.7 – Knee joint with severe osteoarthritis. Articular cartilage becomes disrupted and fragments are released into the synovial fluid, osteophytes grow at the edges of bone and the synovial fluid increases its volume (Adapted from Yavorskyy et al., 2008 [112]).

Joint surfaces are supported by distinct anatomical layers from which articular cartilage is the most superficial (**Fig.1.8**) [111]. In healthy conditions, chondrocytes are organized within a three-dimensional matrix, without any signs of proliferation [111]. Articular cartilage acts as a low-friction, load-bearing surface, experiencing a range of static and dynamic forces which are absorbed by cartilage ECM and subsequently dissipated and transmitted to the chondrocytes [111]. The biomechanical properties of articular cartilage are ensured by the spatial organization of its ECM, whose main constituents are collagens and proteoglycans, in particular Col2a1 and aggrecan, responsible for tensile strength and compressive resistance, respectively [113]. Articular cartilage is divided in a superficial tangential zone with flattened chondrocytes and very few collagen fibrils, a middle zone with thicker collagen fibrils and spherical chondrocytes, and a deep zone, in which collagen fibrils

are thickest and chondrocytes are ellipsoid, perpendicular to the articular surface and grouped in radially arranged columns (**Fig. 1.8**) [111]. The transition between the compliant articular cartilage and stiff subchondral bone is provided by calcified cartilage (**Fig. 1.8**), characterized by typical hypertrophic chondrocytes, able to mineralize their ECM and expressing high levels of Col10a1 [111]. The two types of cartilage are separated by a thick bundle of collagen fibrils termed tidemark (**Fig. 1.8**) [111]. Since cartilage is an avascular tissue, chondrocytes live in a hypoxic environment [91]. Oxygen and nutrients come from the vascular supply in the joint capsule, synovial membrane and subchondral bone [91]. The subchondral bone not only absorbs and distributes loads but is involved in the metabolism of the deeper layers of the articular cartilage [111].

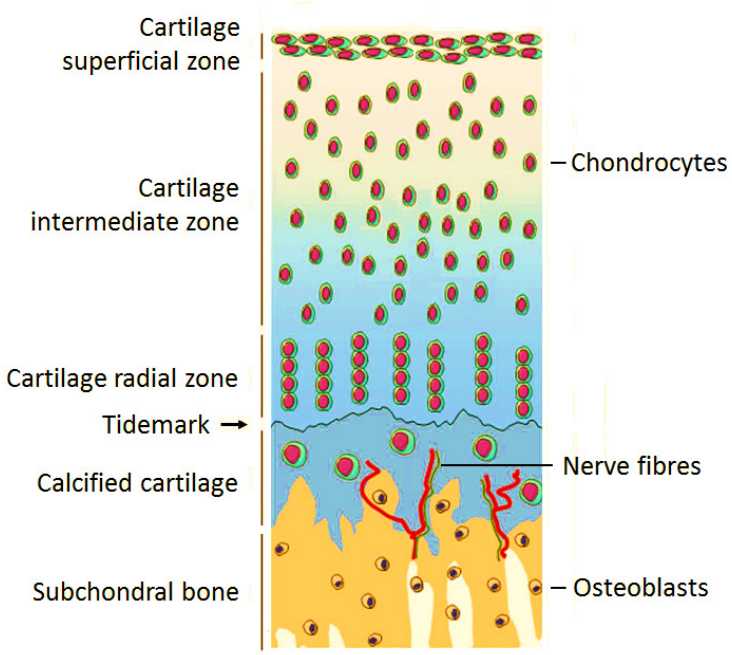

Fig. 1.8 – Schematic representation of cartilage organization in healthy joints before cartilage damage. In each cartilage zone (calcified, radial, intermediate and superficial), chondrocytes have a distinct phenotype and organization. The tidemark separates the non-calcified from the calcified cartilage. The calcified cartilage zone differs from the other cartilage zones by the mineralization of its extracellular matrix, and the presence of vessels (red) and nerve fibres (green) that originate from the subchondral bone (Adapted from Houarda et al., 2013 [91]).

Osteoarthritis is generally the result of abnormal biomechanics, secondary inflammation or enforced inactivity [98], which majorly affect cartilage joint surface areas [91]. As in endochondral ossification, the critical event in OA is based on ECM remodelling

and OA is believed to be a consequence of chondrocytes failure in recovering from disturbed catabolic and anabolic processes [111].

Upon an abnormal stimulus, quiescent chondrocytes undergo a phenotypic shift and become activated, characterized by cell proliferation, cluster formation and increased production of matrix proteins and matrix-degrading enzymes (**Fig. 1.9**) [114]. Chondrocyte differentiation and remodelling are, amongst others, regulated by BMPs, thus impairments in these proteins or their pathways may be involved in chondrocyte hypertrophy and ECM degradation, mainly due to the elevated production of MMP13 [115]. In fact, the main cartilage matrix-degrading enzymes identified in OA are zinc dependent MMPs and ADAMTSs (short for A disintegrin and metalloproteínase with thrombospondin motifs) [91]. Chondrocytes sense mechanical stress and changes in the pericellular matrix, largely through receptors for ECM components [91]. In particular, aggrecan cleavage by ADAMTS5 is believed to uncover a specific receptor to which native Col2a1 binds as a ligand, preferentially inducing and activating MMP13, that in turn will originate Col2a1 remodelling and degradation [116]. The bioactive peptides arising from Col2a1 degradation will boost OA development, stimulating the production by chondrocytes of more MMPs and inflammatory cytokines, such as interleukin 1β (IL-1β) and tumour necrosis factor α (TNF-α) [91]. The presence of IL-1β and TNF-α induce the production of prostaglandin E2 (PGE2) and reactive oxygen species such as nitric oxide (NO), involved in the induction of inflammatory mediators [91]. Cartilage matrix degradation products can also stimulate NF-κB transcription factors, that control the expression of downstream target genes such as MMP13, ADAMTSs, IL-1β, NO synthase (NOS) and cyclooxygenase 2 (COX2), the last involved in PGE2 production [91]. NF-κB also influences the regulated accumulation and remodelling of ECM proteins and has indirect positive effects on downstream regulators of terminal chondrocyte differentiation including β-catenin and Runx2, which are believed to lead to premature chondrocyte differentiation [117]. In fact, the diminished capacity to limit Wnt/β-catenin signalling has been suggested to contribute to cartilage loss [118]. In both OA and RA, the inappropriate regulation of NF-κB transcription factors is one of the major causes of setting an inflammatory response [111]. NF-κB transcription factors and their immediate upstream signalling components represent potential therapeutic targets in OA, because of their pivotal roles in most proinflammatory processes and also in important aspects of chondrocyte differentiation [111]. Adipokines from the white adipose tissue can also act as an endocrine organ, contributing for the induction of inflammatory processes [91]. Interestingly, the presence of adipokines in OA is not only resultant from fat tissue but also from joint cells

including chondrocytes (**Fig. 1.9**), induced by an inflammatory stimuli [119]. In turn, adipokines may induce chondrocytes to enhance the expression of MMPs, NOS and cytokines [91]. Cartilage matrix degradation products are therefore believed to stimulate or feedback amplify further ECM destruction (**Fig. 1.9**) [91]. Chondrocytes at first become activated to try keeping the balance between anabolic and catabolic factors, but this triggers improper maturation, leading to chondrocyte hypertrophy, followed by cartilage degradation, mineralization and vascularization, and the appearance of foci of endochondral ossification such as osteophytes (**Fig. 1.9**) [91]. Cartilage superficial tangential zone gets fibrillated and loses the characteristic flattened chondrocytes, matrix loss occurs and fissures appear (**Fig. 1.9**) [111]. Hypertrophic chondrocytes express genes encoding Runx2, MMP13, and Col10a1, which can all be detected in OA cartilage [91]. Also, there is evidence of cell death and formation of chondrons (disoriented chondrocytes) (**Fig. 1.9**) [111].

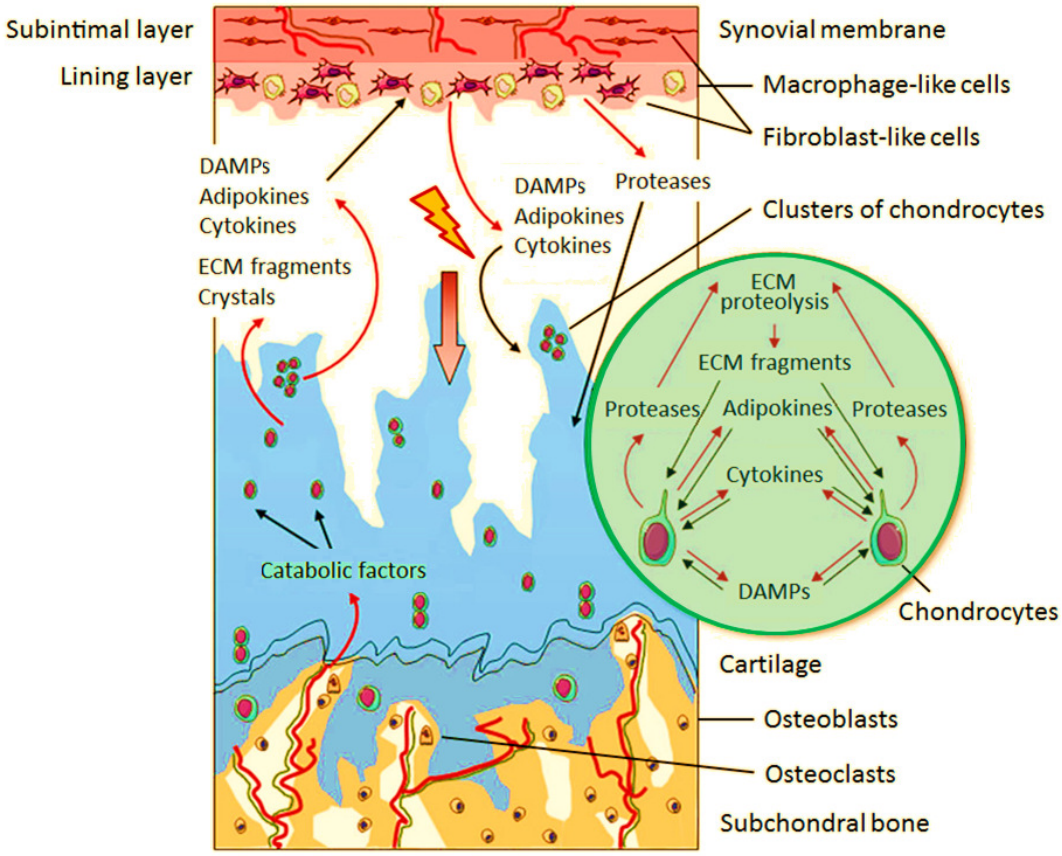

Fig. 1.9 – Schematic representation of joint alterations in osteoarthritis. Cartilage extracellular matrix (ECM) progressively disappears accompanied by phenotypic modifications, including the formation of clusters, catalysis activation, hypertrophic differentiation and chondrocyte loss. Subchondral bone remodelling occurs with the development of vessels (red) located in

vascular channels, which also contain osteoblasts, osteoclasts, and sensory nerves (black). In response to several stimuli, including catabolic factors coming from the subchondral bone, chondrocytes modify their phenotype and express a subset of factors, such as cytokines, damage-associated molecular patterns (DAMPs), and adipokines. Calcium crystals are also released. All these mediators initiate a vicious circle of cartilage degradation and reach the synovial membrane, provoking an inflammatory process with the production of factors by synovial macrophage-like and fibroblast-like cells, which promote inflammation in the synovial membrane and participate in cartilage damage (Adapted from Houarda et al., 2013 [91]).

As a consequence of cartilage degradation, the joint space narrows between adjacent bones [120]. Subchondral bone remodelling takes place particularly in regions beneath articular cartilage damage and is accompanied by increased osteoclast activity, associated to bone resorption and resulting in bone loss [111]. In fact, the imbalance between bone formation and resorption is frequently observed in OA [121]. Ultimately, OA may be considered as a disorganized recapitulation of the maturational phenotype seen in endochondral ossification [91].

The synovial fluid is a viscous ultrafiltrate of plasma with high glycoprotein and hyaluronic acid content, acting as a lubricant, shock absorbing and source of biochemical nutrients to the avascular articular surfaces [122]. Upon OA, molecules and calcium crystals released from the damaged cartilage ECM into the synovial fluid are believed to promote the release of proteolytic enzymes by synovial cells and the recruitment of inflammatory cells into the joint (**Fig. 1.9**) [91]. These secreted damage-associated molecular patterns (DAMPs), also called alarmins, act as ligands of toll-like receptors (TLR) activating inflammatory and catabolic events in articular cartilage and other joint tissues [91,123]. Chondrocytes express TLRs and this expression is upregulated within an osteoarthritic scenario, induced by inflammatory stimuli [124]. Toll-like receptors activation lead to increased expression of downstream inflammation-related genes including MMPs and NOS, via NF-κB signalling [91]. Plasma proteins present in the osteoarthritic synovial fluid may function as DAMPs and thereby contribute to a low-grade inflammatory state [91].

The synovial membrane provides a deformable packing that allows the movement of adjacent tissues [125]. Additionally, the cellular constituents of this tissue are the major source of synovial fluid components, contributing to the unique functional properties of articular surfaces and modulating chondrocytes activity [88]. The synovial membrane is semipermeable controlling the molecular traffic within the joint space, maintaining the composition of the synovial fluid and able to remove the products of chondrocytic

metabolism and articular matrix turnover [88]. Healthy synovial membranes consist of a distinct intimal lining layer of 1-2 cells thickness and a synovial sublining layer (**Fig. 1.9**) [125]. The major cell types composing this tissue are macrophage-like cells, also termed type A synoviocytes, and fibroblast-like cells, or type B synoviocytes (**Fig. 1.9**) [126]. The subintimal layer contains scattered blood vessels, type A synoviocytes, type B synoviocytes, few fat cells and lymphocytes [125]. The structure of the former layer can be of three types: areolar, adipose and fibrous (**Fig. 1.10**), and it is possible to detect the three types within the same membrane both in healthy or pathological conditions [125]. The areolar type (**Fig. 1.10**, **A**) is often crimped into folds, which may disappear when stretched, or may form projections, and contains capillaries immediately beneath the lining cells. The adipose type (**Fig. 1.10**, **B**) is found mainly in fat pads, may be avascular and may lie directly on adipocytes, but it is often separated by a band of collagen-rich substratum. The fibrous type (**Fig. 1.10**, **C**) usually consists of fibrous tissue, such as ligaments or tendons, on which lies an intermittent layer of cells [125]. Lubricin and hyaluronic acid are two of the most important molecules produced by the synovial lining cells, helping protecting and maintaining the integrity of articular cartilage surfaces and reducing friction by providing boundary lubrication at the articular surface [127]. In addition, lubricin reduces the pathologic deposition of proteins at the articular surface [88]. Under healthy conditions, high molecular weight molecules like lubricin and hyaluronic acid are not readily permeable, while small molecules like growth factors and cytokines easily diffuse through the membrane [88]. Macrophage-like synoviocytes express markers of hematopoietic origin consistent with the monocyte-macrophage lineage, such as cluster of differentiation 68 (CD68), and are derived from the bone marrow [128,129]. They migrate to the synovial membrane and become resident cells, although it is not certain if differentiation occurs *in situ* or prior to arrival [129]. Their phenotype is similar to other tissue-resident macrophage populations, they are able to actively phagocyte cell debris and wastes in the joint cavity, and are terminally differentiated with little capacity to proliferate [129]. Fibroblast-like synoviocytes are mesenchymal cells that display many characteristics of fibroblasts, including the expression of collagens type IV and V, and vimentin [129].

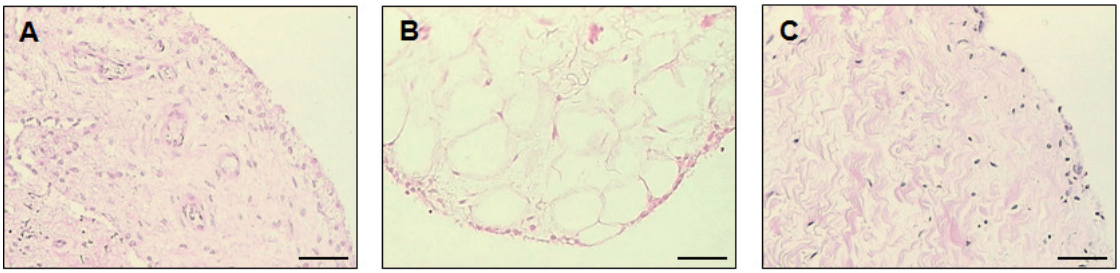

Fig. 1.10 – Healthy human synovial membrane subintimal layer types: Areolar tissue (**A**), adipose tissue (**B**) and fibrous tissue (**C**). Tissue sections were stained with hematoxylin and eosin. Scale bars represents 100 μm (Adapted from Smith, 2011 [125]).

In the setting of OA, cytokines, adipokines and DAMPs attach to the synovial membrane (**Fig. 1.9**) through TLRs present in both type A and B synoviocytes, and initiate synovitis [88]. Synovitis is characterized by increased vascularization, hyperplasia of the lining cells, infiltration of inflammatory cells, and formation of perivascular lymphoid aggregates (**Fig. 1.11**) [87]. Macrophages, T lymphocytes and mast cells are the most abundant cells infiltrating the synovial membrane, although dendritic cells, plasma cells and B lymphocytes may also be present (**Fig. 1.11**) [130]. Upon hyperplasia and infiltration of inflammatory cells, the former promoted by type B synoviocytes that express adhesion molecules able to trap macrophages and lymphocytes [125], the permeability of the membrane is altered [88]. This change is believed to contribute for the decreased concentrations of hyaluronic acid and lubricin observed in the synovial fluid, which worsen cartilage integrity and raise the concentrations of hyaluronic acid in serum [88]. The complement cascade is also one of the major effector mechanisms of immune system activation in OA, complementing the ability of antibodies and phagocytic cells to clear pathogens from the joints [88,131]. Activated type A synoviocytes play a fundamental role as catabolic mediator producers and contribute to the formation of osteophytes, mainly due to the synthesis of TGF-β family members, such as BMP2 [132]. The ensuing synovial cellular response originated by cytokines, adipokines or DAMPs (**Fig. 1.9**), culminates in the activation of specific transcription factors, with NF-κB playing a prominent role [88,114]. The synovial membrane becomes a source of proinflammatory and catabolic products, including ILs, TNF-α, MMPs and ADAMTSs, which imbalance the typical synovial fluid composition and contribute to cartilage degradation (**Fig. 1.9**) [88,98,114,133]. Such alterations can also result in decreased concentrations of cartilage-protecting factors [88]. In response to the produced cytokines by the synovial cells, chondrocytes are activated and start producing more matrix-degrading proteínases, inflammatory mediators and cytokines (**Fig.**

1.9), including IL-1β, TNF-α, MMPs, NOS and PGEs [91]. Feedback amplification events are therefore initiated and this vicious cycle contributes to the negative shift of the balance towards the loss of homeostasis of the joint [91].

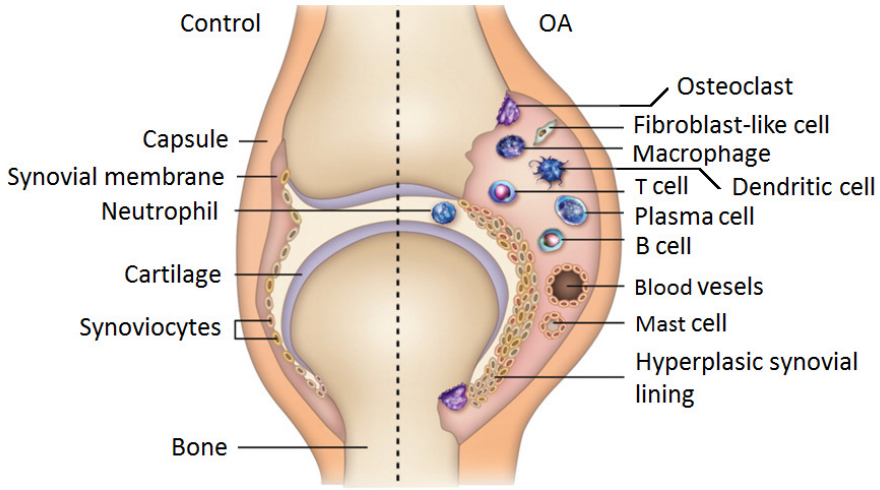

Fig. 1.11 – Synovial membrane changes upon synovitis. The synovial joint is infiltrated by T cells, B cells, macrophages, plasma cells, dendritic cells and mast cells which together with fibroblast-like cells produce cytokines, growth factors, adhesion molecules and matrix metalloproteínases (Adapted from Tanaka, 2009 [134]).

The presence of synovitis in OA is therefore associated with disease progression but also with pain [133]. In fact, OA is the leading cause of disability worldwide largely due to pain, that is the primary symptom of the disease [135]. Unlike many other pain conditions in which the underlying injury typically heals or resolves, OA is a disease that does not resolve, thus, it is typically accompanied by chronic pain [135]. Although the accurate source of pain in OA is still not completely understood, it is believed to be in great extent caused by tissue injury and consequent inflammation, with chemical mediators release, which lead to the activation of peripheral nociceptors that generate and exacerbate the feeling of joint pain [135,136]. Such receptors activation will elicit a painful response to normally innocuous joint movements, like walking, a neurophysiological process known by allodynia [135,136]. Over time this increased neuronal activity from the periphery can cause plasticity changes in the central nervous system and second order neurones in the spinal cord increase their firing rate, enhancing the transmission of pain information to the somatosensory cortex is [136]. This central sensitization phenomenon intensifies pain sensation and can even lead to pain responses in remote regions of the body from the inflamed joint [136].

1.2.2.1 Interplay between ectopic calcification and inflammatory events

Basic calcium crystals and calcium pyrophosphate dihydrate crystals deposition in osteoarthritic cartilage is a common feature of OA [48]. Initially, BCP crystals deposition was associated with end-stage OA, released from bone at time of major cartilage defects, and CPPD crystals deposition was considered an age-related process [48]. However, several clinical and experimental data have provided evidences that cartilage calcification occurs as an active process and that it clearly plays a pathogenic role in OA, promoting crystal-induced stress (**Fig. 1.12**) [48]. Basic calcium phosphate crystals are believed to be the major calcium crystal form associated with OA, identified in 80% to 100% of osteoarthritic cartilage according to different studies, while CPPD prevalence is greater than 20% in people over 80 years old [49,137,138]. Calcium crystals are correlated with OA severity and major joint destruction, although crystal accumulation is also found in a smaller percentage of patients with early OA, indicating that calcifications are also associated with low-grade OA changes [50,137,138]. Calcium pyrophosphate dihydrate crystals occur preferentially in articular tissues (hyaline cartilage, fibrocartilage, intervertebral disk, ligaments, synovial membrane and capsule) and synovial fluid, whereas BCP crystals are frequent in both articular and extra-articular tissues, and in the synovial fluid [49]. Calcium-containing crystals have a direct effect on chondrocytes and synoviocytes. In particular, BCP and CPPD crystals induce the production of MMPs, NO, prostaglandins and inflammatory cytokines such as IL-1β and TNF-α from resident articular cells, increasing the articular inflammation process, cartilage degradation and chondrocyte apoptosis (**Fig. 1.12**) [139-142]. Basic calcium phosphate crystals may also induce synoviocytes proliferation (**Fig. 1.12**) [50]. Interestingly, the crystal-induced stress associated to articular cells seems to rely on physical contact and be size-dependent, thus crystal-cell interactions and respective inflammatory responses are influenced by crystal size and morphology [140]. Accordingly, small crystal sizes of 1 μm result *in vitro* in higher inflammatory responses than 50 μm crystals, and in fact, the detected crystal sizes *in vivo* in OA-affected articular cartilage or synovial membranes are close to 1 μm size [140]. Crystal-induced stress both in chondrocytes and synoviocytes is believed to mainly occur via endocytosis or phagocytosis of particles, leading to intralysosomal crystal dissolution with subsequent elevation of intracellular calcium levels and release of inflammatory cytokines [142]. Crystal phagocytosis can be enhanced by opsonisation by immunoglobulins or complement components [142]. Intracellular mitogen-activated protein kinases (MAPK)

pathways, known to direct cellular responses to a diverse array of stimuli, are also suggested to mediate crystal-induced cellular responses through the activation of NOS [143]. Ultimately, crystal activation may also involve a direct crystal-cell membrane interaction, which can be either due to electrostatic bonds with naked crystal surface or through membrane receptor stimulation by naked or protein-coated crystals [142]. Interestingly, it is postulated that proteins and other substances bound to crystals affect their ability to initiate inflammation [100]. Studies on the effect of kidney stones and crystal effects on VSMCs reinforced older findings showing that synthetic crystals are far more injurious than native crystals and that the substances bound to crystals can dramatically affect cell-crystal interactions [144,145]. In fact, fetuin-A-containing calciprotein particles formation was suggested to help protecting macrophages against proinflammatory effects of the sequestered calcium crystals, while facilitating the clearance of calcium crystals from extracellular fluids [35]. Notably, a circulating MGP-containing CPP was described and suggested to inhibit calcium phosphate crystal precipitation [36], thus mineral binding proteins as fetuin-A, MGP and possibly also GRP, may play a role in such processes, helping to prevent the crystal-induced stress associated with OA. Overall, with the increasing recognition of the importance of inflammation in OA and identification of the innate immune system as a potential mediator of such inflammation, the role of calcium crystals in the development and progression of this disorder gains particular importance. In concordance, the role of calcification inhibitors such as the extra-hepatic VKDPs OC, MGP and GRP, should be further explored and regarded as potential therapeutic targets for OA.

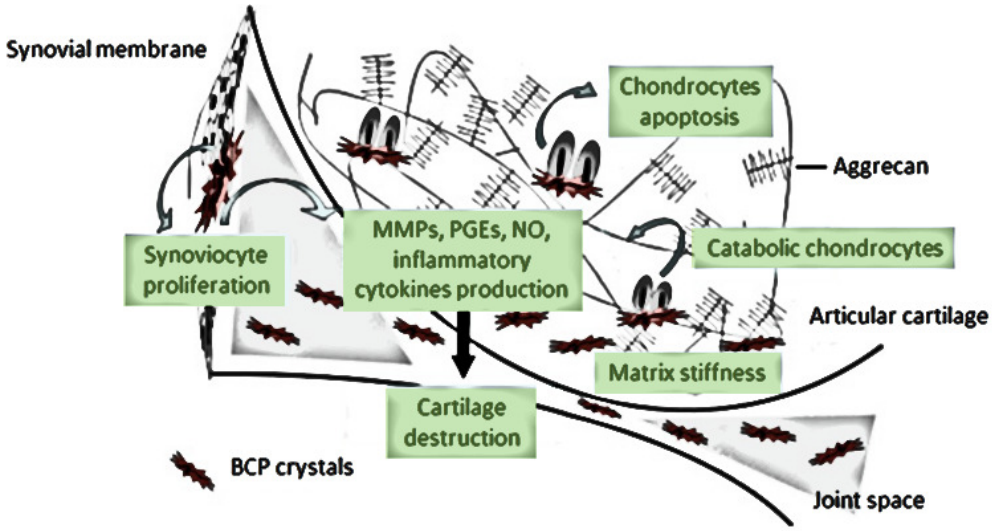

Fig. 1.12 – Model of crystal-induced stress in an osteoarthritic joint. Basic phosphate calcium (BCP) crystals are formed in the articular cartilage by chondrocytes and matrix vesicles and can be released into the joint space when cartilage lesions occur. BCP crystals stimulate synoviocyte proliferation, along with inflammatory cytokine, matrix metalloproteínase (MMP), prostaglandins E (PGE) and nitric oxide (NO) production. BCP crystals also directly induce chondrocytes to produce the same mediators, and undergo apoptosis. MMP production and chondrocyte apoptosis contribute to cartilage destruction. Moreover, cartilage calcifications lead to cartilage stiffness with subsequent altered responses to mechanical stimuli within the cartilage and/or the subchondral bone (Adapted from Ea et al., 2011 [50]).

1.2.3 Models for the study of osteoarthritis

Despite widespread awareness of OA and its devastating impact, the pathogenesis of early OA is not completely understood, hampering the development of effective tools for early diagnosis and disease modifying OA drugs [146]. Moreover, most of the human tissue available for the study of OA is obtained at the time of joint replacement, when OA lesions are at end stage and as a consequence, little can be concluded about the factors that played a role in disease development [146]. Therefore, a whole range of *in vivo* and *in vitro* systems are currently used to study the different aspects of joint physiology in health and disease [147].

In vivo models may provide the most accurate reflections of naturally-occurring OA [148,149]. Reproducing features of OA in animal systems may be extremely important to gain a better understanding of disease mechanisms and to assess responses to potential therapies [147]. In concordance, these are currently the most widely used systems for translating basic findings into therapies for patients [147]. Animal models of OA include naturally occurring OA in aging (experimentally accelerated), transgenic models and surgically or chemically

induced OA [149-151]. Small animals (mice, rats, rabbits and guinea pigs) are most often used to investigate specific disease mechanisms and for pre-clinical drug screenings, for reasons of cost-effectiveness, ease of handling and housing, and opportunity for genetic manipulations [147]. Among these, mice are probably the most commonly used models, in particular the destabilization of the medial meniscus (DMM) surgical model where lesions consistent with that of spontaneous age-related OA are observed [152]. Yet, the high cost of using animal models, the increasing ethical concerns and the need for adequate conditions for animal handling and housing, contrasting with the ease of manipulating and maintaining *in vitro* systems, in addition to models refining, make *in vitro* modelling of OA a desirable approach [147].

In vitro OA models include monolayer cultures, co-cultures, three-dimensional (3D) cultures and explants [153]. Monolayer cultures involve a single layer of cells grown on a flat surface of Petri dishes or culture flasks, allowing cellular expansion from a single sample [153]. This system is the easiest to manipulate and allows the easiest cell observations, measurements and environmental control of all OA models [154]. It is also very suitable for the investigation of distinct isolated pathways [153]. Moreover, there is a rich body of literature to which results can be compared when using monolayer cultures [154]. However, monolayer cultures have the main disadvantages of cells rapidly losing their molecular signature when taken out from the joint environment and the impairment of typical cell-to-cell and cell-protein interactions, due to the absence of normal extracellular matrices cells [153]. Co-cultures systems are able to consider the cross talk between cell types, thus co-cultures of chondrocytes and synoviocytes or synoviocytes and macrophages may contribute to identify potential relevant mechanisms in OA [147,153,155]. Yet, these models have the same disadvantages of monolayer cultures and special attention should be given to the fact that different cell types may require different culture conditions [153]. Three-dimensional cultures correspond to high-density cell pellets obtained by centrifugation and subsequently seeded or not over a synthetic scaffold/matrix [147,156]. These models provide cells a suitable 3D environment, allowing them to secret and build typical *in vivo* components, enable the development of central hypoxia and represent more accurately the real microenvironment where cells reside in tissues [156,157]. The major disadvantages of 3D models relay on the need to first isolate and expand high amounts of cell types, and on the nature of scaffolds, that may induce cells to behave differently than in the natural environment [153]. Ultimately, explants or *ex vivo* models involve the direct culture of a small piece of tissue harvested directly from the host [158]. Explants are inexpensive, easily produced and cells are

maintained in a normal extracellular matrix, resulting in a more controlled and more physiologically relevant OA model than 3D models, maintaining intact both the morphological and biosynthetic cell characteristics [153,158]. Nevertheless, explants are limited in terms of possessing cell death at the edges of the tissue, not allowing many replicates (if any) from the same source, possibly requiring more than one tissue type to maintain viability and being prone to change their physical attributes while in culture [153]. Overall, although *in vitro* models are great tools to study different aspects of OA, the relevance of such models to clinical OA always needs to be carefully interpreted since they may not exactly reflect biological features.

Among *in vitro* models, one of the most commonly used approach to study OA is cytokine-based models. Accordingly, the addition of IL-1β or TNF-α to cell systems of chondrocytes or synoviocytes is a frequent procedure, considering that these cytokines increase the expression of catabolic proteins in both cell types [153]. When using such models, the amounts of loaded cytokines should be carefully considered in order to use a concentration that reflects that existing in naturally occurring OA rather than downstream effects caused by an excess of the added compounds [153]. The amounts of IL-1β and TNF-α assayed in osteoarthritic synovial fluid are usually under 2 ng/mL and close to 3 ng/mL, respectively, while those used to exert an effect *in vitro* are much higher, reaching up to 100 ng/mL of IL-1β and up to 50 ng/mL of TNF-α [153,159,160]. Also, the choice of whether to use a monolayer, a 3D culture or explants will influence the cells response to cytokine stimuli, with monolayer cultures having generally the fastest responses and needing lower amounts of cytokines to exert an effect [153]. Yet, monolayer cultures or co-cultures are limited for the study of extracellular matrix changes and dynamic processes occurring after cytokine stimulation comparing to 3D models [157]. In fact, 3D cartilage cultures stimulated with cytokines and macrophage conditioned medium were described to be the most appropriate OA model, even comparing with animal models, to study aspects of OA progression such as the impacts of NO and PGE2 [157].

Overall, no consensus on the most appropriate model for the representation of particular features of OA has been made since each model has advantages and disadvantages, and its own mechanisms for the induction of a general catabolic process. However, the ease of using monolayer cultures combined with their reproducibility, rapid response to cytokine stimulation and their effectiveness for the study of distinct isolated pathways [153,154], still make this system one of the preferential models to use for the study OA.

1.2.4 Osteoarthritis diagnosis and treatments

Current diagnostic criteria for OA relies on radiographic evaluations and clinical manifestations, including pain symptoms and stiffness of the affected joint [161]. Common clinical approaches to radiographic assessment provide a semi-quantitative judgment of the extent of OA, the most common corresponding to the Kellgren-Lawrence (KL) and the OA research society international (OARSI) classification systems [162]. The OARSI classification system is described to be more appropriated to categorize joint space width, while the KL system to categorize the general OA status of the joint [162]. The KL classification system grades OA from a 0 to 4 stage, in which 0 corresponds to healthy joints and 4 to end stage OA (**Table 1.I**), and the most adequate treatment for each OA patient is defined according to the obtained classification degree [162]. However, OA may be a silent disease for many years before the typical symptoms and radiographic changes emerge, thus articular cartilage damage may have occurred and become irreversible during this long-term subclinical stage [161].

Table 1.I – Kellgren-Lawrence system for classification of OA (Adapted from [162])

Grade	Features
0	No radiographic features of OA
1	Doubtful joint space narrowing and possible osteophytic lipping
2	Definite osteophytes and possible joint space narrowing
3	Moderate multiple osteophytes, definite joint space narrowing, sclerosis, possible bony deformity
4	Large osteophytes, marked joint space narrowing, severe sclerosis and definitely bony deformity

In addition to the late diagnosis of OA, which hampers treatment, there are also no effective DMOADs available as a treatment option to potentially halt or slow disease progression [96]. Therefore current treatments are mainly based on symptom control trying to post-pone whole joint replacement procedures, also termed arthroplasty surgeries, generally only performed in patients with stage 4 OA, according to the KL classification system [162], when all other strategies have failed [96]. Such surgical interventions are highly effective, involving the replacement of the damaged parts of the joint by an artificial device termed

prosthesis [163,164]. The prosthesis is designed to replicate the movement of healthy articulations correcting the existing deformities, thus patients quality of life is significantly improved by the restoration of joint function and consequent enhanced mobility, pain relief and independence [163,164]. Yet, complications may occur at long-term including late infection, wearing of the bearings and loosening of the prosthesis [163]. Prior to arthroplasty, current practices for managing knee OA involve conservative non-pharmacological treatment strategies such as weight loss, aerobic exercise, physical therapy and the use of knee braces [165-167]. Oral analgesics and nonsteroidal anti-inflammatory drugs (NSAIDs) are also commonly administrated to relieve the pain, and they can be helpful for managing OA in the short-term, but are less effective for long-term management [96]. Accordingly, acetaminophen, generally known by paracetamol, is a common first-line therapy in knee OA patients with mild to moderate pain [168]. Nonsteroidal anti-inflammatory drugs (e.g. ibuprofen) are considered superior than oral analgesics to treat joint pain, however they are associated with adverse effects such as gastrointestinal discomfort and therefore a prolonged use should be avoided [168]. Glucosamine/chondroitin is a supplement alleged to be absorbed and incorporated into articular cartilage, thus potentially allowing the halting of OA progression and even promoting a reparative process [169], nevertheless evidences of its positive effect remain inconsistent [168].

Emerging therapies for managing OA involve intra-articular injectables, ranging from corticosteroids, hyaluronic acid and more recently platelet-rich plasma (PRP) or even stem cells [96]. Intra-articular corticosteroid injections for knee OA appear to be effective against pain [170], but they are recommended for short-term applications do to the risk of corticosteroid-induced arthropathies [171]. As a natural component of the synovial fluid, hyaluronic acid injections may help improving joint lubrication and shock absorbing and have proven to be effective relieving knee pain [172]. Platelet-rich plasma injections are believed to help structural repair through its growth factors components [173]. Mesenchymal stromal cells are multipotent cells that can be isolated from several human tissues and their immunomodulatory, reparative, and anti-inflammatory properties have been tested in a variety of animal models, indicating to have potential clinical applications in the field of OA [174].

Ultimately, the existing strategies to treat OA have either limited efficacy or secondary effects and none of them is able to completely cure the disease, thus there is an urging need for continued research with regards to the management of OA. This research should focus on investigating the efficacy of new drugs such as the DMOADs, as well as better understanding their safety profiles [96]. Rather than develop treatments that target symptoms, the emphasis

should be on developing advanced therapies that can slow or prevent further disease progression and hopefully even initiate a regenerative process [96]. Also, the discovery of early OA biomarkers should constitute an extremely valuable tool, in order to manage the disease in its initial stages.

1.2.4.1 Biomarkers for osteoarthritis

Osteoarthritis dramatically needs reliable, quantitative and dynamic tests to identify patients at risk for the progression of the disease, detect early damage and measure the progress of DMOADs targeted against joint destruction [81]. Biomarkers, in addition to magnetic resonance imaging, are tools that can address these therapeutic shortcomings [175]. Structural molecules and fragments derived from cartilage, bone and the synovial membrane, are reported as the most promising candidates for OA biomarkers discovery [81]. These markers are eventually released into biological fluids like the synovial fluid or serum, where they can be more easily detected [176].

Proteomics, a large-scale analysis of proteins that involves isolation, purification, and mass spectrometry (MS) of the proteins of interest, makes it possible to search for such biomarkers in a systemic fashion [177]. Quantitative and high-throughput proteomic techniques have made important contributions for the discovery of complement components, lipoproteins and lower abundance ECM components in body fluids from OA patients [178]. Cartilage proteomic analysis has also been applied to search for candidate OA biomarkers, yet while affinity depletion is usually conducted to remove abundant proteins that mask the signals of less expressed entities in body fluids, cartilage preparation is much more challenging [119]. Cartilage proteomic analysis is mainly limited by dominant collagen and aggrecan levels that overwhelm the signals from other proteins, anionic macromolecules including aggrecan and hyaluronic acid which affect peptide analysis, and cellular proteins from chondrocytes that hinder the identification of ECM proteins [179].

The identification of biomarkers that can be applied more broadly from the very early to the end stages of OA is required, yet advances in the field OA biomarkers still remain challenging [81]. Accordingly, several OA biomarkers are recognized, however most of these molecules represent advanced stages of OA and only a few early stages of the disease [175]. Examples of proposed OA biomarkers are glucosyl-galactosyl-pyridinoline (Glc-Gal-Pyd), correlated with synovial membrane damages, MMP13 and COX2, representing inflammatory markers, and serum cartilage oligomeric matrix protein (COMP), indicative of cartilage

turnover as it represents a cartilage degradation product [180-183]. Since OA is believed to onset at cartilage level, markers of cartilage damage are considered the best candidates to reflect early OA markers [81]. In agreement, one of the few suggested early OA biomarkers are C-terminal telopeptides of Col2a1 (CTX-II), marking Col2a1 degradation [184]. Urine levels of CTX-II have been suggested to access the diagnostic and prognostic of knee OA, and also to be able to evaluate the efficacy of DMOADs [184,185]. In fact, higher urine levels of CTX-II may be identified at stage 1 of the KL classification system [186]. However, the question whether urine CTX-II levels are solely a cartilage degradation biomarker still remains [186].

Overall, the discovery of early OA biomarkers may greatly contribute for managing the disease. The extra-hepatic VKDP GRP, associated to cartilaginous tissues and ectopic calcification in humans [14-16], may represent a candidate biomarker for OA and studies towards unveiling such possible relation should be performed.

1.3 Aims and organization of the thesis

Despite the worldwide burden of OA there is still much to unveil regarding disease incidence and progression. Moreover, OA continues to have a late diagnostic and adequate treatments for this progressive joint disorder are also lacking. Therefore, research in the field of OA may gratefully contribute for new strides benefiting the managing of the pathology. Since one important feature of OA is the occurrence of pathological mineralization, calcification inhibitors may play an important role in the pathogenesis of this disorder. In this line, the main aim of this study was to investigate the association of Gla-rich protein with molecular features of OA, such as ectopic calcification processes. Additionally, studies were conducted to further analyse the potential of GRP as a novel biomarker for OA. Within the scope of this work, Chapter 2 describes the collection and characterization of a biological sample bank suitable for the study of OA, in particular the investigation of GRP potential association with pathological mineralization and inflammatory processes, and the search for candidate OA biomarkers. In Chapter 3, the involvement of GRP with OA was explored through gene expression studies and further analysed through immune-based strategies, which also allowed investigating GRP association with the occurring pathological calcification. Chapter 4 describes the establishment of an *in vitro* cell system that was used to further

explore GRP involvement with OA, in particular calcification and inflammatory events. Finally, Chapter 5 analyses GRP potential as a biomarker for OA and describes the search for alternative candidate OA biomarkers using comparative proteomics. Chapter 6 summarizes the main conclusions of this project and highlights future perspectives for subsequent studies within the scope of this work.

Chapter 2

Collection and characterization of a biological sample bank for the study of osteoarthritis

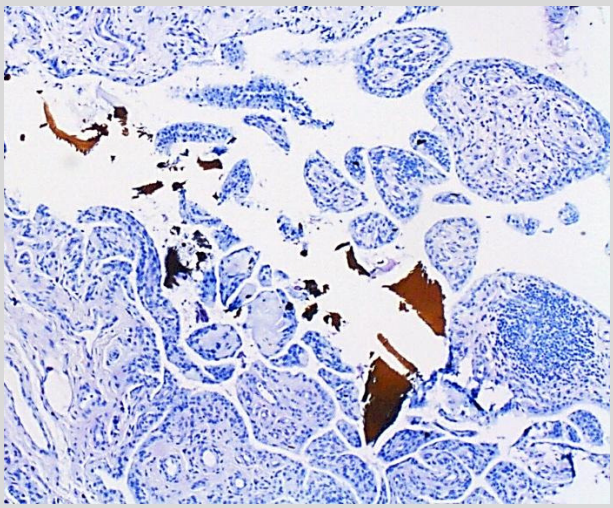

Abstract

Osteoarthritis (OA) is the leading form of degenerative joint disorders, mainly affecting weight bearing joints like the knee and representing the most frequent source of chronic physical disability of the elderly population. Osteoarthritis is believed to onset after articular cartilage damage, later evolving to affect the whole joint. Frequent OA features are the degradation and loss of articular cartilage, subchondral bone changes and occurrence of osteophytes, thickened joints, synovial membrane inflammation and the deposition of calcium crystals in articular tissues, correlated with consequent disease progression. Although new strides have been achieved during the past decade in the field of OA, this degenerative disorder still urges for the discovery of molecular targets and biomarkers that can facilitate early OA prediction, the management of the disease and trials of therapies. The present chapter reports the collection and characterization of a biological sample bank containing human specimens suitable for the study of OA molecular features, by allowing subsequent gene expression studies, histological analysis, proteomic approaches and cell culture development. This biobank comprised samples of knee articular cartilage, subchondral bone, synovial membrane, synovial fluid, and blood, from knee OA patients and individuals with no history of joint disorders. Every collected subject specimen was complemented with medical information, which also included radiographical and biochemical data in the case of the patients, supporting the representation of osteoarthritic or healthy conditions. Tissue histological analysis of the collected material was performed using hematoxylin staining, the von Kossa method and immunohistochemistry, to characterize and evidence the association of osteoarthritic features in the pathological samples, such as cartilage destruction, synovitis and ectopic calcification. This biobank was in particular expected to be useful to investigate the possible association of Gla-rich protein (GRP) with OA molecular features, such as pathological mineralization and inflammatory mechanisms, and the search for candidate OA biomarkers, which will be addressed in the following chapters.

2.1 Introduction

Osteoarthritis (OA) is the most frequent form of degenerative joint disorders, which commonly affects weight-bearing joints like the knee and hip [96,98]. It is one of the most common chronic health conditions and a leading cause of pain and disability among the elderly population [97]. Global estimates indicate that 9.6% of men and 18% of women over 60 years old have symptomatic OA [103]. In USA, OA is responsible for 4 million hospitalizations and the loss of 68 million labour days per year, and the financial burden of the disease has been estimated to be $81 billion in medical costs and $128 billion in total cost per year [101,105]. In Portugal, no published data on specific direct and indirect costs was identified, yet rheumatic diseases are pointed as the first cause for early retirement [103]. knee OA is considered the prevalent form of the disease [97], and recent estimates suggest that its global burden affects approximately 250 million people [101].

Synovial joints are composed of articular cartilage, a synovial cavity between bones filled with synovial fluid, and a capsule, attached to articulating bones and characterized by an outer fibrous membrane and an inner synovial membrane [111]. Osteoarthritis is believed to onset at cartilage level, with extracellular matrix (ECM) remodelling, then evolving to affect the entire joint [91,111]. Frequent OA features are articular cartilage degradation and loss, subchondral bone changes and osteophytes formation, thickening of the joints, synovial membrane inflammation and pathological calcification [99,100].

Articular cartilage has limited ability to recover from disturbed catabolic and anabolic processes, and OA is suggested to result from chondrocytes failure in keeping such balance [111]. In addition to cartilage alterations with age, degeneration may occur in response to inappropriate mechanical stress and inflammatory processes, associated with conditions such as obesity, genetics or trauma, some of the major risk factors for OA development and progression [97,98,107,111]. When the origin of OA is idiopathic, the disease is termed primary OA, whereas if resulting from a known cause, such as joint injuries or diseases, like rheumatoid arthritis (RA), it is categorized as secondary OA [102]. Disruption of the normal resting state of chondrocytes leads to increased production of matrix proteins and matrix-degrading enzymes, inappropriate hypertrophy-like maturation, and eventually cartilage pathological calcification [91]. In fact, cartilage ectopic mineralization is a well-known feature of OA, resulting from factors like the imbalance between inhibitors and stimulators of calcification, alteration of calcium levels, phosphate (Pi) and pyrophosphate (PPi)

metabolism, chondrocyte hypertrophy and cell death [49,50]. Cartilage ectopic calcification is believed to contribute for joint degeneration, mediate and promote inflammatory processes, and is associated with increased OA severity [48,50,137,138].

In the process of OA, ECM degradation products are released from damaged cartilage into the synovial fluid and accumulate in the sinovial membrane [91]. As foreign bodies, an inflammatory response termed synovitis is initiated, characterized by the hyperplasia of lining cells, infiltration of inflammatory cells, increased vascularization and formation of perivascular lymphoid aggregates [87]. Macrophages, T cells and mast cells are the most abundant cell types infiltrating the synovial membrane [130]. In advanced stages of OA, calcium crystals are also detected in the synovial fluid and synovial membrane, believed to be released from the damaged cartilage ECM into the synovial space [88,91].

The diagnosis of OA is currently based on radiographic criteria and clinical manifestations, that only evidence the disease when significant changes have already occurred [81,161]. The Kellgren-Lawrence (KL) classification system is often the used clinical approach to radiographically classify OA, using a scale from 0 to 4, where 0 represents healthy joints and 4, end stage OA [162]. In addition to the absence of diagnostic techniques for early OA, there are no efficient disease modifying OA drugs (DMOADs) to treat the disorder [96]. Hence, biomarkers that can facilitate the early diagnosis of OA, inform the prognosis, and monitor therapeutic trials, are extremely necessary [81,175]. Synovial fluid or serum are the preferable biospecimens for the search of OA biomarkers, because these are easily available and may reflect OA progression [176]. Calcification modulators are interesting candidates as biomarkers for OA, since the presence of intra-articular calcium crystals is suggested to contribute for cartilage destruction in the disorder [48,49]. This prompted the study of Gla-rich protein (GRP), a vitamin K-dependent protein (VKDP) proposed to act as a modulator of calcium availability in the ECM [14,15] and inhibit pathological calcification in the cardiovascular system [16].

The availability of a well characterized and representative biological sample bank, containing osteoarthritic samples and control counterparts, may greatly contribute for the study of OA. Therefore, the present chapter reports (i) the collected tissues and body fluids from control individuals and knee OA patients for the study of representative pathological processes occurring in OA, such as calcification and inflammatory events, and (ii) the histological characterization of the collected tissues, to detect typical cellular alterations associated with the disease. This sample bank allowed the study of GRP associated to OA in Chapters 3 and 4, and the search of novel OA biomarkers in Chapter 5.

2.2 Experimental procedures

2.2.1 Biological material and sample processing

This study complies with the guidelines for good clinical practice, was performed in concordance with the Declaration of Helsinki and approved by the ethics committees of all hospitals and institutions involved. Written informed consent was obtained from all the participants.

Biological material was obtained from patients diagnosed with primary or secondary grade 4 knee OA, according to the KL classification system, who had undergone arthroplasty interventions (total knee replacement) at Centro Hospitalar do Algarve (Departamento de Ortopedia e Traumatologia, Faro, Portugal) or Hospital Particular do Algarve - Gambelas (Departamento de Ortopedia, Faro, Portugal). Doctor Acácio Ramos was the main collaborator involved in the collection of the former biospecimens and respective subject clinical information at both hospitals. The collected samples included articular cartilage, subchondral bone, synovial membrane, synovial fluid and blood. Identical biological material was obtained from subjects with no history of joint diseases, either following autopsy at Delegação do Sul do Instituto Nacional de Medicina Legal e Ciências Forenses (Faro, Portugal) or after arthroscopic procedures (minimally invasive surgeries in which the joint usually is not fully opened), at Centro Hospitalar do Algarve. Blood samples were also obtained from volunteers with no history of joint diseases. Doctor Joana Luz was the main collaborator involved in the collection of control biospecimens and respective subject clinical information at Delegação do Sul do Instituto Nacional de Medicina Legal e Ciências Forenses and Doctor Acácio Ramos at Centro Hospitalar do Algarve.

Cartilage, bone and synovial membrane tissues were collected into RNAlater (Sigma-Aldrich, St. Louis, MO, USA) for RNA extraction, or in sterile 4 % w/v paraformaldehyde solution for histological analysis. The former tissues were also collected for protein extraction purposes, and in this case they were immediately stored at – 20 °C until further use. Osteoarthritic cartilage and synovial membrane tissues for cell culture development were collected in Dulbecco's modified Eagle's medium (DMEM, Invitrogen, Carlsbad, CA, USA) and maintained at room temperature (RT) until processing within 24 h post collection. Synovial fluid and clotted blood samples were centrifuged for 15 min at RT and 3.000 x g,

before storage at – 80 °C until further use. With this centrifugation step, serum samples were obtained from the clotted blood.

2.2.2 Histological techniques

Biospecimens containing both articular cartilage and subchondral bone or cartilage only, fixed in 4% w/v paraformaldehyde, were further processed for histological analysis and embedded in glycol methacrylate or paraffin, respectively, as described [187,188]. Methacrylate embedding was used for the analysis of calcified areas. Synovial membrane samples were processed and embedded in paraffin. All paraffin embedding and part of the paraffin blocks sectioning was performed by Departamento de Anatomia Patológica at Centro Hospitalar do Algarve where technician Alexandra Teixeira was the main collaborator involved. Methacrylate sectioning was performed using a tungsten carbide blade. Longitudinal sections of 5-7 (methacrylate) or 6-8 (paraffin) µm thick were mounted on slides. Hematoxylin staining was used for the identification of structures and morphological features. Mineral deposits were detected using the von Kossa method [187] counterstained with hematoxylin or toluidine blue. Every staining was repeated at least three times using samples of different subjects.

2.2.3 Immunohistochemistry

Immunohistochemistry (IHC) was performed to detect specific antigens in articular cartilage and synovial membrane tissues. Articular cartilage IHC was performed as described [78]. Briefly, antigen retrieval was achieved by incubation with 2 mg/mL hyaluronidase (Sigma-Aldrich) during 1h at 37 °C. Endogenous peroxidase activity was blocked with 3% v/v H_2O_2 in methanol in the dark for 10 min and nonspecific antibody binding was blocked with 0.5% (w/v) bovine serum albumin (BSA) in TBST buffer (15 mM NaCl, 10 mM Tris-HCl buffer pH 8, 0.05% Tween 20). Synovial membrane IHC analysis was performed using a similar procedure, yet antigen retrieval was achieved by boiling in 0.2 % v/v citric acid pH 6.0 for 30 min. Incubations with the primary antibodies mouse monoclonals anti-cartilage oligomeric matrix protein (COMP, 4 µg/mL), anti-cluster of differentiation 3 (CD3, 66.7 µg/mL), anti-CD45 (2 µg/mL) and anti-CD68 (20 µg/mL), from Santa Cruz Biotechnology (Texas, TX, USA), were performed overnight at RT. Peroxidase activity was detected using

the respective peroxidase-conjugated secondary antibodies (Sigma-Aldrich) and ImmPACT NovaRED substrate kit (Vector laboratories Ltd., Peterborough, UK). Negative controls consisted of the substitution of the primary antibody with TBST buffer. Final counterstaining was achieved using hematoxylin. Images were obtained using an Axio Imager Z2 microscope (Zeiss, Jena, Germany) equipped with a digital camera and Axovision imaging software.

2.3 Results

2.3.1 Collection of control and osteoarthritic samples

Knee OA was the selected model to conduct studies within the scope of this project since it is the prevalent OA-affected joint [97]. Biological material was collected during all the time course of this project, from individuals with no history of joint diseases (Control group, **Table 2.I**) and clinically diagnosed knee OA patients (OA group, **Table 2.II**). The collected biospecimens comprised articular cartilage, subchondral bone, synovial membrane tissues, synovial fluid and serum samples (**Tables 2.I** and **2.II**).

Table 2.I – List of collected samples for the Control group and subject clinical information

Control group				
Subjects	**Age**	**Gender**	**Samples**	**Clinical information**
1	52	Male	SF, C, B, SM	*Post mortem* (death by acute myocardial stroke)
2	54	Female	SF, C, B, SM	*Post mortem* (death by drug intoxication)
3	25	Female	S	Arthroscopy (knee trauma)
4	39	Female	S, C, B, SM	Arthroscopy (knee trauma)
5	36	Female	S, C, SM	Arthroscopy (knee trauma)
6	36	Male	S, SM	Arthroscopy (external meniscal lesion)
7	44	Female	SF, C, B, SM	*Post mortem* (death by drug intoxication)
8	47	Male	S, C, B, SM	Arthroscopy (knee trauma)
9	29	Male	S, C, SM	Arthroscopy (knee trauma)
10	18	Female	S, SM	Arthroscopy (knee trauma)
11	67	Female	C, B, SM	*Post mortem* (death by cranial trauma)
12	37	Female	S	No associated pathology
13	26	Female	S	No associated pathology
14	24	Male	S	No associated pathology
15	31	Female	S	No associated pathology

SF, synovial fluid; S, serum; C, cartilage; B, bone; SM, synovial membrane

Table 2.II – List of collected samples for the OA group and subject clinical information

OA group				
Subjects	**Age**	**Gender**	**Samples**	**Clinical information**
1	81	Male	SF, C, B, SM	Secondary OA associated to gout
2	83	Female	SF, C, B, SM	Primary OA, HT
3	71	Female	SF, C, B, SM	Primary OA, DM
4	62	Female	SF, C, B, SM	Primary OA, HT
5	74	Male	SF, C, B	Primary OA, HT
6	83	Female	SF, C, B, SM	Primary OA, obesity
7	72	Male	SF, C, B, SM	Primary OA, dyslipidaemia
8	80	Male	SF, C, B, SM	Primary OA, HT
9	75	Female	SF, C, B, SM	Primary OA, dyslipidaemia
10	63	Male	SF, C, B, SM	Primary OA, HT, dyslipidaemia
11	75	Male	SF, C, B, SM	Primary OA, obesity
12	70	Female	SF, C, B, SM	Secondary OA associated to RA
13	70	Female	C, B, SM	Primary OA, HT
14	71	Female	SF, C, B, SM	Primary OA, HT, DM
15	67	Female	C, B, SM	Primary OA, obesity
16	69	Female	SF, C, B, SM	Primary OA, HT
17	71	Female	SF, C, B, SM	Secondary OA associated to RA
18	72	Female	SF, C, B, SM	Primary OA, DM
19	81	Male	SF, C, B, SM	Primary OA, dyslipidaemia
20	53	Female	SF, C, B, SM	Primary OA, HT
21	64	Female	SF, C, B, SM	Primary OA, obesity
22	69	Female	SF, C, B, SM	Primary OA, obesity
23	72	Male	C, B, SM	Primary OA, HT
24	68	Male	SF, C, B	Primary OA, DM
25	53	Female	SF, S, C, B, SM	Primary OA, HT
26	68	Female	S, C, B, SM	Primary OA, HT, DM
27	80	Female	SF, S, C, B, SM	Primary OA, HT
28	74	Female	SF, S, C, B, SM	Primary OA, obesity
29	68	Female	SF, S, C, B	Primary OA, obesity
30	78	Female	S	Primary OA, dyslipidaemia
31	78	Female	S	Primary OA, HT, DM, obesity
32	74	Female	S	Secondary OA associated to RA
33	84	Female	S	Primary OA, dyslipidaemia
34	62	Male	S	Primary OA, HT, DM
35	78	Female	S	Primary OA, HT

SF, synovial fluid; S, serum; C, cartilage; B, bone; SM, synovial membrane; OA, osteoarthritis; RA, rheumatoid arthritis; HT, arterial hypertension; DM, type II diabetes mellitus

The control group (**Table 1.II**) contained biospecimens collected from 15 subjects, either following autopsy, arthroscopic procedures or volunteers (in the case of blood samples). This group included a reduced number, and in small quantities, of articular cartilage (8), subchondral bone (6), synovial membrane (10) and synovial fluid (3) biospecimens, and 11 serum samples in considerable amounts. The OA group (**Table 2.II**) contained biological material collected from 35 individuals subjected to total knee replacement surgeries. This group included a representative number, in most of the cases in considerable amounts, of articular cartilage (29), subchondral bone (29), synovial membrane (26), synovial fluid (25) and serum (11) samples. The collected biospecimens for the OA group were therefore sufficient for the initial planned experiments of the project, however the collected material for the control group was limited.

All the obtained biospecimens were completed with subject clinical information (**Tables 2.I** and **2.II**) for characterization of the sample groups. The average age of the control group was 38 years old (+/- 13) while in the OA group 72 years old (+/- 8). The prevalence of females was observed in both groups, constituting 67% and 71% of the sample, respectively, in the control and OA group (**Fig. 2.1**). Primary OA was the predominant form of the disease (89% of the individuals, **Fig. 2.2**), while a minority of the subjects presented secondary OA associated to other types of arthritis, namely gout or RA (**Table 2.II**). Patients with primary OA were clinically diagnosed with OA-associated risk factors, including obesity, arterial hypertension, type II diabetes mellitus and dyslipidaemia (abnormal amount of lipids in the blood) [108], with hypertension corresponding to the condition with highest incidence in this group (**Fig. 2.3**).

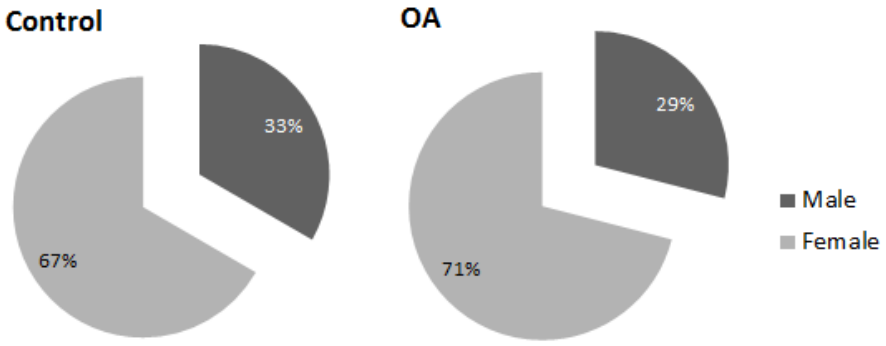

Fig. 2.1 – Predominance of the female gender in the collected control and OA groups.

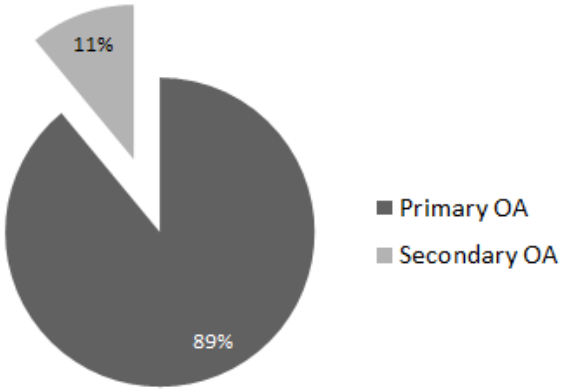

Fig. 2.2 – Higher incidence of primary OA relatively to secondary OA in the collected OA group.

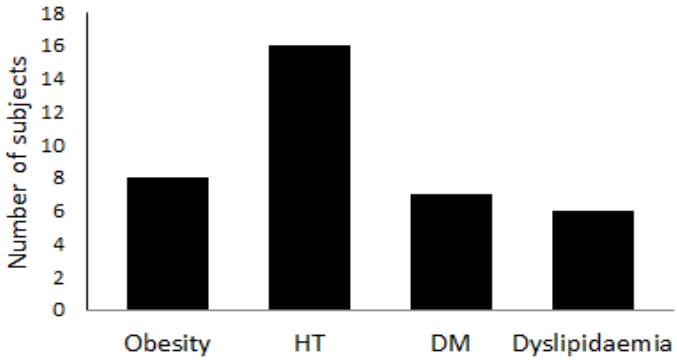

Fig. 2.3 – Primary OA associated-risk factors clinically diagnosed in the OA group. In 31 of the subjects diagnosed with primary OA, 8 suffered from obesity, 16 from arterial hypertension (HT), 7 from type II diabetes mellitus (DM) and 6 from dyslipidaemia.

All OA patients were clinically diagnosed with grade 4 knee OA (end stages of the disease), according to the KL radiographic classification system [162], at Departamento de Ortopedia e Traumatologia of Centro Hospitalar do Algarve or Departamento de Ortopedia of Hospital Particular do Algarve - Gambelas. Features such as the presence of osteophytes, marked joint space narrowing, severe sclerosis, malalignments and bone deformities, were therefore visible in the frontal and lateral plain knee radiographs performed to each patient prior to arthroplasty (**Fig. 2.4**, **A** and **B**, **OA**). For comparisons, frontal and lateral plain radiographs of healthy knees taken at Centro Hospitalar do Algarve are also shown in **Fig. 2.4** (**A** and **B**, **Control**).

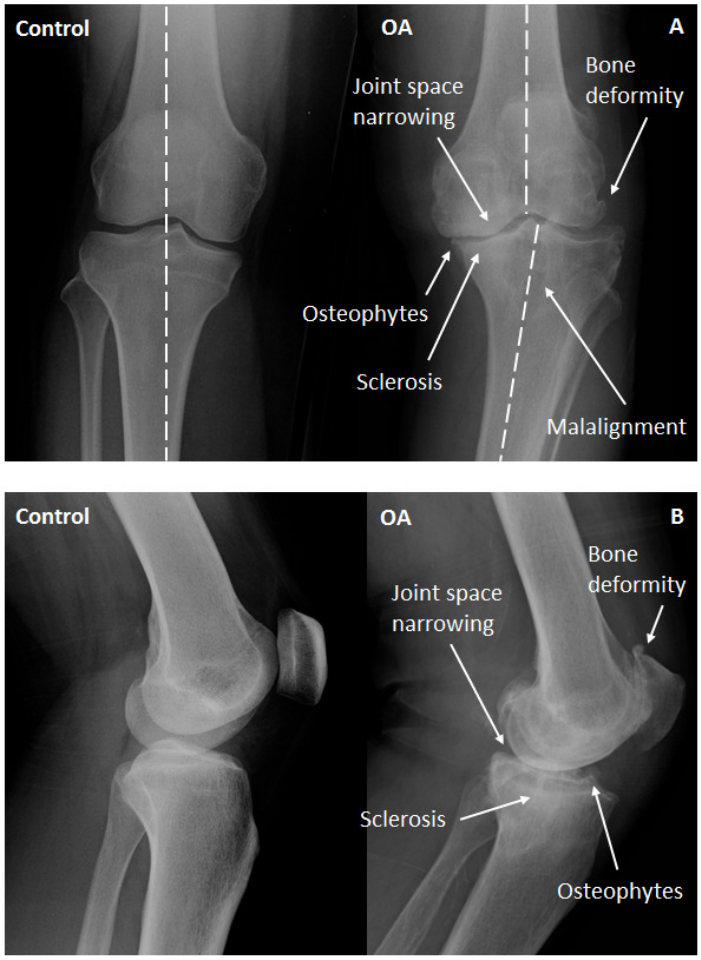

Fig. 2.4 – Frontal (**A**) and lateral (**B**) radiographs of healthy (Control) and Kellgren-Lawrence (KL) grade 4 osteoarthritic knees (OA). Radiographs of the osteoarthritic knees evidence the presence of osteophytes, joint space narrowing, sclerosis and bony deformities. In the osteoarthritic knee frontal scan, the presence of misalignment is also detected (Images supplied by Doctor Acácio Ramos).

Overall, two well characterized groups containing samples representative of healthy and osteoarthritic conditions were collected for the study of OA molecular features. Yet, the collection of control tissues and synovial fluid samples was limited both in total number and quantities, resulting in a control group that was only suitable for a reduced number of applications.

2.3.2 Histological characterization of control and osteoarthritic features among the collected biological material

Histological analysis was performed to further characterize the collected control and osteoarthritic tissues, especially concerning pathological calcification and inflammation features, for subsequent studies of GRP association with these OA characteristics. Control and osteoarthritic tissue sections of articular cartilage and subchondral bone were stained using the von Kossa method, for the analysis of respective calcified structures (**Fig. 2.5**). The brown staining of the subchondral bone and calcified cartilage areas, resultant from von Kossa method, evidenced differences between control and osteoarthritic tidemarks, which were linear in control tissues while irregular in the pathological (**Fig. 2.5**, **B** and **D**). Sites of ectopic calcification were also identified with this staining in 7 of the 12 analysed osteoarthritic tissue sections, representing different subjects, particularly in cartilage tangential layer (**Fig. 2.5**, **C**), whereas no ectopic mineralization was observed in control tissues (**Fig. 2.5**, **A**). Counterstaining with hematoxylin also showed the presence of vascular invasions in the subchondral bone (**Fig. 2.5**, **D**), chondrocyte clusters in cartilage deep zone (**Fig. 2.5**, **D**) and surface fibrillation of cartilage tangential layer in pathological tissues (**Fig. 2.5**, **C**). None of these features was observed in controls, and typical flattened chondrocytes [111] were detected in healthy cartilage tangential layers (**Fig. 2.5**, **A**). Overall, results evidenced several characteristic features of OA [91,111,114] associated to the pathological tissues, with a high prevalence of ectopic mineralization.

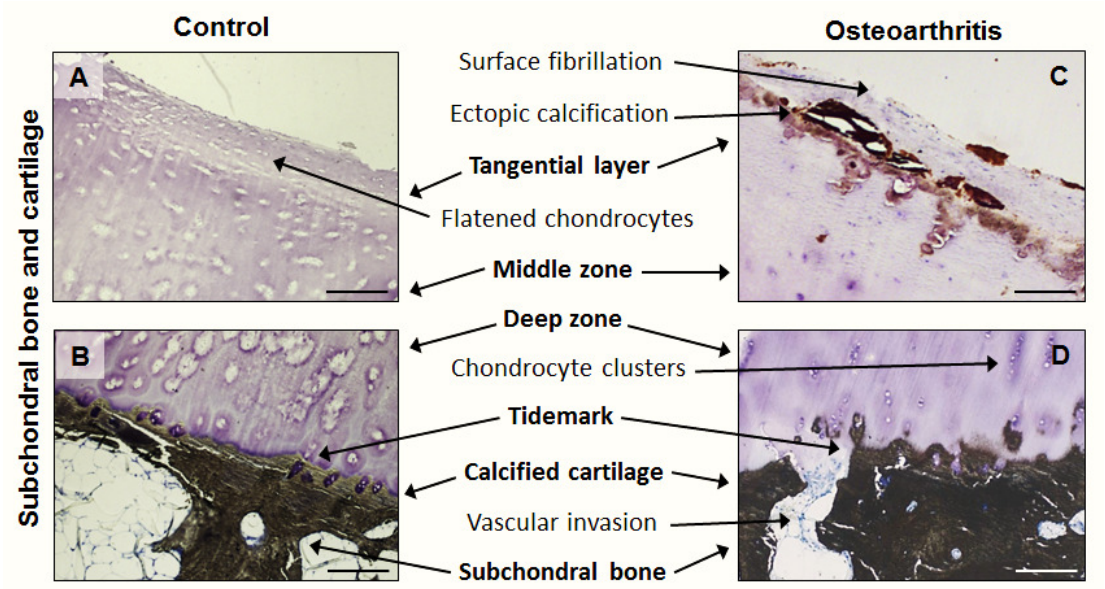

Fig. 2.5 – Histological characterization of control versus osteoarthritic subchondral bone and articular cartilage. Von Kossa staining of control (**A** and **B**) and osteoarthritic tissue sections of subchondral bone and articular cartilage (**C** and **D**) revealing the presence of calcified

areas, some of which ectopic in the osteoarthritic cartilage tissues and mostly in the tangential layer (**C**). Hematoxylin counterstaining allowed the visualization of structures and morphological features in both tissue types. Tissue areas from the subchondral bone to cartilage tangential layer are evidenced in bold. Tissues were embedded with methacrylate. Scale bars represent 100 µm (Adapted from Rafael et al., 2014 [189]).

To further support the osteoarthritic nature of the collected cartilage samples for the OA group, IHC analyses were performed to immunodetect the OA marker COMP, associated to cartilage turnover [183]. The presence of COMP was only detected in pathological samples (**Fig. 2.6**), namely in cartilage ECM (**Fig. 2.6**, **C**), chondrocytes (**Fig. 2.6**, **D**) and ectopic calcification sites (**Fig. 2.6**, **E**).

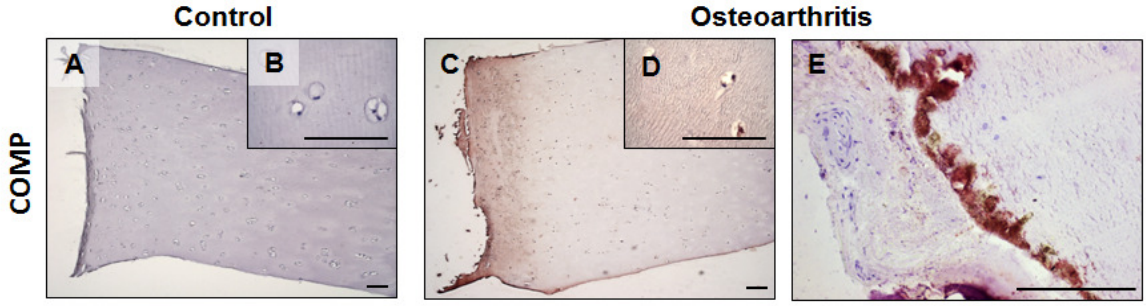

Fig. 2.6 – Immunodetection of cartilage oligomeric matrix protein (COMP) in osteoarthritic cartilage samples. Immunohistochemistry (IHC) was performed using an anti-COMP antibody in control (**A** and **B**) and osteoarthritic samples, without (**C** and **D**) and with ectopic calcification sites (**E**). Positive staining was revealed by a reddish/brown colour. Samples without calcification sites were embedded with paraffin and the remaining with methacrylate, all counterstained with hematoxylin. Scale bars represent 100 µm (Adapted from Rafael et al., 2014 [189]).

Differences between control and osteoarthritic synovial membranes could be observed macroscopically, since the increased volume of the pathological tissues, comparing to controls, was highly frequent (results not shown). To further characterize these differences, the two conditions were histologically analysed using hematoxylin staining (**Fig. 2.7**). Major variations between control and pathological tissues were observed in the membranes lining layers, which were composed by a monolayer of cells in control tissues (**Fig. 2.7**, **A**) and a hyperplasia of cells in osteoarthritic tissues (**Fig. 2.7**, **A**). The presence of mononuclear cell infiltrates in the subintimal layer of the pathological tissues (**Fig. 2.7**, **D**), accompanied by an

increased vascularization (**Fig. 2.7**, **C**), was also detected, in contrast to control tissues, indicating the presence of synovitis in the osteoarthritic membranes [88].

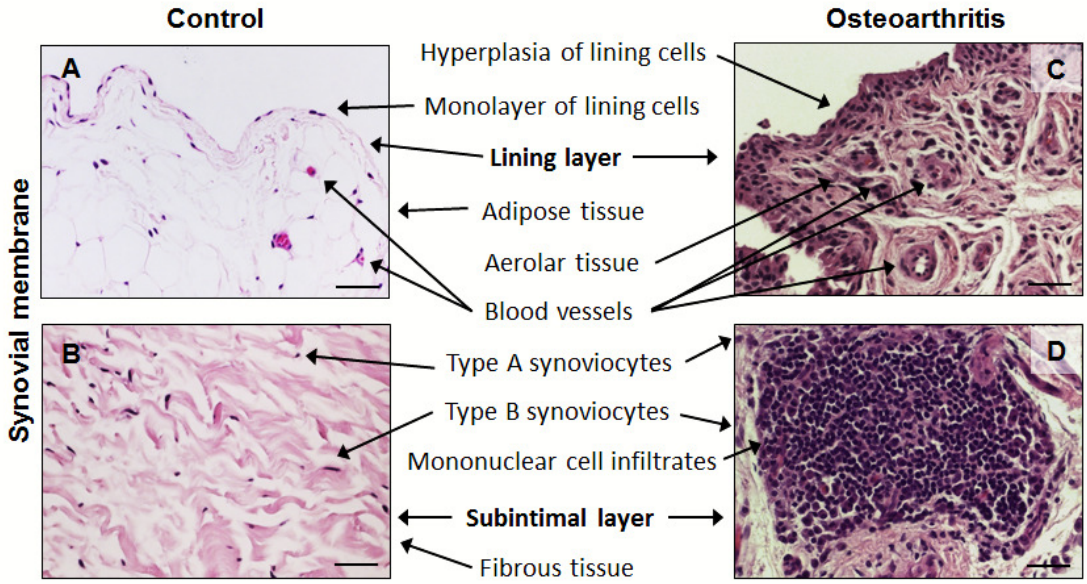

Fig. 2.7 – Histological characterization of control versus osteoarthritic synovial membrane tissues. Hematoxylin staining of control (**A** and **B**) and osteoarthritic synovial membrane tissue sections (**C** and **D**) showing the existing structures and morphological features in both tissue types. Distinct tissue layers are evidenced in bold. The identified cell types and subintimal structure types composing the tissue sections are indicated. Paraffin embedding was performed. Scale bars represent 100 µm (Adapted from Rafael et al., 2014 [189]).

To characterize the types of cells infiltrating the osteoarthritic synovial membranes, IHC analyses were performed using CD45, CD3 and CD68 antibodies (**Fig. 2.8**). Positive staining for CD45 indicated the presence of leucocytes (**Fig. 2.8**, **CD45**) and further staining with CD3 (**Fig. 2.8**, **CD3**) and CD48 (**Fig. 2.8**, **CD68**) suggested the presence of T lymphocytes and macrophages, respectively. The same analyses performed in control tissues did not detect the presence of inflammatory cells (results not shown).

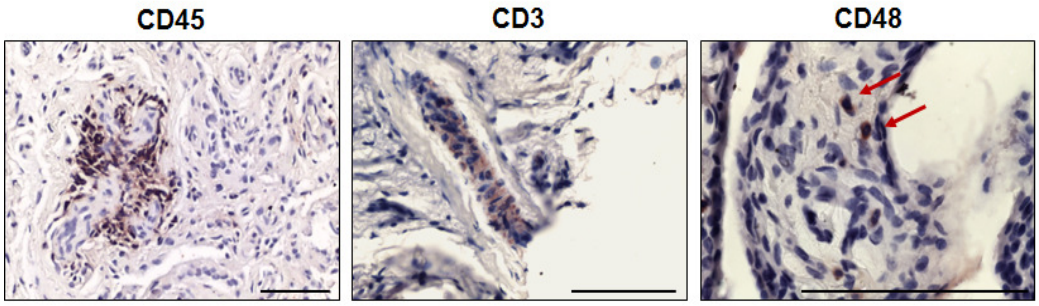

Fig. 2.8 – Immunodetection of T lymphocytes and macrophages in osteoarthritic synovial membranes. Immunohistochemistry (IHC) was performed using anti-CD45 (CD45), anti-CD3 (CD3) and anti-CD68 (CD68) antibodies that mark, respectively, leucocytes, T lymphocytes and macrophages. Red arrows indicate stained cells with anti-CD68 antibody (CD68). Samples were embedded with paraffin and counterstaining with hematoxylin. Scale bars represent 100 µm.

Ultimately, the presence of ectopic calcification was also investigated in synovial membrane tissues using the von Kossa staining (**Fig. 2.9**). Ectopic calcification sites were observed in all 12 analysed tissue sections from different OA patients, at smaller or greater extent depending on the sample, and spread without any apparent specific localization (**Fig. 2.9**, **C** and **D**). In control tissues, no pathological calcification was detected (**Fig. 2.9**, **A** and **B**).

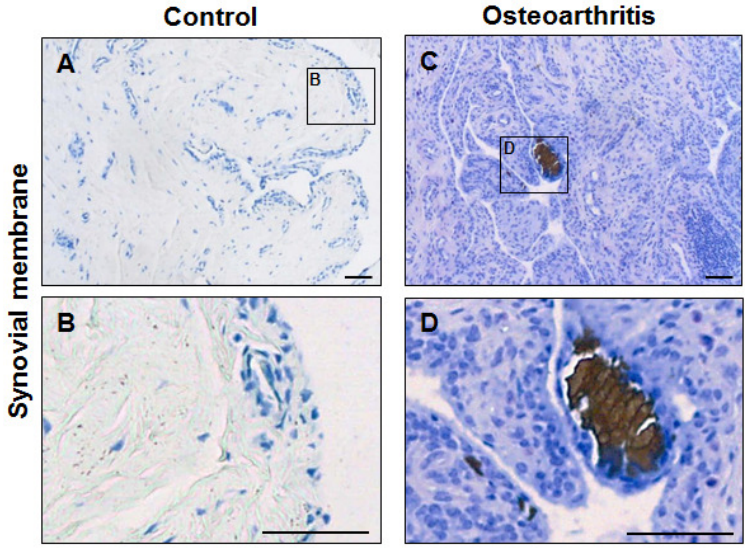

Fig. 2.9 – Detection of ectopic calcification in osteoarthritic synovial membrane through von Kossa staining. Control (**A** and **B**) and osteoarthritic (**C** and **D**) tissue sections of synovial membrane were analysed with von Kossa staining for the detection of pathological

calcification. Samples were embedded in paraffin and counterstained with toluidine blue. Scale bars represent 100 µm.

Altogether, the performed histological sample characterization showed notorious differences between control and osteoarthritic samples. Accordingly, results evidenced the presence of ectopic calcification in both osteoarthritic articular cartilage and synovial membrane tissues, and synovitis in the pathological membranes, clearly indicating their suitability for subsequent studies of GRP association with these OA pathological features in the following chapters.

2.4 Discussion

This chapter describes the collection and characterization of a biological sample bank comprising biospecimens from control individuals and knee OA patients, suitable for the study of OA. Within the scope of this project, this bank was crucial to investigate the involvement of GRP with the pathological mineralization and associated inflammation occurring in the disorder, and the search for candidate OA biomarkers, as further detailed in the following chapters.

Recent studies continue to illustrate the high impact of OA worldwide with increasing incidence [97], motivating the investigation of this disorder particularly focusing in the search for early OA diagnostic tools and the identification of efficient DMOADs to treat the disorder [96]. Osteoarthritis is the first cause of permanent job incapacity, one of the most frequent motifs of inability in the elderly, and one of the main reasons for primary care visits [104]. Therefore, the burden of OA not only involves the health impact of the disorder but also its social and economic weight [104]. knee OA is considered the prevalent form of the disease worldwide [97]. In Portugal, 6% of the population is estimated to be affected by this joint disorder, rheumatic diseases are pointed as the first cause for early retirement and knee OA is also indicated as the prevalent form of the disorder [103]. In concordance, knee arthroplasty interventions are frequent procedures performed at Centro Hospitalar do Algarve (Departamento de Ortopedia e Traumatologia, Faro, Portugal), with estimates of 144 surgeries per year. In addition, in the same hospital, it is estimated that 1200 new cases of different stages of knee OA are diagnosed every year (data supplied by Doctor Acácio Ramos). As a complex multifactorial disease there is still much to unveil about the mechanisms underlying OA, nevertheless, there are several known modifiable and preventable risk factors associated with OA development and progression [97]. Age is the strongest predictor of OA development mainly as consequence of chondrocytes terminal differentiation, which usually occurs around the age of 40 in humans [101,107]. Also, higher risk of developing OA is associated to the female gender, believed to be related with high estrogen levels [99]. In agreement, the collected OA group was characterized by high average age and the prevalence of the female gender. Obesity is also a key risk factor for knee OA, increasing its incidence three-fold and suggested to accelerate the progression of the disease [97]. In this study, obesity was also a present risk factor, with 8 of the 31 primary OA patients suffering from excess of weight. Interestingly, obesity has been described to affect OA not only because of

biomechanical overloading that favours subsequent cartilage degeneration, but also because of the suggested involvement with the metabolic syndrome (MetS) [95]. The MetS corresponds to a cluster of cardiometabolic disorders that result from the increasing prevalence of obesity, having as major components insulin resistance, central obesity, dyslipidaemia and hypertension [108]. Although the precise association between MetS and OA is still unclear, abnormal loading is related with inflammatory and metabolic imbalances in OA in part because it triggers the same signalling pathways as those induced by inflammatory cytokines [91]. Also, and in concordance with MetS association to OA, risk factors that contribute to the syndrome are generally considered risk factors for rheumatic diseases including OA [110]. Interestingly, comorbidities such as dyslipidaemia and hypertension were identified in the OA group of this study. Type II diabetes mellitus is also highly frequent in OA patients and considered a risk factor, although causality was not yet clearly demonstrated [110]. A possible reason for this association is related to hyperglycaemia, which may promote joint inflammation and cartilage degradation through oxidative stress, inflammatory mediators induction and advanced glycosylation end products [190]. Notably, type II diabetes mellitus was also diagnosed in some of the OA group patients. Among secondary OA, diseases that cause inflammation of the joint can also increase the risk of developing the disease later in life [102] and in fact, some of the analysed OA group patients presented secondary OA derived from gout or RA.

Calcium crystals deposition has been associated with destructive arthropathies such as OA [48]. Pathological calcification is believed to modify the biomechanical properties of cartilage, ultimately triggering crystal-induced stress which leads to proinflammatory cytokine and metalloproteinase production, and eventually chondrocyte apoptosis [48]. Calcium crystals have also been found in the synovial fluid and suggested to promote crystal-induced stress on synoviocytes, leading to the worsening of OA [91,123]. For subsequent studies of GRP association to the pathological calcification occurring in OA and associated inflammatory processes, sample histological characterization was performed focusing on these particular features. Accordingly, the presence of ectopic calcification was observed both in osteoarthritic cartilage and synovial membrane tissues, while no pathological mineralization was found in control samples. Also, the presence of synovitis was clearly identified in osteoarthritic synovial membranes, with the immunodetection of macrophages and T cells, described to be the most abundant leucocyte types infiltrating these tissues upon synovitis [87].

Altogether, the provided subject clinical information and specific sample histological characterization confirmed that the collected sample bank was suitable for the study of OA, in particular ectopic calcification and inflammation features, although the number and quantities of most of the biospecimens from the control group was reduced. All the analyses included in this project were therefore planned and the available samples distributed between them, according with the aims of each task, as described in **Table 2.III**. Cartilage, bone and synovial membrane tissue samples, histologically characterized in the present chapter, were further used in Chapter 3 for gene expression analysis and immune-based techniques to get the first insights into GRP association with OA, particularly regarding ectopic calcification processes. Synovial fluid and serum samples were also analysed in Chapter 3 by western blot to detected the presence of GRP in these fluids. Osteoarthritic cartilage and synovial membrane tissues from patient 27 of the OA group (**Table 2.II** and **Table 2.III**) were used in Chapter 4 for the development of an *in vitro* OA cell system, to further study the involvement of GRP in the pathological calcification and inflammatory processes occurring in OA. Osteoarthritic cartilage and synovial fluid samples were used in Chapter 5 for two-dimensional gel electrophoresis (2-DE) analyses aiming to study GRP potential as a biomarker for OA and search for novel OA biomarkers. A comparative proteomic analysis for the search of OA biomarkers was ultimately performed using the available serum samples from the collected sample bank.

Table 3.III – Identification of the samples from the collected biological bank used in the analysis performed in each chapter of this study

Chapter	Analysis	Subjects	
		Control group	OA group
2	Histology	1, 2, 4	1-12
3	Gene expression	1, 2, 4-9, 11	1-11, 13-15, 18-28
	Comparative gene expression	1, 2, 4, 6-9, 11	1-3, 9, 14, 18, 20-23, 25, 27
	SDS-PAGE	1-4	1-13, 16, 17, 27
	Histology	1, 2, 4	1-12, 16, 19, 27, 28
4	Cell culture development	-	27
5	SDS-PAGE	3, 13-15	28-31
	2-DE	6, 10, 12-14	3, 17, 28, 30-32, 35
	Calcium quantification	6, 7, 10-15	28-35
	Comparative proteomics	6, 10, 12-14	28, 30-32, 35

SDS-PAGE, sodium dodecyl sulphate-polyacrylamide gel electrophoresis; 2-DE, two-dimensional gel electrophoresis

2.5 Acknowledgements

The collection of human biological material for this study was only possible due to collaborations with Centro Hospitalar do Algarve (Departamento de Ortopedia e Traumatologia, Faro, Portugal), Hospital Particular do Algarve - Gambelas (Departamento de Ortopedia, Faro, Portugal) and Delegação do Sul do Instituto Nacional de Medicina Legal e Ciências Forenses (Faro, Portugal). In the former hospitals, we gratefully thanks Doctor Acácio Ramos who was the main collaborator involved in the collection of control and osteoarthritic biological material, and respective subject clinical information. Moreover, Doctor Acácio Ramos was always very interested about this project and constantly available to clarify any doubts regarding osteoarthritis medical aspects, therefore all his help was extremely appreciated. At Delegação do Sul do Instituto Nacional de Medicina Legal e Ciências Forenses, we specially thank Doctor Joana Luz who was the main collaborator involved in the collection of control samples and respective subject clinical information. The help of Doctor José Enriquez and technician Alexandra Teixeira, from Centro Hospitalar do Algarve (Departamento de Anatomia Patológica, Faro, Portugal), was also of great value. We gratefully thank Doctor José Enriquez, the head of the department, for allowing this collaboration and analysing several of the obtained histological characterization results, and Alexandra Teixeira for all the tissue paraffin embedding of this chapter and some of the tissue sectioning. This work was funded by projects PTDC/SAUESA/101186/2008 and PTDC/SAU-ORG/112832/2009 from Fundação para a Ciência e Tecnologia (FCT). Part of the work presented in this chapter represents our published results in Rafael et al., 2014 [189].

Chapter 3

Predominance of GRP-F1 in articular tissues and association of undercarboxylated Gla-rich protein with osteoarthritis

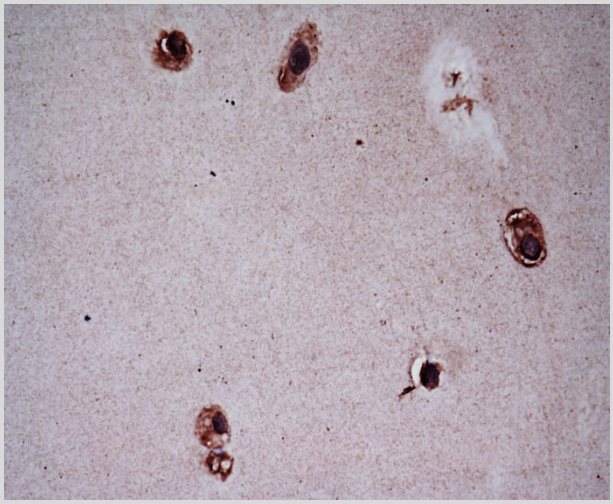

Abstract

The extracellular matrix mineralization of articular tissues is a common feature of osteoarthritis (OA), contributing for disease progression and frequently associated to severe forms of the pathology. Ectopic calcification-related proteins, such as Gla-rich protein (GRP), are therefore potential targets to study the mechanisms involved with OA development. In this chapter, the association of GRP with OA was for the first time investigated at transcription and translational levels. Four alternatively spliced transcripts of GRP gene, GRP-F1, F2, F3, and F4, were previously identified in mice and zebrafish. Using a RT-PCR strategy, two novel GRP splice variants were unveiled in human and termed GRP-F5 and F6. Both alternative transcripts were characterized by the loss of carboxylation motifs and GRP-F6 also lacked secretion motifs. Moreover, GRP-F2, F3, and F4 were not detected in human. Notably, GRP-F1 transcript, corresponding to the full length protein, was found to be the predominant expressed variant in articular tissues, empathizing that it should be the variant with greater contribution for OA development. Moreover, GRP-F1 was shown to be upregulated in osteoarthritic cartilage. GRP accumulation patterns in osteoarthritic tissues and fluids was evaluated using a combination of immune-based techniques, namely western blot, immunohistochemistry and immunofluorescence, and specific antibodies against total, carboxylated (cGRP) and undercarboxylated (ucGRP) GRP. Such approaches demonstrated that both protein forms are immunodetected in human osteoarthritic bone, articular cartilage, synovial membrane, synovial fluid and serum, and accumulated in sites of ectopic calcification. Importantly, it was shown that ucGRP was the predominant entity associated to osteoarthritic cartilage and synovial membrane, whereas cGRP was preferentially accumulated in the same tissues, in control conditions. Similarly, undercarboxylated matrix Gla protein was also the predominant form accumulating in osteoarthritic cartilage, suggesting that the impairment of γ-carboxylation in these vitamin K-dependent proteins might be associated with OA. Overall, the obtained results relate for the first time GRP with OA, indicating the predominance of GRP-F1 transcript in articular tissues, associating GRP to sites of pathological mineralization and clearly relating ucGRP with OA-affected tissues. Moreover, our immunohistochemistry results revealed that GRP association with OA was not restricted to sites of ectopic calcification in synovial membrane tissues, suggesting the involvement in other cell mediated processes, which will be addressed in the following chapter.

3. 1 Introduction

Several determinants are known to contribute for the pathogenesis and progression of osteoarthritis (OA), including the deposition of calcium-containing crystals in articular cartilage [48]. Basic calcium phosphate (BCP) and calcium pyrophosphate dihydrate (CPPD) are the two major forms of calcium crystals accumulating in osteoarthritic cartilage [49,137,138]. In addition, the accumulated crystals are prone to be released into the synovial fluid and spread to other joint tissues, such as the synovial membrane [91,123]. The presence of pathological calcification in OA is associated with increased disease severity, and the regulation of calcium availability and subsequent deposition in chondrocyte extracellular matrix (ECM) is regarded as a determinant factor for disease progression [48,50,137,138]. Cartilage calcification is a multifactorial process including the imbalance between pro-mineralization factors and inhibitors [49,50]. In fact, the dysregulation in the production of mineralization inhibitors has been considered a crucial factor favouring cartilage calcification and the deposition of calcium-containing crystals [50]. Therefore, the role of calcification inhibitors in the pathogenesis of OA was highlighted, prompting the study of vitamin K-dependent proteins (VKDPs), in particular Gla-rich protein (GRP), and its potential association with this joint disorder.

Vitamin K is an essential cofactor for the post-translational modification of VKDPs, where specific glutamate (Glu) residues can be modified to calcium binding γ-carboxyglutamic acid (Gla) residues [1]. Vitamin K is essential for preventing soft tissue mineralization and VKDPs such as osteocalcin (OC), matrix Gla protein (MGP) and, more recently, GRP, are associated with skeletal metabolism [3,56]. Also, subclinical vitamin K levels have been related with increased risk of OA development [82-84] and both OC and MGP proteins have already been associated with the disease. While the presence of undercarboxylated OC (ucOc) in serum is considered a biomarker for OA, associated to vitamin K metabolism deficiency [94], the absence of carboxylated MGP (cMGP) in osteoarthritic chondrocytes was suggested as an important mechanism for increased osteoarthritic cartilage mineralization [92].

Gla-rich protein, the most recently discovered VKDP, is composed by a high density of γ-carboxylated Glu residues which indicated a strong calcium binding capacity [54]. Gla-rich protein mineral binding capacity was further confirmed by several studies showing its accumulation at sites of pathological calcification in human tissues [14-16] and *in vitro*

calcium mineral-binding capacity [15]. Although the function and molecular mechanisms of action remain to be clarified, GRP has been suggested as a modulator of calcium availability in the ECM [14,15] and an inhibitor of calcification in the cardiovascular system depending on its γ-carboxylation status [16]. In concordance, and although GRP-deficient mice did not reveal evident phenotypic alterations in bone and cartilage, GRP knockdown in zebrafish resulted in severe growth retardation and perturbance of skeletal development [72]. Moreover, warfarin treatment mimicked the GRP knockdown phenotype, suggesting an essential role of γ-carboxylation for GRP function [72]. Although GRP has been shown to function as a negative regulator of osteogenic differentiation [74,75] and to be downregulated by bone morphogenetic protein 2 (BMP2) in chondrogenic cells [75], recent data suggested that GRP is upregulated by both runt-related transcription factor 2 (Runx2) and osterix (Osx), stimulating osteoblast differentiation and nodule formation [77]. Altogether, this conflicting data reinforce the need for additional characterization of GRP association with human pathological conditions such as OA. In mice, four alternatively spliced transcripts of GRP gene were identified - GRP-F1, F2, F3, and F4 - differing by exon 2, exon 4, or both, which were associated with early stages of chondrogenesis and suggested as possibly implicated in skeletal pathologies in case of an imbalanced expression [76]. The same variants were also detected in zebrafish [72,73], however, no splice variants were ever described in humans.

In this chapter, GRP potential association with OA was studied for the first time at gene and protein levels, using the biological sample bank described in the previous chapter. Accordingly, here is described (i) the analysis of GRP splice variants existing in the human gene, (ii) the *in silico* characterization of human GRP protein isoforms, (iii) the expression pattern of each variant in control and osteoarthritic tissues, (iv) the immunodetection of total, carboxylated (cGRP) and undercarboxylated (ucGRP) GRP in OA-affected tissues and body fluids, (v) GRP immunodetection in osteoarthritic bony cells, and (vi) the spatial distribution of c/ucGRP in control and osteoarthritic tissues.

3.2 Experimental procedures

3.2.1 Biological material and sample processing

Control and osteoarthritic articular cartilage, subchondral bone and synovial membrane tissues, and osteoarthritic synovial fluid and clotted blood samples, were obtained and processed as described in Chapter 2, section 2.2.1.

3.2.2 RNA extraction

Total RNA was extracted from control and osteoarthritic articular cartilage, bone and synovial membrane samples as described by Chomczynski and Sacchi [191]. RNA concentration was determined by spectrophotometry at 260 nm and quality evaluated by agarose denaturating gel electrophoresis.

3.2.3 Human GRP cDNA amplification

One microgram of total RNA was treated with DNase I (Promega, Madison, WI, USA) and reverse-transcribed using Moloney-murine leukemia virus reverse transcriptase (MMLV-RT), RNase Out (both from Invitrogen, Carlsbad, CA, USA), and an oligo(dT) adapter (5'-ACGCGTCGACCTCGAGATCGATG(T)13-3'), according to manufacturer's recommendations. GRP coding sequences were amplified by nested PCR starting with 250 ng of reverse-transcribed RNA and Taq DNA polymerase (Invitrogen) using primers listed in **Table 3.I** (Complete CDS, CDS nested).

All nested PCR products were size-separated onto a 2 % w/v agarose gel and selected fragments were purified using the GFX Gel Band Purification kit (GE Healthcare, Waukesha, WI, USA), cloned into pCRII-TOPO vector (Invitrogen) and sequenced (Centro de Ciências do Mar, CCMar, Faro, Portugal).

Table 3.I – List of primers used for RT-PCR

Gene	Primer Fw	Primer Rv	Amplicon
18S	GGAGTATGGTTGCAAAGCTGA	ATCTGTCAATCCTGTCCGTGT	Loading control
	GACGCCTGGTCTGCCTTGTGGG	GAAGCCAGGGGAAGCCACTGTAGGT	Complete CDS
	TCCTGGACGGAGCCCCTACCT	ACACGGGGATGCCAATGGTGCTAC	CDS nested
GRP	GTCCCCCAAGTCCCGAGATGAGG	CCTCCACGAAGTTCTCAAATTCATTCC	F1
	TCCTGGACGGAGCCCCTA	GCTTCTGCCTGTTTTCCACTTCAC	F5
	TCCTGGACGGAGCCCCTA	GCTTCTGCCTGTTTTCCATAGACA	F6

3.2.4 Expression profile

To determine the presence of GRP alternative transcripts among several samples of control and osteoarthritic articular cartilage and synovial membrane, specific primers designed in order to specifically amplify each of the splice variants were used (F1, F5 and F6, **Table 3.I**), while human ribosomal 18S was used as a reference gene (18S, **Table 3.I**). RT-PCR amplification was achieved using 25 ng cDNA and SsoFast EvaGreen supermix (Bio-Rad, Richmond, CA, USA) in reactions of 50 cycles.

3.2.5 Genomic sequence analysis

Human genomic sequences (GenBank accession numbers NC_000010) were used to confirm the transcript structure using Spidey mRNA-to-genomic alignment tool at National centre for biotechnology information (NCBI). Prediction of signal peptide, protein targeting, glycosylation and phosphorylation sites was performed using SignalP, TargetP, NetNGlyc, NetOGlyc and NetPhos, respectively, available at Centre for Biological Sequence analysis (CBS) portal (http://www.cbs.dtu.dk/services). All the obtained predictions were confirmed using available tools at Expasy portal (http://www.expasy.org/).

3.2.6 Protein extraction

Two distinct protein extraction procedures were used in this study: mineral-bound proteins were extracted from osteoarthritic bone using a previously described method [192], while total protein extracts were obtained from osteoarthritic articular cartilage and synovial membrane samples using Laemmli buffer.

Bone was reduced to powder using a mortar and liquid nitrogen. A portion of 100 g was washed three times for 8-10 h with a 10-fold excess of 6 M guanidine HCl v/w to remove the proteins that were not sequestered in the mineralized matrix, followed by extensive washes with water and finally with acetone. Mineral-bound proteins were extracted from the clean bone powder using a 10-fold excess of 10 % formic acid during 4 h at 4 °C as described [192]. The resulting soluble acid extract was separated from the insoluble collagenous matrix by fibreglass filtration and dialyzed at 4 °C against 50 mM HCl, using 3500 molecular weight tubing (Spectra-Por 3, Spectrum, Gardena, CA, USA), during 2 days to remove all dissolved mineral. The dialyzed acid extract was freeze-dried, dissolved in 6 M guanidine HCl, 0.1 M Tris pH 9, and dialyzed against 5 mM ammonium bicarbonate to precipitate GRP. The obtained pellet was dissolved in 6 M guanidine HCl, 0.1 M Tris pH 9, and dialyzed against 50 mM HCl. The protein content of the extract was estimated based on the general reference setting that a protein solution with an extinction coefficient (E) of 0.1% (1 mg/ml) produces an absorbance of 1.0 at 280 nm (whit a path length of 1 cm) [193].

Cartilage and synovial membrane samples were reduced to powder using a mortar and liquid nitrogen and 5 g of each tissue were lysed in Laemmli buffer and following sonicated on a Vibra-cell apparatus (Sonics & Materials, Inc., Newtown, MA, USA) using 5 cycles of 30 sec, with intervals of 15 sec on ice, at 60 % amplitude. The protein content of the extracts was estimated by absorbance at 280 nm.

3.2.7 SDS-PAGE and western blot

Aliquots of total protein extracts obtained in the previous section and direct samples of osteoarthritic synovial fluid and serum were dissolved/diluted in lithium dodecyl sulphate (LDS) sample buffer (NuPage, Invitrogen) containing reducing agent, and boiled during 5 min at 95 ^{o}C. Samples were then size-separated by sodium dodecyl sulphate-polyacrylamide gel electrophoresis (SDS-PAGE) on a 4-12 % w/v gradient polyacrylamide precast gel containing 0.1 % w/v SDS (NuPage, Invitrogen) and the protein profiles were revealed by staining with coomassie brilliant blue (CBB) (Bio-Rad). The bony tissue extract profile was also analysed with DBS (Gla-specific stain; 8.5 mM 4-diazobenzene sulfonic acid (Sigma-Aldrich, St. Louis, MO, USA), as described [194].

For western blot (WB) analysis, proteins separated by SDS-PAGE were subsequently transferred onto a nitrocellulose membrane [192]. Detection of total, cGRP and ucGRP was

performed incubating the membranes overnight with the primary antibodies polyclonal rabbit CTerm-GRP [14] and chicken cGRP [15] (5 µg/mL and 1 µg/mL, respectively, GenoGla Diagnostics, Faro, Portugal), and mouse monoclonal ucGRP [15] (7.3 µg/mL, Vitak BV, Maastricht, the Netherlands), respectively. Detection of carboxylated (cMGP) and undercarboxylated (ucMGP) MGP in bony tissue extract was performed using the primary antibodies mouse monoclonals cMGP and ucMGP (10 µg/mL, both from IDS, Bolton, UK). Antibodies were diluted in 5% w/v bovine serum albumin (BSA) powder in TBST (15 mM NaCl, 10 mM Tris-HCl buffer pH 8, 0.05% Tween 20). Immunodetection was achieved using species-specific secondary horseradish peroxidase conjugated antibodies (Sigma-Aldrich) and Western Lightning Plus-ECL (PerkinElmer Inc., Waltham, MA, USA). All WB analysis were repeated at least three times using samples of different subjects. To estimate the molecular weight of the proteins bands both in SDS-PAGE and WB, Precision Plus Protein Dual Xtra Standard (Bio-Rad) was used.

3.2.8 N-terminal amino acid sequence analysis

The mineral-bound protein extract obtained from osteoarthritic bone in section 3.2.6 was separated by SDS-PAGE, as previously described, in several gel lanes and blotted onto a polyvinylidene fluoride (PVDF) membrane (Applied Biosystems, Foster city, CA, USA) for 1 h at constant 80 mA [195]. After transfer, the PVDF membrane was washed with water for 5 min, stained with 0.2% w/v CBB in 50% v/v methanol for 5 min, de-stained with 7.5% v/v acetic acid, 10% v/v methanol until bands were visible, and washed with 20% v/v methanol to remove salts or contaminants. Target bands were cut off for further analysis by automatic Edman degradations, using an Applied Biosystems 491 HT sequencer, at Instituto de Biologia Experimental e Tecnológica (IBET) (Analytical Laboratory, Oeiras, Portugal). The search for protein sequences showing homology with the obtained N-terminal sequences was performed at NCBI in the same institute.

3.2.9 Protein identification by mass spectrometry and data analysis

Protein analysis of the mineral-bound protein extract obtained from osteoarthritic bone in section 3.2.6 was also performed by mass spectrometry (MS). For that, gel bands were excised from SDS-PAGE gels, performed as described in section 3.2.7, and sent to Instituto

de Tecnologia Química e Biológica (ITQB) (Mass Spectrometry Laboratory, Oeiras, Portugal) for subsequent protein sequencing by liquid chromatography-tandem mass spectrometry (LC-MS/MS). Proteins were first in gel digested and the tryptic peptides processed also as described [196]. Protein sequencing was conducted using a Thermo Finnigan LTQ mass spectrometer (Thermo Scientific) coupled with MALDI (matrix-assisted laser desorption/ionization). Protein identification using LC-MS/MS raw data was performed at the same institute with Mascot Daemon software (Matrix science, Boston, MA, USA) and results of the database search were analysed using NCBI.

3.2.10 Histological techniques

Cartilage, bone and synovial membrane samples for histological analysis were embedded in paraffin and glycol methacrylate, then sectioned and analysed with the von Kossa method as described in Chapter 2, section 2.2.2. When sections were counterstained, toluidine blue was the method of choice.

3.2.11 Immunohistochemistry

Immunohistochemistry (IHC) was performed as described in Chapter 2, section 2.2.3, to detect specific antigens in articular cartilage, bone and synovial membrane samples. Antigen retrieval of bone tissue sections was performed by incubation with 2 mg/mL hyaluronidase (Sigma-Aldrich) during 1h at 37 °C. As primary antibodies, polyclonal rabbit CTerm-GRP and chicken cGRP (5 and 1 µg/mL, respectively, GenoGla Diagnostics), and mouse monoclonals ucGRP (7.3 µg/mL, Vitak BV), cMGP and ucMGP (both at 10 µg/mL, IDS) were used. Images were obtained using an Axio Imager Z2 microscope (Zeiss, Jena, Germany) equipped with a digital camera and Axovision imaging software.

3.2.12 Tartrate-resistant acid phosphatase localization

Tissue sections of osteoarthritic bone were saturated with 0.1 M acetate buffer containing 50 mM dehydrated disodium tartrate, pH 5.5. Then, 2 ml of 4 % w/v $NaNO_2$ were added to 1 ml of pararosaniline (PRS) (Sigma-Aldrich) to promote the hexazotization. The incubation media was prepared using 30 ml of the first acetate buffer containing 1 ml

hexazotized PRS, 600 µl 2 % w/v $MgCl_2$ and 2 ml of the enzymatic substrate (2 mg naftol AS-TR phosphate in 2 ml N,N-dimethylformamide). The tartrate-resistant acid phosphatase (TRAP) reaction is sensitive to light, thus, tissue sections were maintained in the dark while in incubation media for 2-3 h. Images were obtained using an Axio Imager Z2 microscope (Zeiss, Jena, Germany) equipped with a digital camera and Axovision imaging software.

3.2.13 Immunofluorescence

Immunofluorescence (IF) analysis were performed in paraffin sections of control and osteoarthritic synovial membrane tissues. Antigen retrieval was performed by boiling in 0.2 % v/v citric acid, pH 6. After peroxidase and nonspecific antibody blockings, performed as described in Chapter 2, section 2.2.3, incubations with the primary antibodies polyclonal chicken cGRP (5 µg/mL, GenoGla Diagnostics) and mouse monoclonals ucGRP (14.6 µg/mL, Vitak BV) were performed overnight at room temperature (RT). Samples analysed with cGRP were then incubated with biotinylated goat anti-chicken antibody (2 µg/mL, Vector laboratories Ltd.) for 1h and then with avidin kit A1100 (Vector laboratories Ltd.) also for 1h at RT. Samples analysed with ucGRP were directly incubated for 1h with the secondary antibody Dylight 549 HAM (Vector laboratories Ltd.) at RT. Negative controls consisted of the substitution of the primary antibody with TBST buffer. Cell nuclei were stained with cell nuclei were stained with 6-diamidino-2-phenylindole (DAPI). Images were obtained using a Zeiss Axioplan 2 (Zeiss, Jena, Germany) equipped with a digital camera and Image-Pro Plus acquisition software (version 6, MediaCybernetics, Bethesda, MD, USA). Final images were processed using Image J Version 1.41m.

3.3 Results

3.3.1 Identification of two novel GRP splice variants in human

The first approach towards investigating the possible association of GRP with OA was the analysis of GRP gene expression in OA-affected tissues. Four GRP splice variants had been previously identified in mouse and zebrafish [72,73,76], thus, the presence of the same transcripts was investigated in osteoarthritic samples of articular cartilage, bone and synovial membrane. For that, a nested RT-PCR strategy was used with primers designed in exons 1 and 5 (**Table 3.I**, Complete CDS and CDS nested and **Fig. 3.1**, **A**), in order to amplify the complete coding sequence including the five exons of GRP gene. Three different fragments were detected in all the analysed tissues with sizes approximately between 300 bp and 500 bp (**Fig. 3.1**, **B**). Genomic sequence analysis revealed that the longest fragment composed of 504 bp (**Fig. 3.1**, **B**), corresponded to the complete open reading frame for full length GRP (GRP-F1, GenBank accession number JX169863). The remaining cDNA fragments of 408 and 342 bp (**Fig. 3.1**, **B**) were also confirmed to be GRP after analysis, however, the sequences were not identical to any of the previously described transcripts, representing two novel GRP splice variants. The two new GRP alternative transcripts were therefore named GRP-F5 and F6 (GenBank accession numbers JX169864 and JX169865, respectively), following the previous nomenclature adopted for mouse and zebrafish models [72,76].

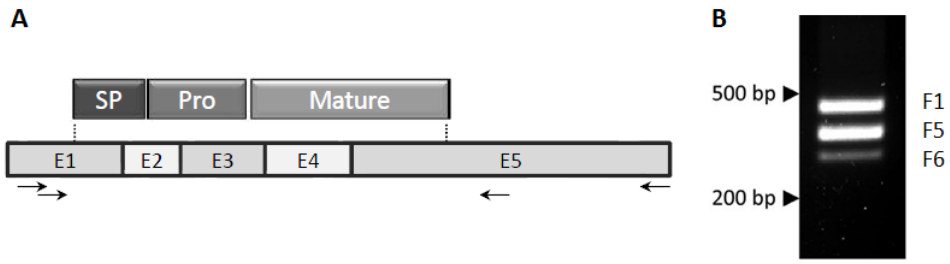

Fig. 3.1 – Schematic representation of the design primers and respective amplified GRP transcripts in human osteoarthritic cartilage. (**A**) Primers localization is indicated by two arrows pairs: the outside set was used in a first PCR, while the internal set was used in a second nested PCR. SP indicates signal peptide; Pro, propeptide; Mature, mature protein; E1 to E5 represent the sequence exons. (**B**) Nested RT-PCR analysis from OA cartilage RNA showing amplification of GRP-F1, F5 and F6 splice variants. Approximated transcript sizes (in base pairs, bp) are indicated (Adapted from Rafael et al., 2014 [189]).

The presence of the newly identified or additional GRP alternative transcripts was investigated in a small group of control and osteoarthritic samples of articular cartilage, bone and synovial membrane and no other GRP splice variant was identified apart from GRP-F1, F5 and F6 (data not shown). These preliminary results were further supported by subsequent studies ongoing in the laboratory using control and osteoarthritic samples of cartilage, bone and synovial membrane, from which a total of 43 GRP positive clones were sequenced, and only the same three variants were detected [189].

3.3.2 *In silico* characterization of human GRP protein isoforms

For the three detected GRP transcripts, GRP-F1, F5 and F6, splicing sites and coding regions were predicted using the Spidey mRNA-to-genomic alignment tool at NCBI (**Fig. 3.2**, **A**). Considering the unprocessed protein isoforms, full length GRP-F1 encodes 138 aa, while the two novel transcripts encode putative proteins of 106 (GRP-F5) and 84 (GRP-F6) aa (**Fig. 3.2**, **B** and **C**). Both GRP-F5 and F6 variants lack exon 3, an exon skipping that had never been described in previously analysed species, which results in the loss of the γ-glutamyl carboxylase (GGCX) recognition site and the furin-like cleavage site (RGKR, **Fig. 3.2**, **A** and **B**). This is of particular interest since the binding to carboxylase and propeptide cleavage occurring in GRP-F1 would be lost, and consequently the γ-carboxylation of Glu residues and mature protein processing could possibly be altered. In addition to the modifications produced in GRP-F5, the F6 variant also lacks exon 2, which codes for the C-terminal region of the signal peptide that will be shorter in this variant (**Fig. 3.2**, **A**-**C**).

Prediction of signal peptide and protein targeting was analysed using SignalP and TargetP CBS tools. The analysis revealed that despite the probability of GRP-F6 shorter signal peptide functionality is lower (D = 0.634) than for F1/F5 variants (D = 0.731), all D-scores were above SignalP algorithm cut off [197], indicating that targeting to the secretory pathway is still possible and cannot be discarded. Moreover, and considering the signal peptide processing for both variants, GRP-F5 and F6 will be 80 and 67 aa long, respectively, comparable to the 74 aa of F1 mature isoform in terms of protein size (**Fig. 3.2**, **C**).

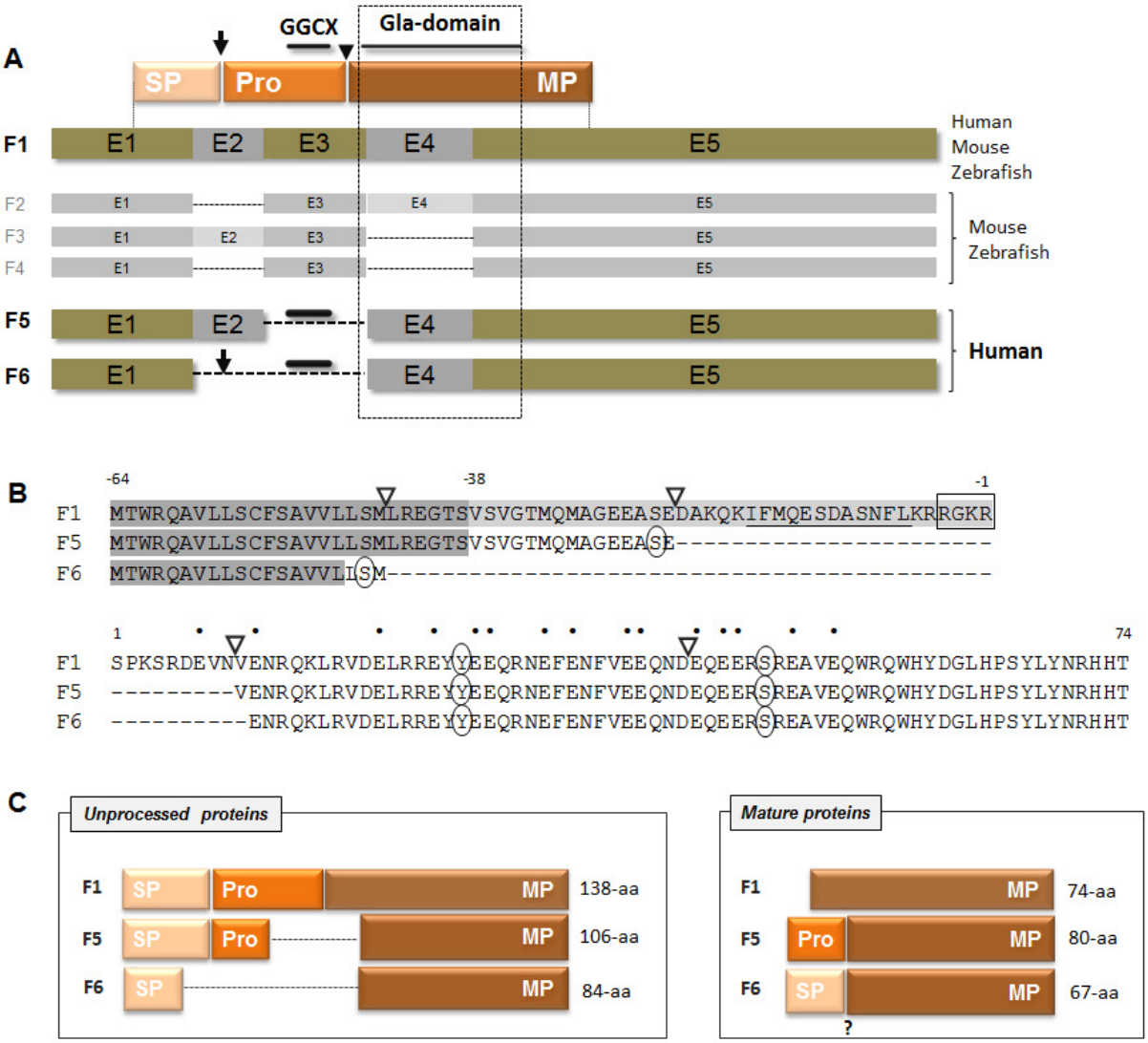

Fig. 3.2 – Identification of novel GRP alternative splice variants in human. (**A**) Schematic representation of the new GRP splice variants (F5 and F6) and previously known data for mouse and zebrafish (F1, F2, F3 and F4) [72,76]. Arrow indicates putative signal peptide cleavage site; arrow head, furin-like cleavage site; SP, signal peptide; Pro, propeptide; MP, mature protein; GGCX, γ-glutamyl carboxylase putative recognition site; E1 to E5 represent the sequence exons. (**B**) Alignment of human GRP splice variants deduced proteins. Triangles indicate intron insertion sites; underlined sequence, GGCX putative recognition site; rectangle, furin-like proteolytic site (RGKR); black dots, putative γ-carboxylated Glu residues; circles, predicted tyrosine and serine phosphorylated residues; signal peptide is shown in dark grey while propeptide in light grey. First residue of mature protein in F1 isoform is assigned as number 1 and signal peptide, propeptide and mature protein are indicated accordingly. (**C**) Unprocessed and mature protein structures and length (aa, on the right) of the three human GRP variants. The question mark highlights the doubt concerning F6 variant signal peptide processing (Adapted from Rafael et al., 2014 [189]).

Regarding post-translational modifications the probability of N- or O-glycosylation and tyrosine or serine phosphorylation was analysed using NetNGlyc, NetOGlyc and NetPhos

tools, respectively, from CBS. Results revealed no indications of glycosylation in any of the human variants, but high probability of phosphorylation in one tyrosine residue in all variants, and in one or two serine residues in GRP-F1 or GRP-F5/F6, respectively (**Fig. 3.2**, **B**).

3.3.3 GRP-F1 variant is the predominant transcript in both control and osteoarthritic tissues

To further explore the expression pattern of human GRP-F1, F5 and F6 transcripts, primers that specifically amplified individual variants were used (**Table 3.I**, F1, F5 and F6, **Fig. 3.3**). These variant-specific primers were strategically designed and validated in the laboratory [189] prior its use in this project. The expression pattern of GRP-F1, F5 and F6 transcripts in control and osteoarthritic cartilage and synovial membrane samples was therefore analysed to investigate a possible association with OA (**Fig. 3.4**). As described in Chapter 2, the reduced number of collected control samples and their low quantities was a limitation in this study, therefore the analysis of gene expression was only quantitatively evaluated by RT-PCR (subject information of each sample used in this analysis is described in Chapter 2, sections 2.3.1 and 2.4.1, **Tables 2.I**, **2.II** and **2.III**). Results suggested a higher expression of GRP-F1 in cartilage samples of OA patients (**Fig. 3.4**, **A**) when compared to controls, while no clear association could be determined in synovial membrane tissues (**Fig. 3.4**, **B**). GRP-F5 was clearly less represented than F1 in both tissue types, (**Fig. 3.4**, **A** and **B**) whereas GRP-F6 could not be detected in any of the analysed cartilage samples, either control or osteoarthritic (**Fig. 3.4**, **A**), but it was found in certain synovial membrane samples (**Fig. 3.4**, **B**) suggesting a restricted expression pattern.

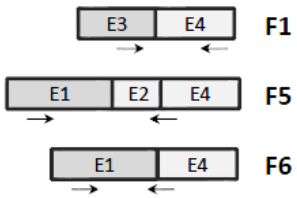

Fig. 3.3 – Schematic representation showing the localization of transcript-specific sets of primers for GRP amplification. F1, F5 and F6 indicate the respective GRP variant and arrows indicate the primers localization. E1 to E4 represent the respective exons (Adapted from Rafael et al., 2014 [189]).

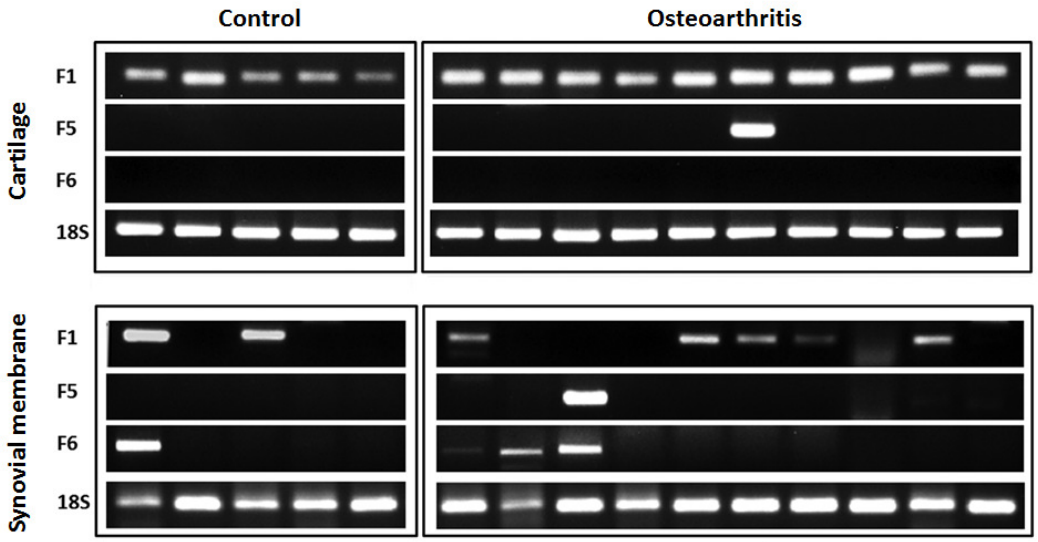

Fig. 3.4 – Evidences for the predominance of GRP-F1 variant in human cartilage and synovial membrane and higher expression in osteoarthritic cartilage. The expression pattern of the three human GRP splice variants (F1, F5 and F6) was investigated in cartilage and synovial membranes of controls and osteoarthritic patients by RT-PCR, using transcript variant specific primers. 18S was used as a loading control (Adapted from Rafael et al., 2014 [189]).

Overall, GRP-F1 transcript appears to be the predominant expressed form in both control and osteoarthritic cartilage and synovial membrane tissues, and with apparent higher expression in OA-affected cartilage comparing to controls, whereas GRP-F5 and F6 are barely or not detectable.

3.3.4 Carboxylated and undercarboxylated GRP forms are accumulated in OA-affected tissues and fluids

After confirming the predominance of GRP-F1 variant, corresponding to the full length GRP, both in control and OA-affected tissues, the patterns of protein accumulation and γ-carboxylation status were studied. For that, three different antibodies against the total (CTerm-GRP), carboxylated (cGRP) and undercarboxylated (ucGRP) GRP forms were used. All three antibodies were developed against synthetic peptides (**Fig. 3.5**) [14,15] and previously tested and validated for conformation specificity using several human tissues, namely breast, skin and heart valves, and calcified aortic valves protein extracts, as described [14-16].

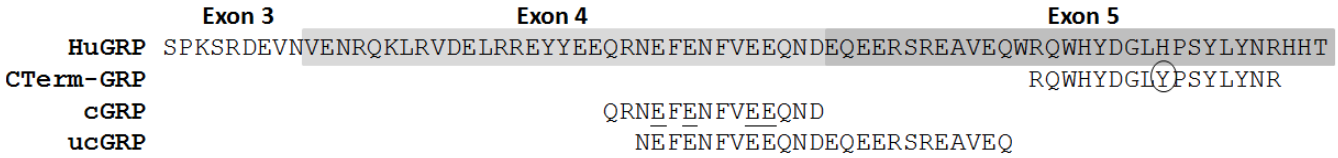

Fig. 3.5 – Total GRP (CTerm-GRP) and conformation-specific antibodies for γ-carboxylated (cGRP) and undercarboxylated (ucGRP) GRP forms. Amino acid sequence alignments of mature human GRP-F1 form (HuGRP), limited to a portion of exon 3 (white) and complete exons 4 (light grey) and 5 (grey), and synthetic peptides used as antigens for development of the three antibodies are shown. Underlined E in cGRP correspond to Gla residues while E in ucGRP to Glu residues. The circle in the peptide sequence used for the development of CTerm-GRP antibody highlights the different amino acid between human and rat GRP sequences (Adapted from Viegas et al., 2014 [15]).

GRP was first identified in sturgeon calcified cartilage [54], thus, a similar extraction procedure, specifically designed to isolate mineral-bound proteins, was chosen to analyse human GRP accumulation in osteoarthritic bone. The content of the mineral-bound protein extract was revealed on SDS-PAGE gels with CBB staining (**Fig. 3.6**, CBB) and the presence of Gla proteins was assessed with DBS analysis (**Fig. 3.6**, DBS). Two protein bands with apparent molecular weights of 13 and 18 kDa were observed with CBB and DBS staining (**Fig. 3.6**, CBB and DBS), indicating the presence of Gla-containing proteins in the extract. Results were correlated with those of sturgeon calcified cartilage extracts, performed under the same gel analysis conditions and where two Gla-containing entities with similar migration behaviours were identified as GRP (18 kDa) and MGP (13 kDa) [54]. Comparing with the sturgeon extract, the two bands showed lower DBS staining intensity in the analysed human osteoarthritic bone extract suggesting a decreased degree of γ-carboxylation.

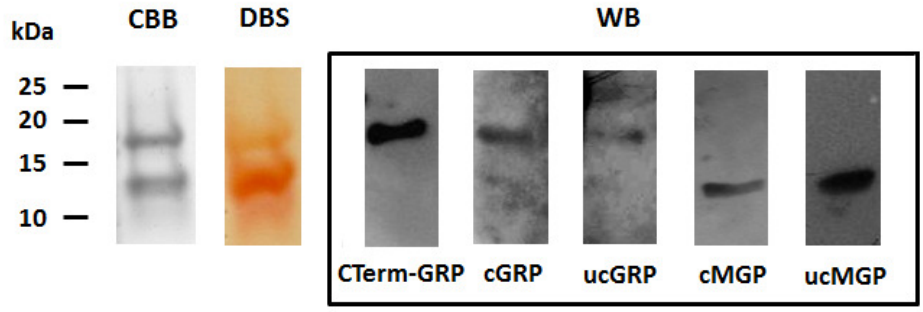

Fig. 3.6 – SDS-PAGE and western blot (WB) analysis of mineral-bound proteins isolated from human osteoarthritic bony extracts. Gels were stained with coomassie brilliant blue (CBB) (20 µg) and diazobenzene sulfonic acid (DBS) (40 µg) and WB analysis (2 µg) were

performed using CTerm-GRP, cGRP, ucGRP, cMGP and ucMGP antibodies. Relevant molecular mass markers (kDa) are indicated on the left of the panels.

The presence of GRP in the human bone extract was further investigated by WB using the three available antibodies and the positive immunodetection of an 18 kDa entity (**Fig. 3.6,** CTerm-GRP, cGRP and ucGRP), indicated the presence of both c/ucGRP forms in this tissue. The presence of MGP in the extract was also investigated by WB and the results showed that the 13 kDa entity visualized with CBB and DBS staining (**Fig. 3.6**, CBB and DBS) could represent MGP, since both c/ucMGP specific antibodies revealed a positive reaction (**Fig. 3.6**, cMGP and ucMGP). Altogether these results evidenced the accumulation of GRP and MGP in the osteoarthritic human bone extract and gave strong indications for the association of both carboxylated and undercarboxylated GRP and MGP protein forms with the bone mineral phase.

In addition to the SDS-PAGE and WB analysis, attempts to further characterize both GRP and MGP protein forms present in the human osteoarthritic bone extract were performed by N-terminal sequencing and LC-MS/MS analysis. Since the initial identification and characterization of GRP from sturgeon calcified cartilage extracts was achieved through N-terminal amino acid sequencing [54], the N-terminal sequence of the 13 and 18 kDa protein bands (**Fig. 3.6**, CBB and DBS) was performed. Results showed that none of the protein bands corresponded to a single protein entity, with multiple amino acids detected in each Edman cycle. However, the first 5 amino acids corresponding to the N-terminal of human MGP were identified in the 13 kDa indicating the presence of MGP (results not shown). Notably, a Glu residue was identified in position 2 where a Gla residue was expected [11], in concordance with WB positive results for undercarboxylated MGP (**Fig. 3.6**, ucMGP). The obtained results for the 18 kDa band evidenced phospholipase A2 as the predominant protein, suggesting that GRP might be present in the extract in very low amounts, which combined with sample complexity, might require more sensitive methods, such as MS, for sequence identification and characterization. Accordingly, both 13 and 18 kDa protein bands were excised from SDS-PAGE gels and analysed by LC-MS/MS. In agreement with the N-terminal sequencing results, MGP was identified as the prevalent protein in the 13 kDa band, whereas GRP tryptic peptides were not detected in the 18 kDa band, and ribonuclease 5 was identified as the predominant protein. These results evidenced that the characterization of GRP protein through sequence determination from complex extracts would be a very challenging task, and

further procedure optimization, and probably additional approaches would be required to achieve this goal.

In parallel, the immunodetection of GRP in human osteoarthritic articular cartilage and synovial membrane was achieved using a previously described extraction method with Laemmli lysis buffer, used to immunodetect GRP in mouse cartilage extracts [78]. The Laemmli extracts were analysed by SDS-PAGE with CBB staining and the presence of GRP investigated through WB (**Fig. 3.7**, CBB and WB). In agreement with the WB results previously obtained for mouse cartilage extracts [78], two positive GRP bands were immunodetected in human cartilage extracts with apparent molecular weights around 16 and 18 kDa (**Fig. 3.7**, WB, C). In the synovial membrane extracts only one GRP positive band of approximately 16 kDa was detected (**Fig. 3.7**, WB, SM). Interestingly, all the bands immunodetected with the CTerm-GRP antibody were also positive for the c/ucGRP conformation-specific antibodies, indicating the presence of both c/ucGRP forms in these OA-affected tissues.

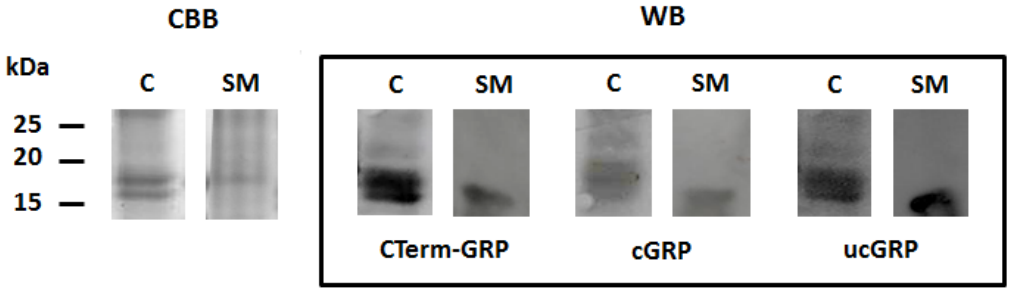

Fig. 3.7 – SDS-PAGE and western blot (WB) analysis of human osteoarthritic articular cartilage and synovial membrane in Laemmli buffer extracts. Gels were stained with coomassie brilliant blue (CBB) (cartilage, C, 50 µg and synovial membrane, SM, 45 µg) and WB analysis (C, 50 µg and SM, 45 µg) were performed using CTerm-GRP, cGRP and ucGRP antibodies. Relevant molecular mass markers (kDa) are indicated on the left of the panels.

Since GRP has been described as a circulating protein [14], its presence in osteoarthritic synovial fluid and osteoarthritic serum was also investigated. For that, direct samples of both fluids were analysed by SDS-PAGE with CBB staining and WB using all the available GRP-specific antibodies (**Fig. 3.8**, CBB and WB). Results showed a single immunoreactive band with 25 kDa of apparent molecular weight (**Fig. 3.8**, WB). The

detected protein band was positive for both c/ucGRP antibodies, although cGRP appeared to be the predominant circulating form in these OA-affected fluids (**Fig. 3.8**, WB).

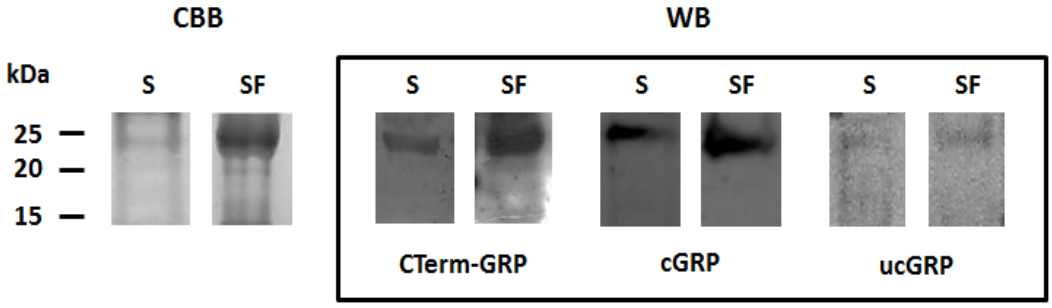

Fig. 3.8 – SDS-PAGE and western blot (WB) analysis of human osteoarthritic synovial fluid and serum samples. Gels were stained with coomassie brilliant blue (CBB) (1 µl of synovial fluid, SF and 1 µl of serum, S) and WB analysis (1 µl of SF and 1 µl of S) were performed using CTerm-GRP, cGRP and ucGRP antibodies. Relevant molecular mass markers (kDa) are indicated on the left of the panels.

Overall, although the presence of c/ucGRP was detected in all analysed samples, further characterization of GRP γ-carboxylation status through N-terminal sequence and LC-MS/MS analysis was hampered, requiring additional studies to determine the pattern of GRP γ-carboxylation and its association with OA-affected tissues. In addition, due to limitations related with control tissue sampling availability (Chapter 2), such studies could not be performed using a SDS-PAGE and WB strategy. In alternative, to investigate GRP accumulation and γ-carboxylation patterns in control and OA-affected tissues, an IHC strategy using the conformation-specific c/ucGRP antibodies was conducted. This experimental approach allows the analysis of protein spatial distribution at the cell level and requires low quantities of tissue samples.

3.3.5 Gla-rich protein is present in bone and associated with human osteoblasts, osteocytes and osteoclasts

Immunohistochemistry analysis of GRP in human osteoarthritic bone and articular cartilage was initially performed using glycol methacrylate and conventional paraffin embedding, the last with previous tissue decalcification. In the methacrylate embedded samples, positive GRP signal was observed in calcified cartilage and bone matrices

(calcification confirmed through von Kossa staining, **Fig. 3.9**, **A**) using the CTerm-GRP antibody, while an uneven signal was detected in the articular cartilage ECM (**Fig. 3.9**, **B**). Resin sections are prone to falling off the slides during IHC [198], thus deplasticization was not performed to prevent tissue lost and the obtained uneven signal in the ECM could be due to lower antibody accessibility and/or effect of antigen retrieval in some areas of the methacrylate tissue section. Because of this constrain, the use of this embedding in these types of tissues was restricted to the analysis of bone and ectopic cartilage calcification.

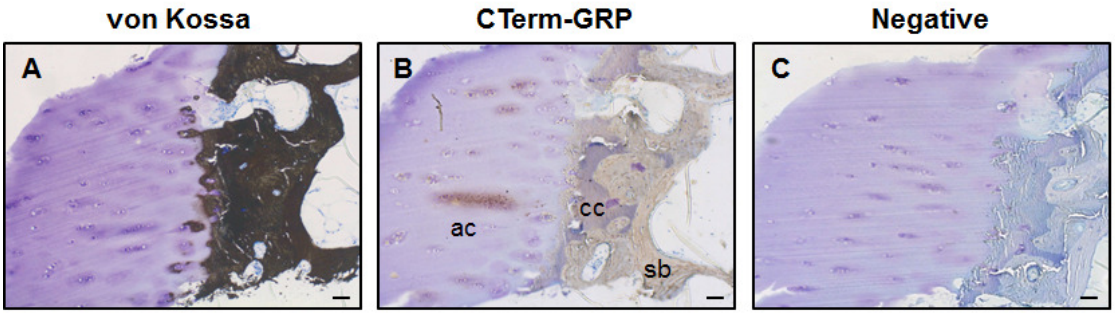

Fig. 3.9 – GRP immunolocalization in human osteoarthritic bone and articular cartilage using methacrylate embedding. Tissue calcified areas where accessed using von Kossa staining (**A**) and GRP immunolocalization in consecutive tissue sections was achieved with CTerm-GRP antibody (**B**). Positive immunoreactive signal was evidenced by the brown colour. Panel **C**, contains a negative control in consecutive sections. Final counterstaining was achieved with toluidine blue. ac, articular cartilage; cc, calcified cartilage; sb, subchondral bone; scale bars represent 50 µm.

For comparison, IHC analysis of the same tissue samples was performed with paraffin embedding. Tissue decalcification prior embedding (confirmed through von Kossa staining, **Fig. 3.10**, **A**) was necessary due to the hard nature of bone that difficults tissue sectioning. IHC analysis with CTerm-GRP antibody revealed a lower positive GRP signal in the bone matrix (**Fig. 3. 10**, **B** and **C**) when compared with the analysis in methacrylate sections (**Fig. 3.9**, **B**). These results suggest protein loss with mineral removal, and are in concordance with the known calcium binding ability of GRP [15]. Interestingly, the preservation of cellular morphology in paraffin allowed the detection of GRP in all three cell types existing in bone: osteoblasts, osteocytes and osteoclasts (**Fig. 3.10**, **C**). Although GRP has been previously detected in rat osteoblasts and osteocytes at mRNA and/or protein levels [14], its association with osteoclasts had never been previously described.

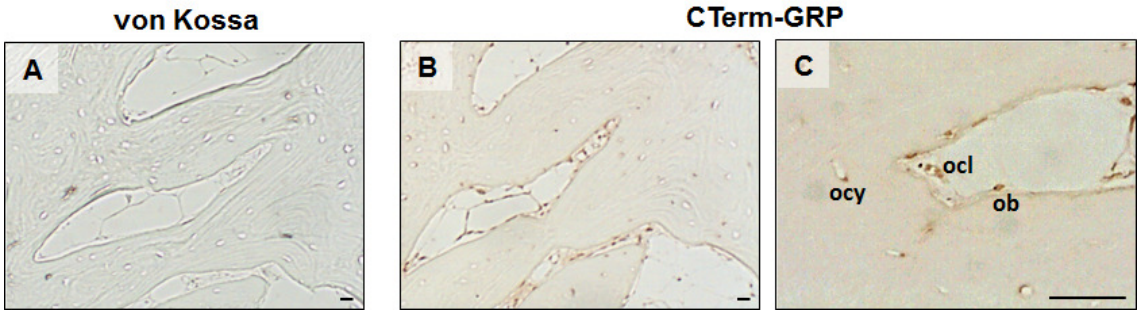

Fig. 3.10 – GRP immunolocalization in human osteoclasts, osteoblasts and osteocytes. Bony tissue was analysed in paraffin tissue sections after tissue decalcification, which was confirmed through von Kossa staining (**A**) and GRP was immunodetected in consecutive tissue sections using CTerm-GRP antibody (**B** and **C**). Positive immunoreactive signal was evidenced by the brown colour. ob, osteoblasts; ocy, osteocytes; ocl, osteoclasts (ocl); scale bars represent 50 µm.

The accumulation of GRP in osteoclasts was further confirmed using TRAP, a marker for osteoclasts and bone resorption [199], and IHC analysis with CTerm-GRP antibody in consecutive tissue sections of osteoarthritic bone. A co-localization of TRAP and GRP was obtained by immunolocalization in consecutive tissue sections (**Fig. 3.11**), indicating, for the first time, the presence of GRP in human osteoclasts, in addition to its detection in osteoblasts and osteocytes.

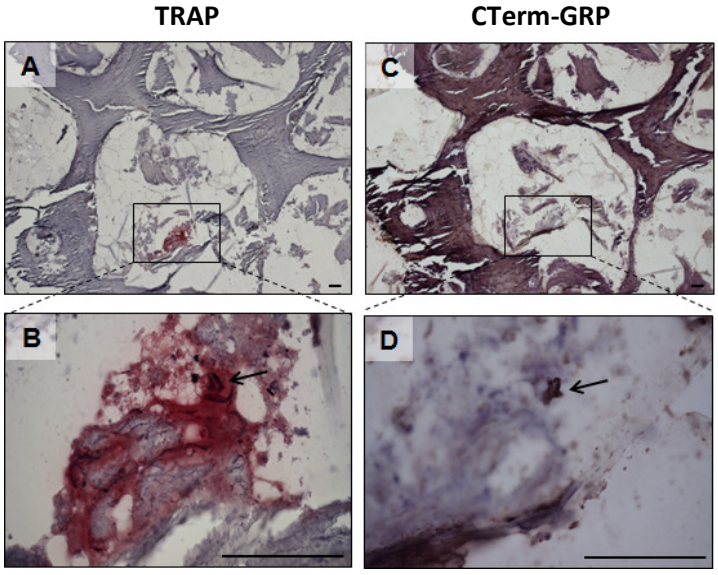

Fig. 3.11 – GRP is immunodetected in human osteoclasts. The reddish colour indicative of endogenous tartrate-resistant acid phosphatase (TRAP) presence (**A** and **B**) was detected in methacrylate osteoarthritic bone tissue sections and co-localized with GRP, using CTerm-

GRP antibody (**C** and **D**) in consecutive sections. Arrows indicate osteoclast localization. Final counterstaining was achieved with hematoxylin. Scale bars represent 50 µm.

3.3.6 Uncarboxylated GRP is the predominant protein form accumulated in osteoarthritic tissues

Gla-rich protein accumulation pattern between control and osteoarthritic samples, and GRP γ-carboxylation status associated with the pathological processes occurring in OA, in particular ectopic calcification events, was analysed by IHC using the conformation-specific antibodies against cGRP and ucGRP protein forms. Synovial membrane samples and articular cartilage samples without adjacent bone or ectopic calcification were embedded in paraffin, while articular cartilage samples containing pathological mineralization were analysed using methacrylate embedding.

Both c/ucGRP forms were found accumulated in control and osteoarthritic chondrocytes (**Fig. 3.12**, **A-D** and **G-J**), although ucGRP was more evident than cGRP in osteoarthritic cartilage ECM, especially in the tangential layer (**Fig. 3.12**, **G-J** and **A-D**, respectively). Also, the majority of the analysed tissue sections of osteoarthritic cartilage samples were characterized by the presence of ectopic calcification (**Fig. 3.12**, **F**), and both cGRP and ucGRP were co-localized at sites of cartilage pathological mineralization (**Fig. 3.12**, **E** and **K**). These observations were confirmed with CTerm-GRP antibody (**Fig. 3.12, L-P**).

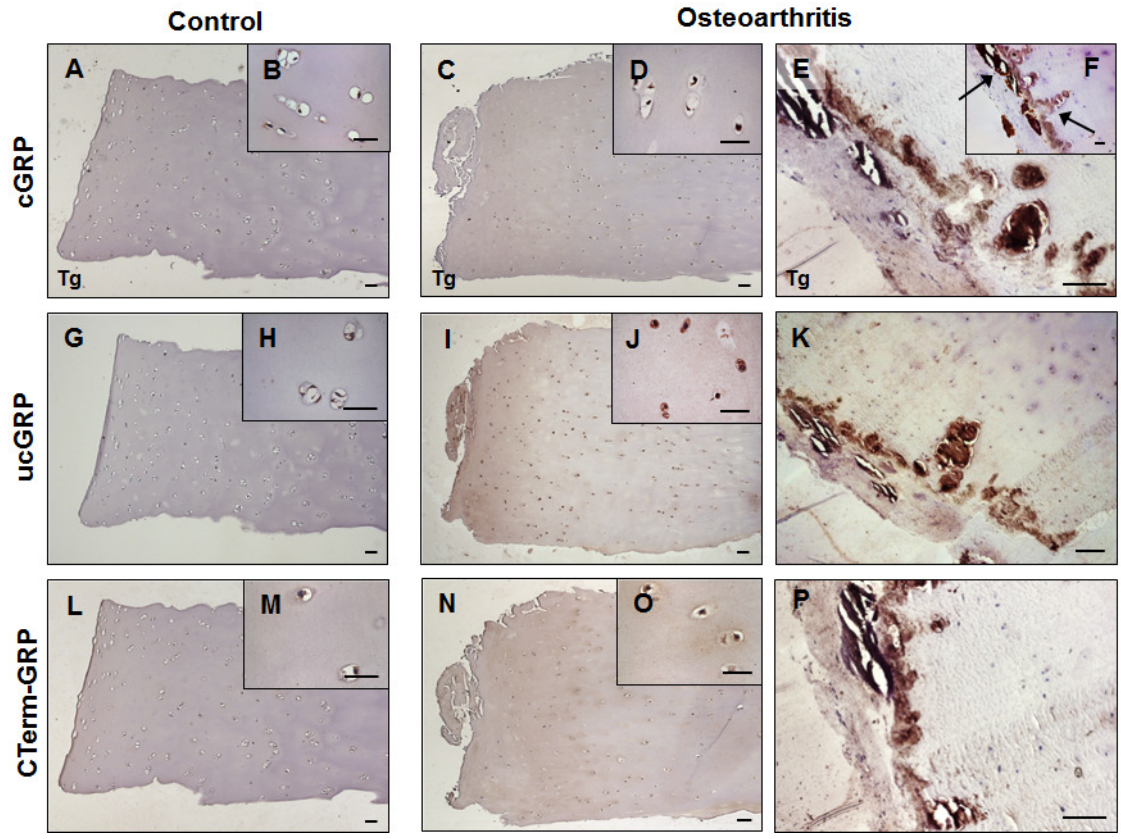

Fig. 3.12 – Undercarboxylated GRP is the predominant form accumulating in osteoarthritic cartilage. Specific antibodies for carboxylated (cGRP) (**A**-**E**), undercarboxylated (ucGRP) (**G**-**K**) and total GRP (CTerm-GRP) (**L**-**P**) were used for immunolocalization in control and osteoarthritic cartilage extracellular matrix (ECM) and chondrocytes, and sites of ectopic calcification in the pathological tissues. Panel **F** represents the von Kossa staining of osteoarthritic cartilage showing sites of pathological mineralization (arrows). Samples without ectopic calcification sites were embedded with paraffin while the remaining with methacrylate and final counterstaining was achieved with hematoxylin. Tg, tangential layer; scale bars represent 50 µm (Adapted from Rafael et al., 2014 [189]).

In parallel, the accumulation of c/ucGRP in the synovial membrane was also analysed (**Fig. 3.13**). Carboxylated GRP accumulation was mainly detected in the lining layer of control tissues (**Fig. 3.13**, **A**), while in osteoarthritic tissues ucGRP was the predominant protein form detected (**Fig. 3.13**, **F**). The presence of pathological mineralization was detected in all analysed samples of osteoarthritic synovial membrane (**Fig. 3.13**, **D**) and at ectopic calcification sites, both cGRP and ucGRP were co-localized (**Fig. 3.13**, **C** and **G**).

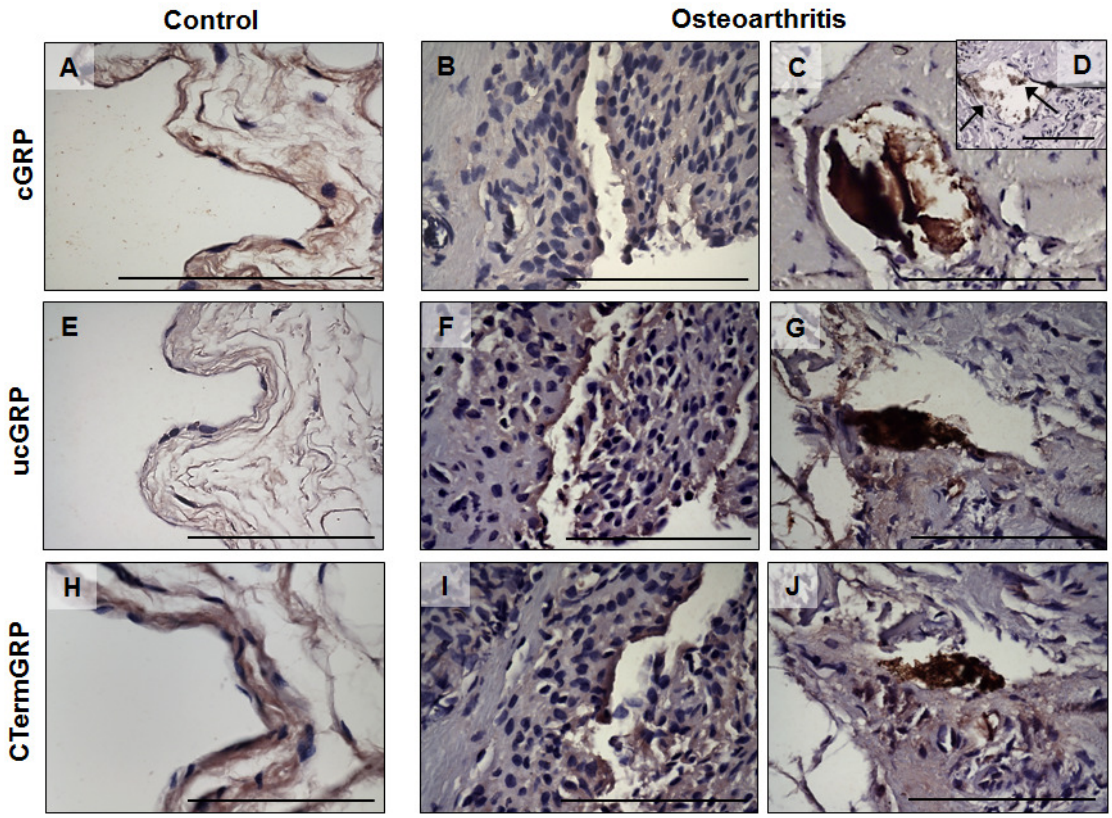

Fig. 3.13 – Undercarboxylated GRP is highly accumulated in osteoarthritic synovial membrane lining cells and both GRP protein forms accumulate at ectopic calcification sites. Specific antibodies for carboxylated (cGRP) (**A**-**C**), undercarboxylated (ucGRP) (**E**-**G**) and total (CTerm-GRP) (**H**-**J**) GRP were used for immunolocalization in the lining layer cells of control and osteoarthritic tissues and sites of ectopic calcification, detected using von Kossa staining (**D**, arrows), in the pathological membranes. Samples were embedded with paraffin and final counterstaining was achieved with hematoxylin. Scale bars represent 50 µm (Adapted from Rafael et al., 2014 [189]).

The prevalence of cGRP in the lining layer of control synovial membranes, contrary to the predominance of ucGRP in osteoarthritic tissues was further confirmed through IF analysis (**Fig. 3.14**).

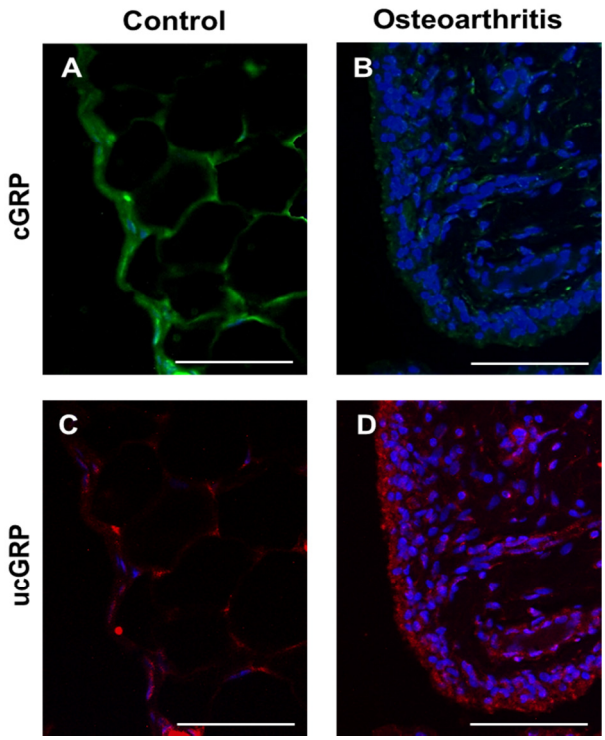

Fig. 3.14 – Undercarboxylated GRP is the predominant form accumulating in osteoarthritic synovial membrane lining cells. Immunofluorescence (IF) imaging was obtained for γ-carboxylated (cGRP) (green, **A-B**) and undercarboxylated GRP (ucGRP) (red, **C-D**) protein forms using the respective specific antibodies. Samples were embedded with paraffin and cell nuclei were stained with DAPI. Scale bars represent 100 µm.

Altogether, the IHC and IF results showing GRP pattern of accumulation in osteoarthritic samples of cartilage and synovial membrane, evidenced the predominance of the ucGRP form in OA-affected tissues, while control cartilage and synovial membrane tissues appear to mainly accumulate the cGRP form.

Since MGP is another VKDP related to ectopic calcification and previously associated with OA [92], the accumulation patterns of the carboxylated (cMGP) and undercarboxylated (ucMGP) MGP forms were also analysed between control and osteoarthritic cartilage and synovial membrane tissues. Immunohistochemistry results showed that, as for GRP, the undercarboxylated form of MGP is highly accumulated in osteoarthritic cartilage when compared to control tissues (**Fig. 3.15**). Moreover, while in control chondrocytes only cMGP is detected, OA chondrocytes only exhibited ucMGP (**Fig. 3.15**, **A**-**D** and **F**-**I**). At sites of ectopic calcification, both MGP protein forms were found co-localized (**Fig. 3.15**, **E** and **J**).

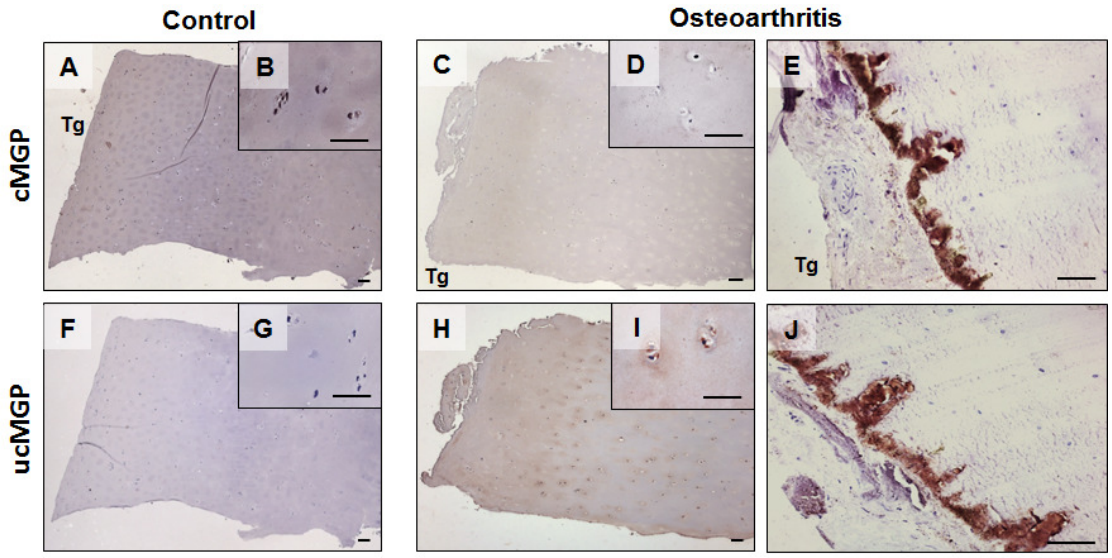

Fig. 3.14 – Undercarboxylated MGP is highly accumulated in osteoarthritic cartilage. Specific antibodies for carboxylated (cMGP) (**A**-**E**) and undercarboxylated (ucMGP) (**F-J**) MGP forms were used for immunodetection in control and osteoarthritic cartilage extracellular matrix (ECM) and chondrocytes, and sites of ectopic calcification in the pathological tissues. Samples without ectopic calcification sites were embedded with paraffin while the remaining with methacrylate and final counterstaining was achieved with hematoxylin. Tg, tangential layer; Scale bars represent 50 µm (Adapted from Rafael et al., 2014 [189]).

In the synovial membrane, no positive MGP signal was detected in control and osteoarthritic lining cells (**Fig. 3.15**, **A** and **C**), while both c/ucMGP were found co-localized at sites of ectopic calcification co-localized (**Fig. 3. 15**, **B** and **D**).

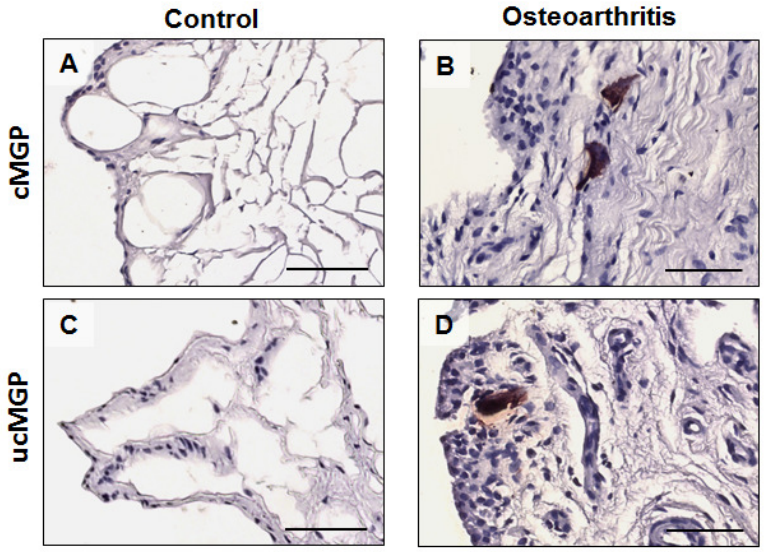

Fig. 3.15 – Both carboxylated and undercarboxylated forms of MGP are accumulated in osteoarthritic synovial membrane ectopic calcification sites. Specific antibodies for carboxylated (cMGP) (**A** and **B**) and undercarboxylated (ucMGP) (**C** and **D**) MGP forms were used for immunodetection in the lining layer cells of control and osteoarthritic tissues and sites of ectopic calcification, in the pathological membranes. Samples were embedded with paraffin and final counterstaining was achieved with hematoxylin. Scale bars represent 50 µm (Adapted from Rafael et al., 2014 [189]).

Overall, the IHC results clearly showed the prevalence of a lower γ-carboxylation status of both GRP and MGP in osteoarthritic conditions and allowed the association of GRP γ-carboxylation impairment with OA pathology.

3.4 Discussion

In this chapter evidences for the involvement of GRP with OA were addressed for the first time, at gene and protein levels. GRP-F1 was found to be the predominant expressed variant in articular cartilage and synovial membrane, and upregulated in osteoarthritic cartilage comparing to controls. Undercarboxylated GRP was found to be the prevalent GRP form accumulated in both osteoarthritic tissues. Moreover, GRP association with OA was not restricted to sites of ectopic calcification evidencing a possible role in other OA-associated processes such as inflammation.

The first evidences for GRP association with OA were obtained from gene expression analysis in OA-affected tissues, which confirmed the consistent presence of the transcript coding for full length GRP (GRP-F1) and unveiled two novel GRP alternative transcripts (GRP-F5 and F6). In contrast, the presence of the previously described mouse and zebrafish splice variants, GRP-F2, F3 and F4 [72,73,76], were not detected in this study. These results were further supported by parallel studies ongoing in the laboratory for screening and identification of additional GRP splice variants using a wide panel of human tissue samples. Despite the extensive efforts and high number of screened GRP clones, no additional spliced transcripts were identified, neither the previously described F2, F3 and F4 GRP transcripts [189]. In addition, the same study failed to detect GRP-F5 and F6 variants in mice using a similar gene expression strategy [189]. Altogether, the results indicated that the newly discovered GRP-F5 and F6 forms may be human-specific, and strongly suggest the prevalence of these variants, in particular GRP-F1, in human, although the possibility that other alternatively spliced transcripts may exist in man cannot be completely excluded.

The discovered GRP-F5 and F6 variants are characterized by the loss of carboxylase binding and propeptide cleavage domains, raising questions about the possibility of altered γ-carboxylation of Glu residues and mature protein processing. Parallel studies ongoing in the laboratory performed transient transfections of HEK293T cells with GRP-mkate2 fusion protein, showing that all protein isoforms were translated and detected intracellularly [189]. Yet, the secretion of the F6 form occurred later than for F1 and F5 variants [189], indicating a lower secretory efficiency as predicted by the 9 aa loss of the signal peptide C-terminus. Detection of Gla residues in the secreted GRP protein isoforms using the M3B Gla-specific antibody, indicated the presence of Gla residues only in GRP-F1 [189], consistent with the predicted loss of γ-carboxylase recognition site in F5 and F6 variants. However, since *in vitro*

cell systems are known to have limited γ-carboxylation capacity, particularly when VKDPs are overexpressed [200], the presence of Gla residues in GRP-F5 and F6 in physiological conditions cannot be completely ruled out.

Despite the identification of novel variants, in addition to the full length GRP-F1, the predominant transcript expressed in control or osteoarthritic tissues was found to be GRP-F1, as also reported for other pathological and control human tissues [15,16,189]. In fact, GRP-F5 and F6 transcripts were found almost restricted to fetal tissues [189] and their biological function in humans should be further evaluated throughout development. Phosphorylation of serine and tyrosine residues are *in silico* predicted for all human putative GRP isoforms, and their occurrence should be further investigated, particularly because three phosphorylated serine residues of human MGP were previously demonstrated to be determinant for its function as a calcification inhibitor in vascular smooth muscle cells [201].

Previous functional studies on GRP had shown contradictory results. While GRP-deficient mice did not exhibit a clear phenotype in bone and cartilage [78], zebrafish functional data indicated an essential role of GRP in skeletal development and calcification [72]. Results here obtained reinforce the notion that the GRP-deficient mouse has shortcomings since the data achieved from this model cannot be directly translated to the human situation [78].

The unequivocal predominant expression of GRP-F1 transcript and the barely detectable expression of GRP-F5 and F6 in the majority of the tissue samples analysed, further supports the fact that the immune-based studies using available GRP antibodies, either CTerm-GRP for total GRP or the conformational c/ucGRP antibodies, should reflect the accumulation pattern of GRP-F1 isoform, with negligible contribution of other variants. Detection of GRP by WB showed a complex patterning with multiple immunodetected bands, ranging from 16 to 25 kDa of apparent molecular weights, depending on the tissue or fluid analysed, although multiple bands were consistently detected with all available anti-GRP antibodies. Since the conformation-specific antibodies were raised against synthetic peptides comprising partial Gla/Glu domains, multiple patterning may represent different degrees of γ-carboxylation. Moreover, since the analysed samples correspond to biological tissues and fluids from different individuals, potentially represents a higher γ-carboxylation heterogeneity. In fact, altered γ-carboxylation status have been shown to modify Gla-containing proteins migration behaviour on SDS-PAGE [202]. Also, similar multiple GRP patterning was recently shown in calcified aortic valves extracts, using the same three

different antibodies against GRP employed in this study, where GRP identity was further confirmed in two out of three immunodetected bands [16].

Attempts to obtain further GRP identification followed by characterization of Gla content in the immunoreactive bands was performed by N-terminal sequence and LC-MS/MS analysis, although the detection of GRP was not achieved using these techniques. N-terminal sequencing is not a high sensitive technique and generally requires pure peptides for an accurate identification [203]. When the protein of interest is present in low amounts in a mixture, as proposed for GRP, assigning the phenylthiohydantoin (PTH)-amino acid derivatives of its sequence will be most unlikely [203]. Mass spectrometry has a higher sensitivity, nevertheless, major problems associated with protein identification using this technique are often related with the generation of peptides suitable for fragmentation, and in the particular case of VKDPs, with the identification of Gla residues [200]. This subject which will be further discussed in Chapter 5. Altogether, protein sequencing results suggested that GRP is a low abundant protein in the analysed extracts, therefore more sensitive and powerful resolution techniques, such as two-dimension gel electrophoresis (2-DE), could be an alternative to obtain further molecular data for protein characterization. The use of this approach will be addressed in Chapter 5.

The comparative IHC results obtained in this chapter revealed the presence of both c/ucGRP and c/ucMGP proteins in osteoarthritic tissues. Such results were not surprising, since it was previously shown that both GRP protein forms coexist, even in control tissues, indicating incomplete γ-carboxylation in physiological conditions [15]. Also, such results were consistent with the knowledge that all extrahepatic VKDPs presently investigated are undercarboxylated in non-vitamin-K-supplemented healthy individuals [204], a condition that might be aggravated in pathological conditions such as OA. At sites of ectopic calcification in osteoarthritic cartilage and synovial membrane co-localization of c/ucGRP and c/ucMGP was clear, evidencing the proteins association to the pathological mineralization occurring in OA and the calcium binding capacity of all forms. In agreement, previous *in vitro* studies evidenced the calcium binging capacity of both c/ucGRP [15]. Moreover, results showed that OA patients accumulate predominantly ucGRP in cartilage and in the lining cells of the synovial membrane, whereas control subjects, showing no signs of mineral deposition in both tissues, exhibit mostly the γ-carboxylated protein in both tissues. Interestingly, the fact that GRP accumulation was not restricted to sites of ectopic calcification in osteoarthritic tissues, evidenced its possible involvement in other OA processes. Overall, the IHC results confirmed the association of GRP with the pathological calcification events occurring in OA and clearly

associate ucGRP to the pathological tissues, suggesting that GRP γ-carboxylation should be crucial for the prevention of pathological features of OA. In concordance, ucGRP predominance relative to cGRP was also recently seen in calcified aortic valves by IHC [16]. Matrix Gla protein immunodetection in this study also supports the relevance of γ-carboxylation for pathology development, since osteoarthritic cartilage tissues showed significantly higher amounts of ucMGP accumulation. Previous studies, both in mice and human, have shown that MGP-deficient chondrocytes are hypertrophic, exhibiting an abnormal maturation and organization that can lead to endochondral ossification due to the lack of this calcification inhibitor [12,65,89]. Specific γ-carboxylase activity has also been found to be higher in cultured control chondrocytes when compared to the ones derived from osteoarthritic tissue, and human osteoarthritic chondrocytes contained significantly less cMGP when compared to control cells [92]. Decreased cMGP, probably reflecting diminished γ-carboxylase activity, has been in fact suggested as responsible for the increased cartilage mineralization occurring in OA [92]. Ultimately, these data reinforce the notion that lower levels of functional VKDPs observed in OA may be the result of decreased γ-carboxylase activity associated with the pathology, possibly accompanied by a loss of vitamin K function that may be intimately related with its subclinical levels in OA [82].

Insufficient vitamin K levels in OA have been associated with impaired functions of MGP and OC, and associated to pathology abnormalities [12,83,94,205]. Accordingly, GRP biosynthesis is also possibly affected by vitamin K availability and consequently related to OA pathophysiological features, however, subclinical vitamin K insufficiency studies in OA have never considered GRP as a target protein. Moreover, vitamin K is not only associated with the prevention of soft tissue mineralization [12,206] but also regarded as protective agent producing anti-inflammatory cytokines that affect articular cartilage and subchondral bone through different molecular mechanisms [26], and ucMGP was also proposed as an inflammatory marker of arthritis through the combined analysis of serum and local synovial fluid accumulation [95]. Thus, the obtained results showing a relation between GRP and MGP γ-carboxylation deficiency and OA might also be linked with recent findings, suggesting that vitamin K metabolism may be associated with synovitis in OA patients [94], evidencing the possibility that GRP may not only be associated with mineralization events but also with inflammatory processes.

Overall, this chapter revealed the existence of two novel GRP spliced variants, that seem to be human-specific, yet evidenced the predominance of GRP-F1 transcript in articular tissues, which is upregulated in osteoarthritic cartilage comparing to controls. Also, lower

levels of γ-carboxylated GRP were shown to be intimately associated with OA pathology, and such impaired γ-carboxylation will most likely affect the ectopic calcification events occurring in OA. Interestingly, the obtained IHC data also suggests GRP involvement in other OA-associated processes. Gla-rich protein γ-carboxylation status correlation with OA-associated mineralization and GRP possible involvement with inflammatory events in OA will be further addressed in the following chapter.

3.5 Acknowledgements

All primary antibodies used in this chapter were kindly provided by GenoGla Diagnostics (Universidade do Algarve, Faro, Portugal) or VitaK BV (University of Maastricht, Maastricht, The Netherlands). We gratefully thank Dr. Cees Vermeer, chief executive officer of VitaK BV, for granting me the opportunity to visit and work at the company's laboratories during a period of time. In fact, all the immunofluorescence analysis performed in this chapter were carried at VitaK BV with the precious help of technicians Marjolein Herfs and Cynthia van't Hoofd, two whom we specially thank. The collaboration of Doctor José Enriquez and technician Alexandra Teixeira, from Centro Hospitalar do Algarve (Departamento de Anatomia Patológica, Faro, Portugal), was also extremelly apreciated. We thank Doctor José Enriquez, the head of the department, for allowing this collaboration, and Alexandra Teixeira, for all tissue paraffin embedding of this chapter and some of the blocks sectioning. Finally, we gratefully thank Dr. Marta Rafael, former Post-Doc at Functional Biochemistry and Proteomics (FBP) research group (CCMar, Universidade do Algarve, Faro, Portugal), for all the help concerning the transcriptional analysis of this chapter. This work was funded by projects PTDC/SAUESA/101186/2008, PTDC/SAU-ORG/112832/2009 and PTDC/SAU-ORG/117266/2010 of the Fundação para a Ciência e Tecnologia (FCT). Part of the work presented in this chapter represents our published results in Rafael et al., 2014 [189].

Chapter 4

Gla-rich protein is a novel cross talk factor linking calcification and inflammation processes in osteoarthritis

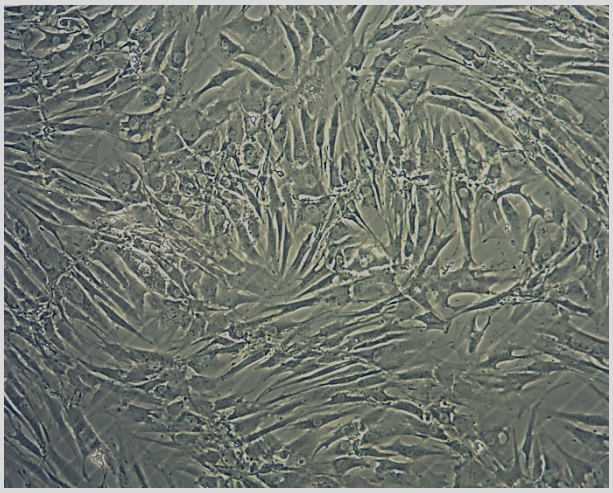

Abstract

Two of the major molecular processes affecting the whole-joint disease osteoarthritis (OA) are inflammation and the pathological mineralization of articular tissues, both events intimately correlated. Gla-rich protein (GRP) was associated to sites of pathological calcification in human osteoarthritic cartilage and synovial membrane tissues in the previous chapter. Moreover, our immunohistochemistry results (Chapter 3) revealed that GRP accumulation was not restricted to sites of ectopic mineralization in osteoarthritic synovial membrane tissues, suggesting a role in other cell mediated processes. In this chapter, the involvement of GRP with OA mineralization and inflammation was investigated using a chondrocyte and synoviocyte monolayer OA cell system. The induced extracellular matrix (ECM) mineralization of the *in vitro* articular model, revealed an upregulation of GRP expression following cell differentiation towards a hypertrophic (chondrocytes) or macrophage-lineage (synoviocytes) phenotype. Also, the induced inflammation of the cell system using the cytokine interleukin 1β, resulted in the increased expression of the inflammatory mediators cyclooxygenase 2 and matrix metalloproteinase 13, concomitant with GRP upregulation. These results further associated GRP with OA-associated mineralization and for the first time, with OA-related inflammatory processes. Importantly, while treatment of articular cells with carboxylated GRP (cGRP) inhibited ECM calcification, treatment with either GRP or GRP-coated basic calcium phosphate crystals, resulted in the down regulation of inflammatory mediators, which was independent of GRP γ-carboxylation status. Thus, while the proposed calcification inhibitory function of cGRP was strengthened in the particular case of OA, our results also strongly suggest the association of GRP with inflammatory processes occurring in this degenerative disorder, apparently independently from its γ-carboxylation status. Since these two processes are widely associated with OA progression, GRP should be considered a strong candidate target to develop new therapeutic approaches for OA.

4. 1 Introduction

Synovial inflammation, also termed synovitis, is frequently observed in osteoarthritis (OA), however, the respective development and how it affects disease progression is still unclear [100]. Abnormal mechanical and oxidative stress resulting from cartilage degradation in OA are associated with the induction of inflammation [91]. Also, another frequent feature known to modulate inflammatory responses in OA pathology is articular tissues ectopic-calcification [139-142]. Although, basic calcium phosphate (BCP) and calcium pyrophosphate dihydrate (CPPD) are the major forms of crystals associated with OA pathology, the first type is more intimately related with primary OA [49,137,138]. The prevailing theory is that proinflammatory and catabolic mediators, such as nitric oxide (NO), cytokines, prostaglandins (PGEs) and matrix metalloproteinases (MMPs), are released from cartilage into the synovial space, and the presence of BCP crystals amplifies the production of such mediators, contributing to whole-joint inflammation and further cartilage degradation [88,91,123].

Vitamin K is essential for preventing soft tissue mineralization [3,56] and it has been further suggested as a protective agent against inflammation [24,25]. While subclinical vitamin K levels have been associated with increased risk of OA development [82-84], several vitamin K-dependent proteins (VKDPs) such as matrix Gla protein (MGP), osteocalcin (OC), and now also Gla-rich protein (GRP) (Chapter 3), have been associated with the disease. The presence of undercarboxylated OC (ucOC) in serum, related to vitamin K metabolism deficiency, is associated to synovitis and considered a risk marker for OA [94]. Moreover, impaired γ-carboxylation of MGP has not only been associated with increased mineralization of osteoarthritic cartilage [92], but also to inflammatory events, with the combined assessment of ucMGP in serum and synovial fluid suggested as a joint inflammatory marker in arthritis patients [95].

Gla-rich protein, proposed to act as a modulator of calcium availability in the extracellular matrix (ECM) [14,15] and an inhibitor of calcification in the cardiovascular system [16], was for the first time associated with OA in Chapter 3. Accordingly, GRP was verified to be upregulated in osteoarthritic cartilage comparing to controls and undercarboxylated GRP (ucGRP) was shown to be the predominant protein form accumulating in osteoarthritic cartilage and synovial membrane. Interestingly, GRP

association with OA was not restricted to ectopic calcification areas, indicating a possible involvement in other osteoarthritic processes such as inflammatory events.

To better understand the pathophysiology of OA, several disease models have been developed in the past years. One of the major barriers overcome by these models is the limitation of human osteoarthritic tissues that are collected only at time of joint replacement, representing end stage lesions [146]. The use of such samples hampers the study of the factors that play a role in disease development [146]. Also, disease models overcome the common limitation of human control samples [153]. A wide variety of *in vitro* cell models are described and, among them, monolayer cell cultures are still one of the most useful tools for the study of OA pathology [153]. Monolayer systems are easy available and easy manipulated, allowing the research of disease causes and progression, and subsequent design and testing of potential therapeutics [153,154].

In this chapter, the involvement of GRP with mineralization and inflammation processes occurring in OA was investigated using an *in vitro* monolayer chondrocyte and synoviocyte cell system. In concordance, here is described (i) the establishment of an *in vitro* cell system aimed at studying OA-associated mineralization and inflammation, (ii) GRP and genes involved in the γ-carboxylation machinery association with OA, (iii) GRP involvement with chondrocytes and synoviocytes induced ECM mineralization and related cell differentiation, (iv) carboxylated GRP (cGRP) ability to reduce mineral deposition in chondrocytes and synoviocytes ECM, (v) GRP association with inflammatory events in OA, (vi) GRP cross talking between calcification and inflammatory events, and (vi) c/ucGRP anti-inflammatory effect in an osteoarthritic scenario.

4.2 Experimental procedures

4.2.1 Biological material and sample processing

Osteoarthritic articular cartilage and synovial membrane tissues were obtained and processed for subsequent cell culture development, as described in Chapter 2, section 2.2.1.

4.2.2 Cell culture development and maintenance

Osteoarthritic articular cartilage and synovial membrane tissues were digested overnight with 2 mg/mL collagenase in DMEM (Invitrogen, Carlsbad, CA, USA) at room temperature (RT). Fragments were washed three times with DMEM, placed in 24-well plates and cultured in the same medium supplemented with 1% v/v penicillin-streptomycin, 1 mM L-glutamine and 10% v/v fetal bovine serum (FBS) at 37 ^{o}C in a humidified atmosphere with 5% CO_2. Osteoarthritis-derived chondrocytes (OA-HAC, osteoarthritic human articular chondrocytes) and synoviocytes (OA-HFLS, osteoarthritic human fibroblast-like synoviocytes) were allowed to migrate from fragments and adhere to the wells for approximately 2 weeks, then collected using trypsin solution (Invitrogen) for cell passage and placed into new plate dishes with fresh media. Cultures were routinely sub-cultured (1:2) at early confluence by trypsinization. The culture media used throughout the study was advanced DMEM (Invitrogen) supplemented with 1% (v/v) penicillin-streptomycin, 1 mM L-glutamine and 10% (v/v) FBS. Cells used in the following experiments were between passages 4 and 14. Cells were observed and photographed with a Motic AE 31 inverted light microscope equipped with a digital camera, using Motic Images Plus 2.0 software.

As controls, primary chondrocytes (NHAC, normal human articular chondrocytes, Lonza, Visp, Switzerland) and synoviocytes (HFLS, human fibroblast-like synoviocytes, ECACC, Sigma-Aldrich, St. Louis, MO, USA) were commercially obtained. A second set of OA and control-derived primary chondrocytes (OAC, osteoarthritic chondrocytes and NC, normal chondrocytes) and synoviocytes (SOAR, osteoarthritic fibroblast-like synoviocytes and SNR, normal fibroblast-like synoviocytes) cultures were developed by collaborators from Grupo de Bioingeniería Tisular y Terapia Celular (Servicio de Reumatología, Instituto de Investigación Biomédica de A Coruña, Complejo Hospitalario Universitario de A Coruña, Sergas, Universidad de A Coruña, A Coruña, Spain) and Centro de Investigación Biomédica

en Red de Bioingeniería, Biomateriales y Nanomedicina (Madrid, Spain) and used to strengthen the results obtained with of the first set of cells.

4.2.3 Cellular proliferation measurement

Cells were seeded in 96-well plates at 2×10^4 cells/well and cultured in DMEM and advanced DMEM supplemented with 1% v/v penicillin-streptomycin, 1 mM L-glutamine and 10% v/v FBS. Both culture conditions were analysed for cell viability using the CellTiter 96 cell proliferation assay (Promega, Madison, WI, USA), following manufacturer's instructions. Briefly, cells were incubated during 1 h with 20 µl of reagent mixture, a tetrazolium compound combined with an electron coupling reagent, and cell proliferation was determined from absorbance at 490 nm. The tetrazolium compound is reduced by cells into a colored formazan product and 1 h was the previously determined optimal incubation period to obtain linearity between the number of cells and formazan absorbance at 490 nm (results not shown).

Cultures in advanced DMEM supplemented with 5.4 mM $CaCl_2$, 500 ng/mL of purified sturgeon GRP [54], human recombinant GRP [15] or bovine MGP [16], 5 ng/mL of interleukin 1β (IL-1β) (Peprotech EC Ltd., London, UK) or 100 µg/mL of produced BCP crystals (section 4.2.12), were also analysed for cell cytotoxicity using the CellTiter 96 cell proliferation assay (Promega) as formerly described.

4.2.4 RNA extraction

Total RNA was isolated from cell cultures as described by Chomczynski and Sacchi [191]. RNA concentration was determined by spectrophotometry at 260 nm and quality evaluated by agarose-denaturating gel electrophoresis.

4.2.5 Amplification of cDNA and quantitative real-time PCR

Five hundred nanograms of total RNA were treated with DNase I (Promega) and reverse-transcribed using Moloney-murine leukemia virus reverse transcriptase (MMLV-RT) (Invitrogen), RNase Out (Invitrogen), and an oligo(dT) adapter (5'-ACGCGTCGACCTCGAGATCGATG(T)13-3'), according to the manufacturer's recommendations.

Quantitative real-time PCR reactions were performed using the StepOne system (Life Technologies, Carlsbad, CA, USA), SsoFast Eva Green Supermix (Bio-Rad, Richmond, CA, USA), 300 nM of forward and reverse gene-specific primers (final concentration) for genes of interest (**Table 4.I**) and a 1:5 dilution of reverse-transcribed RNA solution. The following PCR conditions were used: initial denaturation/enzyme activation step at 95 ºC for 5 min, 50 cycles of amplification (one cycle is 30 s at 95 ºC and 15 s at 66 ºC); 18S was used as a housekeeping gene to normalize expression.

Table 4.I – Gene-specific primers used in this study

Gene	Primer name	Sequence (5' to 3')
18S	18S_F	GGAGTATGGTTGCAAAGCTGA
	18S_R	ATCTGTCAATCCTGTCCGTGT
OC	OC_F	CAGCGAGGTAGTGAAGAGACCCAGG
	OC_R	AGGGCAAGGGGAAGAGGAAAGAAGG
COMP	COMP_F	CTGCCTTCAATGGCGTGGACTTCG
	COMP_R	GGAAGGGGTTCGCCTGCCAATAC
Col2a1	Col2a1_F	CCTCGTGGGTCCCAGGGGTGAA
	Col2a1_R	TGAAGACCTGGAGGGCCCTGTGCG
Col10a1	Col10a1_F	AGCTGCCAAGGCACCATCTCCA
	Col10a1_R	AGTGGGCCTTTTATGCCTGTGGGC
MMP13	MMP13_F	AACCGTATTGTTCGCGTCATGCCAG
	MMP13_R	GATAGCTCTTCTTCCCCTACCCCGC
Vimentin	Vimentin_F	TGCGTCTCTGGCACGTCTTGACCT
	Vimentin_R	AGGGCGTCATTGTTCCGGTTGGCA
CD68	CD68_F	ACAGGACAACCACCACAGGCACCA
	CD68_R	GTGGCAGTGCTGTTGCTTGTTGGA
GRP-F1	GRPF1_F	GTCCCCCAAGTCCCGAGATGAGG
	GRPF1_R	CCTCCACGAAGTTCTCAAATTCATTCC
MGP	MGP_F	TGGAGGCTGGCACCTGATTTTG
	MGP_R	AAAAGGGGTGCAGCCAGACAAG
GGCX	GGCX_F	TTACACAGAGTCGGCGATGGAAGGAT
	GGCX_R	TACTGGATGTCAGGTCTGCGAAA
VKORC1	VKORC1_F	AGGGCAAGGCTAAGAGGCACTGAG
	VKORC1_R	CTGGGCAATGGAAAGAGCTTTGGAGAC
Osx	Osx_F	CAAGGTGTATGGCAAGGCTTCGCA
	Osx_R	TGCTGGCGAGGCAGAAGGTCGGGGCGT
OPN	OPN_F	ACGGACCTGCCAGCAACCGAAGT
	OPN_R	TACTGGATGTCAGGTCTGCGAAA
COX2	COX2_F	TGGTCTGGTGCCTGGTCTGATGATGT
	COX2_R	GCCTGCTTGTCTGGAACAACTGCTCA

4.2.6 Immunofluorescence

Immunofluorescence (IF) was performed in sub-confluent cultures seeded the previous day. Cells were washed with PBS (137 mM NaCl, 2.7 mM KCl, 10 mM sodium phosphate, 1.8 mM potassium phosphate) and fixed for 10 min in 4% v/v paraformaldehyde. Fixed cells were incubated at RT for 1 h with rabbit polyclonal CTerm-GRP (10 µg/mL, GenoGla Diagnostics, Faro, Portugal) or mouse monoclonals cGRP (10 µg/mL, GenoGla Diagnostics), ucGRP [15] (7.3 µg/mL, VitaK BV, Maastricht, The Netherlands) and cluster of differentiation 68 (CD68) (20 µg/mL, Santa Cruz Biotechnology, Texas, TX, USA) primary antibodies. After the first incubations, cells were incubated for 1 h at RT with Alexa488 (anti-rabbit) or Alexa594 (anti-mouse) labelled secondary antibodies (Invitrogen). Cell nuclei were stained with 6-diamidino-2-phenylindole (DAPI). Fluorescence images were obtained using an Axio Imager Z2 microscope (Zeiss, Jena, Germany) equipped with a digital camera and Axovision imaging software. Final images were processed using Image J Version 1.41m.

4.2.7 SDS-PAGE analysis

Aliquots of bovine MGP, purified within the scope of a parallel project [16], were quantified, freeze-dried and dissolved in lithium dodecyl sulphate (LDS) sample buffer (NuPage, Invitrogen) containing reducing agent. Separation was then performed by sodium dodecyl sulphate-polyacrylamide gel electrophoresis (SDS-PAGE) as described in Chapter 3, section 3.7, and the gel stained with coomassie brilliant blue (CBB) (Bio-Rad) and diazobenzene sulfonic acid (DBS) (Sigma-Aldrich). This approach was used to confirm MGP γ-carboxylation status.

4.2.8 Extracellular matrix mineralization assay

To induce ECM mineralization, confluent cultures grown in advanced DMEM were supplemented with either β-glycerophosphate (BPG) salts, inorganic phosphate (Pi), or $CaCl_2$ to final calcium concentrations of 10 mM, 2 mM, and 5.4 mM, respectively. Extracellular matrix mineralization experiments were performed during three weeks with media changes twice a week and each week set as an experimental time point (T0 to T3). Mineral content was detected by von Kossa staining as described [207]. Formation of mineralized nodules in

the ECM was observed and images taken with a Motic AE 31 inverted light microscope equipped with a digital camera and Motic Images Plus 2.0 software.

To analyse the effect of GRP on mineralization and the influence of γ-carboxylation, confluent chondrocytes and synoviocytes were grown for 3 weeks in advanced DMEM under mineralizing conditions ($CaCl_2$) supplemented with 500 ng/mL of cGRP or ucGRP, and compared with cells grown during the same period in the same conditions but without GRP supplementation. The addition of 500 ng/mL of γ-carboxylated MGP (cMGP) was also analysed, as a positive control for calcification inhibition. Sturgeon GRP and human recombinant GRP, purified within the scope of a parallel project [15], were used as cGRP and ucGRP, respectively, while purified bovine MGP [16], was used as cMGP. At appropriate times, calcium/protein ratios of the cell system were determined, as described in section 4.2.9.

4.2.9 Calcium and total protein quantification

At appropriate times, cell cultures grown in control or mineralizing conditions, were washed twice with PBS and mineral was dissolved with 1 M HCl, overnight at 4 °C. Extracellular matrix calcium concentration was determined using a commercially available colorimetric kit (Calcium assay CA-590, Randox, Co. Antrim, UK). Equimolar amounts of NaOH containing 5 % w/v SDS were then used to neutralize the remaining HCl-mineral phase and determine the total protein concentration using the micro BCA protein assay kit (Thermo Scientific, Waltham, MA, USA).

Aliquots of purified sturgeon GRP, human recombinant GRP and bovine MGP, were quantified based on the general reference setting that a protein solution with an extinction coefficient (E) of 0.1% (1 mg/ml) produces an absorbance of 1.0 at 280 nm (whit a path length of 1 cm) [193].

4.2.10 Immunohistochemistry

Osteoarthritic synovial membrane tissues for histological analysis were embedded in paraffin and sectioned as described in Chapter 2, section 2.2.2. Immunohistochemistry (IHC) was performed as described in Chapter 2, section 2.2.3, to detect specific antigens in synovial membrane samples. As primary antibodies, rabbit polyclonal CTerm-GRP (5 µg/mL) and

mouse monoclonal cluster of differentiation 45 (CD45) (2 µg/mL, Santa Cruz Biotechnology, Texas, TX, USA) were used.

4.2.11 Inflammation assay

Confluent chondrocytes and synoviocytes were cultured in advanced DMEM or supplemented with 500 ng/mL of cGRP, ucGRP or cMGP, or 2 µM dexamethasone (DXM), during 24 h. Cells were washed twice with PBS and media was changed for advanced DMEM supplemented with 5 ng/mL of IL-1β for 72 h. At appropriate times, cell media was collected for prostaglandin E2 (PGE2) quantification and cells washed twice with PBS for RNA extraction. Prostaglandin E2 measurement was achieved using an available ELISA kit (Thermo Scientific) following manufacturer's protocol.

4.2.12 Basic calcium phosphate crystals assay

Basic calcium phosphate crystals were produced based on a previously described procedure [15]. Briefly, 2 mM $CaCl_2$ and 10mM sodium phosphate buffer pH 7.0 were incubated for 2 h at 37 ^{o}C, and centrifuged at 20.000 x g for 20 min at RT. The resulting crystals were washed three times with Milli-Q water and reduce to fine particles by sonication during 4 min at a 40 % amplitude (Vibra-cell apparatus, Sonics & Materials, Newtown, MA, USA). Crystals were observed and photographed with a Motic AE 31 inverted light microscope equipped with a digital camera, using Motic Images Plus 2.0 software. The BCP nature of the obtained crystals was confirmed by infrared (IR) spectroscopy at Universidade Nova de Lisboa (Departamento de Química, Lisboa, Portugal).

Protein-mineral complexes were prepared by incubating BCP crystals (100 µg) in Milli-Q water for 30 min at 37 ^{o}C with approximately 500 ng of cGRP, ucGRP or cMGP. Pellets containing BCP crystals and BCP crystals coated to GRP or MGP were added to confluent chondrocytes and synoviocytes and assayed for 72 h (controls had culture media only). At appropriate times, cells were washed twice with PBS prior to RNA extraction and cell media was collected for PGE2 measurement as previously described.

4.2.13 Statistical analysis

GraphPad Prim 6 software (GraphPad Software, Inc., San Diego, CA, USA) was used for graphic design and statistical analysis. Data are presented as mean ($n>2$) ± standard error. Ordinary one-way ANOVA was used for comparisons within the same group. Multiple t-tests were used for comparison between two groups. For two groups submitted to a variable, significance was determined using two-way Anova and multiple comparisons were achieved with the Tukey's test. Statistical significance was defined as $P\leq0.05$ (*), $P\leq0.005$ (**) and $P\leq0.0005$ (***).

4.3 Results

4.3.1 Establishment of an *in vitro* cell model suitable for the study of OA-associated mineralization and inflammation

To further explore the association of GRP with pathological features of OA, namely mineralization and inflammation processes, an OA-derived *in vitro* cell system containing the two main articular cell types was developed. Accordingly, OA-derived primary monolayer cultures of chondrocytes (OA-HAC) and synoviocytes (OA-HFLS) were developed from articular cartilage and synovial membrane tissues, respectively, collected from the knee joint of an OA patient (subject information is described in Chapter 2, sections 2.3.1 and 2.4.1, **Tables 2.II** and **2.III**). Control primary monolayer cultures of chondrocytes (NHAC) and synoviocytes (HFLS) were achieved for comparisons. At early passages, OA-HAC and NHAC cells revealed the typical polygonal morphology of chondrocytes, while OA-HFLS and HFLS cells shown the bipolar morphology characteristic of fibroblast-like synoviocytes (**Fig. 4.1**).

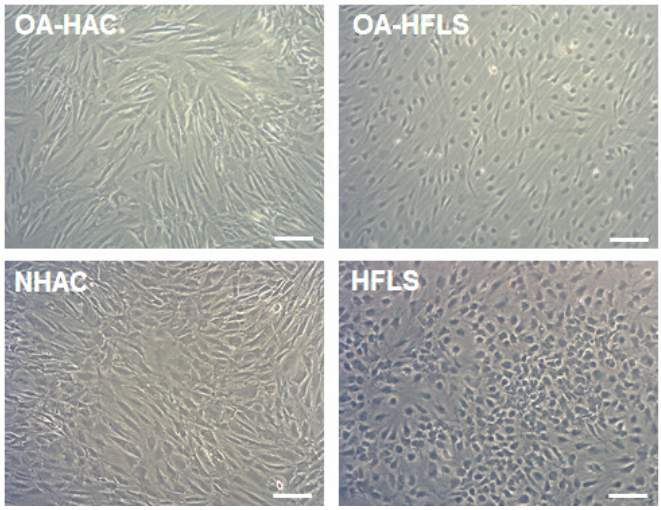

Fig. 4.1 – Phase-contrast micrographs of confluent monolayers of developed OA-derived chondrocytes (OA-HAC) and synoviocytes (OA-HFLS), and commercial control-derived chondrocytes (NHAC) and synoviocytes (HFLS) primary cell lines at passages 4 or 5. Scale bars represent 100 µm.

In order to establish the optimal conditions for the *in vitro* cultivation of OA-derived and control primary cultures, growth performances of OA-HAC, OA-HFLS, NHAC and HFLS cells were analysed in DMEM, previously used for the cultures development, and Advanced DMEM, enriched in normal-serum constituents (**Fig. 4.2**). Higher proliferation capacities for all cell cultures were observed in Advanced DMEM (**Fig. 4.2**), and for that this was the culture media selected for further cells cultivation. Accordingly, cells were grown continuously in Advanced DMEM supplemented with 10% v/v FBS at 37º C and 5% CO_2, and were sub-cultured with a ratio of 1:2 upon reaching confluency. Passaging by trypsinization did not significantly reduce the number of viable cells, and subsequent freezing and thawing did not significantly affect viability (results not shown). At confluence, cells formed confluent monolayers but not multilayer aggregates, and initial morphology (**Fig. 4.1**) was maintained for more than 15 passages.

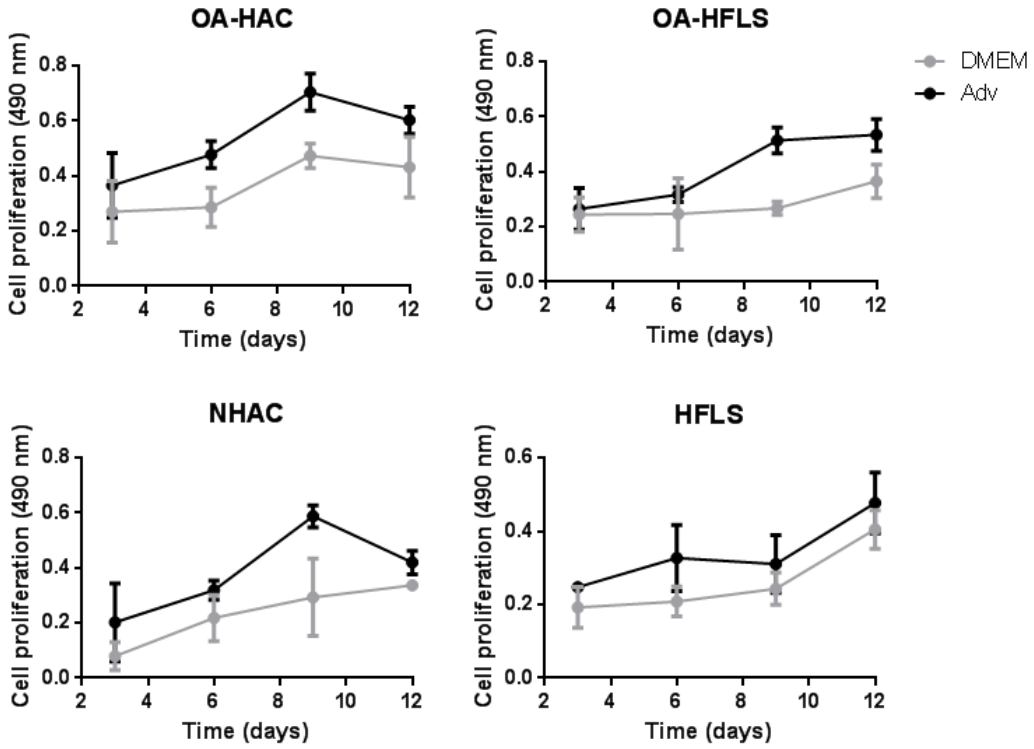

Fig. 4.2 – Control and OA-derived chondrocyte (NHAC/OA-HAC) and synoviocyte (HFLS/OA-HFLS) cultures have higher growth performances in Advanced DMEM (Adv) comparing to DMEM, both supplemented with 10% fetal bovine serum (FBS). Cell proliferation was analysed every 3 days during a 12-day period using a colorimetric method. All experiments were repeated at least three times.

Since synovial membrane tissue is composed of two cell types, macrophage-like and fibroblast-like cells, further characterization of the developed OA-HFLS culture was performed by IF immunodetection of the macrophage marker CD68 (**Fig. 4.3**), to support the apparently predominant fibroblast-like cells phenotype. Results showed a barely detectable staining for CD68 in OA-HFLS cells, in contrast with the high levels found in the macrophage-derived THP1 cells (THP1-MAC), used as positive control (**Fig. 4.3**), indicating an almost absence of macrophage-like cells on the developed synovial membrane-derived primary cultures.

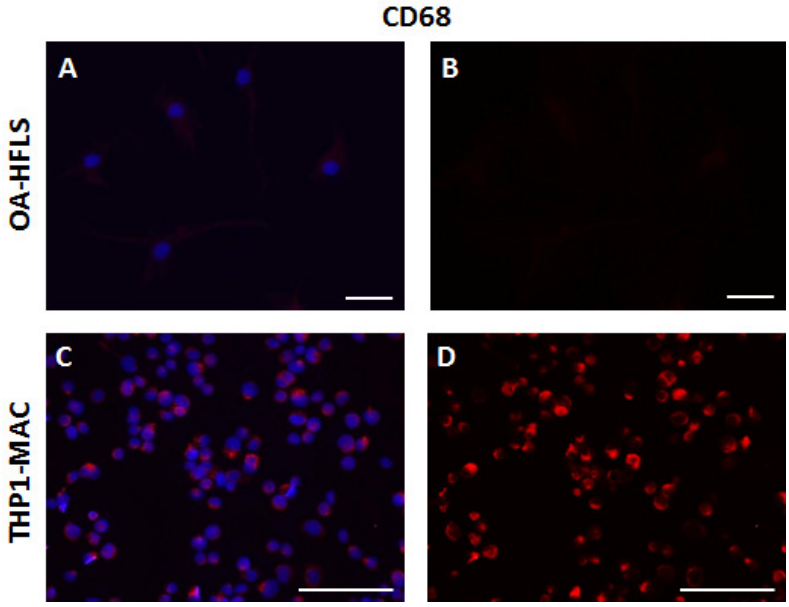

Fig. 4.3 – Evaluation of the macrophage marker cluster of differentiation 68 (CD68) in the developed OA-HFLS primary cell line. Immunofluorescence (IF) analysis of CD68 were performed in OA-HFLS cells (**A** and **B**) and THP1-MAC cells and positive immunoreactions were evidenced by the reddish colour. Cell nuclei were stained with DAPI in panels **A** and **C**. Scale bars represent 100 µm.

Further characterization of control and OA-derived chondrocytes (NHAC/OA-HAC) and synoviocytes (HFLS/OA-HFLS) was achieved through gene expression profiling of differentiation and known OA-related markers (**Fig. 4.4**). Higher levels of OC, cartilage oligomeric matrix protein (COMP) and collagen type X (Col10a1), and lower levels of collagen type II (Col2a1) were detected in OA-HAC cells (**Fig. 4.4**, **A**), confirming an osteoarthritic chondrocyte phenotype. Also, OA-HFLS cells, exhibited higher levels of the

OA-associated gene markers OC, MMP13 and CD68, and lower vimentin expression (**Fig. 4.4**, **B**).

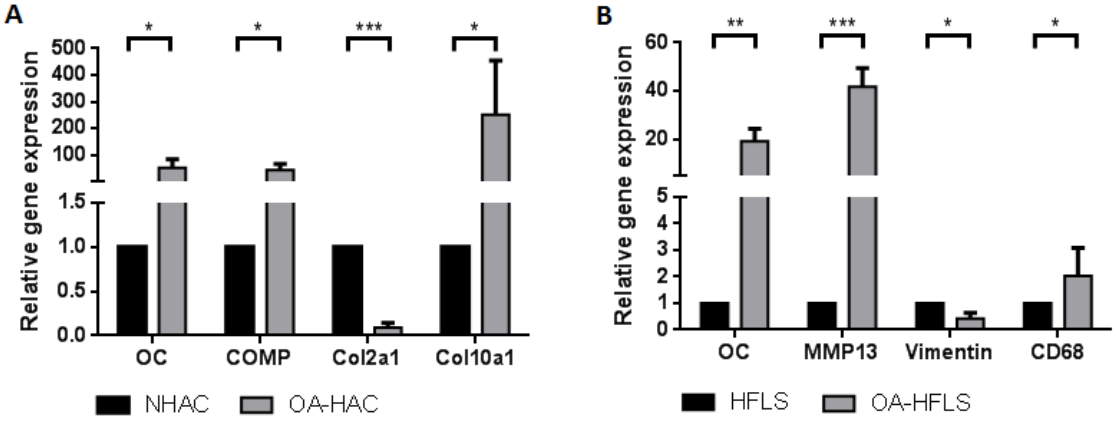

Fig. 4.4 – Gene expression of differentiation and OA markers in control and OA-derived chondrocyte and synoviocyte primary cell cultures. The expression pattern of OA (OC, COMP and MMP13) and differentiation (Cola2, Cola10, CD68 and vimentin) gene markers in control (NHAC) and OA-derived (OA-HAC) chondrocytes (**A**) and control (HFLS) and OA-derived (OA-HFLS) synoviocytes (**B**) was analysed. Values are relative to a reference sample (control cell culture) set to 1. All experiments were repeated at least three times. Multiple t-tests were performed. Statistical significance was defined as P≤0.05 (*), P≤0.005 (**) and P≤0.0005 (***) (Adapted from Cavaco et al., 2015 [208]).

Gene expression results revealed significant differences between control and OA-derived cells, representative of healthy and osteoarthritic conditions, respectively, indicating the suitability of this *in vitro* cell system as a model for the study of osteoarthritis.

4.3.2 Association of GRP and genes involved in the γ-carboxylation machinery with osteoarthritis

The expression pattern of GRP, MGP and genes related to γ-carboxylation processing was analysed in control and OA-derived cultures, to access possible differences between the two conditions (**Fig. 4.5**). GRP was found to be upregulated in both OA-derived cultures (**Fig. 4.5**, **A** and **B**), in agreement with the higher GRP expression associated with OA-affected cartilage described in Chapter 3. MGP was also found to be upregulated in the OA-derived cells (**Fig. 4.5**, **A** and **B**). In contrast, γ-carboxylase (GGCX) and vitamin K epoxide reductase (VKOR) were shown to be downregulated in OA-derived cells (**Fig. 4.5**, **A** and **B**).

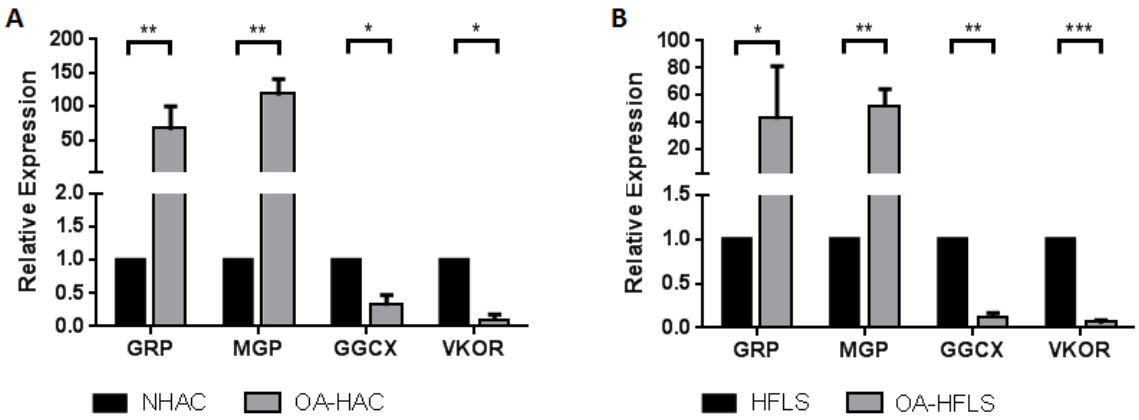

Fig. 4.5 – Gene expression of GRP and genes involved in the γ-carboxylation machinery in control and OA-derived chondrocyte and synoviocyte cell cultures. The expression of GRP, MGP, GGCX and VKOR genes in control (NHAC) and OA-derived (OA-HAC) chondrocytes (**A**) and control (HFLS) and OA-derived (OA-HFLS) synoviocytes was analysed (**B**). Values are relative to a reference sample (control cell culture) set to one. All experiments were repeated at least three times. Multiple t-tests were performed. Statistical significance was defined as P≤0.05 (*), P≤0.005 (**) and P≤0.0005 (***) (Adapted from Cavaco et al., 2015 [208]).

To access GRP γ-carboxylation status in control and OA-derived chondrocytes and synoviocytes, the protein accumulation pattern was analysed by IF using the conformation-specific monoclonal antibodies cGRP and ucGRP and the polyclonal CTerm-GRP recognizing total GRP (**Fig. 4.6**). Both cGRP and ucGRP were detected in pathological and control chondrocytes, whereas only ucGRP was found associated with the OA-HFLS cells, suggesting the predominance of the undercarboxylated form associated with the disease, like observed in Chapter 3.

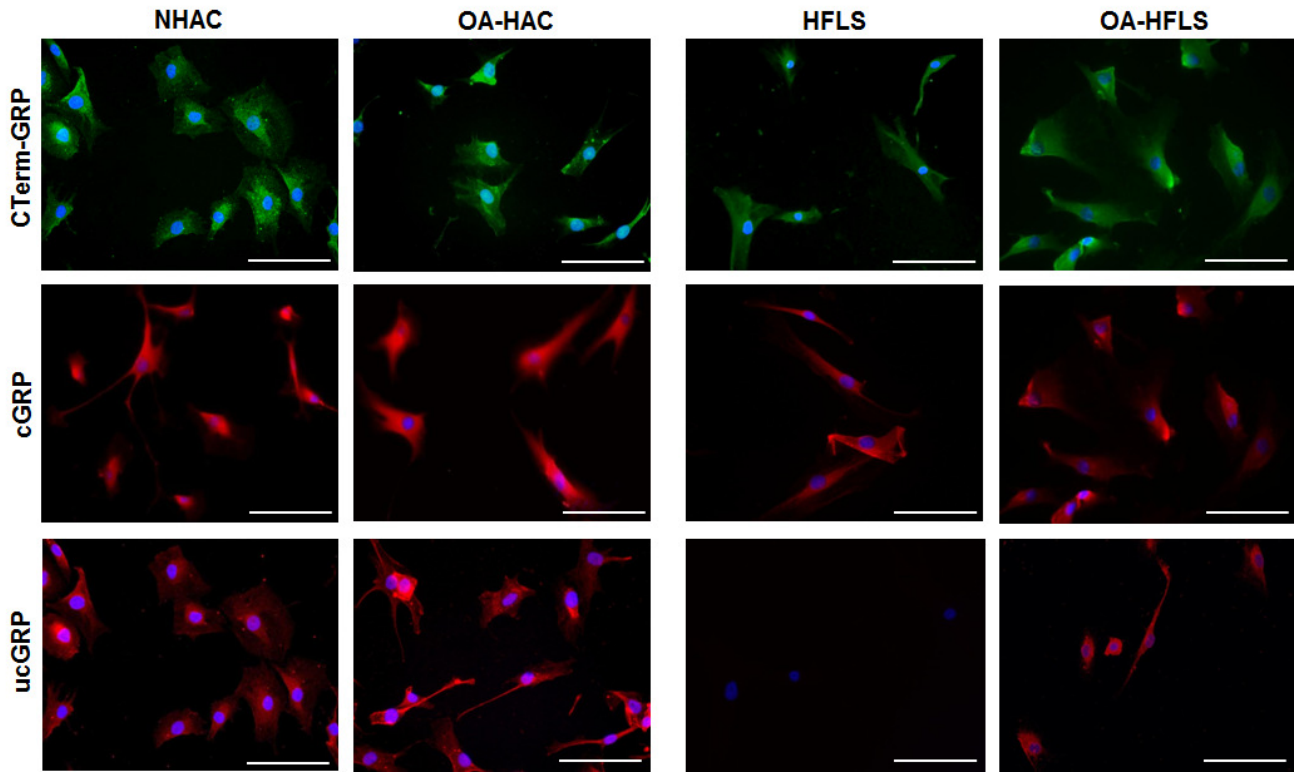

Fig. 4.6 – Accumulation patterns of GRP protein forms in control (NHAC and HFLS) and OA-derived (OA-HAC and OA-HFLS) chondrocytes and synoviocytes, respectively. Immunofluorescence (IF) imaging was obtained for total GRP (CTerm-GRP), γ-carboxylated (cGRP) and undercarboxylated GRP (ucGRP) protein forms using the respective specific antibodies. Cell nuclei were stained with DAPI. Scale bar represents 100 µm. All experiments were repeated at least two times (Adapted from Cavaco et al., 2015 [208]).

Overall, the collected information indicates that OA-derived cells, showing osteoarthritic features, have GRP upregulation and indications of a reduced γ-carboxylation capacity.

4.3.3 Gla-rich protein is associated with calcification and cell differentiation in osteoarthritis

To analyse the association of GRP with pathological mineralization, the *in vitro* model was induced to mineralize its ECM. In chondrocytes, induced ECM mineralization has been previously described [209,210], however, no information was found at the time these studies were conducted for synoviocytes. Therefore, several conditions were tested to promote ECM mineralization in the two cell types, based on existing information [207,209-211]. In agreement, the effect of β-glycerophosphate (BGP), inorganic phosphate (Pi), and $CaCl_2$

supplementation in OA-HAC and OA-HFLS cells was analysed at week 3 of treatment (**Fig. 4.7**). Von Kossa staining and calcium quantification of the mineral deposited in the ECM indicated that both cell cultures were able to mineralize their ECM in all tested conditions but with different levels (**Fig. 4.7**). Although higher calcium levels and mineral deposition were found in chondrocytes, also synoviocytes were shown to produce a mineralized ECM, particularly under $CaCl_2$ treatment (**Fig. 4.7**).

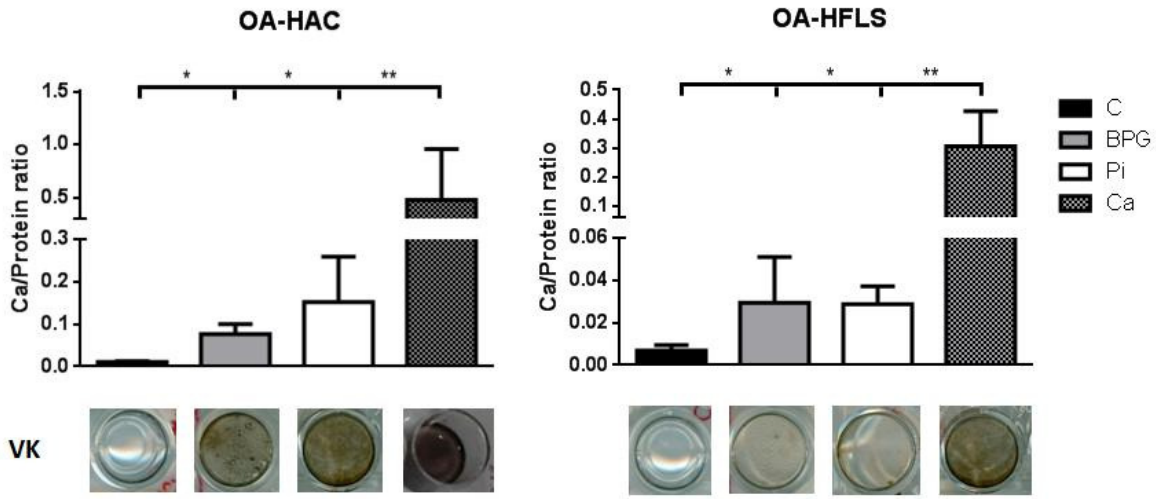

Fig. 4.7 – Comparative analysis of OA-derived chondrocytes and synoviocytes (OA-HAC and OA-HFLS, respectively) *in vitro* mineralization using different supplementations. Mineralization rate and von Kossa staining at week 3 of OA-HAC and OA-HFLS cells induced to mineralize their extracellular matrix (ECM) with 10 mM β-glycerophosphate (BPG), inorganic phosphate (Pi) and 5.4 mM $CaCl_2$ (Ca). C represents control conditions. Calcium accumulation was normalized to protein levels. Data is representative of one experiment. Ordinary one-way ANOVA was performed. Statistical significance was defined as $P \leq 0.05$ (*) and $P \leq 0.005$ (**).

Since higher ECM mineralization was achieved with $CaCl_2$ supplementation in chondrocyte and synoviocyte cell cultures, without affecting cell proliferation capacity (**Fig. 4.8**), subsequent mineralization experiments in control and OA-derived cells were induced with $CaCl_2$ during 3 weeks (**Fig. 4.9**). Von Kossa and calcium quantification results revealed that all cell cultures were able to mineralize their ECM, and higher calcium levels and mineral deposition were found in chondrocyte-derived cultures when compared to synoviocytes, after the 3 weeks of treatment (**Fig. 4.8**, **A** and **B**, T3). Significant differences in calcium quantification between OA and control chondrocytes were evident at week 1 (T1), although during subsequent weeks the differences gradually disappeared.

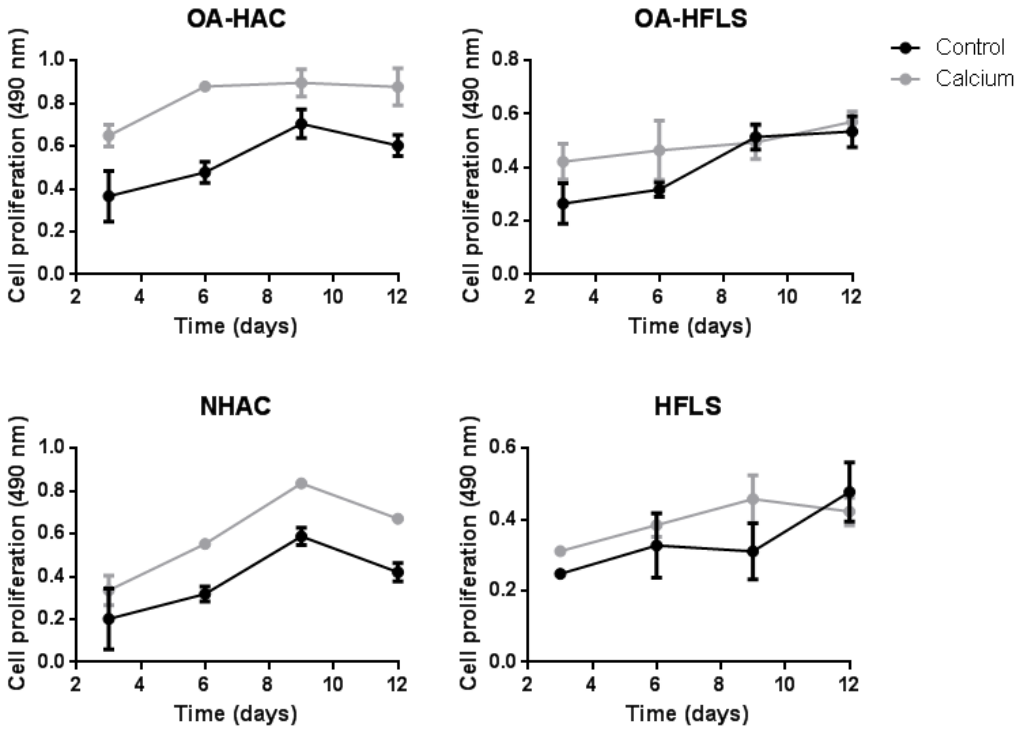

Fig. 4.8 – Effect of 5.4 mM $CaCl_2$ media supplementation on OA-derived and control chondrocytes (OA-HAC and NHAC, respectively) and synoviocytes (OA-HFLS and HFLS, respectively) proliferation. Cell proliferation was analysed every 3 days during a 12-day period using a colorimetric method. All experiments were repeated at least three times.

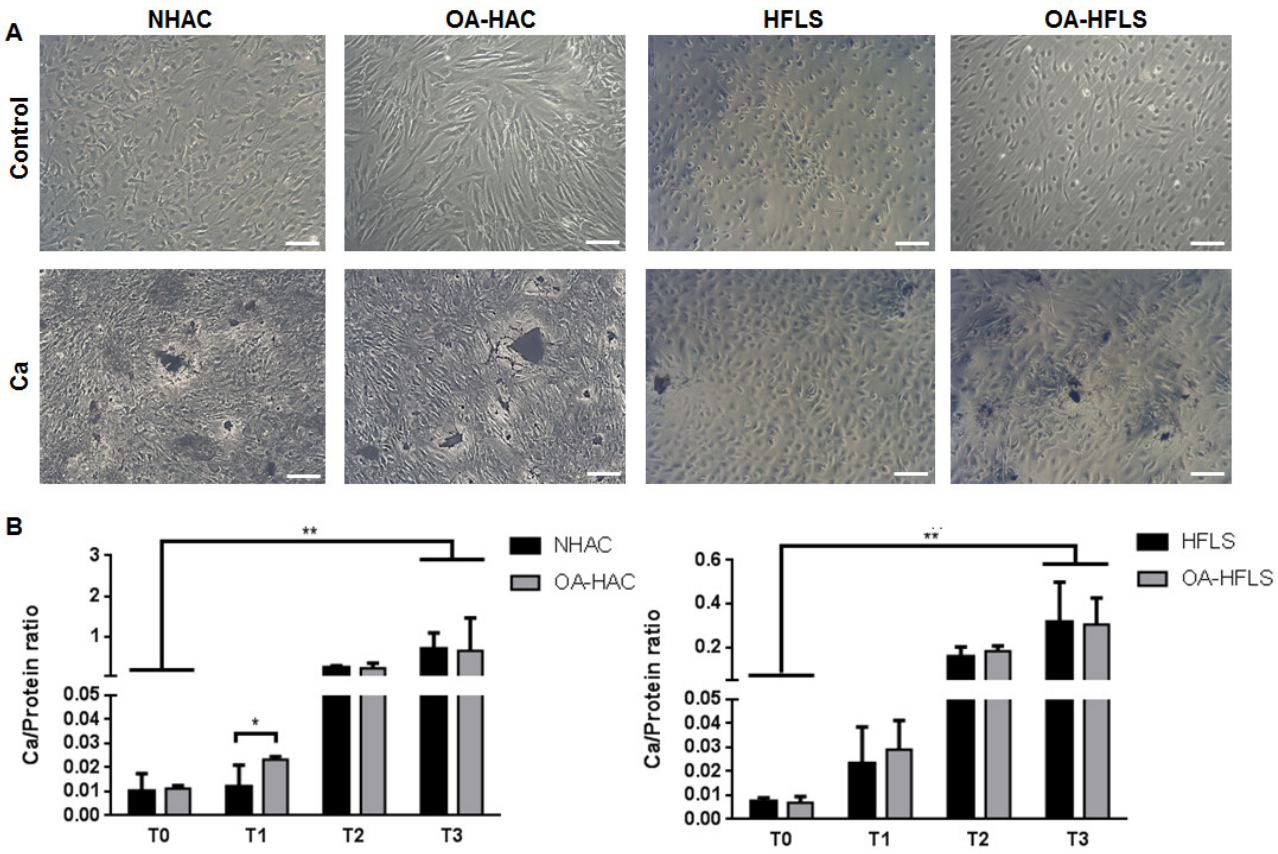

Fig. 4.9 – Control and OA-derived chondrocytes and synoviocytes (NHAC and OA-HAC, and HFLS and OA-HFLS, respectively) are able to mineralize their extracellular matrix (ECM) *in vitro*. (**A**) Representative von Kossa staining at week 3 (T3) in control or induced mineralizing conditions with 5.4 mM $CaCl_2$ (Ca). Scale bar represents 100 µm. (**B**) Mineralization rate determined every week (T0 to T3) with calcium accumulation normalized to protein levels. Data is representative of three independent experiments. Two-way Anova and multiple comparisons were achieved with the Tukey's test. Statistical significance was defined as P≤0.05 (*) and P≤0.005 (**) (Adapted from Cavaco et al., 2015 [208]).

The patterns of gene markers for cell differentiation and mineralization were simultaneously investigated in control and osteoarthritic primary cells to correlate with the calcification process (**Fig. 4.10**). After the first week of treatment (T1), OA-derived chondrocytes showed higher expression levels of GRP, MGP, OC, Osx and Col10a1, and lower levels of Col2a1, compared to control cells (**Fig. 4.10**). The progressive downregulation of Col2a1 simultaneously with the upregulation of Col10a1, Osx and OC throughout the treatment, in both cultures, was consistent with the differentiation occurring in chondrocytes towards a hypertrophic phenotype and ECM calcification (**Fig. 4.10**). The most significant differences between control and OA-derived cells were observed at T1, suggesting that primary OA-derived chondrocytes probably represent later stages of differentiation than control cells, with a faster response to the calcification stimuli. At T3, most of the gene

markers were found similarly expressed, in concordance with the similar levels of calcification obtained for both cultures (**Fig. 4.9**, **B**). Notably, levels and patterns of GRP and Osx gene expression were found similarly upregulated in OA derived chondrocytes throughout mineralization treatment, with higher levels in OA-derived cells at all-time points.

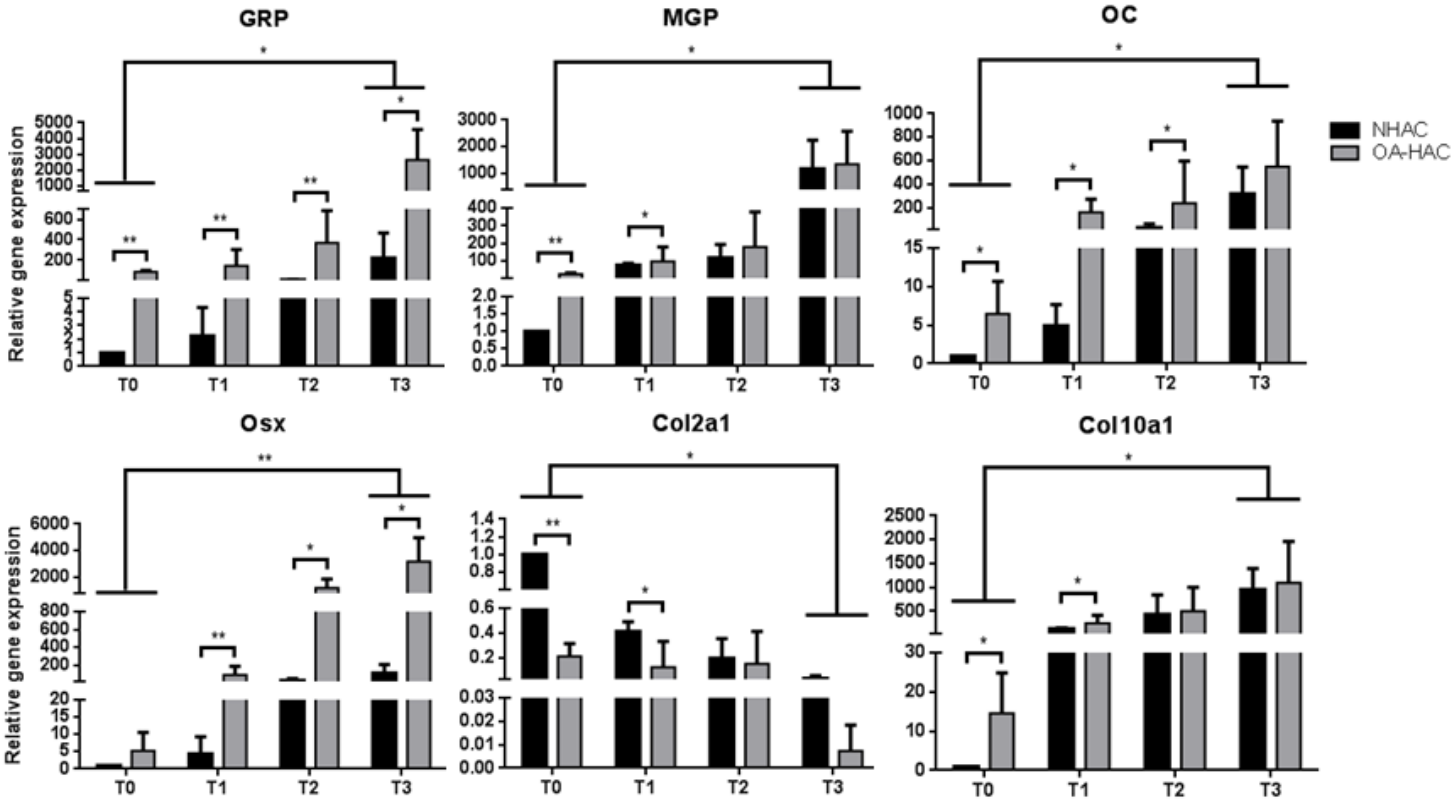

Fig. 4.10 – GRP is associated with calcification and cell differentiation in OA-HAC cells. Gene expression patterns of GRP, mineralization (MGP, OC and Osx) and differentiation (Col2a1 and Col10a1) markers in mineralizing chondrocytes (NHAC and OA-HAC). Gene expression was determined every week during 3 weeks (T0 to T3). Relative gene expression values are relative to the reference sample (control cell culture) and set to 1. Data is representative of three independent experiments. Two-way Anova and multiple comparisons were achieved with the Tukey's test. Statistical significance was defined as $P \leq 0.05$ (*) and $P \leq 0.005$ (**) (Adapted from Cavaco et al., 2015 [208]).

In synoviocytes, vimentin downregulation and CD68 upregulation was observed during induced calcification, in both control and OA-derived cells, suggesting a phenotypic change from fibroblast-like synoviocytes towards a macrophage-lineage (**Fig. 4.11**). Gla-rich protein, MGP, OC and osteopontin (OPN) were gradually upregulated throughout mineralization, with slight differences observed between OA-derived and control cells (**Fig. 4.11**).

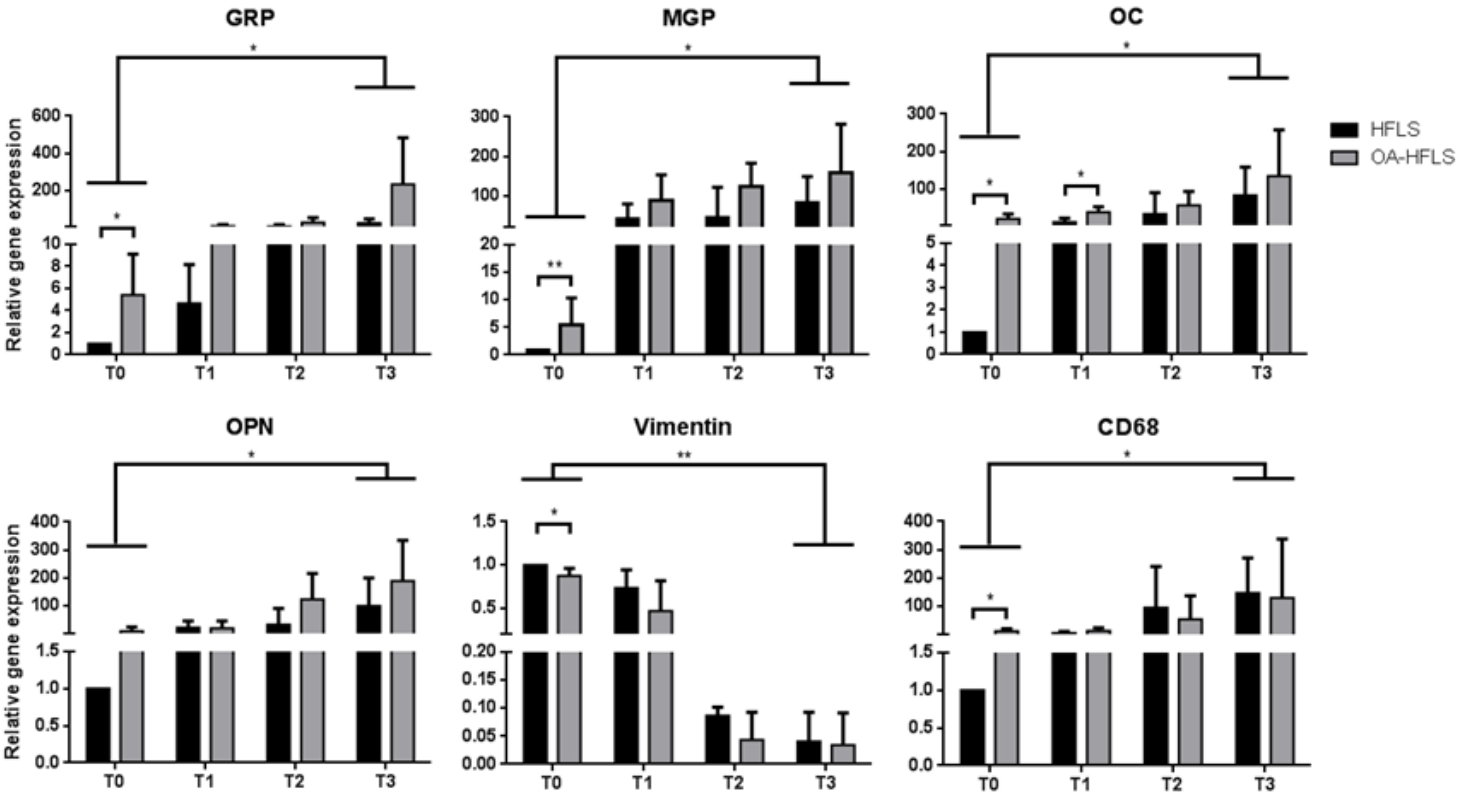

Fig. 4.11 – GRP is associated with calcification and cell differentiation in OA-HFLS cells. Gene expression patterns of GRP, mineralization (MGP, OC and OPN) and differentiation (vimentin and CD68) markers in mineralizing synoviocytes (HFLS and OA-HFLS). Gene expression was determined every week during 3 weeks (T0 to T3). Relative gene expression values are relative to the reference sample (control cell culture) and set to 1. Data is representative of three independent experiments. Two-way Anova and multiple comparisons were achieved with the Tukey's test. Statistical significance was defined as $P \leq 0.05$ (*) and $P \leq 0.005$ (**) (Adapted from Cavaco et al., 2015 [208]).

The results described in this section point for a role of GRP during cell differentiation processes, highly associated with pathological calcification, in agreement with GRP accumulation at sites of ectopic calcification in osteoarthritic articular cartilage and synovial membrane tissues, shown in Chapter 3.

4.3.4 Carboxylated GRP reduces mineral deposition in chondrocytes and synoviocytes ECM

To determine the direct effect of GRP in ECM mineralization of chondrocytes and synoviocytes and further unveil the relevance of its γ-carboxylation status, cells cultured under control and mineralizing conditions where supplemented with cGRP or ucGRP. The effect of the calcification inhibitor cMGP in the mineralizing cells was also analysed as a positive control. Before initiating the analysis, the γ-carboxylation of the used RP-HPLC purified bovine MGP [16] was confirmed by positive DBS staining (red) on SDS-PAGE, a specific staining for Gla-containing proteins (**Fig. 4.12**). Subsequently, cell proliferation assays were performed for both c/ucGRP protein forms and cMGP, to confirm that the protein supplementation had no cytotoxic effect (**Fig. 4.13**).

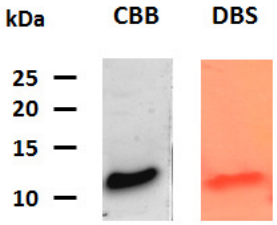

Fig. 4.12 – Evaluation of purity and γ-carboxylation status of purified bovine MGP through SDS-PAGE and DBS staining. Reverse phase-high performance liquid chromatography (RP-HPLC) purified bovine MGP [16] analysis on SDS-PAGE by staining with coomassie brilliant blue (CBB) (5 µg) and diazobenzene sulfonic acid (DBS) (30 µg). Relevant molecular mass markers (kDa) are indicated on the left of the panels.

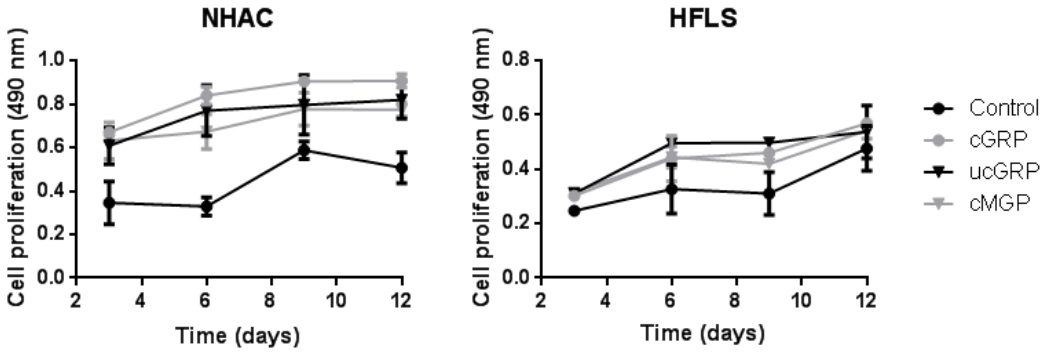

Fig. 4.13 – Effect of 500 ng/mL of carboxylated/undercarboxylated GRP (c/ucGRP) and carboxylated MGP (cMGP) media supplementation on NHAC and HFLS cultures proliferation. Cell proliferation was analysed every 3 days during a 12-day period using a colorimetric method. All experiments were repeated at least three times.

Results showed that the addition of cGRP significantly decreased mineral deposition after three weeks of treatment in both chondrocytes and synoviocytes, while no effect was observed with ucGRP treatment (**Fig. 4.14**). As expected, with cMGP supplementation, a decreased mineral deposition was observed after three weeks of treatment, similar to that induced by cGRP (**Fig. 4.14**).

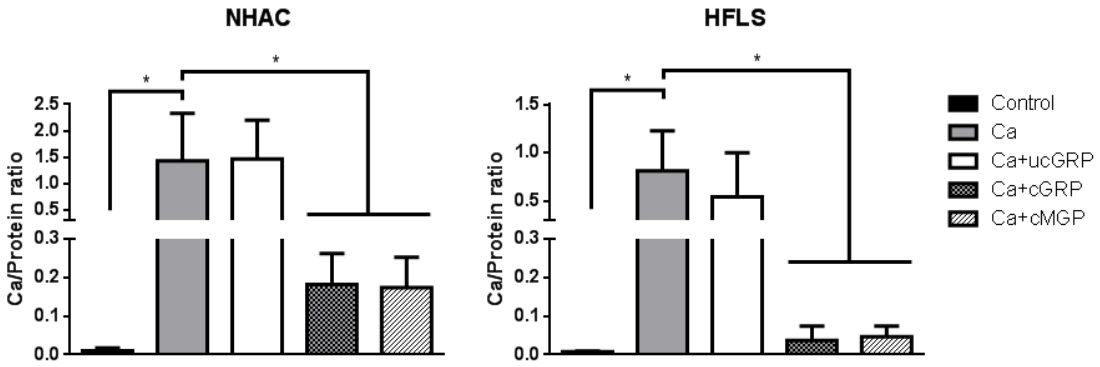

Fig. 4.14 – Carboxylated GRP reduces mineral deposition in chondrocytes (NHAC) and synoviocytes (HFLS) extracellular matrix (ECM). Mineralization rate was determined by calcium measurement using a colorimetric kit (normalized to protein levels) after 3 weeks of treatment with 5.4 mM $CaCl_2$ (Ca) or Ca supplemented with 500 ng/mL undercarboxylated GRP (Ca+ucGRP), carboxylated GRP (Ca+cGRP) or carboxylated MGP (Ca+cMGP). Control corresponds to cells cultured in non-supplement media. Data is representative of three independent experiments. Ordinary one-way ANOVA was performed. Statistical significance was defined as $P \leq 0.05$ (*) (Adapted from Cavaco et al., 2015 [208]).

Similar responses to c/ucGRP and cMGP supplementation were obtained for OA-derived cells, representative of later stages of differentiation (results not shown). These results are in agreement with those presented in section 4.3.3, showing similar expression of calcification and differentiation gene markers between control and OA-derived cells at week 3 of induced mineralization.

4.3.5 Gla-rich protein is associated with inflammatory events in OA

To study the involvement of GRP with mineralization and inflammatory events occurring in OA, the inflammatory response of control and OA-derived chondrocytes and synoviocytes, associated with the induced mineralization, was determined through the expression patterns of OA-related inflammation markers (**Fig. 4.15**). The increased

expression of COX2 and MMP13, throughout the time course indicated that the mineralization stimulus was able to trigger an inflammatory response in both chondrocytes and synoviocytes (**Fig. 4.15**). No significant differences were observed between control and OA-derived cells regarding COX2 and MMP13 expression, except at T0, where COX2 was upregulated in OA-HAC cells and MMP13 in OA-HFLS cells (**Fig. 4.15**), in agreement with the described increased expression of inflammatory mediators in osteoarthritic cells [88,98,114,133].

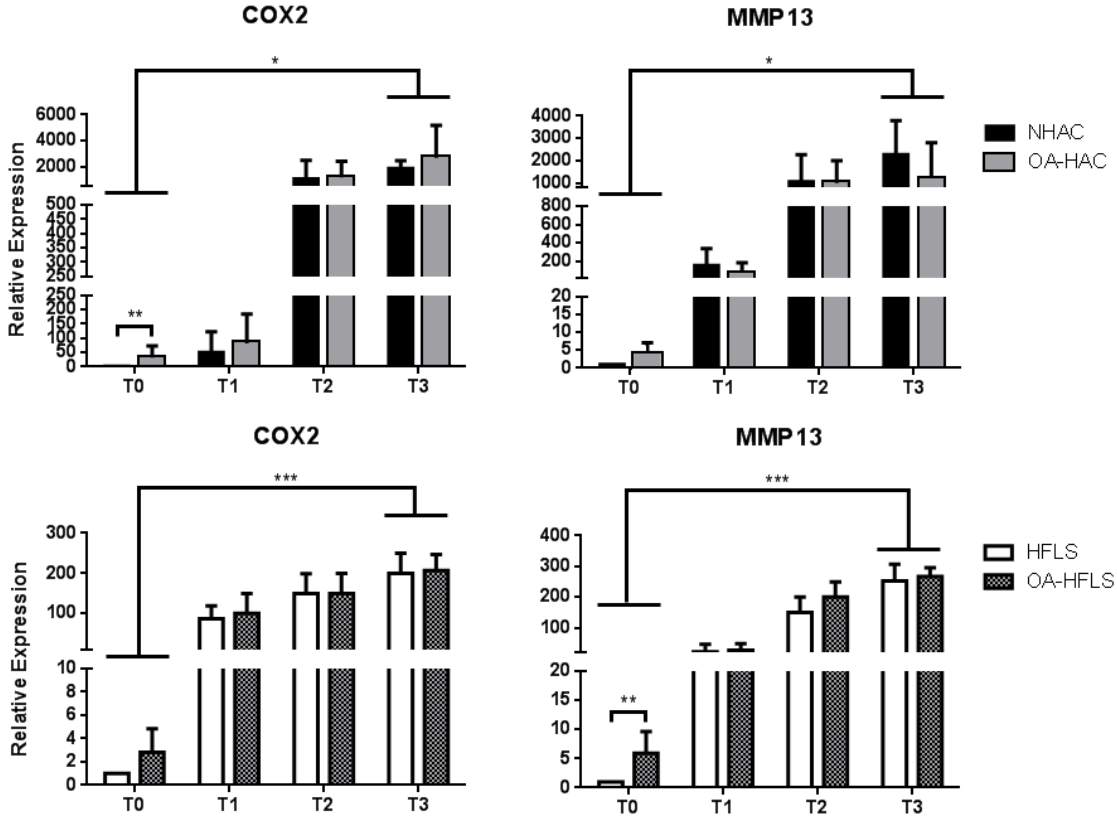

Fig. 4.15 – Gene expression of inflammation markers in control and OA-derived chondrocytes and synoviocytes under mineralization conditions. Cyclooxygenase 2 (COX2) and matrix metalloproteínase 13 (MMP13) gene expression over 3 weeks of mineralizing treatment (5.4 mM calcium) was evaluated in NHAC/OA-HAC and HFLS/OA-HFLS cells. Each week represents a set point (T0 to T3). Values of gene expression are relative to the reference sample (T0) and set to 1. Data is representative of three independent experiments. Two-way Anova and multiple comparisons were achieved with the Tukey's test. Statistical significance was defined as $P \leq 0.05$ (*) and $P \leq 0.005$ (**) (Adapted from Cavaco et al., 2015 [208]).

Interestingly, the upregulation of COX2 and MMP13 gene expression associated to induced EMC mineralization in chondrocytes and synoviocytes was parallel to GRP

upregulation (**Fig. 4.10** and **Fig. 4.11**), suggesting a possible involvement of this VKDP with inflammatory processes. Therefore, GRP hypothetical association with inflammation in OA was further studied *in vivo*, through IHC analysis of GRP and CD45 in consecutive tissue sections of osteoarthritic synovial membrane tissues, showing sites of abnormal infiltration of inflammatory cells (**Fig. 4.16**, **A-D**). CD45 is a selective marker for leukocytes [212], and notably, its positive immunoreactive signal located at sites of inflammatory cells infiltration (**Fig. 4.16**, **A** and **B**) was co-localized with GRP immunoreactive signal (**Fig. 4.16**, **C** and **D**).

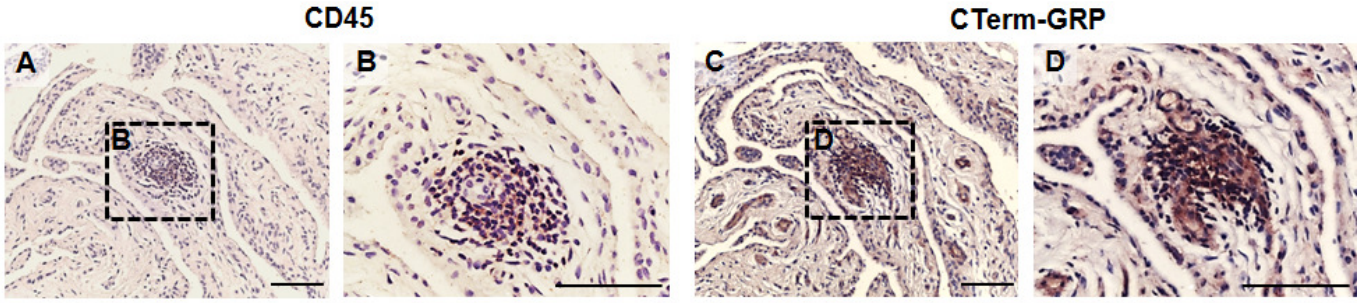

Fig. 4.16 – *In vivo* studies of GRP association with inflammatory events in osteoarthritis. Immunodetection of CD45 (**A** and **B**), showing leukocyte infiltration sites, and total GRP (**C** and **D**, CTerm-GRP antibody) in consecutive sections of osteoarthritic synovial membrane samples. Tissues were embedded with paraffin and final counterstaining was achieved with hematoxylin. Scale bars represent 100 μm (Adapted from Cavaco et al., 2015 [208]).

The involvement of GRP with inflammation was also studied *in vitro* by inducing chondrocytes and synoviocytes with an inflammatory stimulus and evaluating GRP expression pattern. Interleukin-1β was the chosen cytokine to promote an inflammatory response in the cell system using previously described concentrations [130], and after verifying it was not cytotoxic for the cells (**Fig. 4.17**). A sharp rise in GRP expression concomitant with an upregulation of COX2 and MMP13 was obtained 3 h after IL-1β treatment (**Fig. 4.18**). The expression of GRP and inflammatory gene markers was progressively decreased until control levels, from 6 to 72 h of stimulation (**Fig. 4.18**). Since MGP is also associated to calcification events and was previously suggested as a joint inflammatory marker in arthritis patients [95], its expression pattern during IL-1β-induced inflammation was also analysed, and showed a similar pattern of gene expression to that of GRP (**Fig. 4.18**). Both NHAC/OA-HAC and HFLS/OA-HFLS cells responded similarly to the inflammatory stimulus, although control cells appeared to have slightly higher expression

of the four analysed genes 3 h after IL-1β treatment (**Fig. 4.18**). The higher initial response of control cells may reflect an unprecedented contact with inflammatory conditions to which OA-derived cells were probably already exposed.

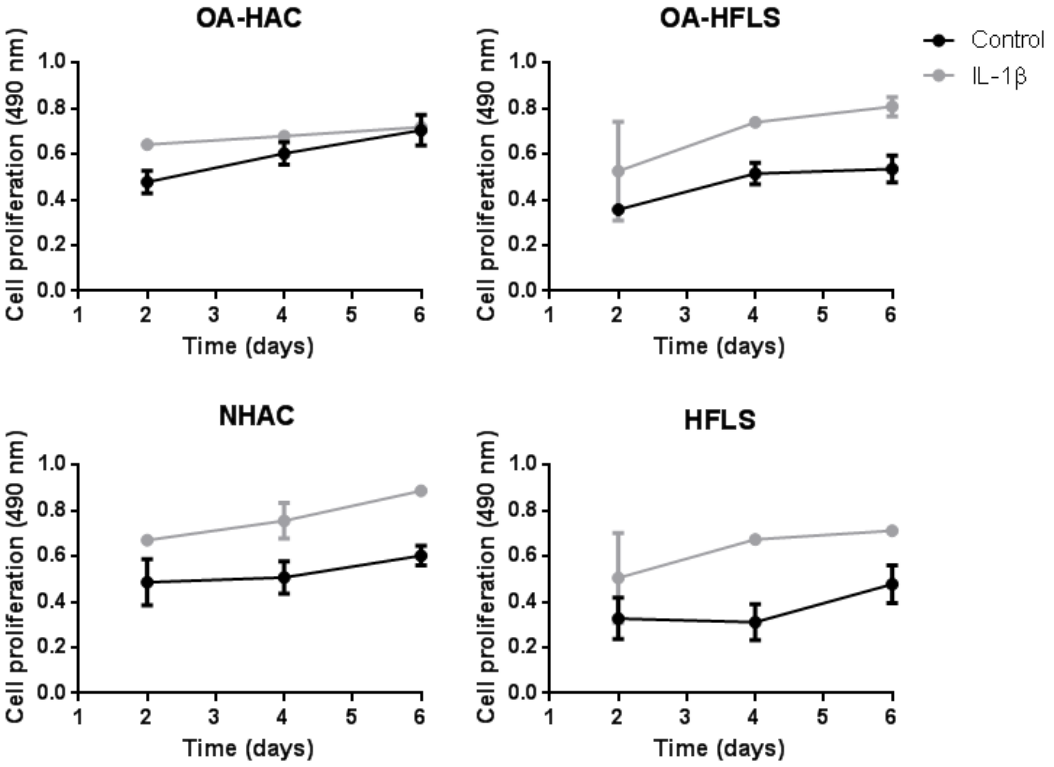

Fig. 4.17 – Effect of 5 ng/mL interleukin 1β (IL-1β) media supplementation on control and OA-derived chondrocytes (NHAC and OA-HAC, respectively) and synoviocytes (HFLS and OA-HFLS, respectively) proliferation. Cell proliferation was analysed every 2 days during a 6-day period using a colorimetric method. All experiments were repeated at least three times.

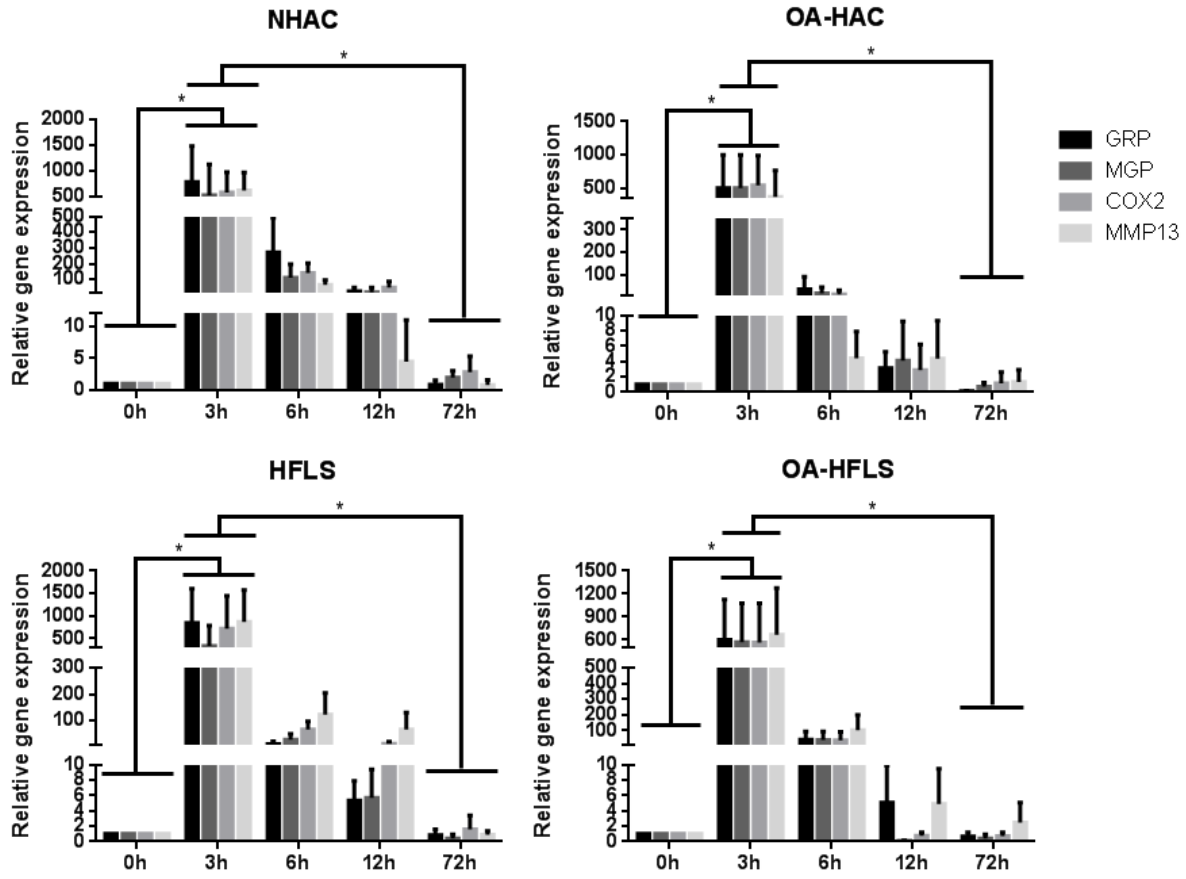

Fig. 4.18 – *In vitro* studies of GRP and MGP association with inflammatory events in osteoarthritis. Gene expression levels of COX2, MMP13, GRP and MGP in NHAC/OA-HAC and HFLS/OA-HFLS cells, after 72 h inflammatory stimulation with 5 ng/mL interleukin 1β (IL-1β). Values are relative to the reference sample (0 h) set to one. Data is representative of three independent experiments. Two-way Anova and multiple comparisons were achieved with the Tukey's test. Statistical significance was defined as P≤0.05 (*)(Adapted from Cavaco et al., 2015 [208]).

Ultimately, the obtained results in this section indicate for the first time a possible association of GRP with the inflammation processes occurring in OA, and further correlate MGP to inflammation in this pathology.

4.3.6 Gla-rich protein is a novel factor in the cross talk between calcification and inflammation processes

Basic calcium phosphate crystals deposition is associated with inflammatory responses in OA [88,91,123]. Since GRP was recently described to be able to bind BCP crystals [15], a study was designed to access the effect of GRP coating to BCP crystals supplementation in the established *in vitro* cell system, in comparison to the effect of supplementing BCP crystals

only. For that, BCP crystals were produced following a previous described procedure [15] and subsequently sonicated, since the induced inflammatory response of these crystals is considered to be size dependent [140]. Optical microscopy observations revealed that crystals were heterogeneous concerning their size, ranging from >1 µm (the optical limit of the used microscope) to approximately 8 µm (**Fig. 4.19**). The nature of the crystals was confirmed to be hydroxyapatite through IR spectroscopy (results not shown).

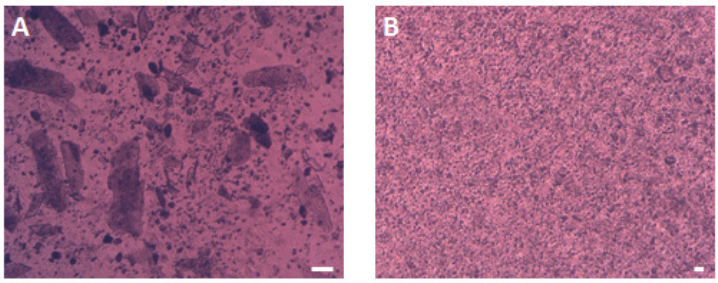

Fig. 4.19 – Micrographs of the basic calcium phosphate (BCP) crystals generated within the scope of this work, before (**A**) and after sonication (**B**). Scale bars represent 10 µm.

Before initiating the experiment, the cytotoxicity of BCP crystals addition to the cell system was evaluated, showing that the treatment did not affect cell proliferation (**Fig. 4.20**). To evaluate the BCP-induced inflammatory responses, control chondrocyte and synoviocyte cells were treated during 72 h with the BCP crystals, in previously described amounts [213] (**Fig. 4.21**). The inflammatory response of BCP crystals coated with c/ucGRP or cMGP was also evaluated (**Fig. 4.21**). The upregulation of COX2 and MMP13 expression in BCP-treated cells confirmed the inflammatory response mediated by the crystals both in chondrocytes and synoviocytes cell cultures (**Fig. 4.21**). Treatment of cells with BCP crystals coated with cGRP or ucGRP resulted in decreased COX2 and MMP13 expression, and similar results were obtained with BCP crystals coated with cMGP (**Fig. 4.21**). Similar results were also obtained with the OA-derived cultures (results not shown).

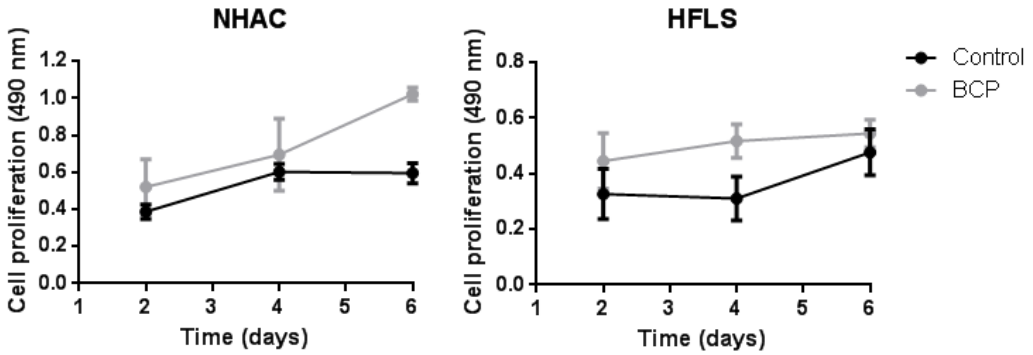

Fig. 4.20 – Effect of 100 µg/mL basic calcium phosphate (BCP) crystals media supplementation on NHAC and HFLS cells proliferation. Cell proliferation was analysed every 2 days during a 6-day period using a colorimetric method. All experiments were repeated at least three times.

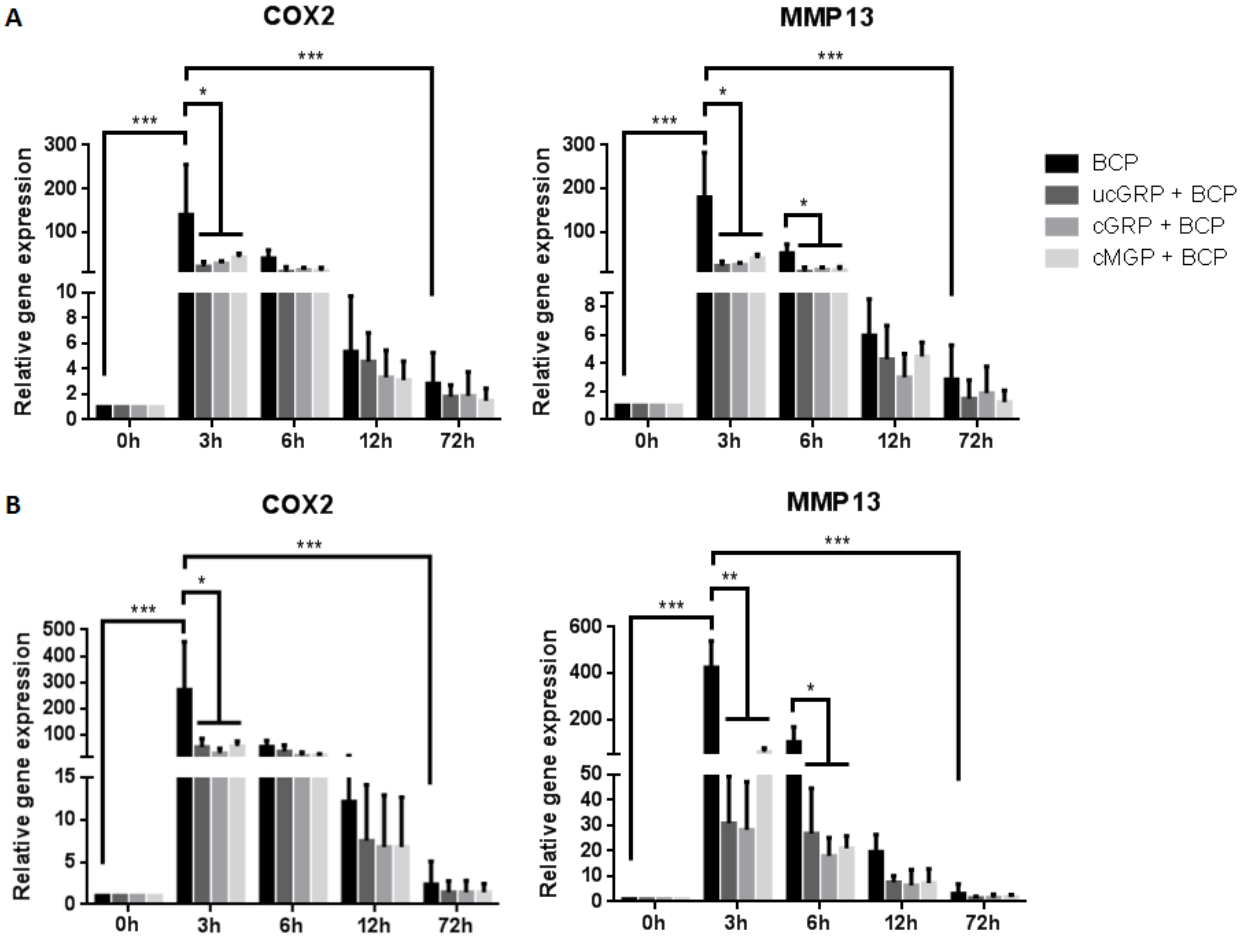

Fig. 4.21 – Effect of GRP and MGP in the inflammatory process promoted by the addition of basic calcium phosphate (BCP) crystals to articular cells. Gene expression of cyclooxygenase 2 (COX2) and matrix metalloproteinase 13 (MMP13) in NHAC (**A**) and HFLS (**B**) cells supplemented for 72 h with basic calcium phosphate (BCP) crystals or BCP crystals coated with undercarboxylated GRP (BCP + ucGRP), carboxylated GRP (BCP + cGRP) or carboxylated MGP (BCP + cMGP) is represented. Values are relative to the reference sample

(untreated cells, 0 h). Data is representative of three independent experiments. Two-way Anova and multiple comparisons were achieved with the Tukey's test. Statistical significance was defined as P≤0.05 (*), P≤0.005 (**) and P≤0.0005 (***) (Adapted from Cavaco et al., 2015 [208]).

A corresponding significant reduction of PGE2 accumulation in control-derived cell media was detected after 72 h of treatment with BCP coated to ucGRP/cGRP protein-mineral complexes when compared with cells treated with BCP crystals (**Fig. 4.22**). Such results further corroborated with the reduction of BCP-induced inflammatory response mediated by GRP-BCP coated crystals.

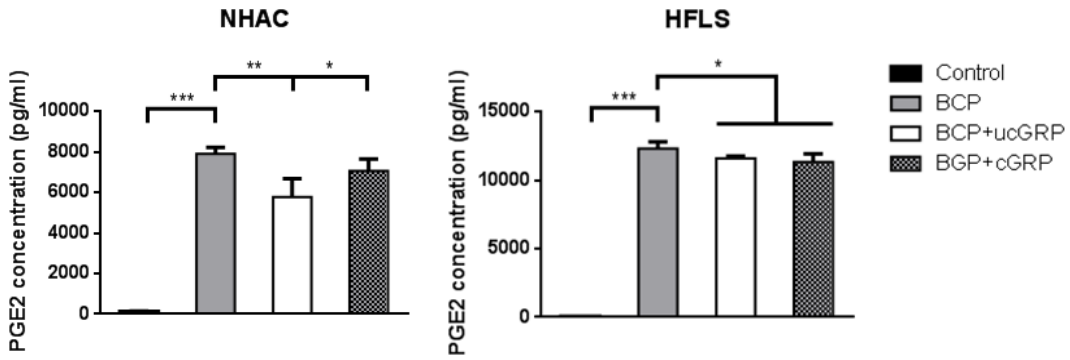

Fig. 4.22 – Effect of GRP in the inflammatory process promoted by the addition of basic calcium phosphate (BCP) crystals to articular cells. Prostaglandin E2 (PGE2) accumulation in NHAC and HFLS conditioned media after 72 h of cells supplementation with BCP crystals (BCP), or BCPs coated with undercarboxylated GRP (BCP + ucGRP) or carboxylated GRP (BCP + cGRP). Control corresponds to culture media of non-treated cells. Ordinary one-way ANOVA was performed. Statistical significance was defined as P≤0.05 (*), P≤0.005 (**) and P≤0.0005 (***) (Adapted from Cavaco et al., 2015 [208]).

Altogether, results showed that both c/ucGRP coating significantly diminished the inflammatory reaction associated with BCP crystals. Accordingly, the collected information points GRP as a new mediator factor linking mineralization and inflammatory processes, independently of its γ-carboxylation status. MGP coating also appears to significantly diminish the inflammatory reaction associated with BCP crystals, although additional studies are required to evaluate the dependency of MGP γ-carboxylation in this process.

4.3.7 Gla-rich protein acts as an anti-inflammatory agent in an osteoarthritic scenario

To determine whether GRP could have an effect on inflammatory processes and if this response was dependent of its γ-carboxylated status, chondrocytes and synoviocytes stimulated with IL-1β were pre-treated with ucGRP/cGRP or dexamethasone (DXM) (**Fig. 4.23**). DXM is a corticosteroid, widely known for its anti-inflammatory effect over IL-1β-mediated responses, and was used as a positive control in amounts according to literature [214]. In both control chondrocytes and synoviocytes systems stimulated with IL-1β, the treatment with either c/ucGRP resulted in significant lower levels of COX2 and MMP13 expression relatively to non-treated cells (**Fig. 4.23**), indicating an anti-inflammatory effect of GRP.

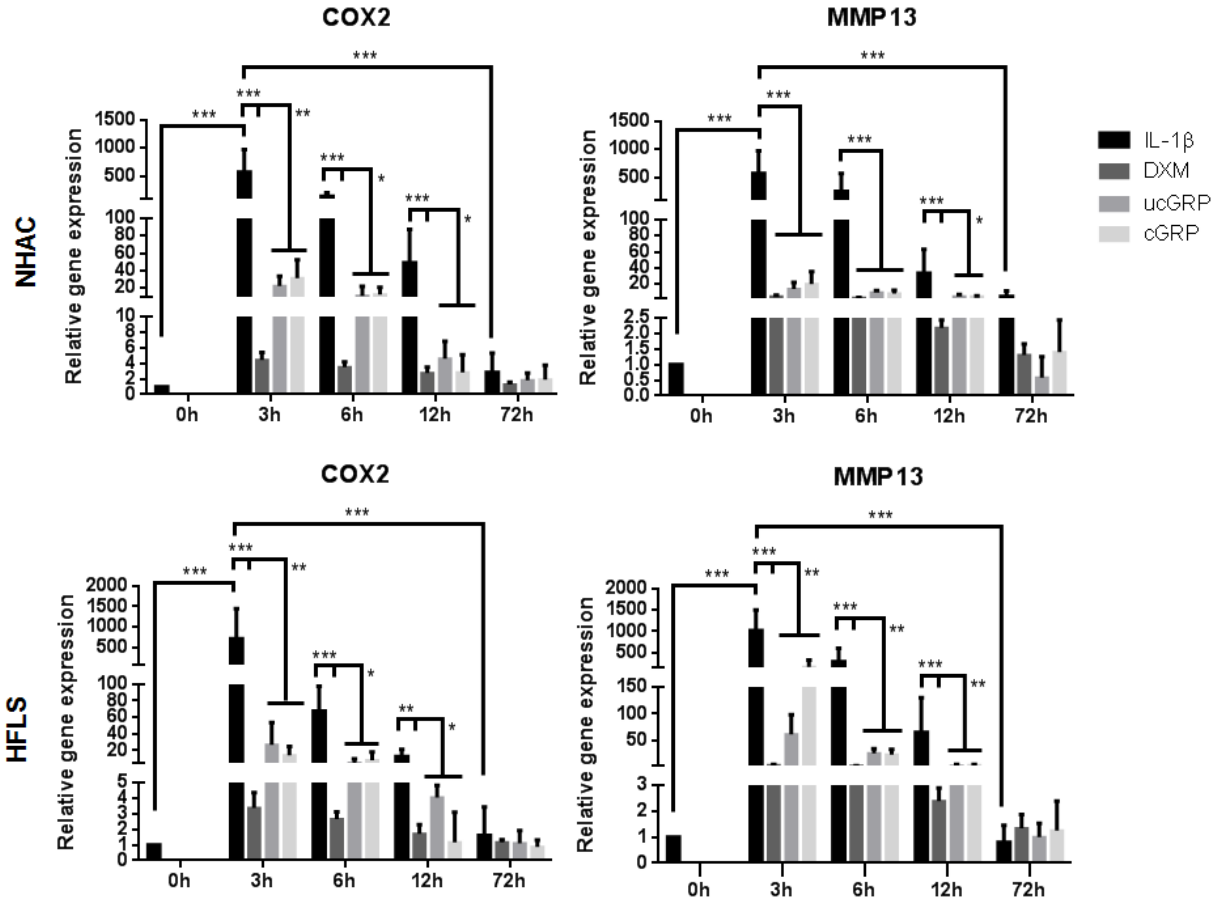

Fig. 4.23 – *In vitro* anti-inflammatory effect of GRP observed through the gene expression of inflammatory mediators in control-derived chondrocytes (NHAC) and synoviocytes (HFLS) stimulated with interleukin 1β (IL-1β). Gene expression of cyclooxygenase 2 (COX2) and matrix metalloproteinase 13 (MMP13) in NHAC and HFLS cells pre-treated with 500 ng/mL of undercarboxylated GRP (ucGRP) or carboxylated GRP (cGRP), or 2 μM dexamethasone (DXM) followed by IL-1β stimulation (5 ng/mL) during 72 h. Cells untreated with GRP or DMX were also analysed (IL-1β). Control corresponds to cells grown in advanced DMEM

only. Values are relative to the reference sample (0 h). Data is representative of three independent experiments. Two-way Anova and multiple comparisons were achieved with the Tukey's test. Statistical significance was defined as P≤0.05 (*), P≤0.005 (**) and P≤0.0005 (***) (Adapted from Cavaco et al., 2015 [208]).

To further confirm these results, PGE2 accumulation in NHAC and HFLS cell media after 24 h of pre-treatment with cGRP and ucGRP was measured (**Fig. 4.24**), and results showed lower levels of PGE2 in media of pre-treated cells relatively to non-treated cells (**Fig. 4.24**).

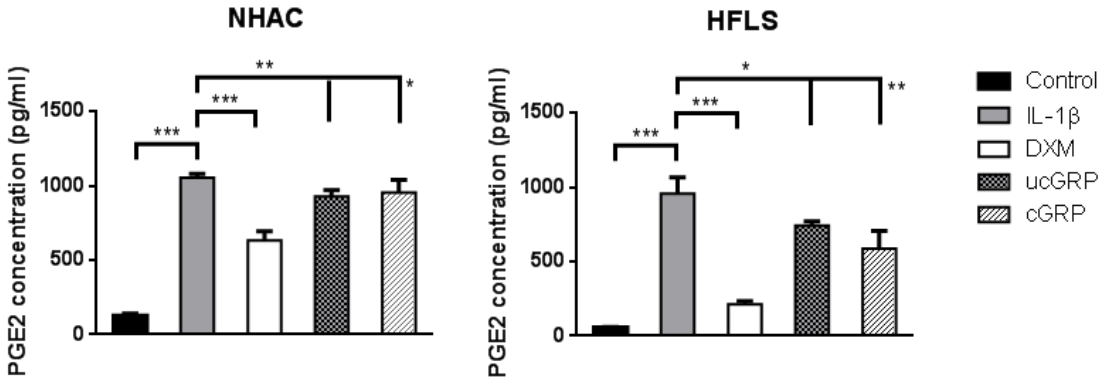

Fig. 4.24 – *In vitro* anti-inflammatory effect of GRP observed through the accumulation of prostaglandin E2 (PGE2) in control-derived chondrocytes (NHAC) and synoviocytes (HFLS) stimulated with interleukin 1β (IL-1β). PGE2 accumulation in cell media of NHAC and HFLS 24 h after a pre-treatment with 500 ng/mL of undercarboxylated GRP (ucGRP) or carboxylated GRP (cGRP), or 2 μM dexamethasone (DXM) followed by IL-1β stimulation (5 ng/mL). Cells without the pre-treatment, only IL-1β stimulation (IL-1β) were also analysed. Control corresponds to culture media of non-treated cells. Ordinary one-way ANOVA was performed. Statistical significance was defined as P≤0.05 (*), P≤0.005 (**) and P≤0.0005 (***) (Adapted from Cavaco et al., 2015 [208]).

A similar anti-inflammatory effect was observed in OA-derived chondrocytes and synoviocytes, but notably, in chondrocytes, the effect of both ucGRP and cGRP on COX2 and MMP13 expression 3 h after IL-1β stimulation, was comparable to that obtained with DXM (**Fig. 4.25**).

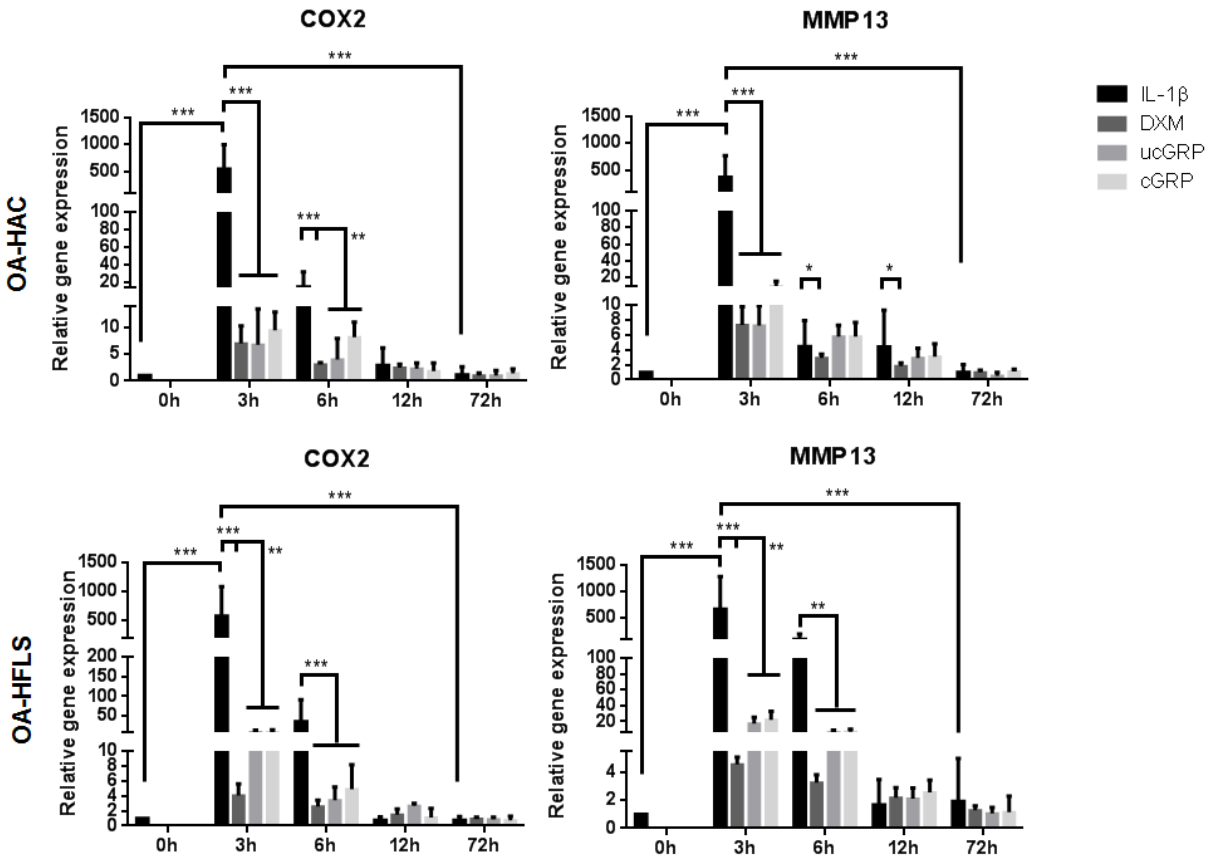

Fig. 4.25 – *In vitro* anti-inflammatory effect of GRP observed through the gene expression of inflammatory mediators in OA-derived chondrocytes (OA-HAC) and synoviocytes (OA-HFLS) stimulated with interleukin 1β (IL-1β). Gene expression of cyclooxygenase 2 (COX2) and matrix metalloproteinase 13 (MMP13) in OA-HAC and OA-HFLS cells pre-treated with 500 ng/mL of undercarboxylated GRP (ucGRP) or carboxylated GRP (cGRP), or 2 µM dexamethasone (DXM) followed by IL-1β stimulation (5 ng/mL) during 72 h. Cells untreated with GRP, MGP or DMX were also analysed (IL-1β). Control corresponds to cells grown in advanced DMEM only. Values are relative to the reference sample (0 h). Data is representative of three independent experiments. Two-way Anova and multiple comparisons were achieved with the Tukey's test. Statistical significance was defined as P≤0.05 (*), P≤0.005 (**) and P≤0.0005 (***)(Adapted from Cavaco et al., 2015 [208]).

Matrix Gla protein effect on inflammatory processes stimulated by IL-1β was also investigated in control chondrocytes and synoviocytes (**Fig. 4.26**). Treatment with cMGP resulted in significant lower levels of COX2 and MMP13 expression relatively to non-treated cells (**Fig. 4.26**), indicating an anti-inflammatory effect of this VKDP. These results were supported by lower PGE2 accumulation in NHAC and HFLS cell media after 24 h of pre-treatment with cMGP (**Fig. 4.27**).

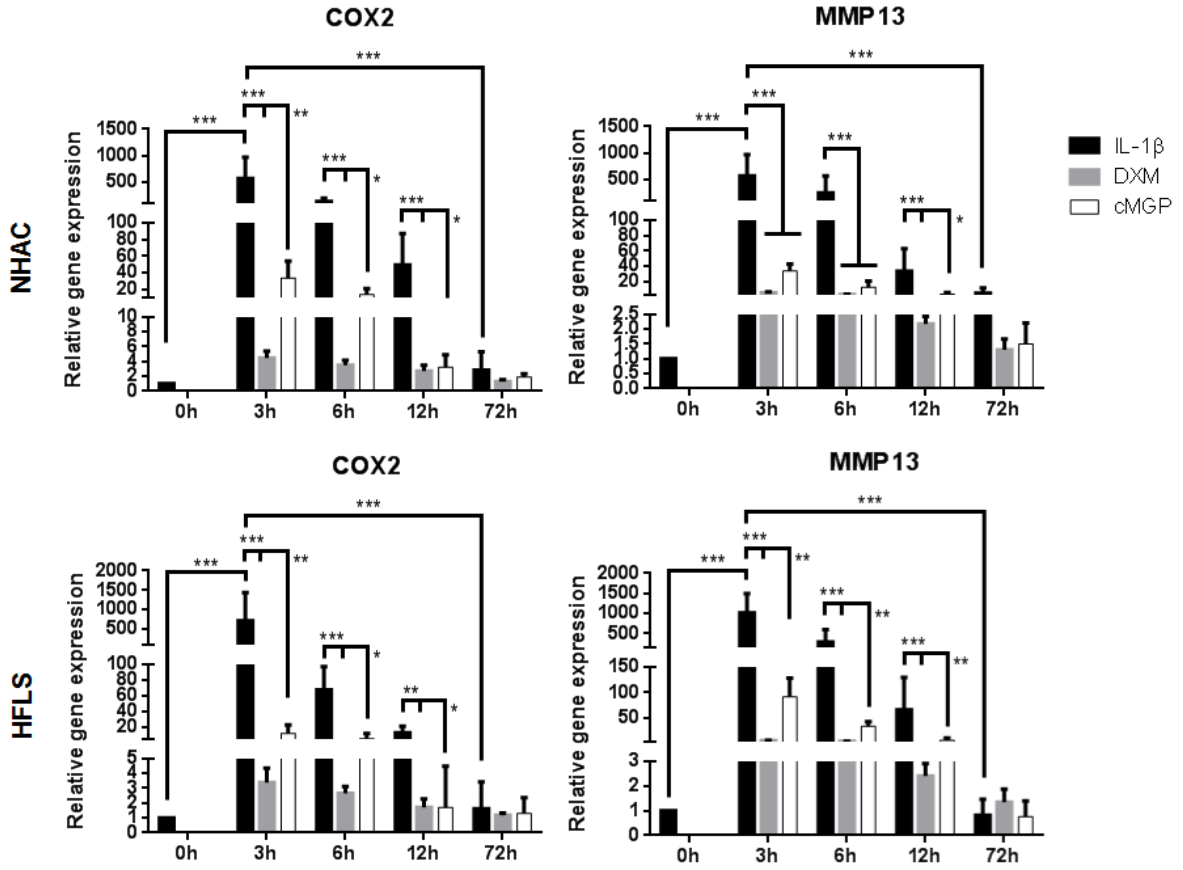

Fig. 4.26 – *In vitro* anti-inflammatory effect of MGP observed through the gene expression of inflammatory mediators in control-derived chondrocytes (NHAC) and synoviocytes (HFLS) stimulated with interleukin 1β (IL-1β). Gene expression of cyclooxygenase 2 (COX2) and matrix metalloproteinase 13 (MMP13) in NHAC and HFLS cells pre-treated with 500 ng/mL of carboxylated MGP (cMGP), or 2 µM dexamethasone (DXM) followed by IL-1β stimulation (5 ng/mL) during 72 h. Cells untreated with MGP or DMX were also analysed (IL-1β). Control corresponds to cells grown in advanced DMEM only. Values are relative to the reference sample (0 h). Data is representative of three independent experiments. Two-way Anova and multiple comparisons were achieved with the Tukey's test. Statistical significance was defined as P≤0.05 (*), P≤0.005 (**) and P≤0.0005 (***).

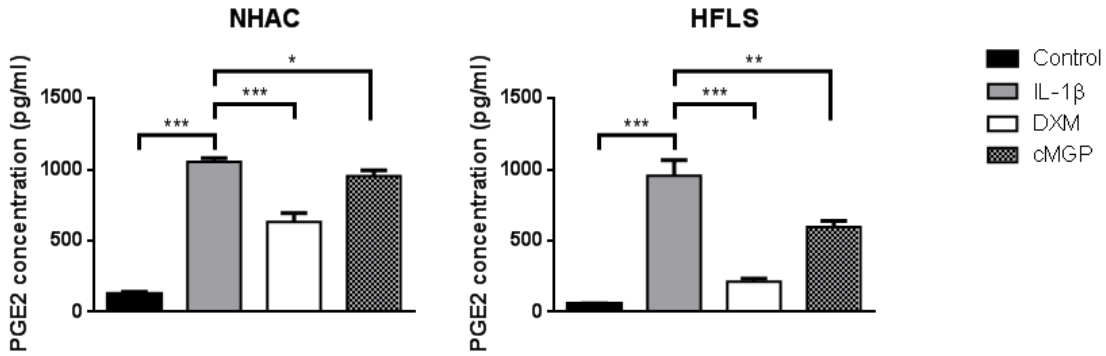

Fig. 4.27 – *In vitro* anti-inflammatory effect of MGP observed through the accumulation of prostaglandin E2 (PGE2) in control-derived chondrocytes (NHAC) and synoviocytes (HFLS) stimulated with interleukin 1β (IL-1β). PGE2 accumulation in cell media of NHAC and HFLS 24 h after a pre-treatment with 500 ng/mL of carboxylated MGP (cMGP) or 2 µM dexamethasone (DXM) followed by IL-1β stimulation (5 ng/mL). Cells without the pre-treatment, only IL-1β stimulation (IL-1β) were also analysed. Control corresponds to culture media of non-treated cells. Ordinary one-way ANOVA was performed. Statistical significance was defined as $P \leq 0.05$ (*), $P \leq 0.005$ (**) and $P \leq 0.0005$ (***).

These results strongly suggest the involvement of GRP with inflammation in OA, indicating that this VKDP might be a powerful anti-inflammatory agent in this pathology, exerting this function independently of its γ-carboxylation status, although further work is required to confirm such indications. MGP also appears to be associated with OA-related inflammatory processes.

4.4 Discussion

In this chapter, the involvement of GRP with two of the major molecular processes affecting OA, mineralization and inflammation, was addressed for the first time. Accordingly, the previously proposed role for GRP as an ECM mineralization inhibitor was strenghned in the particular case of OA and GRP was associated to inflammatory processes occurring in the disease, both in chondrocytes and synoviocytes, the main articular cell types. Moreover, while GRP γ-carboxylation status was shown to be essential for its calcification inhibitor effect, it was apparently irrelevant for the observed GRP anti-inflammatory actions, suggesting differential roles for undercarboxylated and carboxylated GRP.

Most of the collected results in the present chapter were achieved using an *in vitro* chondrocyte and synoviocyte cell system, which allowed studying different parameters of interest in osteoarthritic and control cells. For that, OA-derived primary chondrocytes and synoviocytes were developed and control counterparts were commercially acquired. A second set of OA-derived and control primary chondrocyte and synoviocyte cultures, developed by collaborators as indicated in section 4.2.2, was used to strengthen the results obtained with the first set of cells.

Gla-rich protein gene expression was found to be upregulated in OA-derived chondrocytes and synoviocytes, associated with higher levels of OA-related gene markers such as OC, COMP and Col10a1. These results are in agreement with the increased GRP expression associated with OA, observed in Chapter 3, using control and osteoarthritic cartilage tissue samples. Higher gene levels of the calcification inhibitor MGP were also associated to OA-cells, thus, results are in concordance with the higher demand of calcification inhibitors required to balance the increased cell differentiation and ECM calcification occurring in OA [50,137].

Carboxylated GRP was shown to decrease calcification in both chondrocytes and synoviocytes, and the increase of GRP expression accompanied cell differentiation towards ECM mineralization in both cell types. The upregulation of GRP during osteochondrogenic differentiation, characterized by a decrease in Col2a1 and concomitant increase in Col10a1, was recently shown during osteogenic differentiation of mouse osteoblastic MC3T3 cells, supporting the suggested upregulation of GRP gene by Osx [77]. Nevertheless, previous studies have shown that GRP is repressed by bone morphogenetic protein 2 (BMP2), known to be responsible for Osx upregulation during osteogenesis [75]. These controversial data

emphasize that the molecular mechanism of GRP action requires further clarification. Also, while GRP was suggested as a stimulating factor in osteoblast differentiation and nodule formation [77], previous results have shown an impairment of osteogenic differentiation by GRP using a similar approach [74,75]. Nevertheless, none of these studies has taken into consideration the fact that GRP is a γ-carboxylated protein, and although previous results evidenced that both forms, cGRP and ucGRP, have mineral binding capacity [15], only cGRP is able to inhibit ECM calcification in the vascular system [16]. In concordance, GRP knockdown in zebrafish evidenced severe growth retardation and perturbance of skeletal development, while warfarin treatment mimicked GRP knockdown phenotype, suggesting an essential role of γ-carboxylation for GRP function [72]. The gathered new information using GRP media supplementation in the established cell system strengthens the proposed calcification inhibitory function of GRP and reinforces the importance of its γ-carboxylation status. Carboxylated GRP probably alters calcium availability in the local environment or changes the dynamics of crystal growth [16].

Increased extracellular calcium levels have been shown to drive chondrocyte differentiation towards a mineralizing phenotype, while calcium depletion from culture media maintains a stable cellular phenotype [209]. However, despite the upregulation of GRP in OA-derived cells, GGCX and VKOR genes, coding for crucial enzymes involved in γ-carboxylation [1], were downregulated. This suggests a reduced γ-carboxylation capacity of OA cells, and consequently a decrease in the γ-carboxylation of target proteins such as GRP and MGP. In fact, the predominance of ucGRP and ucMGP in osteoarthritic articular cartilage and synovial membrane samples was previously shown in Chapter 3. Moreover, reduced vitamin K-dependent γ-carboxylase activity was previously reported in OA chondrocytes, and correlated with decreased γ-carboxylation of MGP and increased matrix mineralization [92].

The triggers for articular cartilage calcification associated with OA are still not completely understood. Nevertheless, dysregulation of mineral metabolism, such as calcium and phosphate, and an imbalance in the production of mineralization inhibitors, are crucial factors favouring cartilage calcification and deposition of calcium-containing crystals, like BCPs [49,50]. Also, these are important to avoid chondrocyte phenotype alterations such as hypertrophic differentiation, apoptosis, as well as altered responses to inflammatory cytokines and mediators of inflammation [50]. Interestingly, the obtained results also showed that synoviocytes were able to produce a mineralized ECM, with OC and OPN upregulation and vimentin downregulation. These results were further supported by recent cell culture studies where osteoarthritic synoviocytes were able to produce and accumulate calcium mineral

crystals when stimulated with ATP [215]. Altogether, these findings suggest that synoviocytes are not passive bystanders but are active players in the pathological calcification process occurring in OA, contributing to the production of BCP crystals in OA articular joints.

Calcium crystals have been shown to play an important role in the onset and progression of OA and are considered an early phenomena, affecting the whole joint even before any evidence of cartilage breakdown [50,137,138]. Basic calcium phosphate crystals are therefore found in the cartilage, synovial fluid and synovial membrane of OA patients [49]. The former are currently considered damage-associated molecular patterns (DAMPs), signalling to the immune system a state of stress, and potentially contributing to OA-associated inflammation through the stimulation of articular cells [91,123]. Basic calcium phosphate crystals induce synoviocyte proliferation and the production of inflammatory cytokines, MMPs and prostaglandins, and stimulate articular chondrocytes to produce prodegradative soluble factors, such as nitric oxide, and to undergo apoptosis [50,139-142]. MMPs production and chondrocyte apoptosis contribute to cartilage destruction, while cartilage breakdown products continue driving inflammatory events in a pathological mineralization-inflammation tissue degradation cycle [139-142]. Chapter 3 IHC results evidenced that GRP association to OA was not restricted to ectopic calcification events. In concordance, the possible involvement of GRP with both OA-associated mineralization and inflammation processes was studied through the evaluation of GRP ability to modulate inflammatory events triggered by a mineralization stimulus. COX2 and MMP13 upregulation was observed during mineralization in chondrocytes and synoviocytes and confirmed that, in this cell system, calcification can stimulate proinflammatory signalling that parallels cell differentiation and calcification. Notably, the high expression of COX2 and MMP13 was accompanied by an upregulation of GRP expression. These results reinforce the concept that other cells of the joint, including fibroblast-like synoviocytes and chondrocytes, besides synovial macrophages, directly contribute to the innate immune activation and the production of inflammatory mediators in OA. Importantly, the concomitant increase in GRP expression with inflammation, triggered by mineralization conditions, suggests a calcium-mediated role in inflammatory processes.

Increased GRP expression after inducing inflammation with IL-1β was also verified, with a highly similar pattern to that of the inflammatory markers COX2 and MMP13. These results suggest that the involvement of GRP in inflammatory-mediated processes might not be exclusively mediated by mineralization events, opening new perspectives for GRP as a novel

cross talk factor linking calcification and inflammation processes occurring in articular cells. Such interactions should became relevant for the study of OA development and progression. Regarding the cytokine-based model used to stimulate inflammation *in vitro*, although OA synovial fluid levels of IL-1β are usually under 2 ng/mL [153] and in this study 5 ng/mL were used, differences are not so significant comparing with those typically used to exert an effect *in vitro*, that may reach up to 100 ng/mL [153,159,160]. Therefore, the used quantities of IL-1β should reflect approximately the IL-1β-mediated inflammatory processes occurring in OA.

As previously reported, GRP is able to bind BCP crystals *in vitro* and the calcification inhibitory function of GRP might be through the modulation of crystal formation and/or growth [16]. Moreover, BCP crystals have been suggested to have a direct pathogenic role in OA driving synovial inflammation and cartilage degradation [139-142]. Based on these facts, the potential role of GRP in the inflammatory response mediated by BCP crystals was further investigated in the established cell system. Results clearly demonstrated that coating BCP crystals with GRP reduces the associated proinflammatory effect, protecting cells from the increased expression of MMP13 and COX2 production. It has been proposed that calcium-containing crystals may activate articular cells, either by leading to an increase in intracellular calcium levels after crystal endocytosis, by phagocytosis with consequent intralysosomal crystal dissolution, or through direct crystal-cell membrane interaction [142]. The former may occur via electrostatic bonds with the naked crystal surface or by membrane receptor stimulation with naked or protein-coated crystals [142]. Although the mechanisms behind GRP-BCP mediated anti-inflammatory effect in articular cells are currently unknown, it is possible to speculate that GRP binding to BCP will probably interfere with crystal-cell membrane interaction, modulating the production of proinflammatory mediators. Interestingly, fetuin-A-containing calciprotein particles (CPP), well known for their role in the prevention of uncontrolled mineralization, were recently reported to decrease cytokine production in macrophages, compared with cells stimulated with naked hydroxyapatite crystals [58]. Moreover, serum-derived CPP have been shown to produce a higher protective effect than synthetic CPP in macrophage activation [58], probably reflecting the inhibitory activity of other serum components, such as GRP and MGP. Notably, the association between GRP, MGP and fetuin-A was recently shown at sites of aortic valves calcification. Here, the calcification inhibitory function of both VKDPs was proposed to occur constitutively, via this potent inhibitory system formed by proteins with strong calcium phosphate binding capacity [16]. In the present study, the parallel upregulated gene expression of GRP and MGP in OA-derived chondrocytes and synoviocytes and accompanying cell differentiation towards ECM

mineralization in both cell types, also suggests that the VKDPs may function together against OA-associated pathological calcification. Furthermore, pre-treatment of chondrocytes and synoviocytes with GRP and MGP, followed by IL-1β stimulation, mirrored the anti-inflammatory effect observed with the VKDPs coated BCP crystals, showing a clear anti-inflammatory role by downregulation of the inflammatory modulators COX2 and MMP13, in some cases at levels comparable to DXM. The anti-inflammatory effect of GRP had never been suggested while MGP had already been proposed as an inflammatory marker in arthritis [95,216]. Moreover, the indication that both VKDPs might have parallel functions as anti-inflammatory agents in OA, leads to speculate that GRP and MGP may function together in a complex such as the CPP reported in macrophages, described to act both in the prevention of uncontrolled mineralization and protective effect against cytokine production [58].

Interestingly, the anti-inflammatory mediated effect of GRP was apparently independent of its γ-carboxylation status, suggesting additional functions for undercarboxylated GRP. Despite the fact that undercarboxylated VKDPs have been regarded as non-functional and related to pathological states [217,218], decreased γ-carboxylation of OC has been implicated in the regulation of energy metabolism, with novel metabolic roles [219]. Moreover, in the past decade, vitamin K biological functions other than acting as a coenzyme of GGCX have been proposed, namely regarding anti-inflammatory and antioxidant actions [24,25]. Vitamin K2 has been associated to anti-inflammatory effects through the suppression of the NF-κB pathway, with a dual pro-anabolic and anti-catabolic activity in bone [29]. In fact, inappropriate regulation of anti-catabolic activity in bone has been shown as one of the major causes of setting an inflammatory state in both OA and rheumatoid arthritis (RA) [220]. Although it was shown in this work that GRP is associated to inflammation in osteoarthritic synovial membranes undergoing synovitis, its involvement in immune cells inflammatory responses is presently unclear. Also, additional characterization of the anti-inflammatory activity of GRP and correlation with γ-carboxylation status is necessary to further unveil the molecular pathways involved. Regarding MGP, further work is required to access the impact of its γ-carboxylation status on inflammation.

Notably, the collected data throughout the present chapter evidenced that both control and OA-derived cell cultures, characterized by different gene expression of OA and differentiation markers, and probably reflecting later stages of differentiation in OA-derived cells, responded similarly to all the developed assays. These observations indicate that both pathological calcification inhibition and anti-inflammatory functions exerted by GRP might be effective at different stages of OA development.

Overall, in a context of OA with induced cell hypertrophic differentiation and ECM calcification, the obtained results suggest that the increased expression of VKDPs, such as GRP and MGP, might function to counteract calcification. However, system overload could lead to hampered γ-carboxylation capacity resulting in increased levels of undercarboxylated GRP and MGP. Undercarboxylated GRP might contribute to control the levels of inflammatory mediators through still unknown mechanisms, thereby protecting the joint structures from damage. GRP may therefore be considered a new player acting in osteoarthritic pathological calcification and inflammatory processes, and eventually a potential candidate for therapeutics in OA, which should be further explored.

4.5 Acknowledgements

All primary antibodies used in this chapter were kindly provided by GenoGla Diagnostics (Universidade do Algarve, Faro, Portugal) or VitaK BV (University of Maastricht, Maastricht, The Netherlands). We specially thank Dr. Joana Magalhães, from Grupo de Bioingeniería Tisular y Terapia Celular (Servicio de Reumatología, Instituto de Investigación Biomédica de A Coruña, Complejo Hospitalario Universitario de A Coruña, Sergas, Universidad de A Coruña, A Coruña, Spain) and Centro de Investigación Biomédica en Red de Bioingeniería, Biomateriales y Nanomedicina (Madrid, Spain), for the development of a second set of control and OA-derived primary cell cultures used in this chapter. We gratefully thank Dr. Francisco Blanco, head of Grupo de Bioingeniería Tisular y Terapia Celular, for making the last collaboration possible. The help of Dr. Maria dos Anjos Macedo, from Universidade Nova de Lisboa (Departamento de Química, Lisboa, Portugal), was also extremely appreciated. Dr. Maria dos Anjos was responsible for the infrared analysis of the produced basic calcium phosphate crystals and we specially thank her. Finally, we thank Dr. Marta Rafael and MSc Rúben Costa, former Post-Doc researcher and MSc student, respectively, at Functional Biochemistry and Proteomics (FBP) research group (Centro de Ciências do Mar (CCMar), Universidade do Algarve, Faro, Portugal), the first for her help with the cell system establishment, and the second for his help with the statistical data analysis. This work was funded by projects PTDC/SAUESA/101186/2008, PTDC/SAU-ORG/112832/2009, PTDC/SAU-ORG/117266/2010, PTDC/BIMMEC/1168/2012 and UID/Multi/04326/2013 of Fundação para a Ciência e Tecnologia (FCT). Part of the work presented in this chapter is published in Cavaco et al., 2015 [208].

Chapter 5

Identification of candidate biomarkers for osteoarthritis

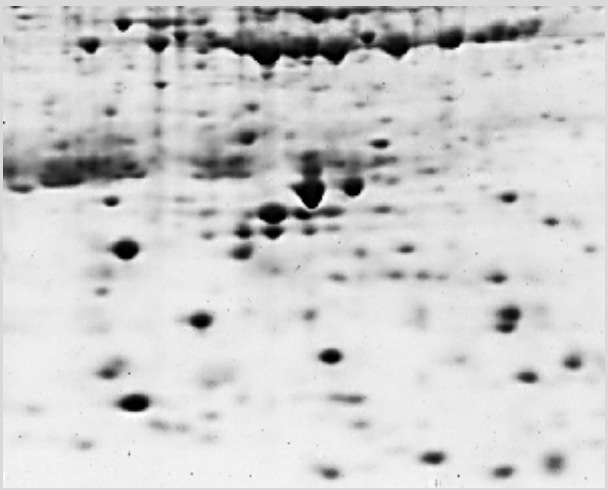

Abstract

The diagnosis of osteoarthritis (OA) is generally based on clinical and radiographic analyses, which are only able to detect the disease after significant joint damage has already taken place. Hence, there is an urgent need to identify reliable biomarkers that facilitate the early diagnosis and contribute to the prognosis and monitoring of therapeutics for OA. Proteomic studies have been used in the field of OA for the search of candidate disease biomarkers, mainly focused on synovial fluid and serum analysis. A common feature found associated with OA is the occurrence of pathological calcification, thus calcification inhibitors such as Gla-rich protein (GRP) or fetuin-A-containing calciprotein particles (CPP) could represent interesting candidates as OA biomarkers. In this chapter, the efforts made to clarify the potential of GRP as a biomarker for OA and to unveil alternative candidate biomarkers for the disease are described. The results obtained from the two-dimensional gel electrophoresis (2-DE) analysis aiming to study GRP as a marker for OA, using knee OA-affected cartilage extracts and GRP purified protein standards, clearly lead to the conclusion that this approach has serious limitations for the analysis of this highly insoluble protein. However, the comparative 2-DE analysis of CPP-like entities isolated from serum of control and osteoarthritic patients, coupled with protein sequencing by liquid chromatography-tandem mass spectrometry analyses, allowed the identification of 19 differentially expressed proteins. Interestingly, some of the identified proteins had been previously associated to OA, strengthening their potential as OA biomarkers. Moreover, the protein content found to be differentially expressed and associated to the fetuin-A-containing CPP-like entities, suggests a possible involvement of this complex with OA, although further work is necessary to elucidate the function of CPP associated to the pathological processes occurring in OA.

5. 1 Introduction

Current criteria for diagnosing osteoarthritis (OA) mainly relies on clinical manifestations and radiographic evaluations of the disease [161]. However, OA may be a silent disorder for many years before typical symptoms and radiographic changes emerge [161]. During this subclinical stage, damage of articular cartilage may have occurred and become irreversible [161]. Thus, it is extremely important to discover reliable biomarkers that can identify patients in risk for the progression of OA, facilitate the earlier diagnosis, contribute for advances in the prognosis and monitor therapeutics for the disease [81]. Structural molecules and fragments derived from cartilage, bone and the synovial membrane, are reported as the most promising candidates for early OA biomarkers discovery [81]. Nevertheless, since most of these extracellular matrix (ECM) turnover and/or cellular metabolism products are released into biological fluids, molecular markers can be measured in the synovial fluid or serum, which are easily obtained comparing with joint tissues [176].

Proteomic studies, a large-scale analysis of proteins involving the isolation, purification and mass spectrometry (MS) of the entities of interest, may enable the search for OA biomarkers in a systemic fashion [177]. Two-dimensional gel electrophoresis (2-DE) has preceded and accompanied the birth of proteomics and it is still one of the most valuable approaches for the separation and visualization of complex protein mixtures [221]. Using 2-DE, proteins are separated by isoelectric focusing (IEF) in the first dimension, and size-separated by sodium dodecyl sulphate-polyacrylamide gel electrophoresis (SDS-PAGE) in the second dimension [221]. High-resolution 2-DE can resolve up to 5.000 different proteins simultaneously, and detect and quantify less than 1 ng of protein per spot [221]. To date, differential expression patterns of proteins in OA have been focussed on synovial fluid or serum proteomic analyses, often using 2-DE approaches [177,179]. The synovial fluid contains higher concentrations of joint degradation products than any other biological fluid, making it an interesting target for assessing joint tissues metabolism analysis [179]. Serum samples containing the same degradation products although more diluted, represent however a more accessible biospecimen [179]. Despite the fact that both fluids contain high abundant proteins that might hamper the detection of lower abundant entities, several methods for affinity depletion of high abundant proteins are currently well described and available [179]. Cartilage 2-DE should provide a more direct insight into the pathogenesis of OA [177], yet the dynamic range of articular cartilage proteins is problematic [179]. The dominant nature of

macromolecules including the network of poorly soluble collagens, highly sulphated proteoglycans and hyaluronan, overwhelm the signals from less abundant proteins [179]. Therefore, a number of strategies for enrichment of the less abundant cartilage proteins and removal of contaminants have been developed, encompassing ultrafiltration, differential protein solubilisation procedures and proteoglycan subtraction [179,222]. Moreover, anionic molecules, such as aggrecan and hyaluronan, interfere with the IEF, making their removal advisable [179,222]. Ultimately, a combination of physical disruption and chemical extraction is generally suggested for articular cartilage protein extraction, which should be followed by proteoglycans removal, protein precipitation and solubilisation [177,179,223]. Importantly, although it is challenging to establish cartilage proteomic analysis methods, studies have reported the results of differential proteomic analysis of cartilage tissues in healthy and OA conditions using 2-DE [224,225].

The occurrence of pathological mineralization is a common feature of OA [48]. Therefore, calcification inhibitors such as Gla-rich protein (GRP), previously suggested as a calcification inhibitor and an anti-inflammatory agent in OA (Chapters 3 and 4), or fetuin-A-containing calciprotein particles (CPP) [57,58], could represent interesting candidates as OA biomarkers. Fetuin-A, is a glycoprotein synthesized in the liver and secreted into circulation, considered the most important systemic inhibitor of soft-tissue calcification [57]. Fetuin-A binds and sequesters mineral nuclei, forming soluble colloidal high molecular weight CPP, inhibiting crystal growth and aggregation [57,58]. This mechanism is believed to facilitate the clearance of calcium crystals from extracellular fluids, that otherwise could seed and possibly promote ectopic calcification [58]. Fetuin-A-containing CPP formation was first discovered in the serum of rats treated with the bone-active bisphosphonate etidronate, suggested to inhibit normal bone mineralization [226]. It was later proposed that this entity could be originated from bone, associated with bone resorption processes [59]. In circumstances where bone formation and resorption are imbalanced, like in OA [121], upon bone resorption increase, calcium phosphate crystal nuclei were probably formed in a bone-remodelling compartment (BRC) and released into the circulation [59]. This process should be accompanied by fetuin-A-containing CPP formation in the BRC, to stop crystal growth [59]. The fetuin-A detected in bone is believed to arise via serum, attracted by its high affinity for hydroxyapatite (HA) [227]. Interestingly, BRC structures were also identified in the vasculature [60], suggesting that calcium crystals and CPP may be formed in other locations, such as sites of pathological calcification. In chronic kidney disease (CKD) patients, serum fetuin-A-containing CPP levels were strongly correlated with coronary artery calcification and the complex was suggested to

reflect extraosseous calcification stress [228]. Fetuin-A-containing CPP formation was also suggested to help protecting macrophages against proinflammatory effects of the sequestered calcium crystals [58]. Notably, CPP entities are not exclusive of serum and were detected in different human body fluids, including the synovial fluid [229]. The same study showed that although the protein content of each fluid-derived CPP mirrored the protein composition of the contacting fluid, entities such as fetuin-A, albumin and apolipoprotein A1, were consistently associated to all complexes and should therefore be considered markers of CPP [229]. The fact that proteins with different functions were observed as CPP constituents, suggests that each complex might interfere with distinct biochemical pathways, thus the identification of the protein content of such entities may be critical to assess their biological activity [229].

In this chapter, efforts were made to clarify the potential of GRP as a biomarker for OA and unveil novel candidate biomarkers for the disease using 2-DE approaches. Therefore, here is described (i) the 2-DE analysis of OA-affected samples aiming to characterize GRP and search for novel OA biomarkers, (ii) the characterization of fetuin-A-containing CPP-like entities isolated from serum and synovial fluid through gel electrophoresis and calcium quantifications, (iii) the analysis of differentially expressed proteins between control and osteoarthritic serum CPP-like entities using comparative 2-DE, and (iv) the identification of differentially expressed proteins in OA, associated to fetuin-A-containing CPP-like entities.

5.2 Experimental procedures

5.2.1 Biological material and sample processing

Osteoarthritic articular cartilage and synovial fluid, and pathological and control clotted blood samples were obtained as described in Chapter 2, section 2.2.1. Cartilage tissues were immediately frozen at – 20 °C after collection, and the biological fluids centrifuged for 15 min at 3.000 x g and room temperature (RT), before storage at – 80 °C until further use.

5.2.2 Sample preparation for proteomic analysis

Articular cartilage protein extraction for subsequent proteomic analysis was achieved using Laemmli buffer, as described in Chapter 3, section 3.2.6.

Synovial fluid samples (1.5 mL) were depleted from high abundant proteins, such as albumin and immunoglobulins, using the ProteoMiner protein enrichment kit (Bio-Rad, Richmond, CA, USA), according to the manufacturer's protocol. The isolation of fetuin-A-containing CPP-like entities from synovial fluid and serum samples was also performed for proteomic analysis, following previously described procedures [228,230]. Briefly, 1.5 mL of fluids were centrifuged for 2 h at 16.000 x g and 4 °C and the supernatants were discarded. Centrifuge tubes were rinsed twice with 150 mM NaCl to wash the obtained pellets and centrifuged for 10 min at 16.000 x g and 4 °C. Final supernatants were discarded.

5.2.3 Total protein and calcium quantification

The protein content of the final cartilage extracts and synovial fluid samples depleted from high abundant proteins, obtained as described in the previous section, was estimated based on the general reference setting that a protein solution with an extinction coefficient (E) of 0.1% (1 mg/ml) produces an absorbance of 1.0 at 280 nm (whit a path length of 1 cm) [193]. Aliquots of purified sturgeon GRP, human recombinant GRP and bovine MGP, obtained within the scope of parallel projects [15,16], were also quantified by absorbance at 280 nm.

Calcium concentrations of the fetuin-A-containing CPP-like entities isolated from synovial fluid and serum as described in the previous section, were estimated after dissolving the pellets in 60 µl of 1 M HCl overnight at 4 ^{o}C, using a commercially available colorimetric kit (Calcium assay CA-590, Randox, Co. Antrim, UK), following the manufacturer's protocol. The protein content of the samples was then estimated after adding equimolar amounts of NaOH containing 0.5% w/v SDS, to neutralize the remaining HCl-mineral phase. Total protein concentrations were measured using the micro BCA protein assay kit (Thermo Scientific, Waltham, MA, USA), according to the manufacturer's protocol. For calcium concentrations, statistical analysis data are presented as mean (n=8) ± standard error, non-paired t-tests were used to compare control and OA groups and statistical significance was defined as $P \leq 0.05$ (*), $P \leq 0.005$ (**) and $P \leq 0.0005$ (***).

5.2.4 SDS-PAGE, native gel and western blot analysis

Freeze-dried aliquots of purified sturgeon GRP, human recombinant GRP and bovine MGP, synovial fluid proteins and CPP-like entities isolated from synovial fluid and serum, were dissolved/diluted in lithium dodecyl sulphate (LDS) sample buffer (NuPage, Invitrogen, Carlsbad, CA, USA) containing reducing agent. Subsequently, samples were size-separated by SDS-PAGE and stained with coomassie brilliant blue (CBB), as indicated in Chapter 3, section 3.2.7.

Fetuin-A-containing CPP-like entities isolated from synovial fluid were also dissolved in a non-denaturant and non-reducing sample buffer (10% v/v glycerol, 0.5 M Tris pH 6.7, 0.5% w/v bromophenol blue) without boiling, for native polyacrylamide gel electrophoresis analysis. Samples were then size-separated on a 7.5 % w/v linear polyacrylamide gel and the protein profiles were revealed with CBB.

Western blot analysis and immunodetection of total GRP was performed as described in Chapter 3, section 3.2.7. Fetuin-A was immunodetected using mouse monoclonal anti-fetuin-A (1 µg/mL, Santa Cruz Biotechnology, Dallas, TX, USA). All WB analysis were repeated at least three times using different osteoarthritic cartilage samples and CPP-like entities obtained from the synovial fluid and serum of different individuals.

5.2.5 Sample preparation for 2-DE

Freeze-dried aliquots of sturgeon GRP were treated with ReadyPrep 2-D Cleanup kit (Bio-Rad), to remove contaminating substances, and resuspended in a mixture of two rehydration/sample buffers from Bio-Rad, namely 66% v/v of ReadyPrep 2-D Starter Kit Rehydration/Sample buffer and 34% v/v of ReadyPrep 2-D Rehydration/Sample buffer 1. The previous mixture resulted in a final buffer composition (8 M urea, 1 M thiourea, 1.5% v/v CHAPS, 0.5% v/v ABS-14, 30 mM DTT, 15 mM Tris, 0.15% v/v Bio-Lyte 3/10 ampholyte, 0.001% bromophenol) indicated for the solubilisation of highly insoluble proteins [231].

Cartilage extracts and synovial fluid samples depleted from high abundant proteins using the ProteoMiner kit (Bio-Rad), were converted into low conductivity samples and/or cleaned from contaminating substances, using ReadyPrep 2-D Cleanup kit. The resulting pellets were dissolved in the mixture of Bio-Rad rehydration/sample buffers.

Freeze-dried aliquots of human recombinant GRP and bovine MGP, and serum isolated CPP-like entities, were directly resuspended/dissolved in the mixture of Bio-Rad rehydration/sample buffers.

5.2.6 Two-dimensional gel electrophoresis

Samples were loaded onto linear immobilized pH gradient (IPG) strips (11 cm, pH 3-10, Bio-Rad). Rehydration proceeded passively overnight. The first dimension IEF was initially ran with a gradient until 150 V for 1h30, then constant 500 V for 1 h, following a gradient until 6000 V for 2 h and finally constant 6000 V for 3 h, with a limiting current of 50 mA per strip. After IEF was complete, strips were sequentially equilibrated in equilibration buffer I (0.375 M Tris-HCl pH 8.8, 20% v/v glycerol, 2% w/v SDS, 6 M urea and 130 mM DTT) and equilibration buffer II (same as buffer I but DTT was replaced by 2.8% w/v iodoacetamide). The second dimension electrophoresis was conducted on 12 % Bis-Tris gels (Bio-Rad) at 180 V until the bromophenol blue reached the bottom of the gel. Proteins separated by analytic 2-DE were visualized with a specific CBB (G-250, Bio-Rad) compatible with MS analysis (34% v/v methanol, 17% w/v aluminium sulphate, 2% v/v phosphoric acid, 1% w/v CBB).

The first comparative 2-DE analysis performed between control and osteoarthritic serum-isolated fetuin-A-containing CPP-like entities was carried using 3 biological replicates (3 gels) of each condition. Based on the power analysis results obtained after comparative gel analysis, as described in section 5.2.8, a final comparative 2-DE analysis of the same samples

was performed using 5 biological replicates of each condition. Following the final comparative gel analysis and selection of differentially expressed spots to be picked, as indicated in section 5.2.8, two master gels were analysed by 2-DE, one containing sample from a control individual and other from an OA patient, and the selected spots were excised from both gels and stored in 0.5 mL tubes at – 20 °C, until further analysis.

5.2.7 *In silico* protein sequence analysis

Isoelectric point predictions of sturgeon and human GRP protein sequences were obtained using Compute pI/Mw tool available at Expasy portal, http://web.expasy.org/compute_pi.

5.2.8 Comparative gel analysis

Comparative gel analysis of fetuin-A-containing CPP-like entities isolated from control and osteoarthritic serum was initiated after gel scanning using a GS-800 Calibrated Imaging Densitometer (Bio-Rad). Progenesis SameSpots software (Nonlinear Dynamics, Quayside, UK) was subsequently used for spot detection, quantification, and matching. The intensities of the spots in each gel were compared and the differentially expressed spots between control and osteoarthritic conditions were highlighted. The initial comparative 2-DE analysis resulted in a power analysis suggesting the use of 4 biological replicates of each condition to obtain results with statistical significance. According to these indications, a final comparative gel analysis was performed and the differentially expressed spots between conditions, with statistical significance of $P \leq 0.05$ based on ANOVA P-value, were selected for spot picking.

5.2.9 Protein identification by mass spectrometry and data analysis

Two-dimensional electrophoresis gels of osteoarthritic cartilage extracts stained with CBB, obtained as described in section 5.2.2, were overlaid with corresponding 2-DE WB membranes of the same sample, with positive GRP immunoreactive signal. The matching protein strikes of the CBB gel with the WB signal were excised and sent to Instituto de

Tecnologia Química e Biológica (ITQB) (Mass Spectrometry Laboratory, Oeiras, Portugal) for protein sequencing and peptide analysis, as described in Chapter 3, section 3.2.9.

The selected differentially expressed spots between control and osteoarthritic serum isolated CPP-like entities, excised from two master gels as indicated in section 5.2.6, were washed with water and acetonitrile, and lyophilized. Dried samples were sent to Life Sciences Research Institute VIB (University of Gent, Gent, Belgium) for protein sequencing by liquid chromatography-tandem mass spectrometry (LC-MS/MS), as described [232]. Briefly, spots were in gel-digested with 50 mM trypsin in 0.1 M NH_4HCO_3 overnight at 37 ^{o}C to generate peptides. Peptide mixtures were transferred to MS compatible vials and analysed by LC-MS/MS on an Orbitrap XL mass spectrometer (Thermo Electron, Bremen, Germany) with injected volumes of 6 µL. Protein identification using LC-MS/MS raw data was performed with Mascot Daemon software (Matrix science, Boston, MA, USA). Results of the database search were analysed using the Knime software program (http://www.knime.org/) and the main biological roles attributed to each identified protein were accessed at UniProt portal (http://www.uniprot.org/).

5.3 Results

5.3.1 Proteomic analysis for the characterization of GRP in OA-affected tissues and discovery of novel osteoarthritis biomarkers

To clarify the potential of GRP as a biomarker for OA, the initial aim of this chapter was to evaluate the expression patterns of GRP between control and osteoarthritic conditions in cartilage tissues, and to identify and characterize GRP protein species present in each condition. Therefore, procedure optimization for the 2-DE analysis of cartilage extracts was conducted and among the tested protein extraction procedures (data not shown), the best results were obtained using Laemmli buffer. Accordingly, final osteoarthritic cartilage extracts for 2-DE were obtained using Laemmli buffer protein extraction followed by a clean-up step, to lower the sample conductivity. CBB staining results evidenced low protein resolution and vertical striking (**Fig. 5.1**, CBB), probably indicative of the interference of collagen and proteoglycans species, in concordance with the known limitations of cartilage 2-DE analysis [177,179]. Nevertheless, the detection of GRP by WB was performed using the CTerm-GRP antibody (**Fig. 5.1**, WB), and showed positive immunodetection in the form of two horizontal strikes (**Fig. 5.1**, WB) at acidic pI, with apparent molecular weights of 16 and 18 kDa, similar to those observed on previous SDS-PAGE analysis (Chapter 3, section 3.3.4, **Fig. 3.7**). In addition to the poor protein resolution indicated by the CBB staining, the horizontal strikes of GRP immunodetection might be associated to different γ-carboxylation degrees of GRP protein forms present in the extract, that should represent a challenge to the IEF. In fact, isoelectric point predictions for human GRP using Compute pI/Mw available at Expasy portal indicate a pI of 5.05, however, γ-carboxylation post-translational modifications are not considered in prediction programs, thus, the observed pI of the strikes ranging from 3 to 5 may indicate different γ-carboxylation degrees of GRP, that should result in different charged entities (**Fig. 5.1**, WB). Moreover, the faint signal obtained by WB in the 2-DE gels compared to previous WB results using SDS-PAGE (Chapter 3, section 3.3.4, **Fig. 3.7**) might indicate protein loss, suggesting poor protein solubilisation in the 2-DE buffer which also interferes with the IEF.

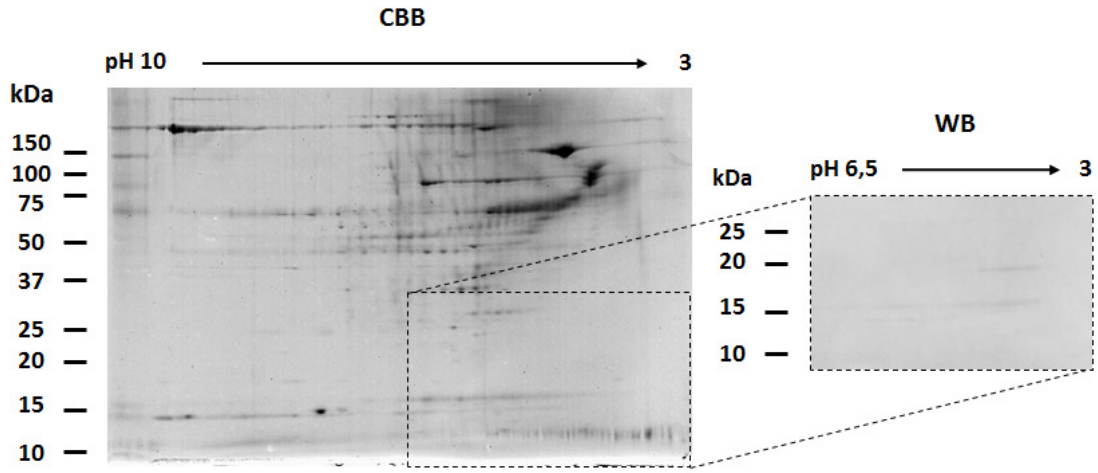

Fig. 5.1 – Two-dimensional gel electrophoresis (2-DE) map of human osteoarthritic articular cartilage extracts obtained with Laemmli buffer (CBB) and GRP immunodetection (WB). Articular cartilage extracts containing 175 µg of total protein were analysed by 2-DE and the protein profile revealed using coomassie brilliant blue (CBB) staining. Western blot (WB) results of the same extract in the same amounts of protein showed the immunodetection of GRP with CTerm-GRP antibody. Relevant molecular mass markers (kDa) and the pH gradient and orientation of the immobilized pH gradient (IPG) strips are indicated.

In order to obtain visible spots with CBB staining in the areas matching GRP positive WB signals (**Fig. 5.1**, WB), 2-DE gels were loaded with double protein amounts, and the corresponding detected strikes were picked and sent to ITQB institute for protein analysis by LC-MS/MS. Although the analysis was focussed on GRP identification and characterization, LC-MS/MS results were only able to identify a vesicle transport protein and tyrosine-rich acidic matrix protein representing the highest score proteins for the 16 kDa and the 18 kDa bands, respectively, and no peptides matching with GRP were found.

To further understand the observed constraints of GRP in the 2-DE analysis of cartilage extracts, aliquots of reverse phase-high performance liquid chromatography (RP-HPLC) purified sturgeon GRP and human recombinant GRP, obtained within the scope of parallel projects [15] and corresponding to fully γ-carboxylated and non-carboxylated GRP forms, respectively, were analysed by 2-DE. Coomassie brilliant blue staining revealed a substantial protein loss of sturgeon GRP, when compared to half of the amount of protein analysed by SDS-PAGE, and poor protein focusing with an apparent pI of 3.5-4 (**Fig. 5.2**, **A**). The protein loss of sturgeon GRP in the 2-DE gel in comparison with SDS-PAGE gels was associated to poor buffer solubilisation, most likely due to the lack of SDS in the 2-DE buffers, in which GRP is highly soluble. The low pI of γ-carboxylated sturgeon GRP, when compared to the isoelectric point predictions of 5.09 for sturgeon noncarboxylated protein

form, further supports the hypothesis that detected GRP strikes located at acidic pI in the osteoarthritic cartilage extracts (**Fig. 5.1**, WB), could represent carboxylated GRP forms. Non-carboxylated GRP was detected as a defined spot with an apparent pI of 5.5-6 (**Fig. 5.2**, **B**), also different from the predicted pI for human GRP, in this case associated to the 33 aa His-V5 tag, present in this recombinant protein [15]. The CBB staining of human recombinant protein, unlike sturgeon GRP, did not reveal a high protein loss (**Fig. 5.2**, **B**), that might be related with the lack of Gla residues. Trying to improve sturgeon GRP 2-DE analysis, the effect of sample clean-up was evaluated (**Fig. 5.2**, **A**), and active rehydration and cup-loading rehydration techniques were also tested (results not shown), yet without further improvements on the final results.

To test the behaviour of another related and highly insoluble γ-carboxylated protein on 2-DE, purified bovine MGP obtained within the scope of a parallel project [16] was analysed (**Fig. 5.2**, **C**). Gel results also showed a considering protein striking effect, indicative of the existence of multiple unfocused spots, possibly due to different MGP γ-carboxylated forms, and poor protein solubilisation in the 2-DE buffers.

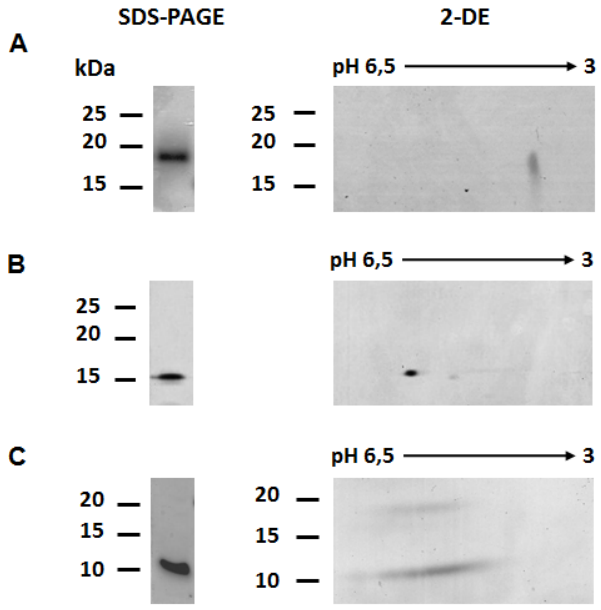

Fig. 5.2 – Two-dimensional gel electrophoresis (2-DE) of purified sturgeon GRP (**A**), human recombinant GRP (**B**) and bovine MGP (**C**) obtained by reverse phase-high performance liquid chromatography (RP-HPLC) [15,16]. Left panels contain the protein profile of 5 µg of purified fractions of sturgeon GRP (**A**), human recombinant GRP (**B**) and bovine MGP (**C**) revealed by SDS-PAGE. Right panels show the 2-DE analysis of 10 µg of sturgeon GRP fractions after a clean-up step (**A**), and 5 µg and 10 µg, respectively, of human recombinant GRP fractions (**B**) and bovine MGP fractions (**C**), without a clean-up. Gels were stained with

coomassie brilliant blue (CBB). Relevant molecular mass markers (kDa) and the pH gradient and orientation of the used immobilized pH gradient (IPG) strip are indicated.

The obtained 2-DE results using the available purified protein standards combined with previous cartilage extracts analysis further evidenced that a 2-DE approach was probably not adequate for GRP analysis, hampering the initial aim of analysing GRP content between control and osteoarthritic conditions using 2-DE.

In addition to the analytical limitations described, the collection of an adequate number of control cartilage samples suitable to perform comparative 2-DE analysis was not achieved, as described in Chapter 2, hindering the initial goal of searching for novel OA biomarkers using cartilage tissue samples. To overcame this situation, attention was focused on biological fluids, the recipients of structural molecules and fragments derived from cartilage, bone and the synovial membrane [176]. Biological fluids are more easily available in terms of sampling and considerably more simple to analyse by 2-DE than joint tissues [176].

The synovial fluid has been shown to be the most valuable biological fluid to assess joint tissue metabolism [179], thus the optimization of procedures for the analysis of osteoarthritic synovial fluid by 2-DE was performed. Final osteoarthritic synovial fluid samples for 2-DE analysis were obtained using an affinity kit for the depletion of high abundant proteins, such as albumin and immunoglobulins, followed by a clean-up step to eliminate kit reagents that might interfere with the IEF. Resulting 2-DE gels stained with CBB (**Fig. 5.3**) showed a good representation of lower abundant proteins, that were more difficult to detected before high abundant protein depletion (data not shown), and good protein resolution. Although the analysis of synovial fluid by 2-DE did not apparently implicate technical challenges, the collection of control synovial fluid samples throughout the project was, once again, a severe constraint (Chapter 2), hampering the performance of comparative analysis using this fluid.

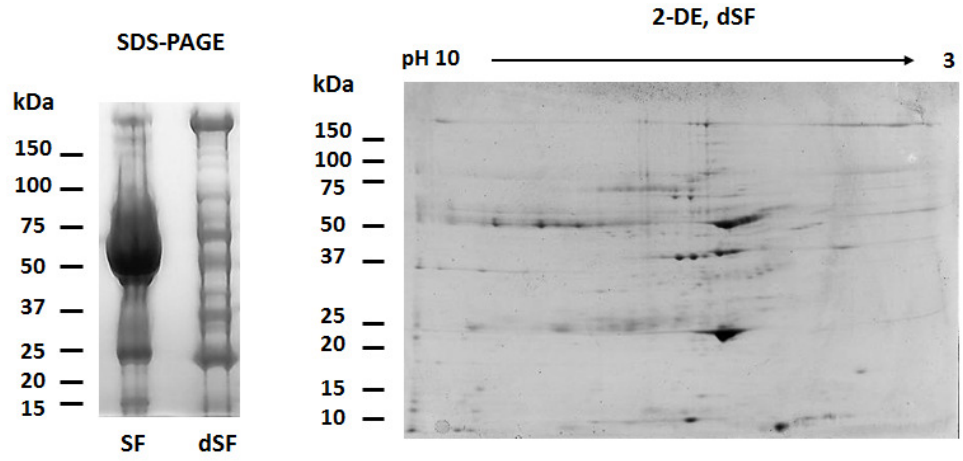

Fig. 5.3 – Two-dimensional gel electrophoresis (2-DE) map of human osteoarthritic synovial fluid after sample depletion of high abundant proteins. Left panel (SDS-PAGE) shows the SDS-PAGE protein profile of direct osteoarthritic synovial fluid samples (1 µl, SF) and samples depleted from high abundant proteins using the Bio-Rad ProteoMiner kit (60 µg, dSF). Right panel (2-DE, dSF), shows the 2-DE analysis of depleted from high abundant proteins osteoarthritic synovial fluid after a clean-up step (150 µg). Gels were stained with coomassie brilliant blue (CBB). Relevant molecular mass markers (kDa) and the pH gradient and orientation of the used immobilized pH gradient (IPG) strip are indicated.

5.3.2 Characterization of fetuin-A-containing CPP-like entities isolated from serum and synovial fluid

Serum samples also contain the diluted degradation products present in the synovial fluid and represent a more accessible biospecimen, thus differential expression patterns of proteins in OA are often focussed on serum proteomic analyses using 2-DE approaches [177,179]. Also, since the occurrence of pathological mineralization is a common feature of OA [48], calcification inhibitors such as fetuin-A-containing calciprotein particles (CPP) [57,58] may represent interesting candidates as OA biomarkers. Therefore, control and osteoarthritic serum preparation for subsequent 2-DE analysis was performed following previously described procedures for the isolation of serum CPP [228,230]. In addition, considering that fetuin-A-containing CPP were also described to exist in the synovial fluid [229], a CPP-like entity derived from osteoarthritic synovial fluid was also analysed. The protein profile of each sample obtained at 16.000 x g was determined by SDS-PAGE, revealing some similarities between the three samples, namely the three main protein bands detected in each protein profile, two of them located between 50 and 70 kDa of apparent molecular weight, and the remaining located around 25 kDa (**Fig. 5.4**, CBB). Since fetuin-A is a well described and crucial component of CPP [229,230], its presence in the isolated CPP-

like entities was confirmed by WB, showing positive fetuin-A immunodetection in all samples (**Fig. 5.4**, WB).

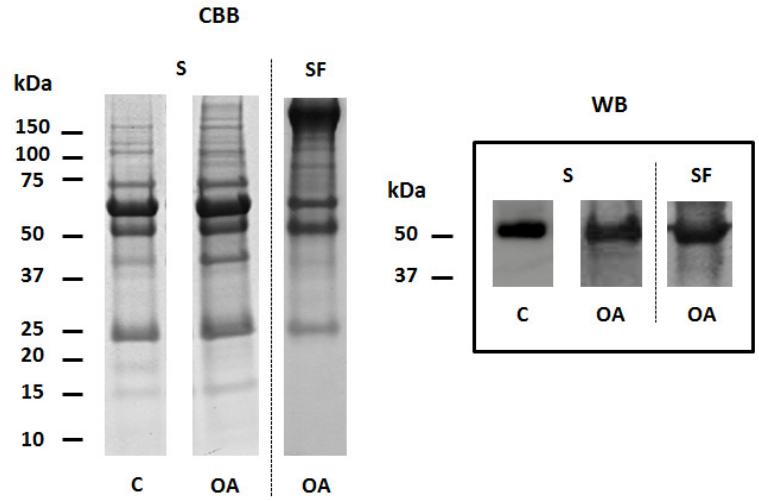

Fig. 5.4 – Protein profiles of fetuin-A-containing calciprotein particles (CPP)-like entities isolated from control and osteoarthritic serum and osteoarthritic synovial fluid, and positive fetuin-A immunodetection in the same samples. Left panel, shows the SDS-PAGE protein profiles stained with coomassie brilliant blue (CBB) of 50 µg of fetuin-A-containing CPP-like entities isolated from control (C) and osteoarthritic (OA) serum (S) and osteoarthritic synovial fluid (SF). Right panel, reveals the immunodetection of fetuin-A by western blot (WB) in the previous samples using the same protein amounts. Relevant molecular mass markers (kDa) are indicated.

Fetuin-A-containing CPP-like entities isolated from osteoarthritic synovial fluid were further characterized using native polyacrylamide gel electrophoresis (**Fig. 5.5**). This approach allows protein separation in their native/folded conformation and could therefore be used to help analysing if the previous visualized entities on SDS-PAGE (**Fig. 5.4**, CBB) were part of a complex. As expected, protein solubilisation in the non-denaturant and non-reducing sample buffer was limited compared with the solubilisation in SDS-containing sample buffer (**Fig. 5.5**), yet a differential pattern was observed between the two gel conditions, indicative of the presence of complexes of proteins in the native gel (**Fig. 5.5**, Native).

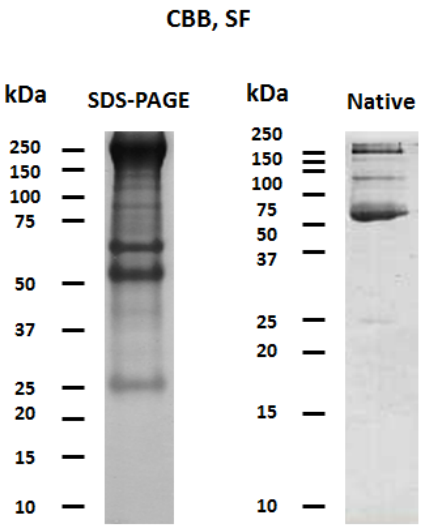

Fig. 5.5 – Protein profiles of fetuin-A-containing calciprotein particles (CPP)-like entities isolated from osteoarthritic synovial fluid (SF) on SDS-PAGE and native gels. Left panel, shows the SDS-PAGE protein profile (50 µg) and right panel the native protein profile (25 µg, corresponding to the maximum volume that could be loaded on the well) of the CPP-like entities stained with coomassie brilliant blue (CBB). Gradient gels of 4-12% acrylamide were used for the SDS-PAGE while linear gels of 7.5% acrylamide for the native gel. Relevant molecular mass markers (kDa) are indicated.

Serum-derived fetuin-A-containing CPP-like entities were further analysed regarding their calcium content. Calcium quantifications were performed in a total of 16 serum samples, 8 of each condition (subject information of the used samples is described in Chapter 2, sections 2.3.1 and 2.4.1, **Tables 2.I**, **2.II** and **2.III**), and revealed higher calcium levels in the CPP-like particles isolated from osteoarthritic samples (**Fig. 5.6**).

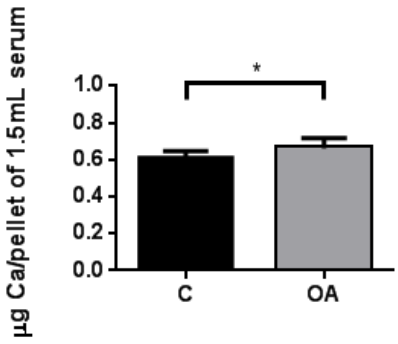

Fig. 5.6 – Calcium levels of CPP-like particles isolated from serum of control (C) and osteoarthritic patients (OA). Pellets were obtained after centrifugation (16.000 x g) of 1.5 mL of original serum and calcium was quantified using a Randox colorimetric kit (Calcium assay CA-590). Data is presented as mean (n = 8) ± standard error. Nonpaired t-tests were used. Statistical significance was defined as $P \leq 0.05$ (*).

The combined results obtained in this section suggest the existence of fetuin-A-containing CPP-like entities in both control and osteoarthritic serum and osteoarthritic synovial fluid, and unveiling the composition of the former complexes might represent a novel approach to study the dysregulated mineralization occurring in OA and potentially uncover new disease biomarkers.

5.3.3 Differentially expressed proteins between control and osteoarthritic serum fetuin-A-containing CPP-like entities

To further access the potential use of CPP-like entities as a source of OA biomarkers, and further explore its protein content, comparative 2-DE was performed between control and osteoarthritic derived samples. A preliminary comparative study was conducted using 3 biological replicates of each condition. SameSpots software gel analysis revealed the existence of differentially expressed spots between control and osteoarthritic samples, and the obtained power analysis estimated the use of 4 biological replicates of each condition in the final analysis, to achieve statistical significant data. Accordingly, final comparative gel analysis was performed using 5 replicates of each condition (subject clinical information for each sample selected for this study is described in Chapter 2, sections 2.3.1 and 2.4.1, **Tables 2.I**, **2.II** and **2.III**) and 19 differentially expressed spots between the two conditions were detected using the previous software (**Fig. 5.7**).

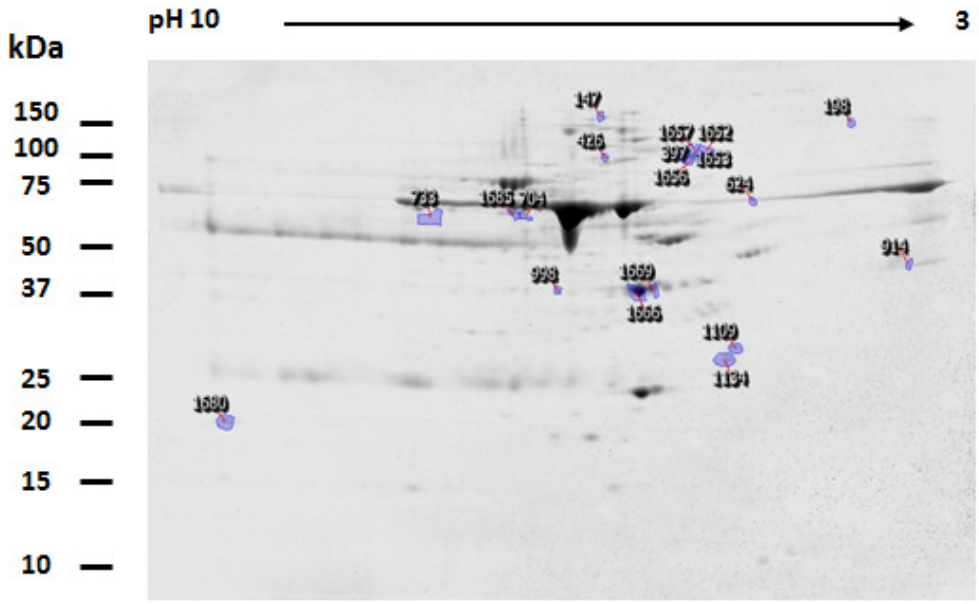

Fig. 5.7 – Differentially expressed proteins between control and osteoarthritic serum isolated CPP-like entities. Comparative two-dimensional gel electrophoresis (2-DE) analysis was performed in control and osteoarthritic samples using 130 µg of total protein. Differentially expressed spots attributed by SameSpots software are evidenced with numbering in a representative gel of a control sample, stained with coomassie brilliant blue (CBB). Relevant molecular mass markers (kDa) are indicated as well as the pH gradient and orientation of the used immobilized pH gradient (IPG) strip.

After final gel analysis, two master gels were run, with the same amounts of total protein previously used for the comparative approach, containing a control and an osteoarthritic sample, respectively. The 19 differentially expressed spots between conditions were excised from both gels, in gel digested with trypsin and further analysed by LC-MS/MS, at Life Sciences Research Institute VIB (University of Gent, Gent, Belgium).

5.3.4 Identification of differentially expressed proteins in osteoarthritis associated to CPP-like entities

All the 19 excised spots from the two master gels analysed by LC-MS/MS, resulted in positive protein identification (**Table 5.I**). The majority of the identified proteins was found upregulated in control conditions, and only two, cytosol aminopeptidase (AMPL) and immunoglobulin γ 1 chain C region (IGHG1) were found upregulated associated to OA (**Table 5.I**).

Table 5.I – Identification of differentially expressed proteins between control and osteoarthritic serum isolated fetuin-A-containing CPP-like entities

Spot	ANOVA (P)	Fold	Accession Number	Protein	Average Normalized volume	
					Control	OA
1657	0,005	9,4	P08514	Integrin α-IIb (ITA2B)	71109	7603
198	0,006	2,7	P14923	Cytosol aminopeptidase (AMPL)	10740	29250
1656	0,006	5,8	P05155	Inter-α-trypsin inhibitor heavy chain H4 (ITIH4)	67720	11670
1652	0,006	5,4	Q9Y490	Vinculin (VINC)	119900	22320
1653	0,008	6,0	Q9NZT1	Serotransferrin (TRFE)	148600	24940
426	0,011	3,1	P61626	Talin 1 (TLN1)	39730	12750
1666	0,014	5,6	P00738	Actin cytoplasmic 1 (ACTB)	1144000	203700
1109	0,015	5,1	P63104	Tropomyosin α 4 chain (TPM4)	117500	23010
147	0,015	2,0	P06280	von Willebrand factor D and EGF domain-containing protein (VWDE)	41930	20700
704	0,017	2,8	P01871	Immunoglobulin mu chain C region (IGHM)	58090	20960
998	0,025	3,3	P60709	Leukocyte elastase inhibitor (ILEU)	25950	7980
1680	0,030	3,0	P23528	Cofilin 1 (COF1)	122800	40790
397	0,033	3,7	P07355	Plakophilin 1 (PKP1)	236400	62360
1685	0,033	2,0	O75083	WD repeat-containing protein 1 (WDR1)	63510	31670
1134	0,036	4,1	P31946	Cathepsin D (CATD)	193400	47180
914	0,036	2,5	Q8N4S0	α-galactosidase A (AGAL)	26820	10870
624	0,044	1,9	P15924	Junction plakoglobin (PLAK)	26810	13940
1669	0,049	3,6	P06727	Apolipoprotein A-IV (APOA4)	188600	52980
733	0,049	4,0	Q86YZ3	Immunoglobulin γ 1 chain C region (IGHG1)	58720	237400

The identified proteins were classified into six groups based on their known biological functions (**Fig. 5.8**). Most of the entities were involved in enzyme catalysis, cell adhesion, defence or cell motility processes; the remaining entities were associated to transport and signal transducing functions (**Fig. 5.8**).

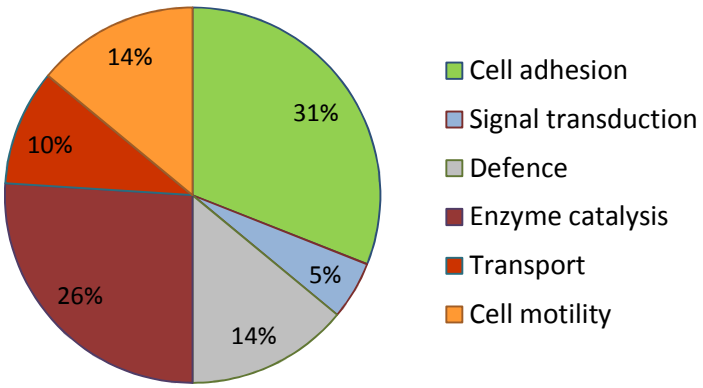

Fig. 5.8 – Differentially expressed proteins identified between control and osteoarthritic serum samples using second-dimension gel electrophoresis (2-DE) were distributed according to known associated functions. ITA2B, VINC, TLN1, PKP1, PLAK and VWDE are related to cell adhesion; WDR1 to signal transduction; IGHM, IGHG1 to immune defense; ITIH4, AMPL, ILEU, CATD, AGAL to enzyme catalysis; TRFE, APOA4 to transport and ACTB, TPM4, COF1 to cell motility.

Among the identified differentially expressed proteins, inter-α-trypsin inhibitor heavy chain H4 (ITIH4), serotransferrin (TRFE), actin cytoplasmic 1/β-actin (ACTB) and apolipoprotein A-IV (APOA4), had been previously associated to serum fetuin-A-containing CPP [228,229], obtained using similar procedures such as those used in this chapter. Moreover, APOA4 [233], leukocyte elastase inhibitor/serpin B1 (ILEU) [234] and cathepsin D (CATD) [235], had already been associated to OA, although the last two not associated to CPP, further supporting their suitability as OA biomarkers.

5.4 Discussion

The main aim of this chapter was the identification of novel candidate OA biomarkers using 2-DE for a potential use in diagnose and monitoring of OA treatments, with a particular focus on GRP. The 2-DE analysis of osteoarthritic cartilage extracts and purified protein standards revealed that the study of GRP using this approach would be a highly challenging task, yet a set of promising candidate biomarkers for OA was identified.

Cartilage tissues can provide a direct insight into the pathogenesis of OA, representing the best biospecimen for early biomarkers discovery [81]. Therefore, to clarify the potential of GRP as a biomarker for OA, a 2-DE approach was used to evaluate the differential expression pattern of GRP between control and osteoarthritic cartilage tissues. The 2-DE analysis was also aimed at favouring GRP protein identification compared to previous performed SDS-PAGE (Chapter 3), allowing GRP separation from other entities by molecular weight and pI. This approach could represent an alternative to further obtain molecular data for GRP identification and characterization of GRP forms existing between control and osteoarthritic conditions. However, GRP 2-DE analysis revealed to be limited by protein loss and ineffective IEF. Optimal protein solubilisation is crucial for 2-DE and in fact, the analysis of insoluble proteins, such as membrane proteins, in common 2-DE buffers, represents a major technical challenge for this approach [236]. To increase protein solubility, detergents with a linear alkyl tail such as the zwitterionic ASB-14 are recommended together with the combination of the nonionic chaotropes urea and thiourea, which ease the solubilisation process by altering the ionic bonds strength and facilitating protein unfolding [231]. However, the use of such buffer composition was not efficient for the 2-DE analysis of the highly insoluble native GRP and MGP proteins. Also, the analysed cartilage osteoarthritic extract was known to contain both carboxylated and undercarboxylated GRP forms (Chapter 3, section 3.3.4, **Fig. 3.7**) and the presence of several GRP protein forms differing on their γ-carboxylation status, representing entities with similar molecular weights and pIs, may have difficult the IEF. Considering the encountered limitations it was not possible to explore GRP potential as a biomarker for OA using 2-DE and it was not surprising that no peptides matching GRP were found when attempting protein identification from the 2-DE gels. Moreover, limitations on GRP protein identification might not only be associated to low protein recovery in the 2-DE gels, but also related to the generation of peptides suitable for fragmentation and known difficulties on the identification of Gla residues [200]. Vitamin K-

dependent proteins may undergo neutral loss of CO_2 from the γ-carboxyl carbon during ionization by matrix-assisted laser desorption/ionization (MALDI) or following collision-induced dissociation tandem MS/MS which may difficult the identification of Gla residues [200]. To further understand GRP limitations on MS analysis, digestion experiments using carboxylated and undercarboxylated GRP purified standards were performed in the laboratory (unpublished results), strongly indicating a very low digestion efficiency of both protein forms with different proteases, including trypsin. This problem was highly aggravated in the case of carboxylated GRP. In fact, the recent identification of GRP by LC-MS/MS was achieved from SDS-PAGE gels but only after using a double trypsin digestion protocol [16].

Subsequent studies focused on the identification of other possible biomarkers for OA using 2-DE. The ideal biospecimens to use for such purpose would be articular cartilage tissue or synovial fluid samples, which best reflect the molecular processes occurring in OA [177,179]. However, an adequate number of control samples to perform a comparative analysis was not achieved for any of the former biospecimens during the time course of this project. Therefore, serum samples containing the diluted degradation products present in the synovial fluid [179] and easily obtained from both control individuals and OA patients, were used to search for candidate OA biomarkers. Fetuin-A-containing CPP are believed to be formed in situations where bone formation and resorption are imbalanced [59] and hypothesised to be associated with ectopic calcification situations [58,229], two features of OA [48,121]. In this line, serum fetuin-A-containing CPP-like entities were used for a comparative analysis to investigate novel associations between these entities and OA.

Nineteen differentially expressed proteins in OA were identified associated to serum CPP-like entities, which were classified into six groups. Most attention was given to proteins grouped within categories previously associated to other fetuin-A-containing serum CPP entities, namely immune defence, enzyme catalysis and transport [229]. Opsonins presence in CPP have been proposed to indicate the complexes propensity to be rapidly phagocytised by the reticuloendothelial system, only accumulating in the fluids in particular situations, such as pathological conditions [229]. Accordingly, the identified immunoglobulins in this study, as opsonins, may be associated with phagocytosis enhancing. In the enzyme catalysis group ILEU, CATD, AMPL and ITIH4, all except AMPL downregulated in osteoarthritic pellets, were highlighted. ILEU and CATD had been previously associated to OA although not related to CPP [234,235]. Osteoarthritic serum low levels of CATD were related to decreased chondrocyte numbers in OA [235], while ILEU decreased urine concentrations suggested as biomarker for OA [234]. Serine proteases are described to contribute for cartilage destruction

[237], thus, the lack of protease inhibitors such as ILEU [238] or ITIH4, previously associated to serum derived-CPP [229], may contribute for OA progression. Interestingly, AMPL upregulation in serum has been associated to high lymphocyte infiltration situations [239], which frequently occurs in osteoarthritic synovial membranes [87]. The identification of the transporters TRFE and APOA4, downregulated in osteoarthritic pellets, was also interesting since they had been previously associated to serum derived-CPP [229]. The iron transporter TRFE may be associated with the induction of iron-dependent processes such as the activation of immune cells [240]. Also, TRFE was previously described to be less accumulated in cases of inflammatory responses [240]. The observation that CPP entities can interact with apolipoproteins suggests that these complexes may influence lipid transport pathways [229]. Notably, impairments in lipid transport resulting in altered levels of adipokines contribute to OA development by inducing the expression of proinflammatory factors as well as degradative enzymes [241], and in fact, low serum levels of APOA4 have been related to OA [233].

The identification of immune regulators, protease inhibitors, and lipid/molecule carriers, some of which previously associated to OA, and the immunodetection of the calcification inhibitor fetuin-A in the CPP-like entities, suggests a possible association of these complexes with osteoarthritic features, namely pathological calcification and inflammatory processes. The higher levels of mineral associated to the osteoarthritic entities, like observed in CKD patients in comparison with control samples [228], also might indicate an association with OA regarding extraosseous calcification stress, as suggested for CKD patients. Yet, no reports were identified associating higher levels of calcium or mineral to osteoarthritic serum, although the presence of calcium crystals is well known in osteoarthritic synovial fluid [112,140]. Nevertheless, it should be referred that although the presented results strongly indicate the existence of a CPP entity that can be differentially associated to OA, additional characterization of the analysed samples is necessary. Cellular components such as platelets and/or microparticles may co-sediment at the low centrifugation speed used for CPP isolation [228], contributing to a final heterogeneous mixture. Indeed, the cellular component ACTB identified in the present study and previously associated to CPP [228,229], was suggested to sediment at this centrifugal force but not to be part of the complex [228]. Also, extracellular vesicles (EVs), capable of efficiently nucleate mineral and known key players in the initiation of physiological and pathological calcification [242,243], may also sediment in serum at such centrifugation speed [244].

Overall, this study contributed for the identification of candidate OA biomarkers that should now be further validated and tested in earlier stages of the disease, to verify their potential as early disease markers. The protein and mineral content associated to the CPP-like entities suggests possible relations of the complex with OA, regarding ectopic calcification and inflammatory processes, thus further work should be performed to elucidate these possible associations.

5.5 Acknowledgements

The CTerm-GRP primary antibody used in this chapter was kindly provided by GenoGla Diagnostics (Universidade do Algarve, Faro, Portugal). We gratefully Dr Kris Gevaert, Jarne Pauwels and An Staes, from the Life Sciences Research Institute VIB (University of Gent, Gent, Belgium) whit which a collaboration was established. Dr Kris Gevaert was the head of project PRIME-XS-0000072 in which protein sequence analysis by mass spectrometry was implicit. Jarne Pauwels and An Staes were responsible for performing the protein sequencing analysis. This work was funded by PTDC/SAUESA/101186/2008, PTDC/SAU-ORG/112832/2009, PTDC/SAU-ORG/117266/2010, PTDC/BIMMEC/1168/2012, and UID/Multi/04326/2013 projects of Fundação para a Ciência e Tecnologia (FCT) and PRIME-XS-0000072 project of VIB.

Chapter 6

General conclusions and future perspectives

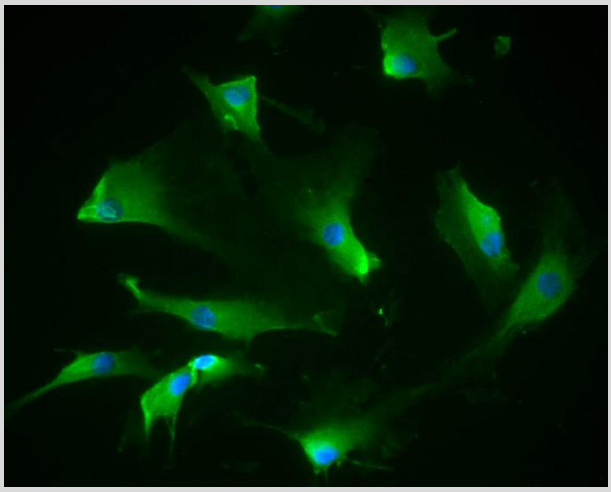

© Sofia Cavaco

6. General conclusions and future perspectives

During the present work new data was collected associating for the first time Gla-rich protein (GRP), the latest discovered vitamin K-dependent protein (VKDP), with the prevalent form of degenerative joint disorders, osteoarthritis (OA). Osteoarthritis is believed to onset after articular cartilage damage, accompanied by tissue inflammation, abnormal bone formation and extracellular matrix (ECM) mineralization [96,99,100]. Also, OA may be a silent disorder for many years before current diagnostic criteria can detect it, allowing irreversible articular cartilage damage to occur, for which there are no effective disease modifying drugs available [81,96]. This multifactorial disease is still poorly understood and additional knowledge is necessary to further uncover pathophysiological mechanisms triggering OA development, as well as the molecular factors and pathways involved in the complexity of pathological processes leading to OA progression [96,101]. Additionally, it is commonly accepted that the discovery of reliable molecular targets and biomarkers benefiting OA management are needed. Gla-rich protein was previously shown to accumulate in mouse and sturgeon cartilage [54,74,75], and at sites of skin and vascular calcification in human [14,15]. Moreover, GRP was proposed as a negative regulator of osteogenesis [74,75]. In this line, the main objective of this project was to investigate the possible involvement of GRP with OA development. Also, we aimed to identify potential OA biomarkers, especially focusing in GRP analysis.

To achieve our aims, a well characterized human biobank was collected during the project to study OA. This biobank comprised samples of knee articular cartilage, subchondral bone, synovial membrane, synovial fluid, and blood, from knee OA patients and individuals with no history of joint disorders. The number and amounts of biospecimens collected from OA patients is now considerable, representing an important achievement; however, the collection of control samples was not equally effective. Yet, the availability of this biobank was crucial for the studies performed in this project, which allowed the association of GRP with the pathological mineralization and inflammation occurring in OA, and the identification of candidate OA biomarkers. A chondrocyte and synoviocyte cell system was also developed within the scope of this project to study GRP association with mineralization and inflammatory mechanisms, complementing the information retrieved from experiments using *in vivo* samples from the biobank. Both the biobank and *in vitro* system are presently available for future studies aiming at further investigating OA-associated molecular features.

GRP association with OA was initially studied at gene expression level using cartilage, synovial membrane and bone tissue samples. Four alternatively spliced transcripts of GRP gene, GRP-F1, F2, F3, and F4, were previously identified in mice and zebrafish [72,73,76]. Here, two novel GRP splice variants were unveiled in human, GRP-F5 and F6, characterized by the loss of carboxylation and secretion motifs, whereas GRP-F2, F3 and F4 were not detected. GRP-F1, corresponding to the full length protein, was shown to be the most relevant variant expressed in cartilage and synovial membrane tissues, suggesting that associations existing between GRP and OA should mainly reflect the contribution of this transcript. GRP-F1 was also found upregulated in osteoarthritic cartilage comparing to control tissues. In concordance, comparative analysis of GRP patterning at transcriptional level using the developed chondrocyte and synoviocyte cell system revealed GRP upregulation in OA-derived cells. GRP association with OA was further explored at translational level using tissue and body fluid samples and conformation-specific antibodies against carboxylated (cGRP) and undercarboxylated (ucGRP) GRP. Although both protein forms were immunodetected in all analysed samples and accumulated at sites of ectopic calcification, ucGRP was shown to be the prevalent form accumulated in osteoarthritic cartilage and synovial membrane. Similarly, matrix Gla protein undercarboxylated form (ucMGP) was found primarily accumulated in osteoarthritic cartilage. Interestingly, comparative gene expression studies using the developed *in vitro* cell system pointed for a reduced γ-carboxylation capacity of OA-derived cells, with decreased expression of genes known to be involved in the γ-carboxylation machinery. Altogether, our results suggest that the impairment of VKDPs γ-carboxylation may be associated with OA. This hypothesis is in agreement with a previous study where the absence of carboxylated matrix Gla protein (MGP) in osteoarthritic chondrocytes and chondrocyte-derived matrix vesicles was suggested to be an important mechanism for the increased mineralization observed in osteoarthritic cartilage [92]. The same study also reported the association of a reduced γ-carboxylase activity in osteoarthritic chondrocytes. Interestingly, our immunohistochemistry results revealed that GRP accumulation was not restricted to sites of ectopic calcification in osteoarthritic synovial membranes, being also accumulated in the lining layer of these tissues and suggesting a role in other cell mediated processes. Moreover, GRP was co-localized with sites of abnormal infiltration of inflammatory cells in consecutive tissue sections of osteoarthritic synovial membranes. The involvement of GRP with OA mineralization and possible association with inflammatory events was further studied using the developed *in vitro* cell system. GRP was shown to be upregulated during induced mineralization and inflammation, associated to cell

differentiation towards ECM mineralization and inflammatory responses, in both chondrocytes and synoviocytes. Importantly, GRP biological functions in OA were highlighted through the inhibition of ECM mineralization and decreased inflammatory response, following GRP supplementation. While γ-carboxylation was required for GRP anti-mineralization function, like previously shown in the cardiovascular system [16], GRP or GRP-coated basic calcium phosphate (BCP) crystals-mediated anti-inflammatory effect was independent of protein γ-carboxylation status, suggesting additional functions for ucGRP. The mechanism behind cGRP calcification inhibition capacity is believed to be related with its ability to alter calcium availability in the local environment or its capacity to change the dynamics of crystal growth [16]. However, the mechanisms behind GRP-mediated anti-inflammatory effect are currently unclear. In the case of GRP-coated BCP crystals, it is possible that GRP binding may interfere with crystal-cell membrane interactions, modulating the production of proinflammatory mediators. In fact, BCP-mediated inflammation is believed to rely on direct physical contact [140], and it is postulated that proteins and other entities bound to these crystals affect their ability to initiate inflammation [100]. Thus, GRP binding to crystals may not only be related with its ability to inhibit ectopic calcification events, but also to crystal-induced inflammatory responses. Interestingly, fetuin-A-containing calciprotein particles (CPP), known for their role in the prevention of pathological mineralization, were reported to decrease cytokine production in macrophages compared with naked hydroxyapatite crystals [58]. Also, serum-derived CPP have been shown to produce a higher protective effect than synthetic CPP in macrophage activation [58]. This protective effect most possibly reflects the inhibitory activity of other serum components, such as GRP. Notably, calcification inhibitors other than fetuin-A have been associated to CPP, including MGP [226,229], indicating that GRP might also be part of such complex. In fact, an association between GRP, MGP and fetuin-A was recently shown at sites of aortic valves calcification and GRP calcification inhibitory function was proposed to occur constitutively via this potent inhibitory system [16]. CPP could function as a chaperone to carry the highly insoluble GRP through circulation and GRP association to CPP might be related with this complex suggested roles as a pathological calcification and inflammatory inhibitor [58]. Accordingly, GRP possible association with these complexes should be further investigated. Our preliminary results also point for an association between MGP and inflammatory processes in OA. In concordance, a previous study suggested that ucMGP was a potential joint inflammatory marker in arthritis patients [95]. Overall, our data suggests that the increased expression of VKDPs, like GRP and MGP, in the context of OA where cell

hypertrophic differentiation and ECM calcification occur, might function to counteract calcification. Yet, system overload may lead to impaired γ-carboxylation capacity resulting in increased levels of ucGRP and ucMGP. Undercarboxylated GRP might contribute to control the levels of inflammatory mediators through still unknown mechanisms, thereby protecting articular joints from damage.

The final part of this project focused on the investigation of candidate OA biomarkers, for a potential use in diagnose and monitoring of disease treatments, with a particular interest on GRP. Since classical two-dimension gel electrophoresis (2-DE) proteomic analysis revealed to be inadequate for the study of GRP, alternative OA biomarkers were searched within CPP-like entities derived from serum samples. The performed 2-DE comparative analysis identified 19 differentially expressed proteins between control and osteoarthritic conditions. Some of these entities had been previously associated to OA, representing the most relevant candidate biomarkers. Moreover, the identification of immune regulators, protease inhibitors and lipid/molecule carriers, and the immunodetection of fetuin-A in the CPP-like entities, strengthens the hypothesis of a possible association of CPP with osteoarthritic pathological calcification and inflammation.

Further characterization of GRP anti-mineralization and putative anti-inflammatory activity, the molecular pathways involved, and correlation with its γ-carboxylation status, is now fundamental to better understand osteoarthritic pathological calcification and inflammatory processes. One of our future perspectives is to further study VKDPs γ-carboxylation impairments associated with OA. Such feature may be originated by vitamin K1 and K2 deficiencies, which in fact have been related with OA. Subclinical vitamin K levels were associated with increased risk of knee OA development [82-84] and vitamin K2 was hypothesized to affect bone turnover [85]. Also, vitamin K has been proposed to exert a protective effect against inflammatory events and oxidative stress [24-26,28,29]. Accordingly, vitamin K should be considered a potential therapeutic/prophylactic agent for OA, and its nutraceutical value should be further evaluated. Studies aiming to relate vitamin K1/K2 supplementation with GRP and MGP γ-carboxylation status and OA, can be conducted using the available cell model and conformation-specific antibodies, although we are aware that *in vitro* cell systems may have limited γ-carboxylation capacity [200], and results should be carefully interpreted. The availability of a system for the immunodetection of GRP in serum should open novel perspectives to establish a relationship between levels of circulating c/ucGRP and the degree of ectopic calcification and inflammatory processes in OA. For that, the development of a specific GRP enzyme-linked immunosorbent assay (ELISA), able to

distinguish different degrees of γ-carboxylation, is currently under development. Macrophages are one of the most abundant cellular type infiltrating the synovial membrane upon OA, generating a broad spectrum of cytokines and immune factors with roles in OA development and progression [130]. To further explore GRP association with the inflammatory processes occurring in OA we can study the effect of GRP supplementation in co-cultures of macrophages with control chondrocytes or synoviocytes, accounting with a macrophage-derived THP-1 cell line available at the laboratory. Nevertheless, we may be limited by the short time-frames in which differentiated monocytic cells can survive in cultures [245], thus an alternative approach is the stimulation of the currently available cell system with conditioned media from the macrophage-derived THP-1 cell line. To collect new knowledge relating GRP with both mineralization and inflammatory events occurring in OA, a three-dimensional (3D) model, where cells can secret and build typical *in vivo* components [156,157], comprising co-cultures of control synoviocytes and monocytic cells over healthy cartilage explants, could be developed. Such system may dynamically mimic OA processes of calcification and cartilage degradation, and respective analysis under control and mineralizing conditions should allow the collection of new data relating GRP with two of the most relevant pathological features associated to OA. To explore the possible association of GRP with CPP, we intend to additionally characterize the serum-derived CPP-like entities obtained in this work, focusing on GRP, MGP and fetuin-A identification. Following, to access new data relative to CPP association with calcification and inflammatory mechanisms in OA, the characterized complexes may be added to the available *in vitro* cell system conditioned media under mineralizing or inflammatory conditions. Regarding the identified candidate biomarkers from the serum-derived CPP-like entities, these should now be validated using western blot or ELISA approaches and subsequently, their expression in earlier stages of the disease should be analysed to verify if they are suitable as early OA markers. The origin of the identified proteins should also be further clarified since although most of them are likely to be components of CPP, the analysed samples may represent an heterogeneous mixture [228,244]. Further morphological characterization can be accomplished in the isolated samples using scanning and transmission electron microscopy. Our efforts to clarify the potential of GRP as a biomarker for OA using comparative proteomic approaches and serum samples will continue, accounting with the recent knowledge acquired from GRP positive identification from calcified aortic valves extracts [16]. We intend to use SDS-PAGE gels instead of 2-DE to improve GRP solubilisation, use a double trypsin digestion for better peptide fragmentation, and mass spectrometry by MALDI-time-of-flight (TOF/TOF),

followed by MS/MS data acquisition, which already proved to be effective for GRP positive identification [16]. Ultimately, the study of extracellular vesicles (EVs) association with OA may be one of our future approaches, since we strongly believe that these entities might be related with the calcification and inflammatory processes described in OA. EVs are considered an emerging area in clinical diagnosis and therapeutics [243], they have a known role on mineralization [41,46] and were shown to be released from synoviocytes and macrophages, with increasing levels upon calcification or inflammatory stimuli [246,247]. Moreover, GRP, MGP and fetuin-A were recently detected inside EVs isolated from the media of cultured aortic segments, and GRP downregulation throughout time in EVs released after a calcifying stimulus suggested that it might act as a blocker of mineral growth and nucleation in EVs in healthy situations [16]. GRP was also recently detected inside EVs derived from chondrocytes and macrophages culture media (laboratory unpublished data). To study a possible association between GRP and EVs in OA we may account with our available cell system, which will enable the study of EVs released from chondrocytes and synoviocytes at structural and compositional levels, during induced mineralization and inflammation processes mimicking OA features.

Overall, this study collected novel and important data associating, for the first time, GRP with molecular features of osteoarthritis. Our new data supports the proposal of GRP as an inhibitor of pathological calcification in this pathology and unravelled an unprecedented association between GRP and inflammatory processes in OA. This work has therefore contributed for new knowledge regarding the pathological calcification and inflammatory processes occurring in OA, evidencing GRP as a new player acting in these mechanisms.

References

1. Tie JK, Stafford DW (2015) Structural and functional insights into enzymes of the vitamin K cycle. J Thromb Haemost 13: 1-12.
2. Stenflo J, Fernlund P, Egan W, Roepstorff P (1974) Vitamin K dependent modifications of glutamic acid residues in prothrombin. Proc Natl Acad Sci 71: 2730-2733.
3. Willems BAG, Vermeer C, Reutelingsperger CPM, Schurgers LJ (2014) The realm of vitamin K dependent proteins: shifting from coagulation toward calcification. Mol Nutr Food Res 58: 1620-1635.
4. Sunnerhagen M, Drakenberg T, Forsen S, Stenflo J (1996) Effect of Ca2+ on the structure of vitamin K-dependent coagulation factors. Haemostasis 26: 45-53.
5. Ellison EH, Castellino FJ (1998) Adsorption of vitamin K-dependent blood coagulation proteins to spread phospholipid monolayers as determined from combined measurements of the surface pressure and surface protein concentration. Biochemistry 37: 7997-8003.
6. Hoang QQ, Sicheri F, Howard AJ, Yang DS (2003) Bone recognition mechanism of porcine osteocalcin from crystal structure. Nature 425: 977-980.
7. Schurgers LJ, Cranenburg EC, Vermeer C (2008) Matrix Gla-protein: the calcification inhibitor in need of vitamin K. Thromb Haemostasis 100: 593-603.
8. Lee NK, Sowa H, Hinoi E, Ferron M, Ahn JD, et al. (2007) Endocrine regulation of energy metabolism by the skeleton. Cell 130: 456-469.
9. Hauschka PV, Lian JB, Gallop PM (1975) Direct identification of the calcium-binding amino acid, gammacarboxyglutamate, in mineralized tissue. Proc Natl Acad Sci 72: 3925-3929.
10. Katagiri T, Takahashi N (2002) Regulatory mechanisms of osteoblast and osteoclast differentiation. Oral Dis 8: 147-159.
11. Price PA, Urist MR, Otawara Y (1983) Matrix Gla protein, a new γ-carboxyglutamic acid-containing protein which is associated with the organic matrix of bone. Biochem Biophys Res Commun 117: 765-771.
12. Luo G, Ducy P, Mckee MD, Pinero GJ, Loyer E, et al. (1997) Spontaneous calcification of arteries and cartilage in mice lacking matrix Gla protein. Nature 386: 78-81.
13. Zebboudj AF, Imura M, Bostrom K (2002) Matrix Gla protein, a regulatory protein for bone morphogenetic protein-2. J Biol Chem 277: 4388-4394.
14. Viegas CSB, Cavaco S, Neves PL, Ferreira A, João A, et al. (2009) Gla-rich protein (GRP) is a novel vitamin K dependent protein present in serum and accumulated at sites of pathological calcifications. Am J Pathol 175: 2288-2298.
15. Viegas CSB, Herfs M, Rafael MS, Enriquez JL, Teixeira A, et al. (2014) Gla-rich protein is a potential new vitamin K target in cancer: evidences for a direct GRP-mineral interaction. Biomed Res Int 18: 10.1155/2014/340216.
16. Viegas CSB, Rafael MS, Enriquez JL, Teixeira A, Vitorino R, et al. (2015) Gla-rich protein (GRP) acts as a calcification inhibitor in the human cardiovascular system. Arterioscler Thromb Vasc Biol 114: 10.1161/ATVBAHA.1114.304823.
17. Shearer MJ, Newman P (2008) Metabolism and cell biology of vitamin K. Thromb Haemostasis 100: 530-547.
18. Walther B, Karl JP, Booth SL, Boyaval P (2013) Menaquinones, bacteria, and the food supply: the relevance of dairy and fermented food products to vitamin K requirements. Adv Nutr 4: 463-473.
19. Okano T, Nakagawa K, Kamao M (2009) *In vivo* metabolism of vitamin K: in relation to the conversion of vitamin K1 to MK-4. Clin Calcium 19: 1779-1787.
20. Rishavy MA, Berkner KL (2012) Vitamin K oxygenation, glutamate carboxylation, and processivity: defining the three critical facets of catalysis by the vitamin K-dependent carboxylase. Adv Nutr 3: 135-148.
21. Stanley TB, Humphries J, High KA, Stafford DW (1999) Amino acids responsible for reduced affinities of vitamin K-dependent propeptides for the carboxylase. Biochemistry 38: 15681-15687.

22. Chatrou ML, Winckers K, Hackeng TM, Reutelingsperger CP, Schurgers LJ (2012) Vascular calcification: the price to pay for anticoagulation therapy with vitamin K-antagonists. Blood Rev 26: 155-166.
23. Price PA, Faus SA, Williamson MK (1998) Warfarin causes rapid calcification of the elastic lamellae in rat arteries and heart valves. Arterios Thromb Vasc Biol 18: 1400-1407.
24. Fujii S, Shimizu A, Takeda N, Oguchi K, Katsurai T, et al. (2015) Systematic synthesis and anti-inflammatory activity of ω-carboxylated menaquinone derivatives - Investigations on identified and putative vitamin K2 metabolites. Bioorg Med Chem 23: 2344-2352.
25. Li J, Wang H, Rosenberg PA (2009) Vitamin K prevents oxidative cell death by inhibiting activation of 12-lipoxygenase in developing oligodendrocytes. J Neurosci Res 87: 1997-2005.
26. Shea MK, Booth SL, Massaro JM, Jacques PF, D'Agostino RB, et al. (2008) Vitamin K and vitamin D status: associations with inflammatory markers in the Framingham Offspring Study. Am J Epidemiol 167: 313-320.
27. Ohsaki Y, Shirakawa H, Hiwatashi K, Furukawa Y, Mizutani T, et al. (2006) Vitamin K suppresses lipopolysaccharide-induced inflammation in the rat. Biosci Biotechnol Biochem 70: 926-932.
28. Ohsaki Y, Shirakawa H, Miura A, Giriwono PE, Sato S, et al. (2010) Vitamin K suppresses the lipopolysaccharide-induced expression of inflammatory cytokines in cultured macrophage-like cells via the inhibition of the activation of nuclear factor κB through the repression of IKKα/β phosphorylation. J Nutr Biochem 21: 1120-1126.
29. Yamaguchi M, Weitzmann MN (2010) Vitamin K2 stimulates osteoblastogenesis and suppresses osteoclastogenesis by suppressing NF-κB activation. Int J Mol Med 27: 3-14.
30. Lawrence T (2009) The nuclear factor NF-kB pathway in inflammation. Cold Spring Harb Perspect Biol 1: 1651-1661.
31. Li J, Lin JC, Wang H, Peterson JW, Furie BC, et al. (2003) Novel role of vitamin K in preventing oxidative injury to developing oligodendrocytes and neurons. J Neurosci Res 23: 5816-5826.
32. Long F, Ornitz DM (2013) Development of the endochondral skeleton. Cold Spring Harb Perspect Biol 5: 8334-8354.
33. Pizette S, Niswander L (2000) BMPs are required at two steps of limb chondrogenesis: formation of prechondrogenic condensations and their differentiation into chondrocytes. Dev Biol 219: 237-249.
34. Kist R, Schrewe H, Balling R, Scherer G (2002) Conditional inactivation of Sox9: a mouse model for campomelic dysplasia. Genesis 32: 121-123.
35. Kobayashi T, Chung UI, Schipani E, Starbuck M, Karsenty G, et al. (2002) PTHrP and indian hedgehog control differentiation of growth plate chondrocytes at multiple steps. Development 129: 2977-2986.
36. Bush PG, Parisinos CA, Hall AC (2008) The osmotic sensitivity of rat growth plate chondrocytes in situ; Clarifying the mechanisms of hypertrophy. J Cell Physiol 214: 621-629.
37. Mueller MB, Tuan RS (2008) Functional characterization of hypertrophy in chondrogenesis of human mesenchymal stem cells. Arthritis Rheum 58: 1377-1388.
38. Studer D, Millan C, Ozturk E, Maniura-Weber K, Zenobi-Wong M (2012) Molecular and biophysical mechanisms regulating hypertrophic differentiation in chondrocytes and mesenchymal stem cells. Eur Cell Mater 24: 118-135.
39. Inada M, Wang YM, Byrne MH, Rahman MU, Miyaura C, et al. (2004) Critical roles for collagenase-3 (Mmp13) in development of growth and in endochondral plate cartilage ossification. Proc Natl Acad Sci USA 101: 17192-17197.
40. Shen G (2005) The role of type X collagen in facilitating and regulating endochondral ossification of articular cartilage. Orthod Craniofac Res 8: 11-17.
41. Balcerzak M, Hamade E, Zhang L, Pikula S, Azzar G, et al. (2003) The roles of annexins and alkaline phosphatase in mineralization process. Acta Biochim Pol 50: 1019-1038.

42. Macrae VE, Davey MG, McTeir L, Narisawa S, Yadav MC, et al. (2010) Inhibition of PHOSPHO1 activity results in impaired skeletal mineralization during limb development of the chick. Bone 46: 1146-1155.
43. Price PA, Toroian D, Lim JE (2009) Mineralization by inhibitor exclusion: the calcification of collagen with fetuin. J Biol Chem 284: 17092-17101.
44. Aubin J, Liu F, Malaval L, Gupta A (1995) Osteoblast and chondroblast differentiation. Bone 17: S77-S83.
45. Mackie EJ, Tatarczuch L, Mirams M (2011) The skeleton: a multi-functional complex organ: the growth plate chondrocyte and endochondral ossification. J Endocrinol 211: 109-121.
46. Vilder EYG, Vanakker OM (2015) From variome to phenome: pathogenesis, diagnosis and management of ectopic mineralization disorders. World J Clin Cases 3: 556-574.
47. Danziger J (2008) Vitamin K-dependent proteins, warfarin, and vascular calcification. Clin J Am Soc Nephrol 3: 1504-1510.
48. Liote F, Ea HK (2014) Clinical implications of pathogenic calcium crystals. Curr Opin Rheumatol 26: 192-196.
49. Ea HK, Liote F (2014) Diagnosis and clinical manifestations of calcium pyrophosphate and basic calcium phosphate crystal deposition diseases. Rheum Dis Clin N Am 40: 207-229.
50. Ea HK, Nguyen C, Bazin D, Bianchi A, Guicheux J, et al. (2011) Articular cartilage calcification in osteoarthritis. Arthritis Rheum 63: 10-18.
51. Rutsch F, Terkeltaub R (2005) Deficiencies of physiologic calcification inhibitors and low-grade inflammation in arterial calcification: lessons for cartilage calcification. Joint Bone Spine 72: 110-118.
52. Ducy P, Desbois C, Boyce B, Pinero G, Story B, et al. (1996) Increased bone formation in osteocalcin-deficient mice. Nature 382: 448-452.
53. Loeser R, Carlson CS, Tulli H, Jerome WG, Miller L, et al. (1992) Articular-cartilage matrix gamma-carboxyglutamic acid containing protein. Characterization and immunolocalization. Biochem J 282: 1-6.
54. Viegas CSB, Simes DC, Laize V, Williamson MK, Price PA, et al. (2008) Gla-rich Protein (GRP), a new vitamin K-dependent protein identified from sturgeon cartilage and highly conserved in vertebrates. J Biol Chem 283: 36655-36664.
55. Heiss A, Eckert T, Aretz A, Richtering W, van Dorp W, et al. (2008) Hierarchical role of fetuin-A and acidic serum proteins in the formation and stabilization of calcium phosphate particles. J Biol Chem 283: 14815-14825.
56. Theuwissen E, Smit E, Vermeer C (2012) The role of vitamin K in soft-tissue calcification. Adv Nutr 3: 166-173.
57. Heiss A, DuChesne A, Denecke B, Grotzinger J, Yamamoto K, et al. (2003) Structural basis of calcification inhibition by alpha 2-HS glycoprotein/fetuin-A. Formation of colloidal calciprotein particles. J Biol Chem 278: 13333-13341.
58. Smith ER, Hanssen E, McMahon LP, Holt SG (2013) Fetuin-A-containing calciprotein particles reduce mineral stress in the macrophage. PLoS One 8: 60904-60920.
59. Price P, Caputo J, Williamson M (2002) Bone origin of the serum complex of calcium, phosphate, fetuin, and matrix Gla protein: biochemical evidence for the cancellous bone-remodeling compartment. J Bone Min Res 17: 1171-1170.
60. Parfitt AM (2001) The bone remodeling compartment: a circulatory function for bone lining cells. J Bone Miner Res 16: 1583-1585.
61. Price PA, Lim JE (2003) The inhibition of calcium phosphate precipitation by fetuin is accompanied by the formation of a fetuin-mineral complex. J Biol Chem 278: 22144-22152.
62. Luo G, D'Souza R, Hogue D, Karsenty G (1995) The matrix Gla protein gene is a marker of the chondrogenesis cell lineage during mouse development. J Bone Miner Res 10: 325-334.
63. Murshed M, Schinke T, Mckee MD, Karsenty G (2004) Extracellular matrix mineralization is regulated locally; different roles of two gla-containing proteins. J Cell Biol 165: 625-630.
64. Roy ME, Nishimoto SK (2002) Matrix Gla protein binding to hydroxyapatite is dependent on the ionic environment: calcium enhances binding affinity but phosphate and magnesium decrease affinity. Bone 31: 296-302.

65. Munroe PB, Olgunturk RO, Fryns JP, Van Maldergem L, Ziereisen F, et al. (1999) Mutations in the gene encoding the human matrix Gla protein cause Keutel syndrome. Nat Genet 21: 142-144.
66. Zebboudj AF, Shin V, Bostrom K (2003) Matrix Gla protein and BMP-2 regulate osteoinduction in calcifying vascular cells. J Cell Biochem 90: 756-765.
67. Uitto J, Jiang Q (2007) Pseudoxanthoma elasticum-like phenotypes: more diseases than one. J Invest Dermatol 127: 507-510.
68. Gheduzzi D, Boraldi F, Annovi G, DeVincenzi CP, Schurgers LJ, et al. (2007) Matrix Gla protein is involved in elastic fiber calcification in the dermis of pseudoxanthoma elasticum patients. Lab Invest 87: 998-1008.
69. Cranenburg EC, Vermeer C, Koos R, Boumans M-L, Hackeng TM, et al. (2008) The circulating inactive form of matrix Gla protein (ucMGP) as a biomarker for cardiovascular calcification. J Vasc Res 45: 427-436.
70. Laize V, Martel P, Viegas CSB, Price PA, Cancela ML (2005) Evolution of matrix and bone γ-carboxyglutamic acid proteins in vertebrates. J Biol Chem 280: 26659-26668.
71. Viegas CSB, Simes DC, Williamson MK, Cavaco S, Laize V, et al. (2013) Ancestral osteocalcin (OC) in Sturgeon: the missing link between bone-related Gla proteins. J Biol Chem 288: 27801-27811.
72. Neacsu CD, Grosch M, Tejada M, Winterpacht A, Paulsson M, et al. (2011) Ucmaa (Grp-2) is required for zebrafish skeletal development. Evidence for a functional role of its glutamate γ-carboxylation. Matrix Biol 30: 369-378.
73. Fazenda C, Silva IAL, Cancela ML, Conceição N (2012) Molecular characterization of two paralog genes encoding Gla-rich protein (Grp) in zebrafish. J Appl Ichthyol 28: 377-381.
74. Tagariello A, Luther J, Streiter M, Didt-Koziel L, Wuelling M, et al. (2008) Ucma-A novel secreted factor represents a highly specific marker for distal chondrocytes. Matrix Biol 27: 3-11.
75. Surmann-Schmitt C, Dietz U, Kireva T, Adam N, Park J, et al. (2008) Ucma, a novel secreted cartilage-specific protein with implications in osteogenesis. J Biol Chem 283: 7082-7093.
76. Le Jeune M, Tomavo N, Tian TV, Flourens A, Marchand N, et al. (2010) Identification of four alternatively spliced transcripts of the Ucma/GRP gene, encoding a new Gla-containing protein. Exp Cell Res 316: 203-215.
77. Lee YJ, Park SY, Lee SJ, Boo YC, Choi JY, et al. (2015) Ucma, a direct transcriptional target of Runx2 and Osterix, promotes osteoblast differentiation and nodule formation. Osteoarth Cartilage 23: 1421-1431.
78. Eitzinger N, Surmann-Schmitt C, Bosl M, Schett G, Engelke K, et al. (2012) Ucma is not necessary for normal development of the mouse skeleton. Bone 50: 670-680.
79. Shroff R, Long DA, Shanahan C (2013) Mechanistic insights into vascular calcification in CKD. J Am Soc Nephrol 24: 179-189.
80. Nguyen C, Bazin D, Daudon M, Chatron-Colliet A, Hannouche D, et al. (2013) Revisiting spatial distribution and biochemical composition of calcium-containing crystals in human osteoarthritic articular cartilage. Arthritis Res Ther 15: 103-115.
81. Ishijima M, Kaneko H, Kaneko K (2014) The evolving role of biomarkers for osteoarthritis. Ther Adv Musculoskel Dis 6: 144-153.
82. Misra D, Booth SL, Tolstykh I, Felson DT, Nevitt MC, et al. (2013) Vitamin K deficiency is associated with incident knee osteoarthritis. Am J Med 126: 243-248.
83. Neogi T, Booth SL, Zhang YQ, Jacques PF, Terkeltaub R, et al. (2006) Low vitamin K status is associated with osteoarthritis in the hand and knee. Arthritis Rheum 54: 1255-1261.
84. Oka H, Akune T, Muraki S, En-yo Y, Yoshida M, et al. (2009) Association of low dietary vitamin K intake with radiographic knee osteoarthritis in Japanese elderly population: dietary survey in a population-based cohort of the ROAD study. J Orthop Sci 14: 687-692.
85. Ishii Y, Noguchi H, Takeda M, Sato J, Yamamoto N, et al. (2012) Distribution of vitamin K2 in subchondral bone in osteoarthritic knee joints. Knee Surg Sports Traumatol Arthrosc 21: 1813-1818.

86. Ziskoven C, Jäger M, Zilkens C, Bloch W, Brixius K, et al. (2010) Oxidative stress in secondary osteoarthritis: from cartilage destruction to clinical presentation? Orthop Rev 23: 23-40.
87. Lange-Brokaar BJE, Ioan-Facsinay A, van Osch GJVM, Zuurmond AM, Schoones J, et al. (2012) Synovial inflammation, immune cells and their cytokines in osteoarthritis: a review. Osteoarth Cartilage 20: 1484-1499.
88. Scanzello CR, Goldring SR (2012) The role of synovitis in osteoarthritis pathogenesis. Bone 51: 249-257.
89. Yagami K, Suh JY, Enomoto-Iwamoto M, Koyama E, et al. (1999) Matrix Gla protein is a developmental regulator of chondrocyte mineralization and, when constitutively expressed, blocks endochondral and intramembranous ossification in the limb. J Cell Biol 147: 1097-1108.
90. Newman B, Gigout L, Sudre L, Grant M, Wallis G (2001) Coordinated expression of matrix Gla protein is required during endochondral ossification for chondrocyte survival. J Cell Biol 154: 659-666.
91. Houarda X, Goldring MB, Berenbauma F (2013) Homeostatic mechanisms in articular cartilage and role of inflammation in osteoarthritis. Curr Rheumatol Rep 15: 375-394.
92. Wallin R, Schurgers LJ, Loeser RF (2010) Biosynthesis of the vitaminK-dependent matrix Gla protein (MGP) in chondrocytes: A fetuin-MGP protein complex is assembled in vesicles shed from normal but not from osteoarthritic chondrocytes. Osteoarth Cartilage 18: 1096-1103.
93. Misra D, Booth SL, Crosier MD, Ordovas JM, Felson DT, et al. (2011) Matrix Gla protein polymorphism, but not concentrations, is associated with radiographic hand osteoarthritis. J Rheumatol 38: 1960-1965.
94. Naito K, Watari T, Obayashi O, Katsube S, Nagaoka I, et al. (2011) Relationship between serum undercarboxylated osteocalcin and hyaluronan levels in patients with bilateral knee osteoarthritis. Int J Mol Med 29: 756-760.
95. Silaghi CN, Fodor D, Cristea V, Crãciun AM (2012) Synovial and serum levels of uncarboxylated matrix Gla-protein (ucMGP) in patients with arthritis. Clin Chem Lab Med 50: 125-128.
96. Fibel KH, Hillstrom HJ, Halpern BC (2015) State-of-the-Art management of knee osteoarthritis. World J Clin Cases 3: 89-101.
97. Allen KD, Golightly YM (2015) Epidemiology of osteoarthritis: state of the evidence. Curr Opin Rheumatol 27: 276-283.
98. Egloff C, Hügle T, Valderrabano V (2012) Biomechanics and pathomechanisms of osteoarthritis. Eur J Med Sci 142: 13583-13597.
99. Abramson SB, Attur M (2009) Developments in the scientific understanding of osteoarthritis. Arthritis Res Ther 11: 227-235.
100. Rosenthal AK (2011) Crystals, inflammation, and osteoarthritis. Curr Opin Rheumatol 23: 170-173.
101. Hunter DJ, Nevitt M, Losina E, Kraus V (2014) Biomarkers for osteoarthritis: current position and steps towards further validation. Best Pract Res Clin Rheumatol 28: 61-71.
102. Samson DJ, Grant MD, Ratko TA, Bonnell CJ, Ziegler KM, et al. (2007) Treatment of primary and secondary osteoarthritis of the knee. Evid Rep Technol Assess 157: 1-157.
103. Pereira D, Ramos E, Branco J (2014) Osteoarthritis. Acta Med Port 27: 1-8.
104. Blanco FJ (2014) Osteoarthritis: something is moving. Reumatol Clin 10: 4-5.
105. Gore M, Tai KS, Sadosky A, Leslie D, Stacey BR (2011) Clinical comorbidities, treatment patterns, and direct medical costs of patients with osteoarthritis in usual care: a retrospective claims database analysis. J Med Econ 14: 497-507.
106. Thomas E, Peat G, Croft P (2014) Defining and mapping the person with osteoarthritis for population studies and public health. Rheumatology 53: 338-345.
107. Van der Kraan PM, Van den Berg WB (2008) Osteoarthritis in the context of ageing and evolution. Loss of chondrocyte differentiation block during ageing. Ageing Res Rev 7: 106-113.

108. Abella V, Scotece M, Conde J, Lopez V, Lazzaro V, et al. (2014) Adipokines, metabolic syndrome and rheumatic diseases. J Immunol Res 2014: 1-15.
109. Fowler-Brown A, Kim DH, Shi L, Marcantonio E, Wee CC, et al. (2015) The mediating effect of leptin on the relationship between body weight and knee osteoarthritis in older adults. Arthritis Rheumatol 67: 169-175.
110. Louati K, Vidal C, Berenbaum F, Sellam J (2014) Association between diabetes mellitus and osteoarthritis: systematic literature review and meta-analysis. Ann Rheum Dis 73: 10.1136/annrheumdis-2014-eular.2509.
111. Madry H, Luyten FP, Facchini A (2011) Biological aspects of early osteoarthritis. Knee Surg Sports Traumatol Arthrosc 20: 401-422.
112. Yavorskyy A, Hernandez-Santana A, McCarthy G, McMahon G (2008) Detection of calcium phosphate crystals in the joint fluid of patients with osteoarthritis - analytical approaches and challenges. Analyst 133: 302-318.
113. Goldring MB, Marcu KB (2009) Cartilage homeostasis in health and rheumatic diseases. Arthritis Res Ther 11: 224-240.
114. Goldring MB, Otero M, Plumb DA, Dragomir C, Favero M, et al. (2011) Roles of inflammatory and anabolic cytokines in cartilage metabolism: signals and multiple effectors converge upon MMP-13 regulation in osteoarthritis. Eur Cell Mater 21: 202-220.
115. van der Kraan PM, Blaney Davidson EN, van den Berg WB (2010) Bone morphogenetic proteins and articular cartilage: To serve and protect or a wolf in sheep clothing's? Osteoarth Cartilage 18: 735-741.
116. Vogel WF, Abdulhussein R, Ford CE (2006) Sensing extracellular matrix: an update on discoidin domain receptor function. Cell Signal 18: 1108-1116.
117. Marcu KB, Otero M, Olivotto E, Borzi RM, Goldring MB (2010) NF-κB Signaling: multiple angles to target OA. Curr Drug Targets 11: 599-613.
118. Corr M (2008) Wnt-β-catenin signaling in the pathogenesis of osteoarthritis. Nat Rev Rheumatol 4: 550-556.
119. Conde J, Gomez R, Bianco G, Scotece M, Lear P, et al. (2011) Expanding the adipokine network in cartilage: identification and regulation of novel factors in human and murine chondrocytes. Ann Rheum Dis 70: 551-559.
120. Bhatia D, Bejarano T, Novo M (2013) Current interventions in the management of knee osteoarthritis. J Pharm Bioallied Sci 5: 30-38.
121. Kumarasinghe DD, Hopwood B, Kuliwaba JS, Atkins GJ, Fazzalari NL (2011) An update on primary hip osteoarthritis including altered Wnt and TGF-β associated gene expression from the bony component of the disease. Rheumatology 50: 2166-2175.
122. MacMullan P, McMahonb G, McCarthy G (2011) Detection of basic calcium phosphate crystals in osteoarthritis. Joint Bone Spine 4: 358-363.
123. Geurts J, van den Brand BT, Wolf A, Abdollahi-Roodsaz S, Arntz OJ, et al. (2011) Toll-like receptor 4 signalling is specifically TGF-beta-activated kinase 1 independent in synovial fibroblasts. Rheumatology 50: 1216-1225.
124. Zhang Q, Hui W, Litherland GJ, Barter MJ, Davidson R, et al. (2008) Differential Toll-like receptor-dependent collagenase expression in chondrocytes. Ann Rheum Dis 67: 1633-1641.
125. Smith MD (2011) The microarchitecture and protective mechanisms in synovial tissue from clinically and arthroscopically normal knee joints. Open Rheumatol J 5: 100-106.
126. Smith MD, Barg E, Weedon H, Papengelis V, Smeets T, et al. (2003) The microarchitecture and protective mechanisms in synovial tissue from clinically and arthroscopically normal knee joints. Ann Rheum Dis 62: 303-307.
127. Hui AY, McCarty WJ, Masuda K, Firestein GS, Sah RL (2012) A systems biology approach to synovial joint lubrication in health, injury, and disease. Wiley Interdiscip Rev Syst Biol Med 4: 15-37.
128. Edwards JC, Willoughby DA (1982) Demonstration of bone marrow derived cells in synovial lining by means of giant intracellular granules as genetic markers. Ann Rheum Dis 41: 177-182.

129. Bartok B, Firestein GS (2010) Fibroblast-like synoviocytes: key effector cells in rheumatoid arthritis. Immunol Rev 233: 233-255.
130. Fioravanti A, Tinti L, Pascarelli NA, Di Capua A, Lamboglia A, et al. (2012) *In vitro* effects of VA441, a new selective cyclooxygenase-2 inhibitor, on human osteoarthritic chondrocytes exposed to IL-1β. J Pharmacol Sci 120: 6-14.
131. Konttinen YT, Ceponis A, Meri S, Vuorikoski A, Kortekangas P, et al. (1996) Complement in acute and chronic arthritides: assessment of C3c, C9, and protectin (CD59) in synovial membrane. Ann Rheum Dis 55: 888-894.
132. Blom AB, van Lent PL, Holthuysen AE, van der Kraan PM, Roth J, et al. (2004) Synovial lining macrophages mediate osteophyte formation during experimental osteoarthritis. Osteoarth Cartilage 12: 627-635.
133. Sokolove J, Lepus CM (2013) Role of inflammation in the pathogenesis of osteoarthritis: Latest findings and interpretations. Ther Adv Musculoskel Dis 5: 77-94.
134. Tanaka K (2009) Iguratimod (T-614): A novel disease-modifying anti-rheumatic drug. Rheumatol Reports 1: 1-4.
135. Neogi T (2013) The epidemiology and impact of pain in osteoarthritis. Osteoarth Cartilage 21: 1145-1153.
136. Hunter DJ, McDougall JJ, Keefe FJ (2008) The symptoms of OA and the genesis of pain. Rheum Dis Clin North Am 34: 623-643.
137. Fuerst M, Bertrand J, Lammers L, Dreier R, Echtermeyer F, et al. (2009) Calcification of articular cartilage in human osteoarthritis. Arthritis Rheum 60: 2694-2703.
138. Fuerst M, Niggemeyer O, Lammers L, Schäfer F, Lohmann C, et al. (2009) Articular cartilage mineralization in osteoarthritis of the hip. BMC Musculoskelet Disord 10: 166.
139. Molloy ES, Morgan MP, Doherty GA, McDonnell B, Hilliard M, et al. (2008) Mechanism of basic calcium phosphate crystal-stimulated cyclooxygenase-1 up-regulation in osteoarthritic synovial fibroblasts. Rheumatology 47: 965-971.
140. Liu YZ, Jackson AP, Cosgrove SD (2009) Contribution of calcium-containing crystals to cartilage degradation and synovial inflammation in osteoarthritis. Osteoarth Cartilage 17: 1333-1340.
141. Ea HK, Chobaz V, Nguyen C, Nasi S, van Lent P, et al. (2013) Pathogenic role of basic calcium phosphate crystals in destructive arthropathies. PLoS One 8: 57352-57360.
142. Ea HK, Liote F (2009) Advances in understanding calcium-containing crystal disease. Curr Opin Rheumatol 21: 150-157.
143. Ea HK, Uzan B, Rey C, Liote F (2005) Octacalcium phosphate crystals directly stimulate expression of inducible nitric oxide synthase throgh p38 and JNK mitogen-activated protein kinases in articular chondrocytes. Arthritis Res Ther 7: 915-926.
144. Ewence A, Bootman M, Roderick H, Skepper J, McCarthy G, et al. (2008) Calcium phosphate crystals induce cell death in human vascular smooth muscle cells. Circ Res 103: 28.
145. Escobar C, Byer K, Khan S (2007) Naturally produced crystals obtained from kidney stones are less injurious to renal tubular epithelial cells than synthetic crystals. British J Urol 100: 891-897.
146. McCoy AM (2015) Animal models of osteoarthritis: comparisons and key considerations. Vet Pathol 52: 803-818.
147. Thysen S, Luyten FP, Lories RJU (2015) Targets, models and challenges in osteoarthritis research. Dis Mod Mech 8: 17-30.
148. Grenier S, Bhargava MM, Torzilli PA (2014) An *in vitro* model for the pathological degradation of articular cartilage in osteoarthritis. J Biomechanics 47: 645-652.
149. Hayami T, Zhuo Y, Wesolowski GA, Pickarski M, Duong T (2012) Inhibition of cathepsin K reduces cartilage degeneration in the anterior cruciate ligament transection rabbit and murine models of osteoarthritis. Bone 50: 1250-1259.
150. Stanton H, Rogerson FM, East CJ, Golub SB, Lawlor KE, et al. (2005) ADAMTS5 is the major aggrecanase in mouse cartilage *in vivo* and *in vitro*. Nature 434: 648-652.
151. Mason RM, Chambers MG, Flannelly J, Gaffen JD, Dudhia J, et al. (2001) The STR/ort mouse and its use as a model of osteoarthritis. Osteoarth Cartilage 9: 85-91.

152. Glasson SS, Blanchet TJ, Morris EA (2007) The surgical destabilization of the medial meniscus (DMM) model of osteoarthritis in the 129/SvEv mouse. Osteoarth Cartilage 15: 1061-1069.
153. Johnson CI, Argyle DJ, Clements DN (2015) *In vitro* models for the study of osteoarthritis Vet J: 10.1016/j.tvjl.2015.1007.1011.
154. Khoruzhenko AI (2011) 2D- and 3D-cell culture. Biopolymers and Cell 27: 17-24.
155. Dominick JB, Matthewsb GL, L. KD (2014) The degradation of chondrogenic pellets using cocultures of synovial fibroblasts and U937 cells. Biomaterials 35: 1185-1191.
156. Edmondson R, Broglie JJ, Adcock AF, Yang L (2014) Three-dimensional cell culture systems and their applications in drug discovery and cell-based biosensors. Assay Drug Dev Technol 12: 207-218.
157. Sun L, Wang X, Kaplan DL (2011) A 3D cartilage-inflammatory cell culture system for the modeling of human osteoarthritis. Biomaterials 32: 5581-5589.
158. Moo EK, Abu Osman NA, Pingguan-Murphy B (2011) The metabolic dynamics of cartilage explants over a long-term culture period. Clinics 66: 1431-1436.
159. Macrory L, Vaughan-Thomas A, Clegg PD, Innes JF (2009) An exploration of the ability of tepoxalin to ameliorate the degradation of articular cartilage in a canine *in vitro* model. BMC Vet Res 5: 25-34.
160. Gabriel N, Innes JF, Caterson B, Vaughan-Thomas A (2010) Development of an *in vitro* model of feline cartilage degradation. J Feline Med Surg 12: 614-620.
161. Zhang Q, Li H, Zhang Z, Yang F, Chen J (2015) Serum metabolites as potential biomarkers for diagnosis of knee osteoarthritis. Dis Markers doi:10.1155/2015/684794.
162. Riddle DL, Jiranek WA, Hull JR (2013) Validity and reliability of radiographic knee osteoarthritis measures by arthroplasty surgeons. Orthopedics 36: 25-32.
163. Djahani O, Rainer S, Pietsch M, Hofmann S (2013) Systematic analysis of painful total knee prosthesis, a diagnostic algorithm. Arch Bone Jt Surg 1: 48-52.
164. Bonutti PM, Mont MA, McMahon M, Ragland PS, Kester M (2004) Minimally invasive total knee arthroplasty. J Bone Joint Surg Am 86: 26-32.
165. Messier SP, Mihalko SL, Legault C, Miller GD, Nicklas BJ, et al. (2013) Effects of intensive diet and exercise on knee joint loads, inflammation, and clinical outcomes among overweight and obese adults with knee osteoarthritis: the IDEA randomized clinical trial. J Am Med Assoc 310: 1263-1273.
166. Kirkley A, Webster-Bogaert S, Litchfield R, Amendola A, MacDonald S, et al. (1999) The effect of bracing on varus gonarthrosis. J Bone Joint Surg Am 81: 539-548.
167. Haim A, Rubin G, Rozen N, Goryachev Y, Wolf A (2012) Reduction in knee adduction moment via non-invasive biomechanical training: a longitudinal gait analysis study. J Biomech 45: 41-45.
168. Richmond J, Hunter D, Irrgang J, Jones MH, Levy B, et al. (2009) Treatment of osteoarthritis of the knee (nonarthroplasty). J Am Acad Orthop Surg 17: 591-600.
169. Noyszewski EA, Wroblewski K, Dodge GR, Kudchodkar S, Beers J, et al. (2001) Preferential incorporation of glucosamine into the galactosamine moieties of chondroitin sulfates in articular cartilage explants. Arthritis Rheum 44: 1089-1095.
170. Micu MC, Bogdan GD, Fodor D (2010) Steroid injection for hip osteoarthritis: efficacy under ultrasound guidance. Rheumatology 49: 1490-1494.
171. Nakazawa F, Matsuno H, Yudoh K, Watanabe Y, Katayama R, et al. (2002) Corticosteroid treatment induces chondrocyte apoptosis in an experimental arthritis model and in chondrocyte cultures. Clin Exp Rheumatol 20: 773-781.
172. Chevalier X, Jerosch J, Goupille P, van Dijk N, Luyten FP, et al. (2010) Single, intra-articular treatment with 6 ml hylan G-F 20 in patients with symptomatic primary osteoarthritis of the knee: a randomised, multicentre, double-blind, placebo controlled trial. Ann Rheum Dis 69: 113-119.
173. Petrera M, De Croos JN, Iu J, Hurtig M, Kandel RA, et al. (2013) Supplementation with platelet-rich plasma improves the *in vitro* formation of tissue-engineered cartilage with enhanced mechanical properties. Arthroscopy 29: 1685-1692.

174. Singh A, Goel SC, Gupta KK, Kumar M, Arun GR, et al. (2014) The role of stem cells in osteoarthritis: An experimental study in rabbits. Bone Joint Res 3: 32-37.
175. Lotz M, Pelletier JM, Christiansen C, Brandi M-L, Bruyère O, et al. (2013) Value of biomarkers in osteoarthritis: current status and perspectives. Ann Rheum Dis 72: 1756-1763.
176. Addison S, Coleman ER, Feng S, McDaniel G, Kraus VB (2009) Whole body bone scintigraphy provides a measure of total body burden of osteoarthritis for the purpose of systemic biomarker validation. Arthritis Rheum 60: 3366-3373.
177. Chan PMB, Zhu L, Wen CY, Chiu KY (2015) Subchondral bone proteomics in osteoarthritis: current status and perspectives. J Orthop Translat 3: 71-77.
178. Mobasheri A (2012) Osteoarthritis year 2012 in review: biomarkers. Osteoarth Cartilage 20: 1451-1464.
179. Hsueh M-F, Önnerfjord P, Kraus VB (2014) Biomarkers and proteomic analysis of osteoarthritis. Matrix Biol 39: 56-66.
180. Garnero P, Piperno M, Gineyts E, Christgau S, Delmas P, et al. (2001) Cross sectional evaluation of biochemical markers of bone, cartilage, and synovial tissue metabolism in patients with knee osteoarthritis: relations with disease activity and joint damage. Ann Rheum Dis 60: 619-626.
181. Wei F, Zhou J, Wei X, Zhang J, Fleming BC, et al. (2012) Activation of Indian hedgehog promotes chondrocyte hypertrophy and upregulation of MMP-13 in human osteoarthritic cartilage. Osteoarth Cartilage 20: 755-763.
182. Amin AR, Attur M, Patel RN, Thakker GD, Marshall PJ, et al. (1997) Superinduction of cyclooxygenase-2 activity in human osteoarthritis-affected cartilage. Influence of nitric oxide. J Clin Invest 99: 1231-1237.
183. Verma P, Dalal K (2013) Serum cartilage oligomeric matrix protein (COMP) in knee osteoarthritis: a novel diagnostic and prognostic biomarker. J Orthop Res 31: 999-1006.
184. Reijman M, Hazes JM, Bierma-Zeinstra SM, Koes BW, Christgau S, et al. (2004) A new marker for osteoarthritis: cross-sectional and longitudinal approach. Arthritis Rheum 50: 2471-2478.
185. Conrozier T, Balblanc JC, Richette P, Mulleman D, Maillet B, et al. (2012) Early effect of hyaluronic acid intra-articular injections on serum and urine biomarkers in patients with knee osteoarthritis: an open-label observational prospective study. J Orthop Res 30: 679-685.
186. van Spil W, Drossaers-Bakker K, Lafeber F (2013) Associations of CTX-II with biochemical markers of bone turnover raise questions on its tissue origin: data from CHECK, a cohort study of early osteoarthritis. Ann Rheum Dis 72: 29-36.
187. Ortiz-Delgado JB, Simes DC, Viegas CSB, Schaff BJ, Sarasquete C, et al. (2006) Cloning of matrix Gla protein in amarine cartilaginous fish, Prionace glauca: preferential protein accumulation in skeletal and vascular systems. Histochem Cell Biol 126: 89-101.
188. Witten PE, Villwock W (1997) Growth requires bone resorption at particular skeletal elements in a teleost fish with acellular bone. J Appl Ichthyol 13: 149-158.
189. Rafael MS, Cavaco S, Viegas CSB, Santos S, Ramos A, et al. (2014) Insights into the association of Gla-rich protein and osteoarthritis, novel splice variants and γ-carboxylation status. Mol Nutr Food Res 10.1002/mnfr.201300941.
190. Berenbaum F (2011) Diabetes-induced osteoarthritis: from a new paradigm to a new phenotype. Ann Rheum Dis 70: 1354-1356.
191. Chomczynski P, Sacchi N (1987) Single-step method of RNA isolation by acid guanidinium thiocyanate phenol chloroform extraction. Anal Biochem 162: 156-159.
192. Simes DC, Williamson MK, Ortiz-Delgado JB, Viegas CSB, Price PA, et al. (2003) Purification of matrix Gla protein from a marine teleost fish, Argyrosomus regius: calcified cartilage and not bone as the primary site of MGP accumulation in fish. J Bone Min Res 18: 244-259.
193. Noble JE, Bailey MJA (2009) Quantitation of protein. Method enzymol 463: 73-95.
194. Vermeer C, Jie KS, Knapen MH (1995) Role of vitamin K in bone metabolism. Annu Rev Nutr 15: 1-22.

195. Simes DC, Williamson MK, Schaff BJ, Gavaia PJ, Ingleton PM, et al. (2004) Characterization of osteocalcin (BGP) and matrix Gla protein (MGP) fish specific antibodies: validation for immunodetection studies in lower vertebrates. Calcif Tissue Int 74: 170-180.
196. Gobom J, Nordhoff E, Mirgorodskaya E, Ekman R, Roespstorff P (1999) Sample purification and preparation technique based on nano-scale reversed-phase columns for the sensitive analysis of complex peptide mixtures by matrix-assisted laser desorption/ionization mass spectrometry. J Mass Spectrom 34: 105-116.
197. Petersen TN, Brunak S, von Heijne G, Nielsen H (2011) SignalP 4.0: discriminating signal peptides from transmembrane regions. Nat Methods 8: 785-786.
198. Torgersen JS, Takle H, Andersen O (2009) Localization of mRNAs and proteins in methyl methacrylate-embedded tissues. J Histochem Cytochem 57: 825-830.
199. Hayman AR, Jones SJ, Boyde A, Foster D, Colledge WH, et al. (1996) Mice lacking tartrate-resistant acid phosphatase (Acp 5) have disrupted endochondral ossification and mild osteopetrosis. Development 122: 3151-3162.
200. Hallgren KW, Zhang D, Kinter M, Willard B, Berkner KL (2013) Methylation of γ-carboxylated Glu (Gla) allows detection by liquid chromatography-mass spectrometry and the identification of Gla residues in the γ-glutamyl carboxylase. J Proteome Res 12: 2365-2374.
201. Schurgers LJ, Spronk HMH, Skepper JN, Shanahan CM (2007) Post-translational modifications regulate matrix Gla protein function: importance for inhibition of vascular smooth muscle cell calcification. J Thromb Haemost 5: 2503-2511.
202. Cavaco S, Williamson MK, Rosa J, Roberto V, Cordeiro O, et al. (2014) Teleost fish osteocalcin 1 and 2 share the ability to bind the calcium mineral phase. Fish Physiol Biochem 40: 731-738.
203. Speicher KD, Gorman N, Speicher DW (2001) UNIT 11.10 N-Terminal Sequence Analysis of Proteins and Peptides. Curr Protoc Protein Sci Unit–11.10: 10.1002/0471140864.ps0471141110s0471140808.
204. Vermeer C, Theuwissen E (2011) Vitamin K, osteoporosis and degenerative diseases of ageing. Menopause Int 17: 19-23.
205. Price PA, Williamson MK, Haba T, Dell RB, et al. (1982) Excessive mineralization with growth plate closure in rats on chronic warfarin treatment. Proc Natl Acad Sci USA 79: 7734-7748.
206. Shroff RC, Shanahan CM (2007) The vascular biology of calcification. Semin Dial 20: 103-109.
207. Pombinho AR, Laize V, Molha DM, Marques SMP, Cancela ML (2004) Development of two bone-derived cell lines from the marine teleost Sparus aurata; evidence for extracellular matrix mineralization and cell-type-specific expression of matrix Gla protein and osteocalcin. Cell Tissue Res 315: 393-406.
208. Cavaco S, Viegas CSB, Rafael MS, Ramos A, Magalhães J, et al. (2015) Gla-rich protein is involved in the cross-talk between calcification and inflammation in osteoarthritis. Cell Mol Life Sci: 10.1007/s00018-00015-02033-00019.
209. Nakatani S, Mano H, Ryanghyok IM, Shimizu J, Wada M (2006) Excess magnesium inhibits excess calcium-induced matrix-mineralization and production of matrix gla protein (MGP) by ATDC5 cells. Biochem Biophys Res Commun 348: 1157-1162.
210. Tabcheh L, Bianchi A, Clément A, Jouzeau JY, Kempf H (2014) Phosphate-induced mineralization of tracheal smooth muscle and cartilage cells. Biomed Mater Eng 24: 37-45.
211. Shalhoub V, Shatzen EM, Ward SC, Young J-Y, Boedigheimer M, et al. (2010) Chondro/osteoblastic and cardiovascular gene modulation in human artery smooth muscle cells that calcify in the presence of phosphate and calcitriol or paricalcitol. J Cell Biochem 111: 911-921.
212. Hendrickx A, Bossuyt X (2001) Quantification of the leukocyte common antigen (CD45) in mature B-cell malignancies. Cytometry 46: 336-339.
213. Nguyen C, Lieberherr M, Bordat C, Velard F, Côme D, et al. (2012) Intracellular calcium oscillations in articular chondrocytes induced by basic calcium phosphate crystals lead to cartilage degradation. Osteoarth Cartilage 12: 1399-1408.

214. Sadowski T, Steinmeyer J (2001) Effects of non-steroidal antiinflammatory drugs and dexamethasone on the activity and expression of matrix metalloproteinase-1, matrix metalloproteinase-3 and tissue inhibitor of metalloproteinases-1 by bovine articular chondrocytes. Osteoarth Cartilage 9: 407-415.
215. Sun Y, Mauerhan DR, Franklin AM, Zinchenko N, Norton HJ, et al. (2014) Fibroblast-like synoviocytes induce calcium mineral formation and deposition. Arthritis: 10.1155/2014/812678.
216. Thomsen SB, Rathcke CN, Zerahn B, Vestergaard H (2010) Increased levels of the calcification marker Matrix Gla Protein and the inflammatory markers YKL-40 and CRP in patients with type 2 diabetes and ischemic heart disease. Cardiovasc Diabetol 9: 86-93.
217. Schurgers LJ, Teunissen KJ, Knapen MH, Kwaijtaal M, van Diest R, et al. (2005) Novel conformation-specific antibodies against matrix gamma-carboxyglutamic acid (Gla) protein: undercarboxylated matrix Gla protein as marker for vascular calcification. Arterioscler Thromb Vasc Biol 25: 1629-1633.
218. Cranenburg EC, Schurgers LJ, Vermeer C (2007) Vitamin K: The coagulation vitamin that became omnipotent. Thromb Haemostasis 98: 120-125.
219. Zoch ML, Clemens TL, Riddle RC (2015) New insights into the biology of osteocalcin. Bone: 10.1016/j.bone.2015.1005.1046.
220. Roman-Blas JA, Jimenez SA (2006) NF-κB as a potential therapeutic target in osteoarthritis and rheumatoid arthritis. Osteoarth Cartilage 14: 839-848.
221. Santucci L, Bruschi M, Ghiggeri GM, Candiano G (2015) The latest advancements in proteomic two-dimensional gel electrophoresis analysis applied to biological samples. Methods Mol Biol 1243: 103-125.
222. Ruiz-Romero C, Calamia V, Carreira V, Mateos J, Fernandez P, et al. (2010) Strategies to optimize two-dimensional gel electrophoresis analysis of the human joint proteome. Talanta 80: 1552-1560.
223. Cillero-Pastor B, Ruiz-Romero C, Carames B, Lopez-Armada MJ, Blanco FJ (2010) Proteomic analysis by two-dimensional electrophoresis to identify the normal human chondrocyte proteome stimulated by tumor necrosis factor a and interleukin-1beta. Arthritis & Rheum 62: 802-814.
224. Guo D, Tan W, Wang F, Lv Z, Hu J, et al. (2008) Proteomic analysis of human articular cartilage: identification of differentially expressed proteins in knee osteoarthritis. Joint Bone Spine 75: 439-444.
225. Parra-Torres NM, Cazares-Raga FE, Kour JB (2014) Proteomic analysis of rat cartilage: the identification of differentially expressed proteins in the early stages of osteoarthritis. Proteome Sci 12: 55-66.
226. Price PA, Thomas GR, Pardini AW, Figueira WF, Caputo JM, et al. (2002) Discovery of a high molecular weight complex of calcium, phosphate, fetuin, and matrix γ-carboxyglutamic acid protein in the serum of etidronate-treated rats. J Biol Chem 277: 3926-3934.
227. Price P, Williamson M, Nguyen TMT, Than TN (2004) Serum levels of the fetuin-mineral complex correlate with artery calcification in the rat. J Biol Chem 279: 1594-1600.
228. Hamano T, Matsui I, Mikami S, Tomida K, Fujii N, et al. (2010) Fetuin-mineral complex reflects extraosseous calcification stress in CKD. J Am Soc Nephrol 21: 1998-2007.
229. Martel J, Young D, Young A, C-Y. W, Chen C-D, et al. (2011) Comprehensive proteomic analysis of mineral nanoparticles derived from human body fluids and analyzed by liquid chromatography–tandem mass spectrometry. Anal Biochem 418: 111-125.
230. Price PA, Nguyen TMT, Williamson MK (2003) Biochemical characterization of the serum fetuin-mineral complex. J Biol Chem 278: 22153-22160.
231. Rabilloud T (2009) Detergents and chaotropes for protein solubilization before two-dimensional electrophoresis Methods Mol Biol 528: 259-267.
232. Vranakis I, Bock P, Papadioti A, Tselentis Y, Gevaert K, et al. (2012) Quantitative proteome profiling of C. burnetii under tetracycline stress conditions. Plos one 7: 33599-33607.

233. Fernandez-Costa C, Calamia V, Fernandez-Puente P, Mateos J, Rocha B, et al. (2013) Haptoglobin chains as potential biomarkers in serum of osteoarthritis disease. Arthritis Rheum 65: October 2013 Abstract Supplement.
234. Henrotin Y, Gharbi M, Deberg M, Pauw E (2011) Biomarker for osteoarthritis and/or other ageing-related diseases, and use thereof EP2131199 A1.
235. Olszewska-Slonina D, Matewski D, Jung S, Olszewski KJ, Czajkowski R, et al. (2013) The activity of cathepsin D and alpha-1 antitrypsin in hip and knee osteoarthritis. Acta ABP Biochima Polonica 60: 99-106.
236. Trimpin S, Brizzard B (2009) Analysis of insoluble proteins. Biotechniques 46: 409-419
237. Jaovisidha K, Etim A, Yamakawa K, Masuda I, Gohr CM, et al. (2006) The serine protease inhibitor trappin-2 is present in cartilage and synovial fluid in osteoarthritis. J Rheumatol 33 318-325.
238. Benarafa C, Priebe GP, Remold-O'Donnell E (2007) The neutrophil serine protease inhibitor serpinb1 preserves lung defense functions in Pseudomonas aeruginosa infection. J Exp Med 204: 1901-1909.
239. Sugaya N, Kanno T, Nlrasawa M, Mltamura K, Takeuchl Y, et al. (1990) Increased activities of cytosol aminopeptidase and lactate dehydrogenase in serum originate from lymphocytes in necrotizing lymphadenitis. Clin Chem Lab Med 36: 304-306.
240. Fischer R, Trudgian DC, Wright C, Thomas G, Bradbury LA, et al. (2012) Discovery of candidate serum proteomic and metabolomic biomarkers in ankylosing spondylitis. Mol Cell Proteomics 11: 1-11.
241. Zhuo Q, Yang W, Chen J, Wang Y (2012) Metabolic syndrome meets osteoarthritis. Nat Rev Rheumatol 8: 729-737.
242. New SEP, Aikawa E (2013) The role of extracellular vesicles in De Novo mineralization: An aditional novel mechanism of cardiovascular calcification. Arterioscler Thromb Vasc Biol 33: 1753-1758.
243. Malda J, Boere J, van de Lest CHA, van Weeren PR, Wauben MHM (2016) Extracellular vesicles - new tool for joint repair and regeneration. Nat Rev Rheumatol 12: 243-249.
244. Taylor DD, Shah S (2015) Methods of isolating extracellular vesicles impact down-stream analyses of their cargoes. Methods 87: 3-10.
245. Estrella JL, Kan-Sutton C, Gong X, Rajagopalan M, Lewis DE, et al. (2011) A novel in vitro human macrophage model to study the persistence of Mycobacterium tuberculosis using vitamin D3 and retinoic acid activated THP-1 macrophages. Front Microbiol 2: 1-16.
246. Ismail N, Wang Y, Dakhlallah D, Moldovan L, Agarwal K, et al. (2013) Macrophage microvesicles induce macrophage differentiation and miR-223 transfer. Blood 121 984-995.
247. Kato T, Miyaki S, Ishitobi H, Nakamura Y, Nakasa T, et al. (2014) Exosomes from IL-1β stimulated synovial fibroblasts induce osteoarthritic changes in articular chondrocytes. Arthritis Res Ther 16: 163-174.

Appendices - Manuscripts

RESEARCH ARTICLE

Insights into the association of Gla-rich protein and osteoarthritis, novel splice variants and γ-carboxylation status

Marta S. Rafael[1], Sofia Cavaco[1], Carla S. B. Viegas[1,2], Sofia Santos[1], Acácio Ramos[3], Brecht A. G. Willems[4], Marjolein Herfs[4], Elke Theuwissen[4], Cees Vermeer[4] and Dina C. Simes[1,2]

[1] Centre of Marine Sciences (CCMAR), University of Algarve, Faro, Portugal
[2] GenoGla Diagnostics, University of Algarve, Faro, Portugal
[3] European Board of Orthopedics and Traumatology, Algarve Medical Centre, Faro, Portugal
[4] VitaK, Maastricht University, The Netherlands

Received: December 16, 2013
Revised: February 20, 2014
Accepted: April 2, 2014

Scope: Gla-rich protein (GRP) is a vitamin K dependent protein, characterized by a high density of γ-carboxylated Glu residues, shown to accumulate in mouse and sturgeon cartilage and at sites of skin and vascular calcification in humans. Therefore, we investigated the involvement of GRP in pathological calcification in osteoarthritis (OA).

Methods and results: Comparative analysis of GRP patterning at transcriptional and translational levels was performed between controls and OA patients. Using a RT-PCR strategy we unveiled two novel splice variants in human—GRP-F5 and F6—potentially characterized by the loss of full γ-carboxylation and secretion functional motifs. GRP-F1 is shown to be the predominant splice variant expressed in mouse and human adult tissues, particularly in OA cartilage, while an overexpressing human cell model points it as the major γ-carboxylated isoform. Using validated conformational antibodies detecting carboxylated or undercarboxylated GRP (c/uc GRP), we have demonstrated cGRP accumulation in controls, whereas ucGRP was the predominant form in OA-affected tissues, colocalizing at sites of ectopic calcification.

Conclusion: Overall, our results indicate the predominance of GRP-F1, and a clear association of ucGRP with OA cartilage and synovial membrane. Levels of vitamin K should be further assessed in these patients to determine its potential therapeutic use as a supplement in OA treatment.

Keywords:
Alternative splicing / γ-Carboxylation / Gla-rich protein / Osteoarthritis / Vitamin K

Additional supporting information may be found in the online version of this article at the publisher's web-site

1 Introduction

Gla-rich protein, or GRP, is the newest vitamin K-dependent protein (VKDP), first identified in sturgeon calcified cartilage; the mature protein exhibits an extensive γ-carboxyglutamic acid (Gla) domain—16 Gla residues in this species—suggesting a strong calcium-binding capacity [1]. The association of GRP to pathological calcification in human skin and vascular tissues was shown by detection of protein accumulation at sites of mineral deposition in cases of dermatomyositis, pseudoxanthoma elasticum, and chronic kidney disease, further supporting the notion that GRP strongly binds to calcium mineral deposits [2].

Osteoarthritis (OA) is a common degenerative joint disease characterized by progressive loss of articular cartilage, accompanied by tissue inflammation, causing pain and disability [3]. Current treatments of OA pathology have limited efficacy and various side effects, urging the need to identify novel therapeutic and prophylactic agents for treatment

Correspondence: Dr. Dina C. Simes, CCMAR, University of Algarve, Campus de Gambelas, 8005-139 Faro, Portugal
E-mail: dsimes@ualg.pt
Fax: +351-289800069

Abbreviations: **c/uc**, carboxylated/undercarboxylated; **COMP**, cartilage oligomeric matrix protein; **ECM**, extracellular matrix; **GRP**, Gla-rich protein; **MGP**, matrix Gla protein; **OA**, osteoarthritis; **OC**, osteocalcin; **VKDP**, vitamin K-dependent protein

and prevention. Vitamin K represents an interesting candidate due to its determinant role in skeletal metabolism, either through bone and cartilage VKDPs, osteocalcin (OC), and matrix Gla-protein (MGP) or, more recently, GRP [4–6]. In fact, several studies have now evidenced that subclinical vitamin K levels are associated with an increased risk of developing knee OA [7–9]. At cellular level, OA results from the failure of chondrocytes to maintain the appropriate balance between synthesis and degradation of extracellular matrix (ECM) components, followed by the occurrence of ectopic calcification [3]. In later stages, this results in the formation of bony outgrowths at the joint margin (osteophytes), altered subchondral bone architecture and synovial membrane inflammation [3, 10]. Osteoarthritis has been reported to be directly associated with basic calcium phosphate crystals deposition either in the articular cartilage, synovial fluid, or synovial membrane [11–15]. The regulation of calcium availability and subsequent deposition in the ECM is also reported to be determinant for disease progression, which prompted us to investigate the relation between calcium mineral deposition and GRP expression and accumulation. Furthermore, GRP, also named Ucma (upper zone of growth plate and cartilage matrix associated protein), was reported as a specific cartilage-associated protein and suggested to be a negative regulator of osteogenic differentiation in mice [16]. Four alternatively spliced transcripts of the Ucma/GRP gene were reported in mouse chondrocytes and shown to be associated with the early stages of chondrogenesis [17]. Recently, an Ucma/GRP-deficient mouse model was produced and no association with calcification mechanisms was found during skeletal development, although it should be noted that ageing or pathological conditions were not yet described in this model [18].

Here, we report for the first time the identification of two novel alternatively splice variants of human GRP and a new alternative transcript in mouse. Using an overexpressing human cell model, we were able to demonstrate that although all human isoforms could be secreted, GRP-F1 (corresponding to the full length protein) is the predominant γ-carboxylated protein isoform. We also demonstrate the prevalence of the GRP-F1 splice variant, both in mouse and human adult tissues, in particular in OA cartilage where results point to a higher expression. Comparative analysis of γ-carboxylation status reveals the prevalence of cGRP in healthy control samples, both in cartilage and synovial membrane; this is in contrast to OA-affected tissues that produce significantly more ucGRP, suggesting that GRP may become an additional vitamin K target to beneficially affect OA pathology.

2 Materials and methods

2.1 Biological material and sample processing

Knee articular cartilage and synovial membrane samples were obtained from osteoarthritic patients who had undergone total knee replacement surgery; control samples (cartilage, synovial membrane, and all adult human tissues analyzed) were obtained either from subjects with no history of joint disease following autopsy at Algarve Medical Centre or by arthroscopy (cartilage and synovial membrane samples). Fetal samples were collected from 37 to 40 gestational weeks' stillbirths at HPP Cascais Hospital. Samples were immediately collected into RNAlater (Sigma-Aldrich, St. Louis, MO, USA) or sterile 4% w/v PFA solution for RNA extraction or histological analysis, respectively. For histological preparation, samples were embedded either in paraffin or glycol methacrylate as described [19, 20]. Mineral deposits were detected using the von Kossa method counterstained with hematoxylin. This study was approved by the ethical committees of Algarve Medical Centre and HPP Cascais Hospital. Mouse tissue samples were collected from 9 weeks old male black 6 mice, washed in PBS followed by immediate RNA extraction.

2.2 RNA extraction

Total RNA was extracted from human and mouse tissues as described by Chomczynski and Sacchi [21], RNA concentration determined by spectrophotometry at 260 nm and quality evaluated by agarose-denaturating gel electrophoresis.

2.3 Human and mouse GRP cDNA amplification

One microgram of total RNA was treated with DNase I (Promega, Madison, WI, USA), and reverse-transcribed using Moloney-murine leukemia virus reverse transcriptase, RNase Out (both from Invitrogen, Carlsbad, CA, USA), and an oligo(dT) adapter (5′-ACGCGTCGACCTCGAGATCGATG $(T)_{13-}$3′), according to manufacturer's recommendations. Human and mouse GRP-coding sequences were amplified by nested PCR starting with 250 ng of reverse-transcribed RNA and *Taq* DNA polymerase (Invitrogen) using primers listed in Supporting Information Table 1. All nested PCR products were size-separated onto a 2% w/v agarose gel and selected fragments were purified using the GFX Gel Band Purification kit (GE Healthcare, Waukesha, WI, USA), cloned into pCRII-TOPO vector (Invitrogen) and sequenced (CCMAR, Faro, Portugal).

2.4 Expression profile

To determine the presence of GRP alternative transcripts in a broad number of tissues both from human and mouse, primers were designed in order to specifically amplify each of the splice variants, while human ribosomal 18S and mouse GAPDH were used as loading controls (Supporting Information Table I). RT-PCR amplification was achieved using 25 ng cDNA and SsoFast Eva Green supermix (Bio-Rad, Richmond, CA, USA) in reactions of 50 cycles.

2.5 Sequence analysis

Human and mouse genomic sequences (GenBank accession numbers NC_000010 and NC_000068), respectively, were used to confirm transcripts structure using Spidey mRNA-to-genomic alignment tool at NCBI. Prediction of signal peptide, protein targeting, and phosphorylation sites was performed using SignalP, TargetP, and NetPhos 2.0, respectively, available at http://www.cbs.dtu.dk/services.

2.6 Protein expression in HEK293T cells

The complete coding sequence of human GRP alternative transcripts was cloned into the pmkate2-N vector (Evrogen, Moscow, Russia), producing a fusion protein where the GRP C-terminus is fused to the mkate2 N-terminus (primers used for directional cloning are listed in Supporting Information Table 1); mkate is a far-red fluorescent protein usually used to tag and solubilize proteins of interest [22]. Transfections of HEK293T cells, cultured in DMEM (Invitrogen) supplemented with 10% v/v fetal bovine serum (Sigma-Aldrich) were performed using the calcium/phosphate method, and conditioned media were collected after 48 or 72 h. Total cell extracts were obtained using RIPA buffer and protein content was determined using a micro BCA kit (Thermo Scientific, Waltham, MA, USA).

2.7 Protein size-separation and Western blot

Aliquots of total protein extracts were size-separated on a 4–12% w/v gradient polyacrylamide precast gel containing 0.1% w/v SDS (NuPage, Invitrogen) and transferred onto a nitrocellulose membrane as previously described [23]. Detection of γ-carboxylated proteins was performed using 5 μg/mL of M3B antibody (American Diagnostica Inc., Stamford, CT, USA); mkate2/GRP fusion proteins were detected using 0.2 μg/mL tRFP (Evrogen) and GRP using 5 μg/mL of CTerm-GRP (GenoGla Diagnostics, Faro, Portugal) produced against the C-terminus of rat GRP peptide following a previously described procedure [2]. Immunodetection was achieved using species-specific secondary horseradish peroxidase conjugated antibodies (Sigma-Aldrich) and Western Lightning Plus-ECL (PerkinElmer Inc., Waltham, MA, USA).

2.8 Immunolocalization

Immunohistochemistry was performed in paraffin or glycol methacrylate tissue sections to detect antigens in soft and calcified tissues, respectively [24]. Antigen retrieval of cartilage and synovial membrane tissue sections was performed by incubation with 2 mg/mL hyaluronidase (Sigma-Aldrich) and by boiling in 0.2% v/v citric acid pH 6.0, respectively. After peroxidase and nonspecific antibody blockings, incubations with the primary antibodies polyclonal rabbit CTerm-GRP [2], and chicken cGRP (5 and 1 μg/mL, respectively (GenoGla Diagnostics); mouse monoclonals ucGRP (7.3 μg/mL, Vitak BV, Maastricht, the Netherlands), cMGP and ucMGP (both at 10 μg/mL, IDS, Boldon, UK) and cartilage oligomeric matrix protein (COMP; 4 μg/mL, Santa Cruz) were performed O/N at RT. Conformational-specific carboxylated/undercarboxylated (c/uc) GRP antibodies were produced against the following peptides: QRNEFENFVEEQND (E residues are γ-carboxylated) and NEFENFVEEQNDEQEERSREAVEQ, respectively (Viegas et al., in press). Peroxidase activity was detected using the respective peroxidase-conjugated secondary antibodies (Sigma-Aldrich) and ImmPACT NovaRED substrate kit (Vector laboratories Ltd, Peterborough, UK). Negative controls consisted of the substitution of the primary antibody with TBST. Final counterstaining was achieved using hematoxylin.

3 Results

3.1 Identification of novel GRP splice variants in human and mouse

The presence of GRP splice variants was investigated through a nested RT-PCR strategy using human osteoarthritic cartilage and bone and cartilage from wild type murine femurs; primers designed in exons 1 and 5 were used to amplify the complete or partial GRP complete coding sequence, respectively (Supporting Information Fig. 1 and Supporting Information Table 1). For both human and mouse GRP we have identified different fragments (Fig. 1A), corresponding to novel splice variants. The longest human cDNA fragment is 504-bp long and contains the complete open reading frame for full-length GRP (GRP-F1, GenBank accession number JX169863), while after sequencing two cDNA fragments of 408- and 342–bp (Fig. 1A) were confirmed to be coding for two hitherto undiscovered GRP protein isoforms. The new splice variants were named GRP-F5 and F6 (GenBank accession numbers JX169864 and JX169865, respectively; Fig. 1B) following previous nomenclature adopted for mouse and zebrafish [6,17,25]. We have then performed an extensive search of GRP splice variants in other cartilage and synovial membrane samples, both from control and OA patients, and no other GRP alternative transcript was further identified. In addition, the same set of splice variants was also amplified from several other human tissues (heart and skin, among others, results not shown) further suggesting that these novel GRP splice variants might be species-specific.

Regarding mouse GRP splice variants, we were able to detect the GRP-F1, F2, F3 and F4 transcripts previously described [17], and a new one of 178-bp corresponding to GRP-F7 (Fig. 1A and B, Supporting Information Fig. 1B). Although we have sequenced approximately 40 clones from different tissues, no GRP-F5 and F6 have been identified in mice, reinforcing the notion of a possible species-specificity.

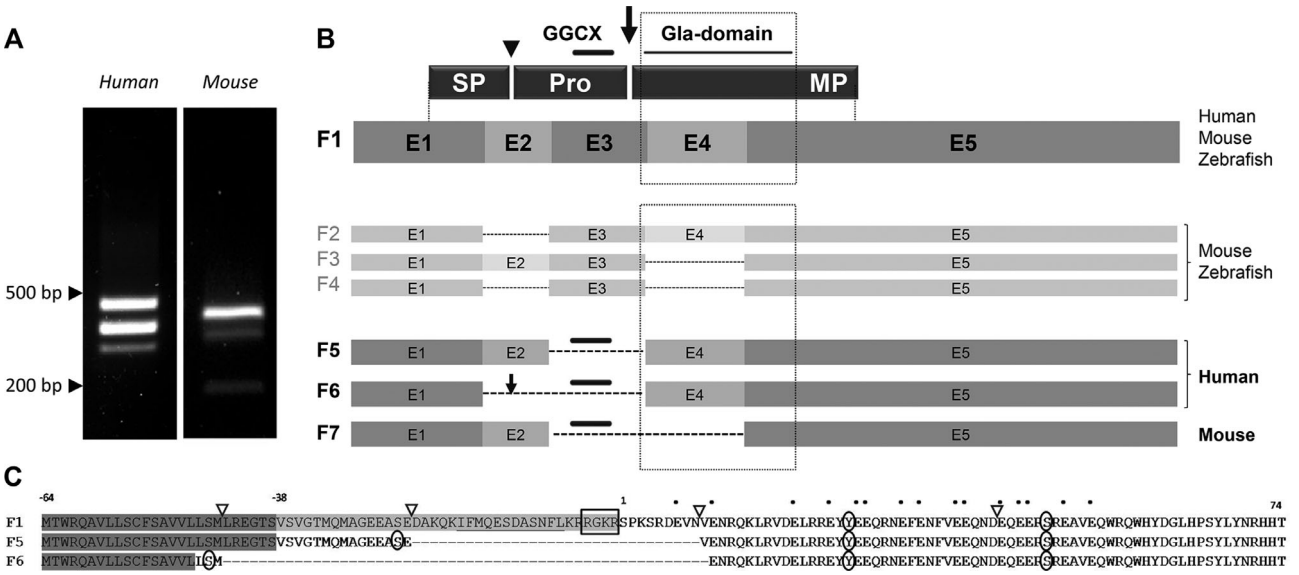

Figure 1. Identification of novel GRP alternative splice variants in human and mouse. (A) RT-PCR from RNA isolated from OA human articular cartilage and bone and cartilage (femur) of wild-type black-6 mice. For both mouse and human, several PCR products were amplified, cloned, and sequenced, respectively, and further identified as different GRP splice variants. Transcript sizes (bp) are indicated on the right side of the panel. (B) Schematic representation of GRP-splice variants, including an overview of our results (human F5 and F6 and mouse F7) and previously published data for mouse and zebrafish [6, 17, 25]. Arrow head indicates putative signal peptide cleavage site; arrow is furin-like cleavage site; SP indicates signal peptide; Pro, propeptide; MP, mature protein, and GGCX, γ-glutamyl carboxylase putative recognition site. (C) Alignment of human GRP-splice variants deduced proteins. Triangles indicate intron insertion sites; underlined sequence indicates γ-glutamyl carboxylase (GGCX) putative recognition site; a rectangle shows the furin-like proteolytic site (RGKR); black dots sign putative γ-carboxylated Glu residues; circles indicate predicted tyrosine and serine phosphorylated residues; signal peptide is shown in dark gray, while propeptide in light gray. First residue of mature protein in F1 isoform is assigned as number 1 and signal peptide, propeptide, and mature protein are indicated accordingly.

3.2 In silico characterization of human GRP protein isoforms

For each detected transcript (Fig. 1A), splicing sites and coding regions were predicted using the Spidey mRNA to genomic alignment tool at NCBI (Fig. 1B and Supporting Information 1A). Considering nonprocessed protein isoforms, full length GRP-F1 encodes 138-aa, whereas the two novel transcripts encode putative proteins of 106 (GRP-F5) and 84 amino acids (GRP-F6), respectively (Fig. 1B and C, and Supporting Information Fig. 1A). Both GRP-F5 and F6 variants lack exon 3, an exon skipping that has never been described in previously analyzed species (mouse and zebrafish, [6, 17, 25], Fig. 1B), resulting in the loss of the γ-glutamyl carboxylase recognition site (GGCX) and the furin-like cleavage site for propeptide processing (RGKR, Fig. 1B and C). Conversely, F6 lacks both exons 2 and 3 which, in addition to the modifications produced in GRP-F5, will also be translated with a shorter signal peptide (Fig. 1B–C, and Supporting Information 1A). Although the probability of this shorter signal peptide functionality is lower than for GRP-F1/F5 (calculated D-score for F1/F5 is 0.731 and for F6 0.634, both above SignalP algorithm cutoff [26]), the prediction shows that targeting to the secretory pathway is still a possible event. Overall, and considering signal peptide processing for both variants, GRP-F5 and F6 will be 80- and 67-aa long, that is, comparable to the 74-aa F1 mature isoform in terms of protein size (Fig. 1C). Although no *N*- or *O*-glycosylation post-translational modifications were in silico predicted, two (GRP-F1) and three (GRP-F5 and F6) serine and tyrosine residues exhibit high probability of phosphorylation (Fig. 1C).

3.3 Production and characterization of GRP isoforms in HEK293T cells

To determine mature protein processing and evaluate γ-carboxylation of Glu residues, we have performed transient transfections of HEK293T cells with GRP-mkate2 fusion proteins of theoretical molecular weights of approximately 43, 39 and 37 kDa for GRP-F1, F5, and F6, respectively. Our results indicate that 48h after transfection, the three fusion proteins are translated and can be detected in total cell extracts, but only the GRP-F1 and F5 isoforms are secreted, while GRP-F6 remains intracellularly (Fig. 2A); identification of secreted GRP-F1 isoform was further confirmed by LC-MS/MS (data not shown). Nevertheless, 72 h after transfection, GRP-F6 is also found in conditioned media (Fig. 2A), confirming

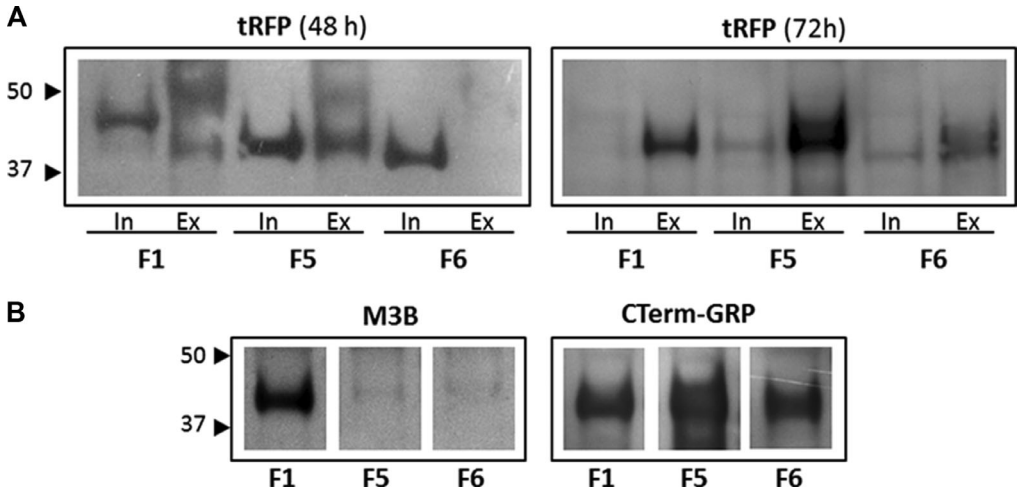

Figure 2. Analysis of secretion and γ-carboxylation potential of human GRP protein isoforms. GRP-mkate2 fusion proteins were expressed in HEK293T cells and intracellular extracts (In) and/or conditioned media (Ex) were analyzed by SDS-PAGE followed by Western blot. (A) mkate2 detection was achieved with specific antibody (tRFP) at 48 or 72 h after transient transfection. (B) Immunodetection of γ-carboxylated and GRP protein in conditioned media, 72 h after transfection, using M3B and CTerm-GRP antibodies, respectively. Relevant molecular weights in kDa are indicated on the left side of panels.

theoretical predictions indicating a lower secretory potential due to an incomplete signal peptide and a time-dependent secretion of GRP isoforms. γ-carboxylation status of secreted GRP isoforms was then investigated using a Gla-specific antibody (monoclonal M3B antibody) and the CTerm-GRP, which reacts with both carboxylated or undercarboxylated GRP forms with results evidencing GRP-F1 as the major γ-carboxylated isoform produced in this human cell system (Fig. 2B).

3.4 Expression pattern of human and mouse GRP transcripts

Primers were strategically designed to specifically amplify individual transcripts (Supporting Information Table 1 and Supporting Information Fig. 2) and confirmed to amplify only the target sequence for each of the splice variants except for murine GRP-F3. In this case, several sets of primers were tested but all exhibited unspecific amplification.

For human samples, our results show GRP-F1 transcript as predominant and almost ubiquitously expressed (Fig. 3A), both in fetal and adult tissues. On the other hand, GRP-F5 and F6 are barely or not detectable in most adult tissues, although in the fetal tissues analyzed their expression is clearly detected in cartilage, heart, and skin (Fig. 3A).

For murine samples, both GRP-F1 and F7 were found mainly expressed in calcified tissues formed by bone and/or cartilage (ear, femur, foot, tail, tibia) and also in heart, testis and thymus (Fig. 3B), while F2 and F4 splice variants were not detected in any of the tissues analyzed. The GRP-F3 expression pattern was not determined since we were not able to develop a specific set of primers (Supporting Information Fig. 2B).

3.5 Gene expression analysis of GRP transcripts in human control and osteoarthritic tissues

Due to the number of samples available (Supporting Information Table 2) we have only analyzed GRP gene expression levels under saturating PCR conditions (50 cycles) in the two major OA affected tissues. The results indicate higher expression of GRP-F1 in cartilage of OA patients (Fig. 4A) when compared to controls, while no association could be determined in synovial membrane samples (Fig. 4B). GRP-F5 was clearly less represented (Fig. 4) than F1 in both tissues, while GRP-F6 could not be detected in any of the cartilage samples analyzed, in control or OA, but it was found in certain synovial membrane samples (Fig. 4), suggesting a restricted pattern of expression.

3.6 Differential accumulation pattern of c/ucGRP in control and osteoarthritic tissues

While no calcification was observed in control samples (Fig. 5A and C), ectopic calcifications were detected in the tangential layer of osteoarthritic cartilage (Fig. 5B and D). The presence of GRP was then investigated by IHC and both cGRP and ucGRP co-localized at sites of cartilage calcification (Fig. 5I and N); these observations were confirmed with CTerm-GRP antibody (Fig. 5O–S). The two protein forms were found accumulated in control and osteoarthritic

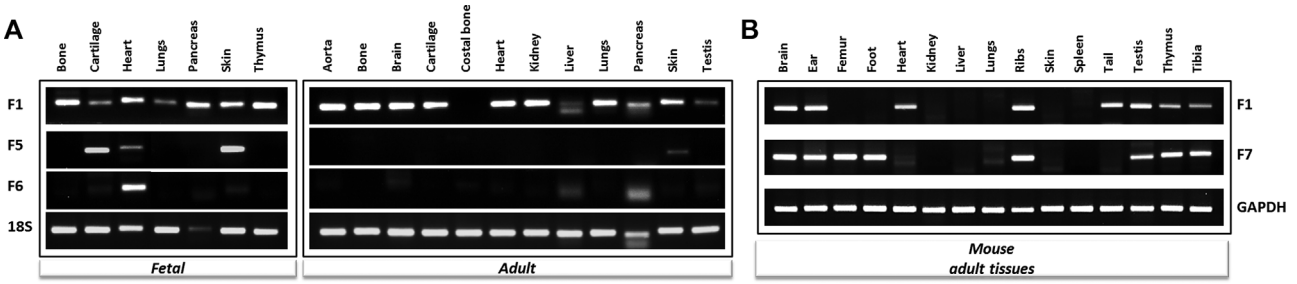

Figure 3. GRP-F1 is the predominant splice variant in human tissues. The qualitative expression profile of known GRP alternative transcripts was investigated by RT-PCR in fetal and adult human (A) and adult mouse (B) tissues. 18S and mouse GAPDH were used as loading controls for sample integrity.

chondrocytes (Fig. 5E–H and J–M), although ucGRP was more evident than cGRP in osteoarthritic cartilage matrix (Fig. 5J–M; and 5E, H, respectively). In contrast to GRP, control chondrocytes exhibited cMGP accumulation while pathological counterparts exhibited ucMGP only (Supporting Information Fig. 3A–D and F–I), both MGP protein forms were co-localized with sites of ectopic calcifications (Supporting Information Fig. 3E and J). Moreover, ucMGP accumulation was shown to be more predominant in the ECM of osteoarthritic cartilage than in that of controls (Supporting Information Fig. 3F, G, H, and I). Immunohistochemical analysis of COMP, a well-established marker of OA [27], showed protein accumulation only in pathological chondrocytes ECM and ectopic calcification sites (Supporting Information Fig. 3K–O). Altogether, our results show that the tangential layer of cartilage is the most affected tissue area, where not only COMP, but also ucGRP and ucMGP accumulate to considerable higher levels than in the corresponding healthy tissue.

Synovial membranes showed substantial histological differences between controls and OA patients (Fig. 6A–C). OA samples exhibited a higher number and altered pattern of lining cells, accompanied by the presence of ectopic calcifications (Fig. 6B–C). Immunodetection of total GRP, using CTerm-GRP antibody, showed protein accumulation within synovial membrane lining cells both in control and OA samples (Fig. 6D and E). Using conformational antibodies, ucGRP accumulation was detected in the OA tissues lining layer, whereas only cGRP was detected in the lining layer of control tissues (Fig. 6D, E, G, H, J, and K). In addition, both cGRP and ucGRP were detected at sites of ectopic calcifications (Fig. 6F, I, and L), a result also confirmed with CTerm-GRP antibody (Fig. 6F). While no MGP was detected in control and OA synovial membrane lining cells (Supporting Information Fig. 4A–D), carboxylated and ucMGP were both found co-localized with ectopic calcifications (Supporting Information Fig. 3B and D).

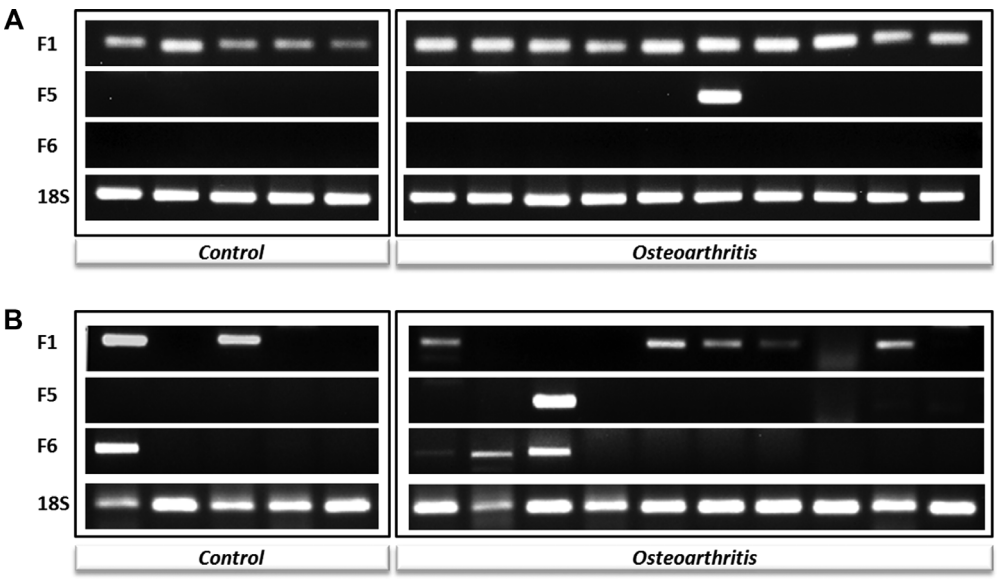

Figure 4. Osteoarthritic cartilage evidences higher GRP-F1 expression over controls. The presence of the three human GRP splice variants was investigated in cartilage (A) and synovial membranes (B) of controls and osteoarthritic patients; 18S was used as a loading control.

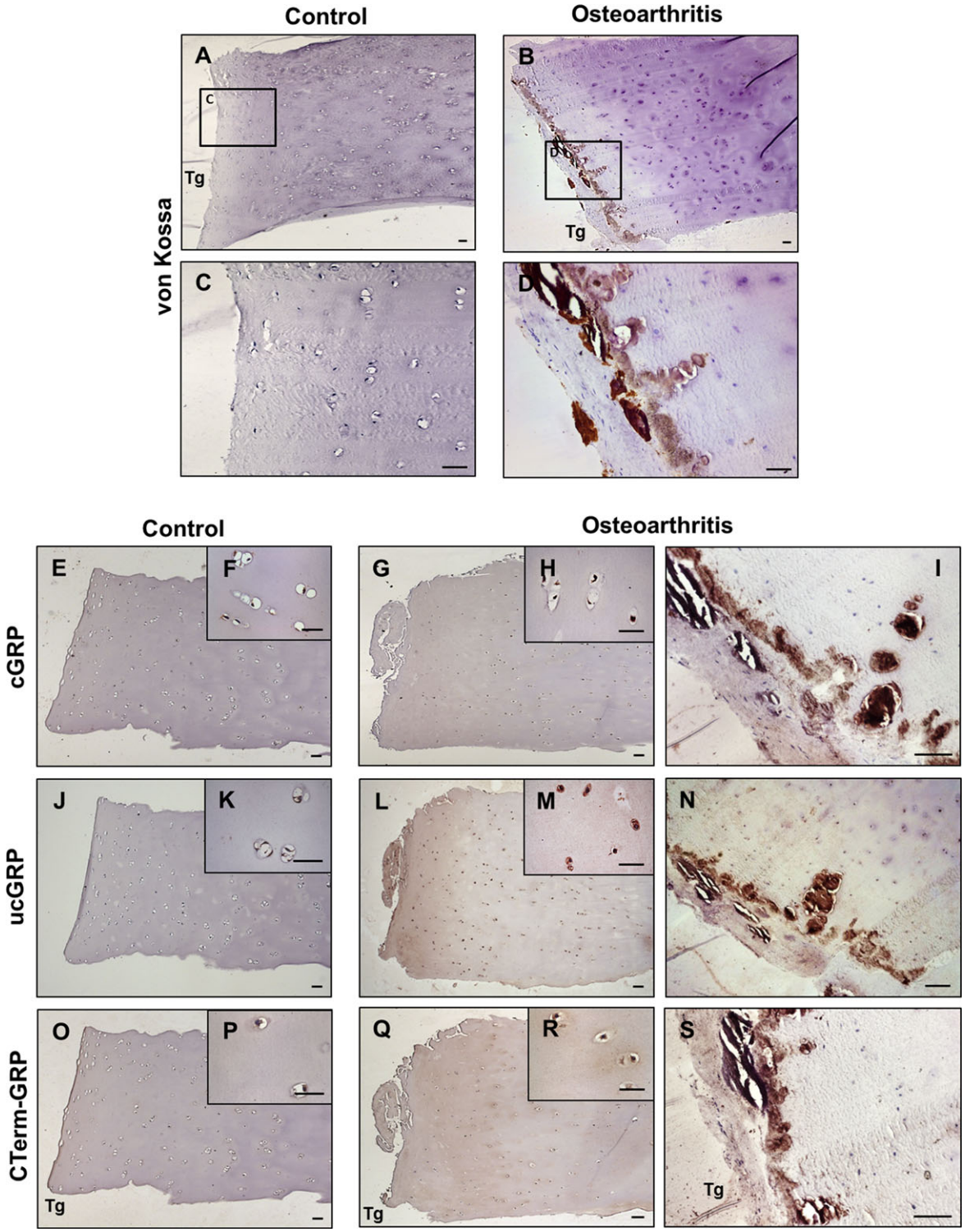

Figure 5. Undercarboxylated GRP (ucGRP) is predominant in osteoarthritic cartilage. The presence of ectopic calcifications was investigated by von Kossa staining in osteoarthritic (B and D) and control (A and C) cartilage samples. Specific antibodies for cGRP, and ucGRP (N–J) and CTerm-GRP (O–S) were used to immunodetect carboxylated (cGRP), undercarboxylated GRP (ucGRP) and total (t-GRP) protein forms. *Tg*, tangential layer. Scale bars represent 50 μm.

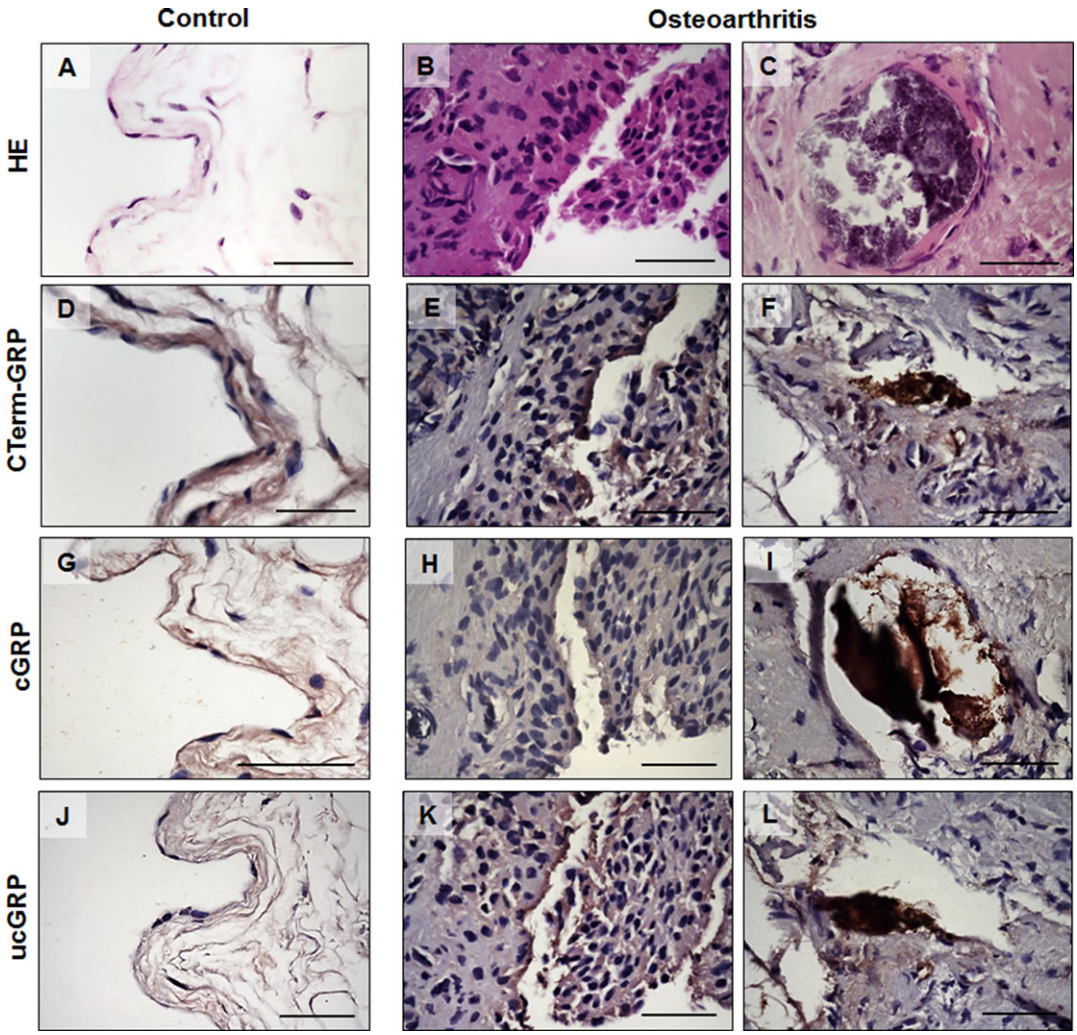

Figure 6. Undercarboxylated GRP is highly accumulated in osteoarthritic synovial membrane lining cells. Hematoxylin eosin (HE) staining shows severe histological changes between control (A) and osteoarthritic (B) synovial membrane lining cells and evidences ectopic calcifications within OA samples (C). Total GRP (D–F), carboxylated (G–I), and undercarboxylated (J–L) accumulation was detected using respective CTerm-GRP, cGRP, and ucGRP antibodies. Scale bars represent 50 μm.

4 Discussion

GRP is the newest member of VKD family of proteins and exhibits the highest density of Gla residues ever described, suggesting a strong affinity for calcium [1]. The protein, first named Ucma for 'unique cartilage matrix associated protein' [28], was identified as a VKDP protein [1] and demonstrated to have a wide tissue expression in rat [1] and zebrafish [25]. GRP/UCMA was also shown to be highly accumulated in mouse, rat, and Adriatic sturgeon cartilage [1, 28]. This work is a follow-up study on the previously reported association of GRP with calcinosis in skin and vascular diseases [2] by further investigating a possible relationship between GRP and OA due to the reported association of ectopic calcification and this pathology [15].

Gene expression studies performed in OA-associated tissues confirmed the consistent presence of the transcript coding for full-length GRP protein (GRP-F1), and unveiled two novel GRP alternative transcripts [6, 17, 25]. Furthermore, our extensive efforts to detect splice variants F2, F3 and F4 in human samples were unsuccessful, while GRP-F5 and F6 were only detected in humans; the possibility that other variants might exist cannot be completely ruled out, but our data strongly indicate the prevalence of these three GRP transcripts. Our gene expression data demonstrate that GRP-F1 is the most abundant transcript in almost all adult human tissues analyzed, while GRP-F5 and F6 were mostly restricted to fetal development emphasizing that the biological function of GRP splice variants in humans should be further evaluated throughout development. In addition to F3 and F4 transcripts, suggested to be involved in early chondrogenesis [17], a new alternative transcript was also identified in mice (GRP-F7), although we did not find murine homologs of human GRP-F5 and F6. The identification of a novel murine

transcript might be, as previously suggested [17], related to a time-dependent expression of GRP variants. It is still noteworthy that all described splice variants (human, mouse or zebrafish) preserve the GRP-coding frame and that a modular alteration of the protein product has been proposed to be an evidence of protein product functionality [29]. Also, phosphorylation of serine and tyrosine residues are in silico predicted for all human putative GRP isoforms and their occurrence should be further investigated. This is of particular interest, since three phosphorylated serine residues of human MGP were previously demonstrated to be determinant for its function as a inhibitor of calcification in vascular smooth muscle cells [30].

Recent functional studies on GRP showed contradictory results: while GRP-deficient mice did not exhibit a clear phenotype in bone and cartilage [18], zebrafish functional data suggested an essential role of GRP in skeletal development and calcification [6]. Our results reinforce the notion that the GRP-deficient mouse has shortcomings since the data obtained from this model cannot be directly translated to the human situation [18].

In this respect, and since variants F5 and F6 appear to be human-specific and are characterized by the loss of essential domains that may alter GRP function, we have further explored their secretory and γ-carboxylation potentials as well as for F1. All protein isoforms were translated and detected intracellularly; however, F6 secretion occurs later than F1 and F5 isoforms, indicating a lower efficiency during the secretory process as predicted by the 9-aa loss of the signal peptide C-terminus. Detection of Gla residues in the secreted GRP-protein isoforms, using the M3B Gla-specific antibody, showed clear specific immunoreactivity with the F1 isoform, suggesting that this is a γ-carboxylated protein. However, since in vitro cell systems are usually not able to fully γ-carboxylate overexpressed VKDPs, the presence of Gla residues in GRP-F5 and F6 cannot be completely ruled out. Further studies should be performed to determine the Gla content in the three GRP isoforms, since our functional in vitro cell model has been described to possess a limited γ-carboxylation potential [31], while comparative studies on mineral binding capacity of different GRP isoforms might also bring new insights into the relevance of protein three dimensional structure and carboxylation status for its functionality.

The selective expression of GRP-F1 transcript supports the use of our antibodies, either the total GRP CTerm-GRP or conformational c/ucGRP antibodies, and IHC results should reflect the accumulation of the GRP-F1 isoform-only. Although, the conformational anti-GRP antibodies monospecificity against native GRP species is still under investigation in our laboratory—as we cannot as yet discard the possibility of residual overlapping detection of c/ucGRP protein forms—these antibodies were found to have high specificity towards the respective synthetic GRP-related peptides used as antigens (Viegas et al., in press).

Our comparative data clearly shows the colocalization of undercarboxylated GRP at sites of ectopic calcification of both cartilage and synovial membrane in OA. Moreover, control subjects, showing no signs of mineral deposition in both tissues, exhibit only γ-carboxylated protein in their ECM and lining cells. Altogether, these results suggest that GRP γ-carboxylation should be crucial for calcium mineral formation inhibition. Furthermore, MGP immunodetection also supports the relevance of γ-carboxylation for pathology development, since OA mineralized cartilage showed significantly higher amounts of ucMGP. Previous studies, both in mice and human, have shown that MGP-deficient chondrocytes are hypertrophic, exhibiting an abnormal maturation, and organization that can lead to endochondral ossification [5, 32, 33]. Specific γ-carboxylase activity has been further found to be higher in cultured control chondrocytes when compared to the ones derived from osteoarthritic tissue [34]; the same study evidences that matrix vesicles isolated from OA human articular cartilage also contained significantly less cMGP when compared to those isolated from control tissue [34]. Undercarboxylated MGP was also proposed to be used as an inflammatory marker of arthritis through the combined analysis of serum and local synovial fluid ucMGP [35], further pointing to the relevance of carboxylation levels of VKDPs in OA. Overall these data reinforce the notion that lower levels of functional VKDPs might result from a decreased γ-carboxylase activity in OA, possibly accompanied by a loss of vitamin K function that might be intimately related with its subclinical levels [9]. In fact, all extra-hepatic Gla-proteins analyzed thus far were found to be undercarboxylated in non-vitamin K-supplemented healthy individuals [36].

The combined study of local and serum levels of carboxylated and undercarboxylated GRP with vitamin K1 and K2 serum levels in OA patients will definitely strengthen our present findings, since vitamin K is known to act either as a substrate for the vitamin K epoxide reductase, an essential cofactor for γ-carboxylation, or as a protective agent associated to the production of certain inflammatory cytokines affecting articular cartilage and subchondral bone through different molecular mechanisms [37]. Insufficient vitamin K levels have been proposed to cause impaired functions not only of MGP but also OC and associated to abnormalities observed in OA [4, 5]. GRP biosynthesis is also most possibly affected by vitamin K availability and consequently related to OA pathophysiological features, such as cartilage mineralization and synovial membrane inflammation. Accordingly, recent studies have demonstrated a clear association between knee OA and subclinical vitamin K insufficiency [7–9], but none of them has considered GRP as a target protein. Our results showing a relation between GRP and MGP γ-carboxylation deficiency and OA are also in agreement with recent findings, suggesting that vitamin K metabolism may be associated with synovitis in OA patients, and that serum undercarboxylated OC could be a biomarker for OA [38]. The novel association of both phylloquinone (vitamin K1) and menaquinone

(vitamin K2) deficiency with the disease further suggests the use of vitamin K as a potential therapeutic/prophylactic agent for OA [39]. We are currently collecting a representative number of OA patients and controls sera samples to determine and compare levels of (i) vitamin K1 and K2 and (ii) c/uc GRP protein forms, for which we are developing an ELISA detection kit (industrial application reported in the international patent request PCT/PT2009000046). We strongly believe that the integrated study of these parameters together with clinical and biochemical characterizations will unravel new insights into OA pathology progression and severity.

This work was funded by projects PTDC/SAU-ESA/101186/2008, PTDC/SAU-ORG/112832/2009 and PTDC/SAU-ORG/117266/2010 from the Portuguese Science and Technology Foundation (FCT) and partially supported by CCMAR funding and grant PEst-C/MAR/LA0015/2011. M.S. Rafael, S. Cavaco, and C.S.B. Viegas were the recipients of the FCT fellowships SFRH/BPD/89188/2012, SFRH/BD/60867/2009 and SFRH/BPD/70277/2010, respectively. We would like to thank Nuno R. dos Santos and Mónica T. Fernandes (CBME/University of Algarve, Faro) for providing mice samples and Philip Hublitz (EMBL, Monterotondo, Italy) for plasmids. We also thank the following Portuguese institutions and hospitals for providing human tissue samples used in this study, namely the South Delegation of National Institute of Legal Medicine and Forensic Sciences, Public Institute; HPP, Hospital of Santa Maria, Faro; HPP, Hospital of Cascais.

The authors have declared no conflict of interest.

5 References

[1] Viegas, C. S. B., Simes, D. C., Laizé, V., Williamson, M. K. et al., Gla-rich protein (GRP), a new vitamin K-dependent protein identified from sturgeon cartilage and highly conserved in vertebrates. *J. Biol. Chem.* 2008, *283*, 36655–36664.

[2] Viegas, C. S. B., Cavaco, S., Neves, P. L., Ferreira, A. et al., Gla-rich protein is a novel vitamin K-dependent protein present in serum that accumulates at sites of pathological calcifications. *Am. J. Pathol.* 2009, *175*, 2288–2298.

[3] Abramson, S. B., Attur, M., Developments in the scientific understanding of osteoarthritis. *Arthritis Res. Ther.* 2009, *11*, 227–235.

[4] Price, P. A., Williamson, M. K., Haba, T., Dell, R. B. et al., Excessive mineralization with growth plate closure in rats on chronic warfarin treatment. *Proc. Natl. Acad. Sci. USA* 1982, *79*, 7734–7748.

[5] Luo, G., Ducy, P., McKee, M. D., Pinero, G. J. et al., Spontaneous calcification of arteries and cartilage in mice lacking matrix GLA protein. *Nature* 1997, *386*, 78–81.

[6] Neacsu, C. D., Grosch, M., Tejada, M., Winterpacht, A., et al., Ucmaa (Grp-2) is required for zebrafish skeletal development. Evidence for a functional role of its glutamate γ-carboxylation. *Matrix Biol.* 2011, *30*, 369–378.

[7] Neogi, T., Booth, S. L., Zhang, Y. Q., Jacques, P. F. et al., Low vitamin K status is associated with osteoarthritis in the hand and knee. *Arthritis Rheum.* 2006, *54*, 1255–1261.

[8] Oka, H., Akune, T., Muraki, S., En-yo, Y. et al., Association of low dietary vitamin K intake with radiographic knee osteoarthritis in the Japanese elderly population: dietary survey in a population-based cohort of the ROAD study. *J. Orthop. Sci.* 2009, *14*, 687–692.

[9] Misra, D., Booth, S. L., Tolstykh, I., Felson, D. T. et al., Vitamin K deficiency is associated with incident knee osteoarthritis. *Am. J. Med.* 2013, *126*, 243–248.

[10] Sellam, J., Berenbaum, F., The role of synovitis in pathophysiology and clinical symptoms of osteoarthritis. *Nat. Rev. Rheumatol.* 2010, *6*, 625–635.

[11] Liu, Y. Z., Jackson, A. P., Cosgrove, S. D., Contribution of calcium-containing crystals to cartilage degradation and synovial inflammation in osteoarthritis. *Osteoarthr. Cartil.* 2009, *17*, 1333–1340.

[12] Fuerst, M., Bertrand, J., Lammers, L., Dreier, R. et al., Calcification of articular cartilage in human osteoarthritis. *Arthritis Rheum.* 2009, *60*, 2694–2703.

[13] O'Connell, J. X., Pathology of the synovium. *Am. J. Clin. Pathol.* 2000, *114*, 773–784.

[14] Hernandez-Santana, A., Yavorskyy, A., Loughran, S. T., McCarthy, G. M. et al., New approaches in the detection of calcium-containing microcrystals in synovial fluid. *Bioanalysis* 2011, *3*, 1085–1091.

[15] Ea, H.-K., Nguyen, C., Bazin, D., Bianchi, A. et al., Articular cartilage calcification in osteoarthritis: insights into crystal-induced stress. *Arthritis Rheum.* 2011, *63*, 10–18.

[16] Surmann-Schmitt, C., Dietz, U., Kireva, T., Adam, N. et al., Ucma, a novel secreted cartilage-specific protein with implications in osteogenesis. *J. Biol. Chem.* 2008, *283*, 7082–7093.

[17] Le Jeune, M., Tomavo, N., Tian, T. V., Flourens, A. et al., Identification of four alternatively spliced transcripts of the Ucma/GRP gene, encoding a new Gla-containing protein. *Exp. Cell Res.* 2010, *316*, 203–215.

[18] Eitzinger, N., Surmann-Schmitt, C., Bösl, M., Ucma is not necessary for normal development of the mouse skeleton. *Bone* 2012, *50*, 670–680.

[19] Witten, P. E., Villwock, W., Growth requires bone resorption at particular skeletal elements in a teleost fish with acellular bone (*Oreochromis niloticus*, Teleostei: Cichlidae). *J. Appl. Ichthyol.* 1997, *13*, 149–158.

[20] Ortiz-Delgado, J. B., Simes, D. C., Viegas, C. S. B., Schaff, B. J. et al., Cloning of matrix Gla protein in a marine cartilaginous fish, *Prionace glauca*: preferential protein accumulation in skeletal and vascular systems. *Histochem. Cell Biol.* 2006, *126*, 89–101.

[21] Chomczynski, P., Sacchi, N., Single-step method of RNA isolation by acid guanidinium thiocyanate-phenol-chloroform extraction. *Anal. Biochem.* 1987, *162*, 156–159.

[22] Shcherbo, D., Merzlyak, E. M., Chepurnykh, T. V, Fradkov, A. F. et al., Bright far-red fluorescent protein for whole-body imaging. *Nat. Methods* 2007, *4*, 741–746.

[23] Simes, D. C., Williamson, M. K., Ortiz-Delgado, J. B., Viegas, C. S. B. et al., Purification of matrix Gla protein from a marine

teleost fish, Argyrosomus regius: calcified cartilage and not bone as the primary site of MGP accumulation in fish. *J. Bone Miner. Res.* 2003, *18*, 244–259.

[24] Schurgers, L. J., Teunissen, K. J. F., Knapen, M. H. J., Kwaijtaal, M. et al., Novel conformation-specific antibodies against matrix gamma-carboxyglutamic acid (Gla) protein: undercarboxylated matrix Gla protein as marker for vascular calcification. *Arterioscler. Thromb. Vasc. Biol.* 2005, *25*, 1629–1633.

[25] Fazenda, C., Silva, I. A. L., Cancela, M. L., Conceição, N., Molecular characterization of two paralog genes encoding Gla-rich protein (Grp) in zebrafish. *J. Appl. Ichthyol.* 2012, *28*, 377–381.

[26] Petersen, T. N., Brunak, S., von Heijne, G., Nielsen, H., SignalP 4.0: discriminating signal peptides from transmembrane regions. *Nat. Methods* 2011, *8*, 785–786.

[27] Tseng, S., Reddi, A. H., Di Cesare, P. E., Cartilage oligomeric matrix protein (COMP): a biomarker of arthritis. *Biomark. Insights* 2009, *4*, 33–44.

[28] Tagariello, A., Luther, J., Streiter, M., Didt-Koziel, L. et al., Ucma—a novel secreted factor represents a highly specific marker for distal chondrocytes. *Matrix Biol.* 2008, *27*, 3–11.

[29] Xing, Y., Lee, C. J., Protein modularity of alternatively spliced exons is associated with tissue-specific regulation of alternative splicing. *PLoS Genet.* 2005, *1*, e34.

[30] Schurgers, L. J., Spronk, H. M. H., Skepper, J. N., Shanahan, C. M., Post-translational modifications regulate matrix Gla protein function: importance for inhibition of vascular smooth muscle cell calcification. *J. Thromb. Haemost.* 2007, *5*, 2503–2511.

[31] Hallgren, K. W., Zhang, D., Kinter, M., Willard, B. et al., Methylation of γ-carboxylated glu (Gla) allows detection by liquid chromatography-mass spectrometry and the identification of Gla residues in the γ-glutamyl carboxylase. *J. Proteome Res.* 2013, *12*, 2365–2374.

[32] Munroe, P. B., Olgunturk, R. O., Fryns, J. P., Van Maldergem, L. et al., Mutations in the gene encoding the human matrix Gla protein cause Keutel syndrome. *Nat. Genet.* 1999, *21*, 142–144.

[33] Yagami, K., Suh, J. Y., Enomoto-Iwamoto, M., Koyama, E. et al., Matrix GLA protein is a developmental regulator of chondrocyte mineralization and, when constitutively expressed, blocks endochondral and intramembranous ossification in the limb. *J. Cell Biol.* 1999, *147*, 1097–1108.

[34] Wallin, R., Schurgers, L. J., Loeser, R. F., Biosynthesis of the vitamin K-dependent matrix Gla protein (MGP) in chondrocytes: a fetuin-MGP protein complex is assembled in vesicles shed from normal but not from osteoarthritic chondrocytes. *Osteoarthr. Cartil.* 2010, *18*, 1096–1103.

[35] Silaghi, C. N., Fodor, D., Cristea, V., Crăciun, A. M., Synovial and serum levels of uncarboxylated matrix Gla-protein (ucMGP) in patients with arthritis. *Clin. Chem. Lab. Med.* 2012, *50*, 125–128.

[36] Vermeer, C., Theuwissen, E., Vitamin K, osteoporosis and degenerative diseases of ageing. *Menopause Int.* 2011, *17*, 19–23.

[37] Shea, M. K., Booth, S. L., Massaro, J. M., Jacques, P. F. et al., Vitamin K and vitamin D status: associations with inflammatory markers in the Framingham Offspring Study. *Am. J. Epidemiol.* 2008, *167*, 313–320.

[38] Naito, K., Watari, T., Obayashi, O., Katsube, S. et al., Relationship between serum undercarboxylated osteocalcin and hyaluronan levels in patients with bilateral knee osteoarthritis. *Int. J. Mol. Med.* 2012, *29*, 756–760.

[39] Ishii, Y., Noguchi, H., Takeda, M., Sato, J. et al., Distribution of vitamin K2 in subchondral bone in osteoarthritic knee joints. *Knee Surg. Sports Traumatol. Arthrosc.* 2013, *21*, 1813–1818.

Cell. Mol. Life Sci.
DOI 10.1007/s00018-015-2033-9

Cellular and Molecular Life Sciences

ORIGINAL ARTICLE

Gla-rich protein is involved in the cross-talk between calcification and inflammation in osteoarthritis

Sofia Cavaco[1] · Carla S. B. Viegas[1,2] · Marta S. Rafael[1] · Acácio Ramos[3] · Joana Magalhães[4,5] · Francisco J. Blanco[4] · Cees Vermeer[6] · Dina C. Simes[1,2]

Received: 5 July 2015 / Revised: 25 August 2015 / Accepted: 27 August 2015

Abstract Osteoarthritis (OA) is a whole-joint disease characterized by articular cartilage loss, tissue inflammation, abnormal bone formation and extracellular matrix (ECM) mineralization. Disease-modifying treatments are not yet available and a better understanding of osteoarthritis pathophysiology should lead to the discovery of more effective treatments. Gla-rich protein (GRP) has been proposed to act as a mineralization inhibitor and was recently shown to be associated with OA in vivo. Here, we further investigated the association of GRP with OA mineralization–inflammation processes. Using a synoviocyte and chondrocyte OA cell system, we showed that GRP expression was up-regulated following cell differentiation throughout ECM calcification, and that inflammatory stimulation with IL-1β results in an increased expression of COX2 and MMP13 and up-regulation of GRP. Importantly, while treatment of articular cells with γ-carboxylated GRP inhibited ECM calcification, treatment with either GRP or GRP-coated basic calcium phosphate (BCP) crystals resulted in the down-regulation of inflammatory cytokines and mediators of inflammation, independently of its γ-carboxylation status. Our results strengthen the calcification inhibitory function of GRP and strongly suggest GRP as a novel anti-inflammatory agent, with potential beneficial effects on the main processes responsible for osteoarthritis progression. In conclusion, GRP is a strong candidate target to develop new therapeutic approaches.

Keywords Osteoarthritis · Gla-rich protein · ECM mineralization · Gamma-carboxylated GRP · Inflammation

Electronic supplementary material The online version of this article (doi:10.1007/s00018-015-2033-9) contains supplementary material, which is available to authorized users.

✉ Dina C. Simes
dsimes@ualg.pt

1 Centre of Marine Sciences (CCMAR), University of Algarve, Campus de Gambelas, 8005-139 Faro, Portugal

2 GenoGla Diagnostics, Centre of Marine Sciences (CCMAR), University of Algarve, Faro, Portugal

3 Department of Orthopedics and Traumatology, Algarve Medical Centre (CHAlgarve), Faro, Portugal

4 Grupo de Bioingeniería Tisular y Terapia Celular (GBTTC-CHUAC), Servicio de Reumatología, Instituto de Investigación Biomédica de A Coruña (INIBIC), Complejo Hospitalario Universitario de A Coruña (CHUAC), Sergas, Universidad de A Coruña (UDC), A Coruña, Spain

5 Centro de Investigación Biomédica en Red de Bioingeniería, Biomateriales y Nanomedicina (CIBER-BBN), Madrid, Spain

6 VitaK, Maastricht University, Maastricht, The Netherlands

Introduction

Osteoarthritis (OA) is the leading form of degenerative joint diseases [1] characterized by progressive loss of articular cartilage, abnormal bone formation, tissue inflammation and synovial proliferation, culminating in pain, loss of joint function and disability [2, 3]. At the cellular level, OA results from abnormal chondrocyte differentiation into a hypertrophic phenotype and impairment of the homeostatic balance between synthesis and degradation of their extracellular matrix (ECM). This phenotype is commonly associated with ECM mineralization that can result from basic calcium phosphate (BCP) crystals deposition [4] contributing to disease progression [5]. Crystal deposition in OA is not unique for cartilage and has also

Published online: 04 September 2015

been reported in the synovial fluid and membrane, where it modulates inflammatory responses [6, 7]. The prevailing theory is that proinflammatory and catabolic mediators, such as nitric oxide, cytokines, prostaglandins and matrix metalloproteinases (MMPs) [5, 7, 8], are released from cartilage into the synovial space, and that the presence of calcium crystals amplifies the production of such mediators, contributing to joint inflammation and cartilage degradation [5, 7].

Osteoarthritis prevention and treatment are still limited impelling the need to identify novel targets and biomarkers for prevention, therapeutics and prophylactic treatment [9]. An interesting candidate is vitamin K, which is critical for preventing soft tissue mineralization [10, 11]. Moreover, vitamin K was also suggested as a protective agent against inflammation [12]. Vitamin K is an essential cofactor for the post-translational modification of vitamin K-dependent proteins (VKDPs), where specific glutamic acid (Glu) residues can be modified to calcium binding γ-carboxyglutamic acid (Gla) residues [13]. While subclinical vitamin K levels have been associated with an increased risk of OA development [14, 15], several VKDPs, such as matrix Gla protein (MGP), osteocalcin (OC), and recently Gla-rich protein (GRP), have been associated with the disease. Moreover, the presence of undercarboxylated OC in serum, resultant of vitamin K insufficiency, is considered as a risk marker for OA [16]. Importantly, impaired γ-carboxylation of MGP has been associated with increased mineralization of osteoarthritic cartilage [15], whereas also levels of undercarboxylated MGP in synovial fluid and serum were recently suggested as a potential inflammatory marker of arthritis [17].

GRP is the newest member of the VKDP family. It was first identified in sturgeon calcified cartilage and characterized by the presence of 15 putative Gla residues in man [18], but its function and molecular mechanisms of action remain to be further clarified. GRP has been suggested to act as a modulator of calcium availability in the ECM [19, 20], and an inhibitor of calcification in the cardiovascular system [21]. However, conflicting data, particularly associated to its function in mouse skeletal tissues, reinforce the need for additional characterization of GRP potential association to human pathological conditions such as OA. While GRP-deficient mice did not reveal evident phenotypic alterations in bone and cartilage [22], zebrafish knockdown studies highlighted the essential role of GRP in skeletal development and calcification [23]. Although GRP has been shown to function as a negative regulator of osteogenic differentiation [24, 25] and to be down-regulated by bone morphogenetic protein 2 (BMP-2) in chondrogenic cells [24], recent data suggested that GRP is up-regulated by both runt-related transcription factor 2 (Runx2) and osterix (Osx) stimulating osteoblast differentiation and nodule formation [26]. Our previous studies revealed a differential pattern of GRP gene expression and protein accumulation between control and osteoarthritic human articular cartilage and synovial membrane tissues. Furthermore, we verified that GRP accumulation was not restricted to sites of ectopic calcification [27], suggesting the involvement of this VKDP in cell-mediated processes other than ECM calcification in OA.

In this context, and to further understand the relevance of GRP for OA etiology, we used an in vitro cell system to study the relationship between GRP and the mineralization and inflammatory processes involved in OA development and progression. Our results demonstrate the involvement of GRP in calcification processes associated to OA-affected tissues, supporting a previously proposed role for GRP as a novel biomarker for calcification-related diseases. Moreover, we describe, for the first time, a new role for GRP in inflammatory events, and propose this VKDP as a novel factor linking the two main pathological processes responsible for OA development and progression.

Materials and methods

Biological material and sample processing

Knee articular cartilage and synovial membrane samples were obtained from osteoarthritic patients who had undergone arthroplasty surgeries. Tissues were collected in Dulbecco's Modified Eagle's Medium (DMEM, Invitrogen, Carlsbad, CA, USA) for cell culture preparation and in formalin for histological processing, followed by paraffin embedding as described [28]. This study was approved by the ethics committees of the hospitals involved, and written informed consent was obtained from all the participants.

Cell culture development and maintenance

Tissues, both articular cartilage and synovial membrane, were digested overnight with 2 mg/mL collagenase in DMEM at room temperature (RT). Fragments were washed three times with DMEM, placed in 24-well plates, and cultured in the same medium supplemented with 1 % (v/v) penicillin–streptomycin, 1 mM L-glutamine and 10 % (v/v) fetal bovine serum (FBS), at 37 °C in a humidified atmosphere with 5 % CO_2. OA-derived chondrocytes (OA-HAC, osteoarthritic human articular chondrocytes) and synoviocytes (OA-HFLS, osteoarthritic human fibroblast-like synoviocytes) were allowed to migrate from fragments and adhere to wells for approximately 2 weeks, then collected using trypsin solution (Invitrogen) for cell passage, and placed into new plate dishes with fresh media. Cultures

were routinely sub-cultured (1:2) at early confluence by trypsinization. Cellular proliferation measurements indicated higher growth performance using advanced DMEM (Invitrogen) supplemented with 1 % (v/v) penicillin–streptomycin, 1 mM L-glutamine and 10 % (v/v) FBS when compared with DMEM. Therefore, advanced DMEM was used throughout the study, in all cell lines. Cells used in the experiments were between passages 4 and 14.

Control primary chondrocytes (NHAC, Lonza, Visp, Switzerland) and synoviocytes (HFLS, ECACC, Sigma-Aldrich, St. Louis, MO, USA) were commercially obtained. A second set of OA and control-derived primary chondrocytes cultures (OAC and NC, respectively) and primary synoviocytes cultures (SOAR and SNR, respectively) were obtained using well-defined methodology [29, 30], and used to confirm the results obtained with of the first set of cells.

Cellular proliferation measurement

Cells were seeded in 96-well plates at 2×10^4 cells/well and cultured in DMEM and advanced DMEM supplemented with 1 % (v/v) penicillin–streptomycin, 1 mM L-glutamine and 10 % (v/v) FBS and both culture conditions were analyzed for cell viability at appropriate times using the CellTiter 96 cell proliferation assay (Promega, Madison, WI, USA), following manufacturer's instructions. Cell viability of cultures supplemented with 5.4 mM $CaCl_2$, 500 ng/mL of sturgeon cGRP or human recombinant ucGRP [20], 5 ng/mL of interleukin 1β (IL-1β) or 100 μg/mL of BCP crystals (prepared as described below) was also determined using the same procedure.

RNA extraction, cDNA amplification and quantitative real-time PCR (qPCR)

Total RNA was isolated from cell cultures as described by Chomczynski and Sacchi [31]. RNA concentration was determined by spectrophotometry at 260 nm and quality evaluated by agarose-denaturing gel electrophoresis. Five hundred ng of total RNA was treated with DNase RQ-I (Promega) and reverse transcribed using Moloney-murine leukemia virus reverse transcriptase (MMLV-RT, Invitrogen), RNase Out (Invitrogen), and an oligo(dT) adapter (ACGCGTCGACCTCGAGATCGATG$(T)_{13}$), according to manufacturer's recommendations.

Quantitative real-time PCR reactions were performed using the StepOne system (Life Technologies, Carlsbad, CA, USA), SsoFast Eva Green Supermix (Bio-Rad, Richmond, CA, USA), 300 nM of forward and reverse gene-specific primers (final concentration) for genes of interest (Online Resource 1) and a 1:5 dilution of reverse-transcribed RNA reaction mixture. The following PCR conditions were used: initial denaturation/enzyme activation step at 95 °C for 5 min, 50 cycles of amplification (one cycle is 30 s at 95 °C and 15 s at 66 °C); 18S was used as a housekeeping gene to normalize expression.

Immunofluorescence and immunohistochemistry

Immunofluorescence (IF) was performed in sub-confluent cultures, seeded the previous day. Cells were washed with PBS and fixed for 10 min in 4 % (v/v) paraformaldehyde. Fixed cells were incubated at RT for 1 h with CTerm-GRP (10 μg/mL, GenoGla Diagnostics, Faro, Portugal), mouse monoclonal cGRP (10 μg/mL, GenoGla Diagnostics) or mouse monoclonal ucGRP [20] (7.3 μg/mL, VitaK BV, Maastricht, The Netherlands) primary antibodies, followed by incubation for 1 h, at RT with Alexa488 or Alexa594 labeled secondary antibodies (Invitrogen), respectively. Fluorescence images were obtained using an Axio Imager Z2 microscope (Zeiss, Jena, Germany) equipped with a digital camera and AxioVision imaging software. Final images were processed using Image J Version 1.41 m.

Immunohistochemistry (IHC) was performed in paraffin tissue sections of osteoarthritic synovial membrane as described [32]. Antigen retrieval was performed by boiling tissue sections in 0.2 % (v/v) citric acid pH 6.0, followed by endogenous peroxidase and nonspecific antibody blocking and incubations with CTerm-GRP (5 μg/mL) or mouse monoclonal cluster of differentiation 45 (CD45, 2 μg/mL, Santa Cruz Biotechnology) primary antibodies. Peroxidase activity was detected using the respective peroxidase-conjugated secondary antibodies (Sigma-Aldrich) and ImmPACT NovaRED substrate kit (Vector laboratories Ltd., Peterborough, UK). Sections were counterstained with hematoxylin.

ECM mineralization assay

To induce mineralization of the ECM, confluent cultures grown in advanced DMEM were supplemented with $CaCl_2$ to a final calcium concentration of 5.4 mM. The experiment was performed during 3 weeks with media changes twice a week and each week set as an experimental time point (*T*0–*T*3). Mineral content was detected by von Kossa staining as described [33]. Formation of mineralized nodules in the ECM was observed under a Motic AE 31 inverted light microscope.

To analyze the effect of GRP on mineralization, confluent chondrocytes and synoviocytes were grown for 3 weeks in advanced DMEM under mineralizing conditions supplemented with 500 ng/mL of cGRP or ucGRP and compared with respective controls. At appropriate times, calcium/protein ratios were determined, as described below.

Calcium and total protein quantification

At appropriate times, cell cultures grown in control or mineralizing conditions were washed twice with PBS and mineral was dissolved overnight with 1 M HCl, at 4 °C. ECM calcium concentration was then determined using a commercially available kit (Calcium assay CA-590, Randox, Co. Antrim, UK). Equimolar amounts of NaOH containing 5 % (w/v) SDS were then used to neutralize the remaining HCl-mineral phase and determine total protein concentration using the micro BCA protein assay kit (Thermo Scientific, Waltham, MA, USA). Results are thus presented as calcium/protein ratios.

Inflammation assay

Confluent chondrocytes and synoviocytes were cultured in advanced DMEM or supplemented with 500 ng/mL of cGRP, 500 ng/mL of ucGRP or 2 μM dexamethasone (DXM) during 24 h. Cells were washed twice with PBS and media were changed for advanced DMEM supplemented with 5 ng/mL of IL-1β for 72 h. At appropriate times, cell media were collected for prostaglandin E2 (PGE2) quantification and cells washed twice with PBS for RNA extraction. PGE2 measurement was achieved using an available ELISA kit (Thermo Scientific) following manufacture's protocol.

Protein mineral complex (PMC) assay

BCP crystals were produced based on a previously described procedure, and the resulting crystals were washed three times with Milli-Q water and reduce to fine particles by sonication (Vibra-cell apparatus, Sonics & Materials, Inc., Newtown, MA, USA) [21, 34]. PMCs were prepared by incubating BCP crystals (100 μg) in Milli-Q water for 30 min at 37 °C with approximately 500 ng of cGRP or ucGRP [21]. Pellets containing PMCs or BCP crystals were added to confluent chondrocytes and synoviocytes and assayed for 72 h (controls consist of culture medium only). At appropriate times, cells were washed twice with PBS prior to RNA extraction and cell media were collected for PGE2 measurement as previously described.

Statistical analysis

Data are presented as mean ($n > 2$) ± standard error. Ordinary one-way ANOVA was used for comparisons within the same group. Multiple t tests were used for comparison between two groups. For two groups submitted to a variable, significance was determined using two-way ANOVA and multiple comparisons were achieved with the Tukey's test. Statistical significance was defined as $P \leq 0.05$ (*), $P \leq 0.005$ (**) and $P \leq 0.0005$ (***).

Results

GRP and genes involved in the γ-carboxylation machinery are associated with osteoarthritis

The association of GRP with OA was analyzed on chondrocyte and synoviocyte primary cell cultures, the two main cell types involved in OA pathology. Human articular chondrocytes and fibroblast-like synoviocytes, either control (NHAC and HFLS, respectively) or derived from OA patients (OA-HAC and OA-HFLS, respectively), were characterized by gene expression profiling of differentiation and known OA-related markers, and correlated with the expression of GRP, MGP, and genes related to γ-carboxylation processing. The obtained results showed higher levels of OC, cartilage oligomeric matrix protein (COMP) and collagen type X (Col10a1), and lower levels of collagen type II (Col2a1) in OA-HAC cells (Fig. 1a), confirming an osteoarthritic chondrocyte phenotype. Also, OA-HFLS cells, exhibited higher levels of the OA-associated gene markers OC, MMP13 and CD68, and lower vimentin expression (Fig. 1a).

GRP and MGP were found to be up-regulated in both OA-derived cultures, OA-HAC and OA-HFLS, while γ-carboxylase (GGCX) and vitamin K epoxide reductase (VKOR) were shown to be expressed at lower levels than in control-derived cells (Fig. 1b), suggesting an increased production of VKDPs, but an impaired γ-carboxylation capacity in OA-derived cells. To access GRP γ-carboxylation status, the protein accumulation pattern was analyzed in OA and control cells by IF using the conformation-specific monoclonal antibodies cGRP and ucGRP, and the polyclonal CTerm-GRP recognizing total GRP (Fig. 2). In concordance with previously reported data from osteoarthritic cartilage and synovial membrane tissue samples [27], both cGRP and ucGRP were detected in pathological and control chondrocyte cells, while only ucGRP was found associated with the OA-HFLS cells.

Overall, the results indicate that OA-derived cells showing osteoarthritic gene expression patterns have GRP up-regulation and indications of a reduced γ-carboxylation capacity.

Calcification and cell differentiation in OA are correlated with GRP expression

The calcification capacity of both NHAC/OA-HAC and HFLS/OA-HFLS cells was assessed by von Kossa staining (Fig. 3a) and by calcium quantification of the mineral

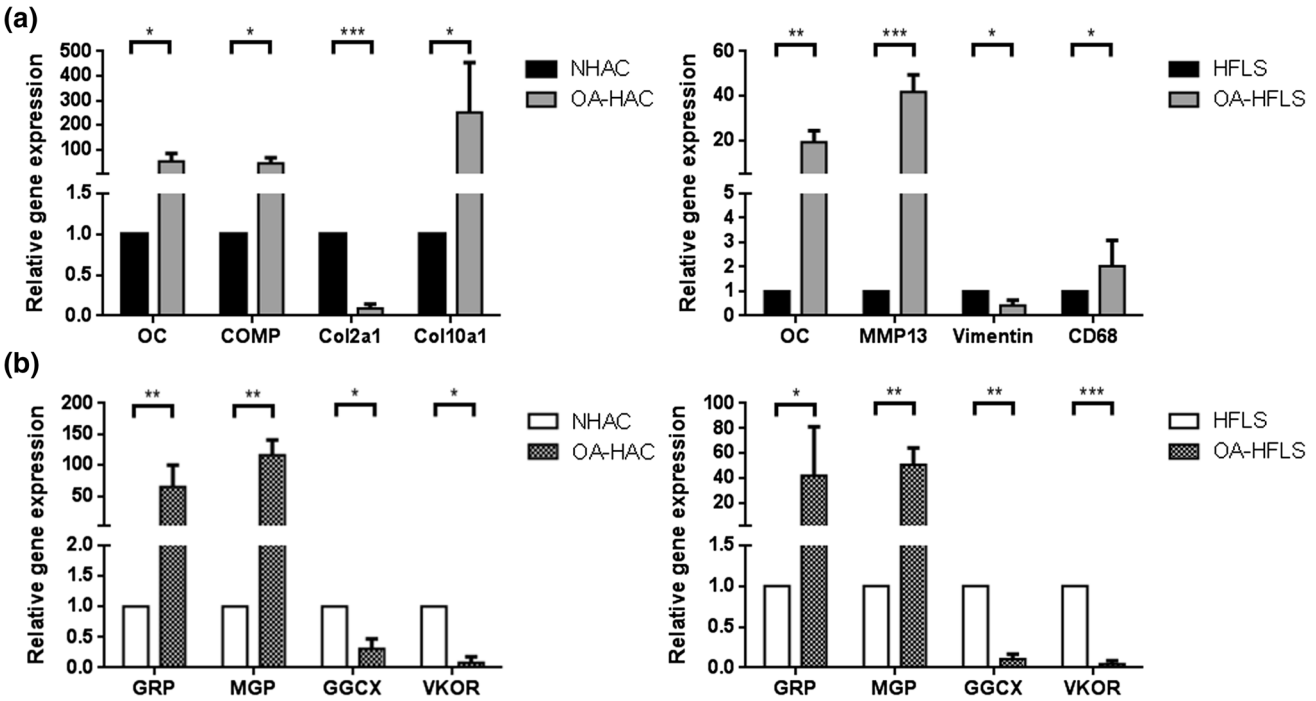

Fig. 1 Characterization of control and osteoarthritic-derived (OA) chondrocyte and synoviocyte cell cultures through gene expression patterns determined by qPCR. **a** Expression of OA (OC, COMP and MMP13) and differentiation (Cola2a1, Cola10a1, CD68 and vimentin) gene markers in control (NHAC and HFLS) and OA-derived (OA-HAC and OA-HFLS) chondrocytes and synoviocytes. **b** Expression of VKDP-related genes (GRP, MGP, GGCX and VKOR) in control and OA-derived chondrocytes and synoviocytes. Values are relative to a reference sample (control cell culture) set to 1. All experiments were repeated at least three times. Multiple *t* tests were performed. Statistical significance was defined as $P \leq 0.05$ (*), $P \leq 0.005$ (**) and $P \leq 0.0005$ (***)

deposited in the ECM (Fig. 3b). The results showed that all cell cultures were able to mineralize their ECM, although after the 3 weeks of treatment higher calcium levels and mineral deposition were found in chondrocyte-derived cultures when compared to synoviocytes (Fig. 3a, b, *T*3). Significant differences in calcium quantification between OA and control chondrocytes were evident at week 1 (*T*1), although during subsequent weeks the differences gradually disappeared.

The expression patterns of gene markers for cell differentiation and mineralization were simultaneously investigated, in control and OA-derived primary cells to determine their correlation with calcification. After the first week of treatment (*T*1), OA-HAC cells showed higher expression levels of GRP, MGP, OC, Osx and Col10a1, and lower levels of Col2a1, compared to control NHAC cells (Fig. 4a). The progressive down-regulation of Col2a1 in parallel with the up-regulation of Col10a1, Osx and OC throughout the treatment in both cultures is consistent with differentiation occurring in chondrocytes towards a hypertrophic phenotype and ECM calcification.

The most significant differences between control and OA-derived cells were observed at *T*1, suggesting that, under calcification stimulating conditions the already altered phenotype of primary OA-derived cells induces a faster response. However, at *T*3 most of the gene markers were found similarly expressed, in concordance with the similar levels of calcification obtained for both cultures (Fig. 3b). Notably, levels and patterns of GRP and Osx gene expression were found similarly up-regulated in OA-derived chondrocytes, throughout mineralization treatment, with higher levels in OA-derived cells at all-time points. In synoviocytes, vimentin down-regulation and CD68 up-regulation were observed during induced calcification, in both OA-derived and control cells; this is suggestive for a phenotypic change from fibroblast-like synoviocytes towards a macrophage lineage, while GRP, MGP, OC and osteopontin (OPN) were gradually up-regulated throughout mineralization, with only minor differences observed between OA-derived and control cells (Fig. 4b).

Carboxylated GRP is able to reduce mineral deposition in articular cells ECM

To determine the direct effect of GRP in ECM mineralization of chondrocytes and synoviocytes, and further unveil the relevance of its γ-carboxylation status, cells cultured under control and mineralizing conditions were supplemented with ucGRP or cGRP. Cell proliferation assays were performed for both GRP protein forms to

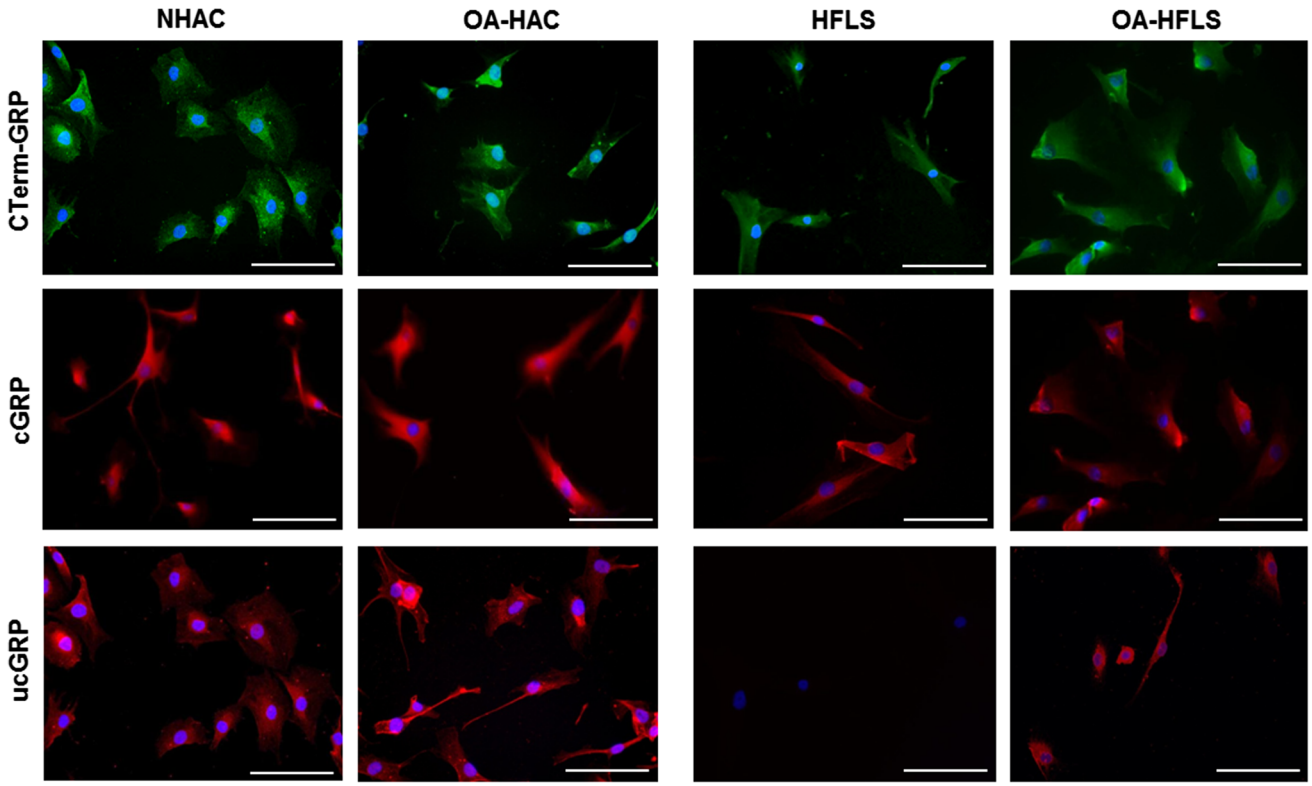

Fig. 2 Accumulation patterns of GRP protein forms in both control (NHAC and HFLS) and OA (OA-HAC and OA-HFLS)-derived chondrocytes and synoviocytes. Immunofluorescence imaging was obtained for total GRP (CTerm-GRP), γ-carboxylated (cGRP) and undercarboxylated GRP (ucGRP) protein forms using specific antibodies. Cell nuclei were stained with DAPI; *scale bar* represents 100 μm. All experiments were repeated at least twice

confirm that the treatment was not cytotoxic (data not shown). The results showed that the addition of cGRP significantly decreased mineral deposition after 3 weeks of treatment, in both control (Fig. 5) or OA-derived (results not shown) chondrocytes and synoviocytes, while no effect was observed with ucGRP treatment.

GRP is associated with inflammatory events in OA

To study the interplay between mineralization and inflammatory events in OA, the inflammatory response of chondrocytes and synoviocytes under mineralization conditions was determined by analyzing the expression patterns of inflammation markers. Increased expression of COX2 and MMP13, throughout the time course indicated that a mineralization stimulus is able to trigger the inflammatory response in both cells systems (Fig. 6a). Since in this model, GRP was also found to be up-regulated with mineralization treatment (Fig. 4), we have further studied the possible relation between GRP and inflammation by inducing chondrocytes and synoviocytes with an inflammatory stimulus and evaluating GRP expression pattern. A sharp rise in GRP gene expression concomitant with an increase in COX2 and MMP13 expression was obtained at 3 h after IL-1β treatment (Fig. 6b). From 6 to 72 h of stimulation, the expression of GRP and inflammatory gene markers had progressively decreased until control levels. To evaluate the association of GRP with inflammation in vivo, the presence of GRP in osteoarthritic synovial membrane was determined by IHC and the results showed co-localization of GRP with CD45 positive cells, indicative of leucocytes (Fig. 6c–f).

GRP is a novel factor in the cross-talk between calcification and inflammation processes

Since BCP crystals deposition has been associated with inflammatory responses in OA, and GRP binding capacity to calcium crystals has been previously reported [21], chondrocytes and synoviocytes were treated with BCP crystals and BCP crystals coated with either cGRP/ucGRP (PMCs), during 72 h, to evaluate the inflammatory response. Up-regulation of COX2 and MMP13 expression in BCP-treated cells confirmed the inflammatory response mediated by BCP crystals, both in synoviocytes and chondrocytes cell systems, while treatment of cells with non-cytotoxic doses of PMCs, containing either cGRP or ucGRP, resulted in decreased COX2 and MMP13 expression (Fig. 7a). A corresponding significant reduction of

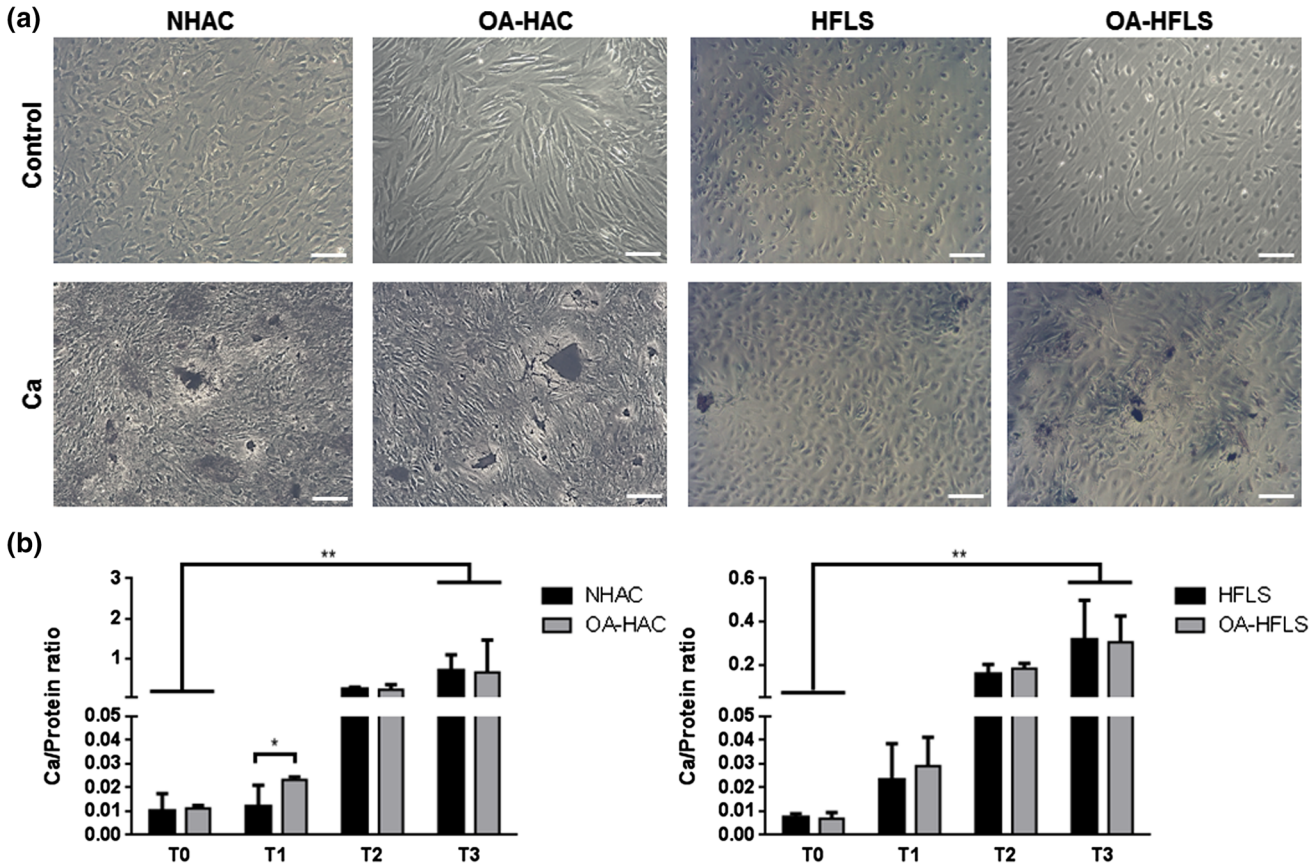

Fig. 3 In vitro ECM mineralization of control and OA-derived chondrocytes and synoviocytes (NHAC and OA-HAC, and HFLS and OA-HFLS, respectively). **a** Representative von Kossa staining at week 3 (*T*3) in control or induced mineralizing conditions with 5.4 mM $CaCl_2$ (Ca). *Scale bar* represents 100 μm. **b** Mineralization rate was determined every week (*T*0–*T*3) through calcium quantification normalized to protein levels. Data are representative of three independent experiments. Two-way Anova and multiple comparisons were achieved with the Tukey's test. Statistical significance was defined as $P \leq 0.05$ (*) and $P \leq 0.005$ (**)

PGE2 accumulation in cell media was detected after 72 h of treatment with PMCs, when compared with cells treated with BCP crystals (Fig. 7b). Altogether, our results showed that GRP coating significantly diminished the inflammatory reaction associated with BCPs, and point GRP as a new mediator factor linking mineralization and inflammatory processes.

GRP acts as an anti-inflammatory agent in osteoarthritis

To determine if GRP had a direct effect on inflammatory processes and if this response was dependent of its γ-carboxylated state, chondrocytes and synoviocytes, stimulated with IL-1β, were pre-treated with ucGRP/cGRP or DXM, the latter used as a control anti-inflammatory agent. In both cell systems stimulated with IL-1β, the treatment with either ucGRP/cGRP, resulted in significant lower levels of COX2 and MMP13 expression relative to non-treated cells (Fig. 8a), indicating an anti-inflammatory effect of GRP. To further confirm these results, PGE2 accumulation in cell media after 24 h of pre-treatment with cGRP and ucGRP (Fig. 8b) was measured, and the results showed lower levels of PGE2 in media of cells pre-treated with both protein forms relative to non-treated cells. Moreover, a similar anti-inflammatory effect was observed in OA-HAC and OA-HFLS cells. Notably, the ucGRP/cGRP effects on COX2 and MMP13 expression were comparable with levels obtained after 3 h of IL-1β stimulation in cells pre-treated with DXM, particularly in chondrocytes (Online Resource 2). The 3-h stimulation period corresponds with the inflammatory peak response. These results strongly suggest that GRP might be a powerful anti-inflammatory agent in OA that can exert its function independent of its γ-carboxylation status.

Discussion

In this study, we demonstrate for the first time the involvement of GRP, the most recently discovered VKDP, in the two major molecular processes affecting

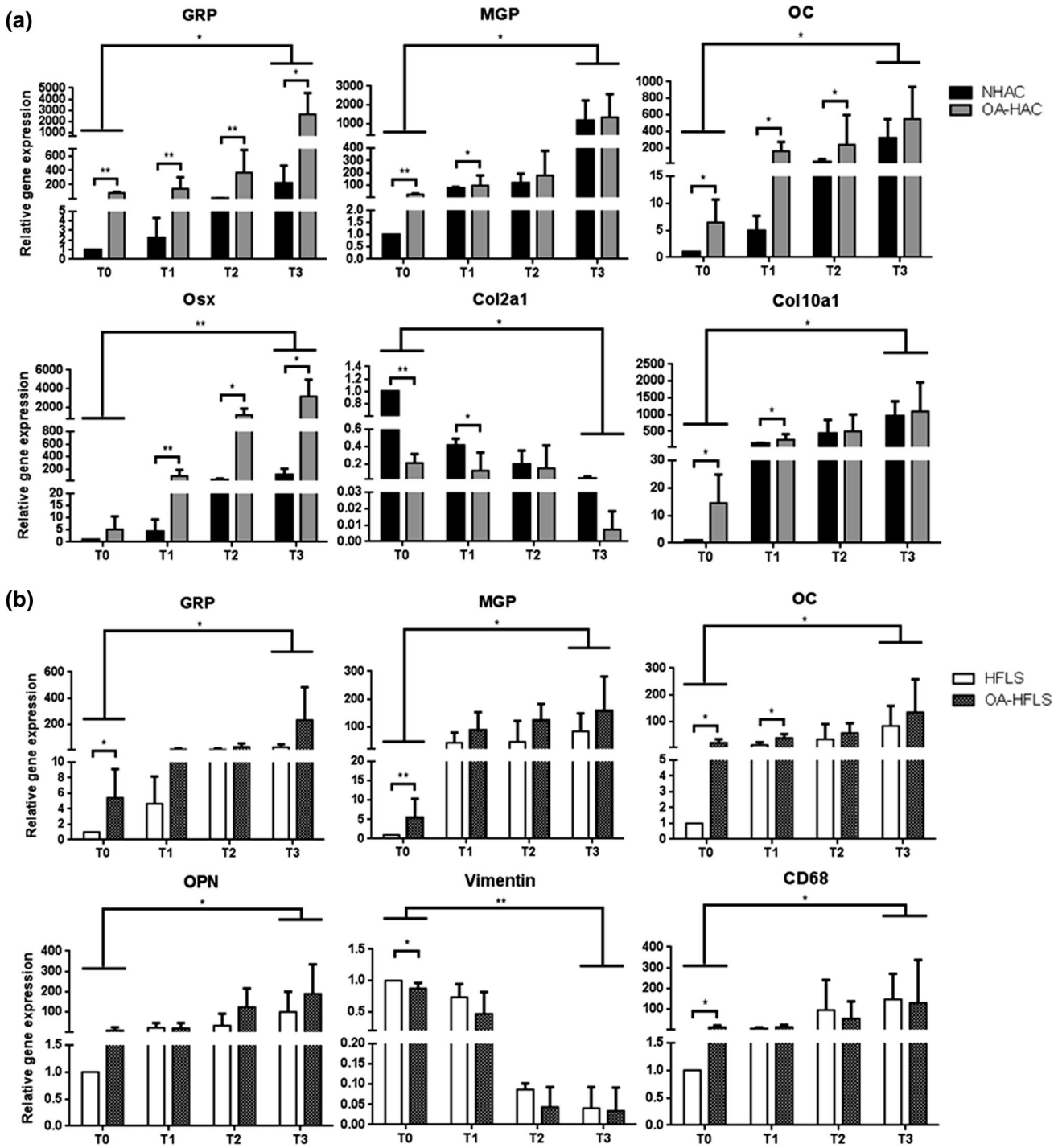

Fig. 4 Association of GRP with calcification and cell differentiation in osteoarthritis. **a** Gene expression patterns of GRP, mineralization (MGP, OC and Osx) and differentiation (Col2a1 and Col10a1) markers during induced mineralization of chondrocytes (NHAC and OA-HAC). **b** Gene expression patterns of GRP, mineralization (MGP, OC and OPN) and differentiation (vimentin and CD68) markers during induced mineralization of synoviocytes (HFLS and OA-HFLS). Gene expression was determined every week during 3 weeks (*T0*–*T3*). Gene expression values are relative to the reference sample (control cell culture) and set to 1. Data are representative of three independent experiments. Two-way Anova and multiple comparisons were achieved with the Tukey's test. Statistical significance was defined as $P \leq 0.05$ (*) and $P \leq 0.005$ (**)

osteoarthritis: mineralization and inflammation of articular tissue. GRP appears to be functioning as an ECM mineralization inhibitor and as an anti-inflammatory agent, both on chondrocytes and synoviocytes, the two main articular cell types. Moreover, while GRP γ-carboxylation was shown to be essential for its calcification inhibitor effect, it

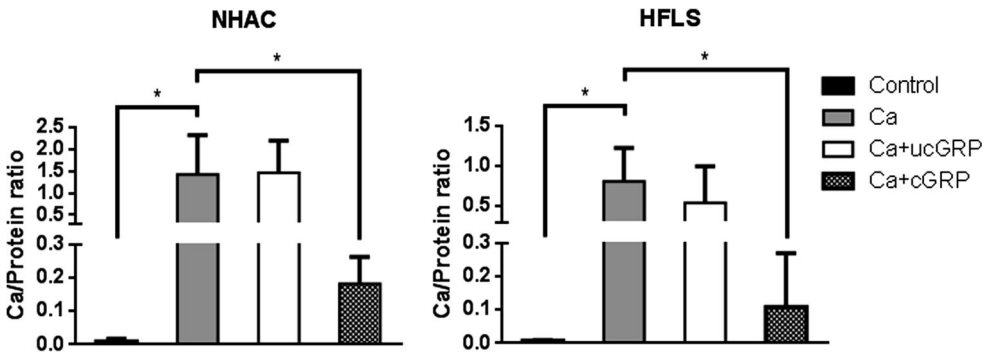

Fig. 5 Effect of GRP in ECM mineral deposition in chondrocytes and synoviocytes. Mineralization rate was determined by calcium measurement (normalized to protein levels) after 3 weeks of NHAC and HFLS cells treatment with 5.4 mM $CaCl_2$ (Ca), or supplemented with 500 ng/mL of ucGRP (Ca+ucGRP) or cGRP (Ca+cGRP). Control corresponds to cells cultured in non-supplemented media. Data are representative of three independent experiments. Ordinary one-way ANOVA was performed. Statistical significance was defined as $P \leq 0.05$ (*)

was apparently irrelevant for its anti-inflammatory action, pointing to differential roles for undercarboxylated and carboxylated GRP.

GRP gene expression was found to be up-regulated in OA-derived chondrocytes and synoviocytes, and was associated with higher levels of the calcification inhibitor MGP and OA-related gene markers such as OC, COMP and Col10a1. The results here obtained are in concordance with our previous studies with biological samples, where we showed an increase in GRP expression associated with OA [27], and also with the higher demand of calcification inhibitors, required to balance increased cell differentiation and ECM calcification occurring in OA [4]. Moreover, γ-carboxylated GRP was shown to decrease calcification in both chondrocytes and synoviocytes, and the increase in GRP expression accompanied cell differentiation towards ECM mineralization, in both cell systems. The up-regulation of GRP during osteochondrogenic differentiation, characterized by a decrease in Col2a1 and concomitant increase in Col10a1, was recently shown during osteogenic differentiation of MC3T3 cells, supporting the suggested up-regulation of GRP gene by Osx [26]. Nevertheless, previous studies have shown that GRP is repressed by BMP2, a protein known to be responsible for Osx up-regulation during osteogenesis [24]. These controversial data emphasize that the molecular mechanism of GRP action requires further clarification. Moreover, while GRP was suggested to act as a stimulating factor in osteoblast differentiation and nodule formation [26], previous data have shown an impairment of osteogenic differentiation by GRP [24, 25]. None of these studies have taken into consideration the fact that GRP is a γ-carboxylated protein, and we have shown that although both forms, cGRP and ucGRP, have mineral-binding capacity, only cGRP is able to inhibit ECM calcification in the vascular system [21]. In concordance, GRP knockdown in zebrafish resulted in severe growth retardation and perturbance of skeletal development, while warfarin treatment mimicked the GRP knockdown phenotype, suggesting an essential role of γ-carboxylation for GRP function [23]. Our new data, using GRP media supplementation in chondrocyte and synoviocyte cell cultures, strengthen the proposed calcification inhibitory function of GRP and reinforce the importance of its γ-carboxylation status, probably acting by decreasing calcium availability in the local environment, or changing the dynamics of crystal growth [21]. Increased extracellular calcium levels have been shown to drive chondrocyte differentiation towards a mineralizing phenotype, while calcium depletion from culture media maintains a stable cellular phenotype [35]. GGCX and VKOR are two crucial enzymes involved in γ-carboxylation [13]. Remarkably, the increase of GRP and MGP expression in OA-derived cells was associated with a down-regulation of GGCX and VKOR genes, suggesting a reduced capacity of OA cells, and consequently a decrease in the γ-carboxylation of target proteins such as GRP and MGP. In fact, we have previously shown a predominance of ucGRP and ucMGP in biological OA samples [27]. Moreover, reduced vitamin K-dependent γ-carboxylase activity has been reported in OA chondrocytes and correlated with (1) decreased γ-carboxylation of MGP and (2) increased matrix mineralization [36]. Although the triggers for articular cartilage calcification associated with OA are still not completely understood, dysregulation of mineral metabolism such as calcium and phosphate and an imbalance in the production of mineralization inhibitors are crucial factors favoring cartilage calcification and deposition of calcium-containing crystals, such as BCPs. It should be noted that these factors that trigger articular calcification are important to avoid chondrocyte phenotype alterations such as hypertrophic differentiation, apoptosis, as well as altered responses to inflammatory cytokines and mediators of inflammation

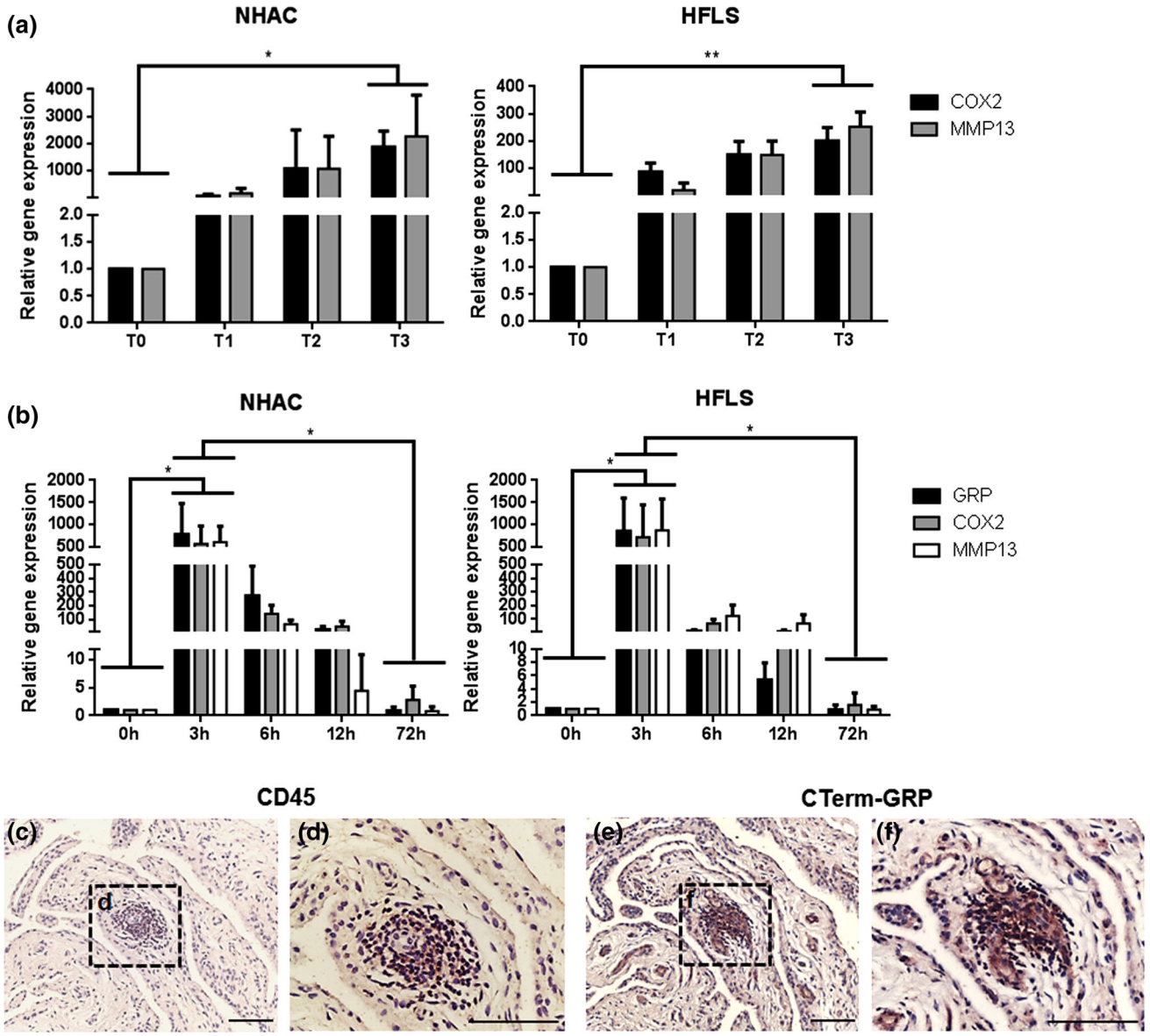

Fig. 6 In vitro and in vivo studies of GRP association with inflammatory events in osteoarthritis. **a** Gene expression of COX2 and MMP13 over 3 weeks of mineralizing treatment (5.4 mM calcium) in NHAC and HFLS (each week a set point, *T*0–*T*3). Values of gene expression are relative to the reference sample (*T*0) and set to 1. Data are representative of three independent experiments. Two-way Anova and multiple comparisons were achieved with the Tukey's test. Statistical significance was defined as $P \leq 0.05$ (*) and $P \leq 0.005$ (**). **b** Gene expression levels of COX2, MMP13 and GRP in NHAC and HFLS cells, after 72-h inflammatory stimulation with 5 ng/mL IL-1β. Values are relative to the reference sample (0 h). Data are representative of three independent experiments. Two-way Anova and multiple comparisons were achieved with the Tukey's test. Statistical significance was defined as $P \leq 0.05$ (*). **c–f** Immunodetection of CD45, showing leucocyte infiltration sites (**c** and **d**) and total GRP (**e** and **f**, CTerm-GRP antibody) in consecutive sections of osteoarthritic synovial membrane samples. Counterstaining with HE; *sale bar* represents 100 μm

[37]. Interestingly, we also showed that synoviocytes were able to produce a mineralized ECM with up-regulation of OC and OPN, and down-regulation of vimentin, suggesting a possible contribution of synoviocytes to the production of BCPs in OA articular joint. BCPs have been shown to play an important role in the onset and progression of OA [5], and are considered to be early phenomena affecting the whole joint, occurring even before any evidence of cartilage breakdown [4]. BCPs have been found in the synovial fluid, synovial membrane and cartilage from OA patients [4, 6, 7], and are currently considered a damage-associated molecular pattern (DAMP). The underlying mechanism is thought to be the signaling to the immune system a state of stress [8], and potentially contributing to OA-associated inflammation through stimulation of articular cells [6, 7]. Besides their effect on synoviocyte

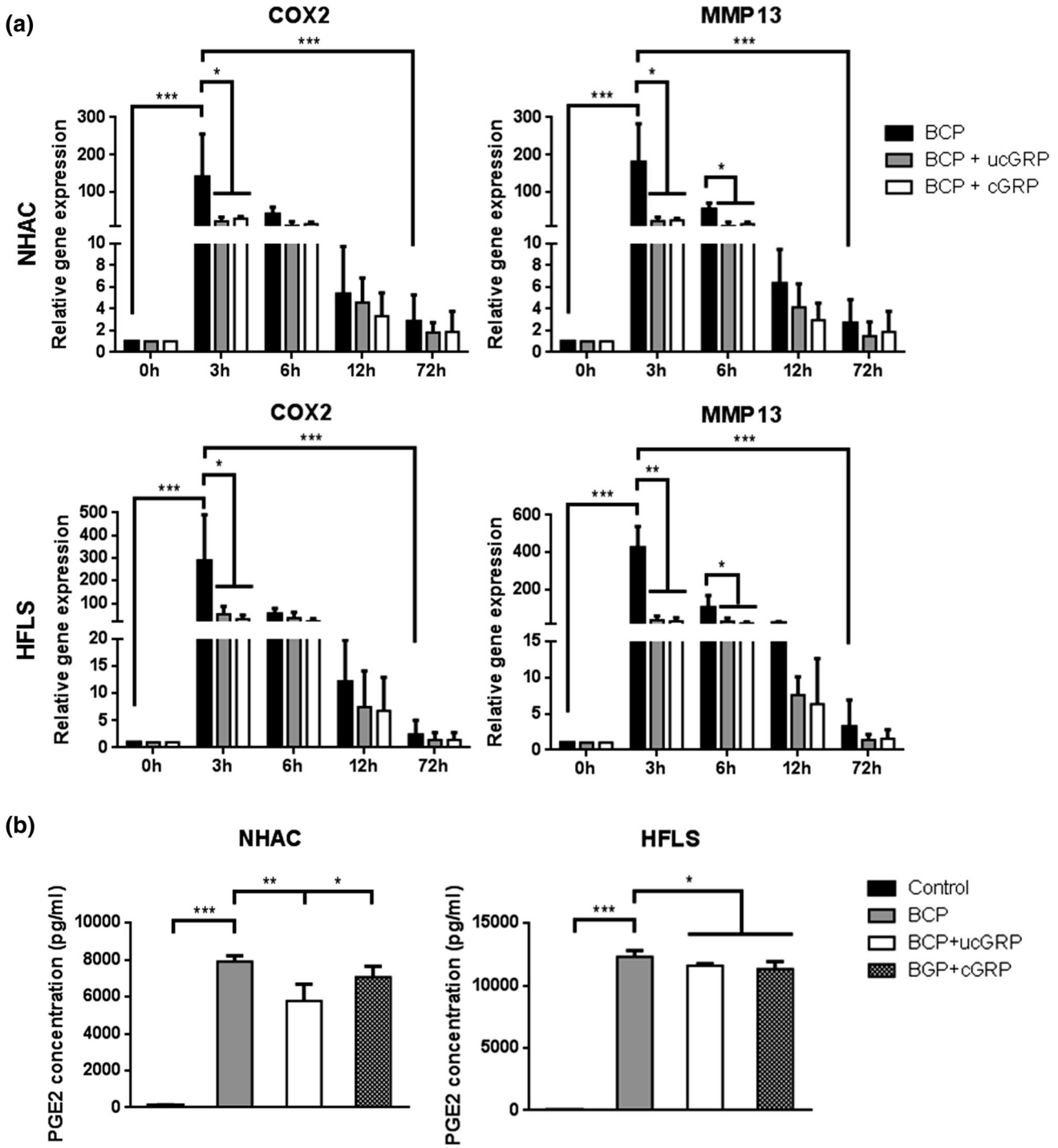

Fig. 7 Effect of GRP in the inflammatory process promoted by the addition of BCP crystals to articular cells. **a** Gene expression of COX2 and MMP13 in NHAC and HFLS cells supplemented for 72 h with BCP crystals (BCP) or BCPs coated with ucGRP (BCP + ucGRP) or cGRP (BCP + cGRP). Values are relative to the reference sample (untreated cells 0 h). Data are representative of three independent experiments. Two-way Anova and multiple comparisons were achieved with the Tukey's test. Statistical significance was defined as $P \leq 0.05$ (*), $P \leq 0.005$ (**) and $P \leq 0.0005$ (***). **b** PGE2 accumulation in NHAC and HFLS conditioned media of cells treated for 72 h as described in **a**. Control corresponds to culture media of non-treated cells. Ordinary one-way ANOVA was performed. Statistical significance was defined as $P \leq 0.05$ (*), $P \leq 0.005$ (**) and $P \leq 0.0005$ (***)

proliferation, along with production of inflammatory cytokines, MMPs and prostaglandins, BCP crystals also induce articular chondrocytes to produce prodegradative soluble factors such as nitric oxide and to undergo apoptosis [5, 7, 8]. Production of MMPs and chondrocyte apoptosis contributes to cartilage destruction, while

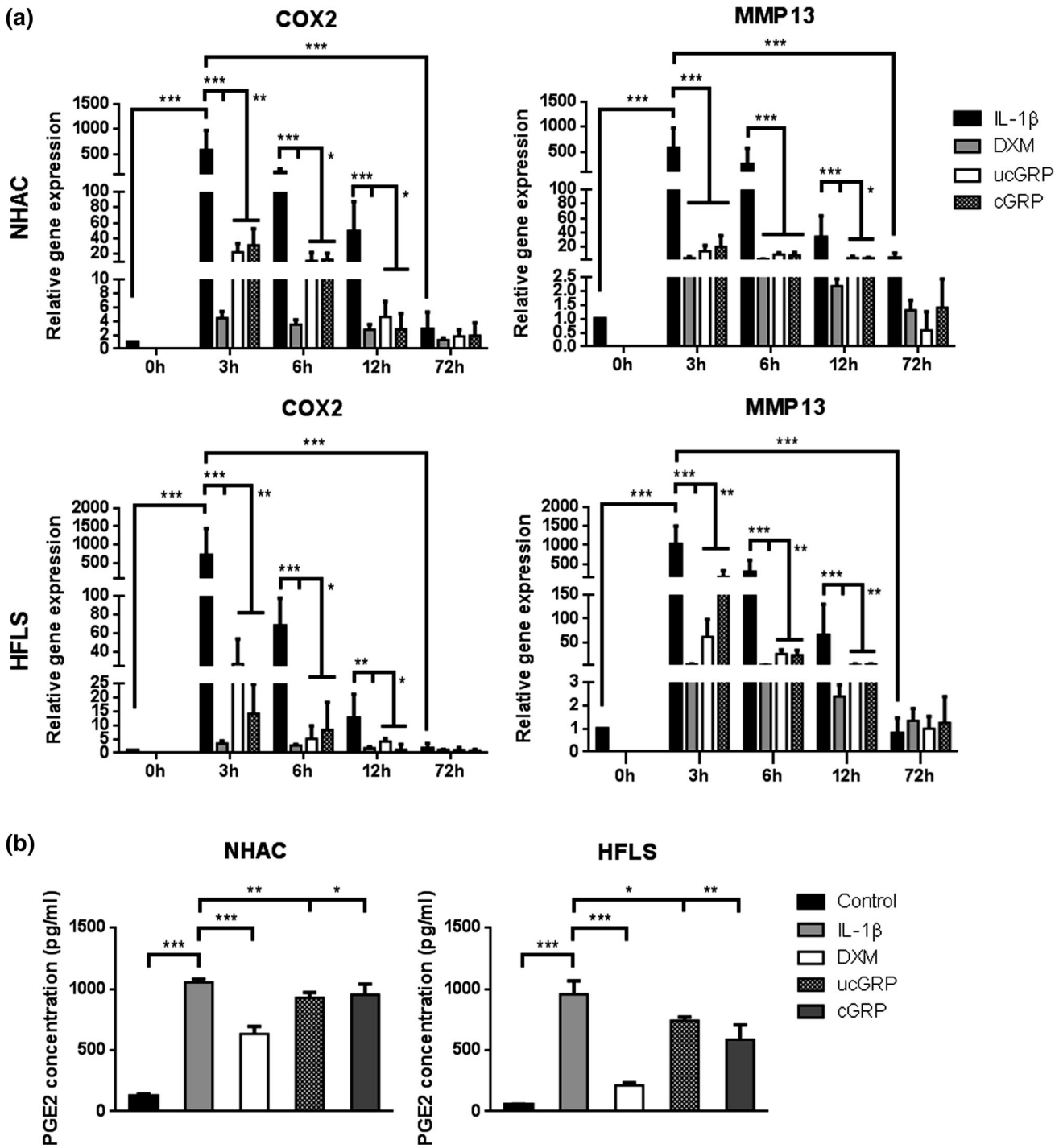

Fig. 8 Effect of GRP in chondrocytes and synoviocytes under in vitro inflammatory conditions mimicking osteoarthritis. **a** Gene expression of COX2 and MMP13 in NHAC and HFLS cells pre-treated with 500 ng/mL of ucGRP or cGRP or 2 μM dexamethasone (DXM) followed by IL-1β stimulation (5 ng/mL) during 72 h. Cells untreated with GRP or DMX were also analyzed (IL-1β). Control corresponds to cells grown in advanced DMEM only. Values are relative to the reference sample (0 h). Data are representative of three independent experiments. Two-way Anova and multiple comparisons were achieved with the Tukey's test. Statistical significance was defined as $P \leq 0.05$ (*), $P \leq 0.005$ (**) and $P \leq 0.0005$ (***). **b** PGE2 accumulation in cell media of NHAC and HFLS treated for 24 h as described in (**a**). Control corresponds to culture media of non-treated cells. Ordinary one-way ANOVA was performed. Statistical significance was defined as $P \leq 0.05$ (*), $P \leq 0.005$ (**) and $P \leq 0.0005$ (***)

cartilage degradation products drive inflammatory events in a pathological mineralization–inflammation tissue degradation cycle [5, 7]. To unveil the role of GRP in the mineralization–inflammation processes associated with OA, we decided to investigate the effect of GRP-induced modulation of inflammatory conditions triggered by a mineralization stimulus. COX2 and MMP13 up-regulation was observed during mineralization in chondrocytes and synoviocytes and confirmed that calcification can stimulate proinflammatory signaling that parallels cell differentiation, whereas calcification is also accompanied by an up-regulation of GRP expression. These results reinforce the concept that also other cells of the joint, including fibroblast-like synoviocytes and chondrocytes, directly contribute to the innate immune activation and cytokine production in OA [8]. Moreover, the concomitant increase in GRP expression with inflammation, triggered by mineralization conditions, indicates a calcium-mediated role for GRP in the inflammatory processes. However, our experiments also showed increased GRP expression after inducing inflammation with IL-1β, with a highly similar pattern to the inflammatory markers COX2 and MMP13. These results suggest that the involvement of GRP in inflammatory-mediated processes might not be exclusively mediated by mineralization events, opening new perspectives for GRP as a novel cross-talk factor linking calcification and inflammation processes occurring in articular cells that should become highly relevant for the study of OA development and progression.

As previously reported, GRP is able to bind BCP crystals in vitro and the calcification inhibitory function of GRP might be through modulation of crystal formation and/or growth [21]. Moreover, BCPs have been suggested to have a direct pathogenic role in OA, driving synovial inflammation and cartilage degradation [5]. Based on these facts, we decided to further investigate the potential role of GRP in the inflammatory response mediated by BCPs in the articular cell system. Our results clearly demonstrate that coating BCP crystals with GRP reduces its proinflammatory effect, protecting cells from the increased expression of MMP13 and PGE2 production. It has been proposed that calcium-containing crystals may activate articular cells by either leading to an increase in intracellular calcium levels after crystal endocytosis or phagocytosis, with consequent intralysosomal crystal dissolution, through direct crystal-cell membrane interaction, that may occur via electrostatic bonds with the naked crystal surface, or by membrane receptor stimulation with naked or protein-coated crystals [37]. Although the mechanisms behind a GRP-BCP mediated anti-inflammatory effect in articular cells are currently unknown, we speculate that GRP binding to BCP will probably interfere with crystal–cell membrane interaction, thus modulating the production of proinflammatory mediators. It is interesting to note that, compared with naked hydroxyapatite crystals, fetuin-A-containing calciprotein particles (CPP), well known for their role in the prevention of uncontrolled mineralization, were recently reported to decrease cytokine production in macrophages [38]. Moreover, serum-derived CPP have been shown to produce a higher protective effect than synthetic CPP in macrophage activation [38], probably reflecting the inhibitory activity of other serum components, such as GRP. We have recently shown an association between GRP, fetuin-A and MGP at sites of aortic valves calcification, and proposed that the calcification inhibitory function of GRP may occur constitutively via this potent inhibitory system formed by proteins with strong calcium phosphate binding capacity [21]. Furthermore, pre-treatment of chondrocytes and synoviocytes with GRP followed by IL-1β stimulation mirrored the anti-inflammatory effect observed with GRP-coated BCPs. This is consistent with an anti-inflammatory role by down-regulation of cytokines and MMPs production, in some cases at levels comparable to DXM. Interestingly, the anti-inflammatory-mediated effect of GRP was apparently independent of its γ-carboxylation status, suggesting additional functions for undercarboxylated GRP. Although undercarboxylated VKDPs are generally regarded as non-functional and related to pathological states [32, 39], decreased γ-carboxylation of OC has been implicated in the regulation of energy metabolism, with novel metabolic roles [40]. This area is still under debate, however, and whether carboxylated or uncarboxylated osteocalcin acts as the active hormone in energy metabolism remains to be clarified. Moreover, in the past decade, vitamin K biological functions other than acting as a coenzyme of GGCX have been proposed, namely the anti-inflammatory effect of vitamin K2 through suppression of the NF-kB pathway with a dual pro-anabolic and anti-catabolic activity in bone [41]. In fact, inappropriate regulation of anti-catabolic activity in bone has been shown as one of the major causes of setting an inflammatory state in both OA and rheumatoid arthritis [42]. Although we have shown in this work that GRP is associated to inflammation in osteoarthritic synovial membrane undergoing synovitis, a process characterized by lymphocytes and plasma cells infiltration [43], its involvement in immune cells inflammatory responses is presently unclear. Also, additional characterization of the anti-inflammatory activity of GRP and correlation with γ-carboxylation status is necessary to further unveil the molecular pathways involved.

Overall, we propose that in a context of OA with induced cell differentiation and ECM calcification, the increased expression of VKDPs such as GRP and MGP might function to counteract calcification. However, system overload could lead to hampered γ-carboxylation

capacity resulting in increased levels of undercarboxylated GRP, which might contribute to control the levels of inflammatory mediators through still unknown mechanisms, and thereby protecting the joint structures from damage. Moreover, our results have shown that the effects of GRP in both calcification and inflammation processes were similar in control and OA-derived cell cultures, indicating that GRP can exert its function as calcification inhibitor and mediator of inflammation at different OA stages. Therefore, it is a potential candidate for therapeutics in OA, acting at both calcification and inflammation processes.

Acknowledgments This work was funded by projects PTDC/SAU-ORG/112832/2009, PTDC/SAU-ORG/117266/2010 and PTDC/BIM-MEC/1168/2012, and also through Project UID/Multi/04326/2013, all from the Portuguese Science and Technology Foundation (FCT). S. Cavaco, C. S. B. Viegas and M. S. Rafael were the recipients of the FCT fellowships SFRH/BD/60867/2009, SFRH/BPD/70277/2010 and SFRH/BPD/89188/2012, respectively. Authors acknowledge the Orthopedics and Traumatology Service, Algarve Medical Centre (CHAlgarve), Faro, for providing the biological samples used in this study, and to Rheumatologic and Orthopedic Services of CHUAC for their help in obtaining cartilage samples. CIBER-BBN is a Spanish initiative from ISCIII.

References

1. Egloff C, Hügle T, Valderrabano V (2012) Biomechanics and pathomechanisms of osteoarthritis. Eur J Med Sci 142:w13583
2. Abramson SB, Attur M (2009) Developments in the scientific understanding of osteoarthritis. Arthritis Res Ther 11:227–235
3. Blanco FJ (2014) Osteoarthritis: something is moving. Reumatol Clin 10:4–5
4. Fuerst M, Bertrand J, Lammers L, Dreier R, Echtermeyer F, Nitschke Y, Nitschke Y, Rutsch F, Schäfer FK, Niggemeyer O, Steinhagen J, Lohmann CH, Pap T, Rüther W (2009) Calcification of articular cartilage in human osteoarthritis. Arthritis Rheum 60:2694–2703
5. Rosenthal AK (2011) Crystals, inflammation, and osteoarthritis. Curr Opin Rheumatol 23:170–173
6. Hernandez-Santana A, Yavorskyy A, Loughran ST, McCarthy GM, McMahon GP (2011) New approaches in the detection of calcium-containing microcrystals in synovial fluid. Bioanalysis 3:1085–1091
7. Liu YZ, Jackson AP, Cosgrove SD (2009) Contribution of calcium-containing crystals to cartilage degradation and synovial inflammation in osteoarthritis. Osteoarth Cartil 17:1333–1340
8. Sokolove J, Lepus CM (2013) Role of inflammation in the pathogenesis of osteoarthritis: latest findings and interpretations. Ther Adv Musculoskel Dis 5:77–94
9. Kraus VB, Blanco F, Englund M, Karsdal MA, Lohmander LS (2015) Call for standardized definitions of osteoarthritis and risk stratification for clinical trials and clinical use. Osteoarth Cartil 23:1233–1241
10. Shroff RC, Shanahan CM (2007) The vascular biology of calcification. Semin Dial 20:103–109
11. Luo G, Ducy P, Mckee MD, Pinero GJ, Loyer E, Behringer RR, Karsenty G (1997) Spontaneous calcification of arteries and cartilage in mice lacking matrix Gla protein. Nature 386:78–81
12. Shea M, Booth SL, Massaro JM, Jacques PF, D'Agostinho RB, Dawson-Hughes B, Ordovas JM, O'Donnell CJ, Kathiresan S, Keaney JF Jr, Vasan RS, Benjamin EJ (2008) Vitamin K and vitamin D status: associations with inflammatory markers in the Framingham Offspring Study. Am J Epidemiol 167:313–320
13. Wallin R, Wajih N, Hutson SM (2008) VKORC1: a warfarin-sensitive enzyme in vitamin K metabolism and biosynthesis of vitamin K-dependent blood coagulation factors. Vitam Horm 78:227–246
14. Misra D, Booth SL, Tolstykh I, Felson DT, Nevitt MC, Lewis CE, Torner J, Neogi T (2013) Vitamin K deficiency is associated with incident knee osteoarthritis. Am J Med 126:243–248
15. Neogi T, Booth SL, Zhang YQ, Jacques PF, Terkeltaub R, Aliabadi P, Felson DT (2006) Low vitamin K status is associated with osteoarthritis in the hand and knee. Arthritis Rheum 54:1255–1261
16. Naito K, Watari T, Obayashi O, Katsube S, Nagaoka I, Kaneko K (2011) Relationship between serum undercarboxylated osteocalcin and hyaluronan levels in patients with bilateral knee osteoarthritis. Int J Mol Med 29:756–760
17. Silaghi C, Fodor D, Cristea V, Crăciun AM (2012) Synovial and serum levels of uncarboxylated matrix Gla-protein (ucMGP) in patients with arthritis. Clin Chem Lab Med 50:125–128
18. Viegas CSB, Simes DC, Laizè V, Williamson MK, Price PA, Cancela ML (2008) Gla-rich Protein (GRP), a new vitamin K-dependent protein identified from sturgeon cartilage and highly conserved in vertebrates. J Biol Chem 283:36655–36664
19. Viegas CSB, Cavaco S, Neves PL, Ferreira A, João A, Williamson MK, Price PA, Cancela ML, Simes DC (2009) Gla-rich protein (GRP) is a novel vitamin K dependent protein present in serum and accumulated at sites of pathological calcifications. Am J Pathol 175:2288–2298
20. Viegas CSB, Herfs M, Rafael MS, Enriquez JL, Teixeira A, Luís I, van 't Hoofd C, João A, Maria VL, Cavaco S, Ferreira A, Serra M, Theuwissen E, Vermeer C, Simes, DC (2014) Gla-rich protein is a potential new vitamin K target in cancer: Evidences for a direct GRP-mineral interaction. Biomed Res Int. doi:10.1155/2014/340216
21. Viegas CSB, Rafael M, Enriquez JL, Teixeira A, Vitorino R, Luís IM, Costa RM, Santos S, Cavaco S, Neves J, Willems B, Vermeer C, Simes DC (2015) Gla-rich protein (GRP) acts as a calcification inhibitor in the human cardiovascular system. Arterioscler Thromb Vasc Biol 35:399–408
22. Eitzinger N, Surmann-Schmitt C, Bosl M, Schett G, Engelke K, Hess A, von der Mark K, Stock M (2012) Ucma is not necessary for normal development of the mouse skeleton. Bone 50:670–680
23. Neacsu CD, Grosch M, Tejada M, Winterpacht A, Paulsson M, Wagener R, Tagariello A (2011) Ucmaa (Grp-2) is required for zebrafish skeletal development. Evidence for a functional role of its glutamate γ-carboxylation. Matrix Biol 30:369–378
24. Surmann-Schmitt C, Dietz U, Kireva T, Adam N, Park J, Tagariello A, Onnerfjord P, Heinegård D, Schlötzer-Schrehardt U, Deutzmann R, von der Mark K, Stock M (2008) Ucma, a novel secreted cartilage-specific protein with implications in osteogenesis. J Biol Chem 283:7082–7093
25. Tagariello A, Luther J, Streiter M, Didt-Koziel L, Wuelling M, Surmann-Schmitt C, Stock M, Adam N, Vortkamp A, Winterpacht A (2008) Ucma-A novel secreted factor represents a highly specific marker for distal chondrocytes. Matrix Biol 27:3–11
26. Lee YJ, Park SY, Lee SJ, Boo YC, Choi JY, Kim JE (2015) Ucma, a direct transcriptional target of Runx2 and Osterix, promotes osteoblast differentiation and nodule formation. Osteoarth Cartil. doi:10.1016/j.joca.2015.03.035
27. Rafael MS, Cavaco S, Viegas CSB, Santos S, Ramos A, Willems B, Herfs M, Theuwissen E, Vermeer C, Simes DC (2014) Insights into the association of Gla-rich protein and osteoarthritis, novel

splice variants and γ-carboxylation status. Mol Nutr Food Res. doi:10.1002/mnfr.201300941
28. Ortiz-Delgado JB, Simes DC, Viegas CSB, Schaff BJ, Sarasquete C, Cancela ML (2006) Cloning of matrix Gla protein in amarine cartilaginous fish, Prionace glauca: preferential protein accumulation in skeletal and vascular systems. Histochem Cell Biol 126:89–101
29. Burguera EF, Vela AA, Magalhães J, Meijide-Faílde R, Blanco FJ (2014) Effect of hydrogen sulfide sources on inflammation and catabolic markers on interleukin 1β-stimulated human articular chondrocytes. Osteoarth Cartil 22:1026–1035
30. Cillero PB, Martin M, Arenas J, Lopez-Armada MJ, Blanco FJ (2011) Effect of nitric oxide on mitochondrial activity of human synovial cells. B Musculoskelet Disord 12:1471–2474
31. Chomczynski P, Sacchi N (1987) Single-step method of RNA isolation by acid guanidinium thiocyanate phenol chloroform extraction. Anal Biochem 162:156–159
32. Schurgers LJ, Teunissen KJ, Knapen MH, Kwaijtaal M, van Diest R, Appels A, Reutelingsperger CP, Cleutjens JP, Vermeer C (2005) Novel conformation-specific antibodies against matrix gamma-carboxyglutamic acid (Gla) protein: undercarboxylated matrix Gla protein as marker for vascular calcification. Arterioscler Thromb Vasc Biol 25:1629–1633
33. Pombinho AR, LaizéV Molha DM, Marques SMP, Cancela ML (2004) Development of two bone-derived cell lines from the marine teleost Sparus aurata; evidence for extracellular matrix mineralization and cell-type-specific expression of matrix Gla protein and osteocalcin. Cell Tissue Res 315:393–406
34. McCarthy GM, Westfall P, Masuda I, Christopherson PA, Cheung HS, Mitchell PG (2001) Basic calcium phosphate crystals activate human osteoarthritic synovial fibroblasts and induce matrix metalloproteinase-13 (collagenase-3) in adult porcine articular chondrocytes.Ann Rheum Dis Aquat Organ 60:399–406
35. Nakatani S, Mano H, Ryanghyok IM, Shimizu J, Wada M (2006) Excess magnesium inhibits excess calcium-induced matrix-mineralization and production of matrix gla protein (MGP) by ATDC5 cells. Biochem Biophys Res Commun 348:1157–1162
36. Wallin R, Schurgers LJ, Loeser RF (2010) Biosynthesis of the vitamin K-dependent matrix Gla protein (MGP) in chondrocytes: a fetuin-MGP protein complex is assembled in vesicles shed from normal but not from osteoarthritic chondrocytes. Osteoarth Cartil 16:1096–1103
37. Ea HK, Nguyen C, Bazin D, Bianchi A, Jérôme G, Pascal R, Daudon M, Frédéric Lioté (2011) Articular cartilage calcification in osteoarthritis. Arthritis Rheum 63:10–18
38. Smith ER, Hanssen E, McMahon LP, Holt SG (2013) Fetuin-A-containing calciprotein particles reduce mineral stress in the macrophage. PLoS One 8:e60904
39. Cranenburg EC, Schurgers LJ, Vermeer C (2007) Vitamin K: the coagulation vitamin that became omnipotent. Thromb Haemostasis 98:120–125
40. Zoch ML, Clemens TL, Riddle RC (2015) New insights into the biology of osteocalcin. Bone. doi:10.1016/j.bone.2015.05.046
41. Yamaguchi M, Weitzmann M (2010) Vitamin K2 stimulates osteoblastogenesis and suppresses osteoclastogenesis by suppressing NF-κB activation. Int J Mol Med 27:3–14
42. Roman-Blas JA, Jimenez SA (2006) NF-κB as a potential therapeutic target in osteoarthritis and rheumatoid arthritis. Osteoarthritis Cartilage 14:839–848
43. Pobirci O, Bogdan F, Pobirci DD, Rosca E, Petcu CA (2011) The study of synovities with articular inflammatory liquid, through clinical-statistical, histological and immunohistochemical methods. Rom J Morphol Embryol 52:333–338